IDŐJÁRÁS

QUARTERLY JOURNAL
OF THE HUNGARIAN METEOROLOGICAL SERVICE

CONTENTS

****

http://www.met.hu/firat/ido-e.html

VOL. 103 ∗ NO. 1 ∗ JANUARY–MARCH 1999

IDŐJÁRÁS

Quarterly Journal of the Hungarian Meteorological Service

Editor-in-Chief
G. MAJOR

Executive Editor
M. ANTAL

Editorial Office: P.O. Box 39, H-1675 Budapest, Hungary or
Gilice tér 39, H-1181 Budapest, Hungary
E-mail: gmajor@met.hu or *antal@met.hu*
Fax: (36-1) 290-7387

Subscription by

mail: IDŐJÁRÁS, P.O. Box 39, H-1675 Budapest, Hungary;
E-mail: gmajor@met.hu or *antal@met.hu*; *Fax: (36-1) 290-7387*

IDŐJÁRÁS
Quarterly Journal of the Hungarian Meteorological Service
Vol. 103, No. 1, January–March 1999, pp. 1–18

A preliminary estimation of the nitrogen compounds exchange between the atmosphere and a Spruce forest

László Horváth[1], **Soren Christensen**[2], **Ernő Führer**[3], **Sugárka Kelecsényi**[4], **Róbert Mészáros**[5], **Zoltán Nagy**[1] and **Tamás Weidinger**[5]

[1]*Hungarian Meteorological Service,*
H-1675 Budapest, P.O. Box 39, Hungary; e-mail: lhorvath@met.hu
[2]*University of Copenhagen, Zoological Institute, Department of Population Biology,*
15 Universitetsparken, 2100 Copenhagen, Denmark
[3]*Forest Research Institute, 1023 Budapest, Frankel Leó u. 42/44, Hungary*
[4]*Ministry for Environmental Protection, 1117 Budapest, Fő u. 44/50, Hungary*
[5]*Eötvös Loránd University, Department of Meteorology,*
1117 Budapest, Pázmány Péter sétány 1, Hungary

(Manuscript received 30 September 1998; in final form 8 February 1999)

Abstract—On the basis of a one and a half year investigation carried out at a forestry station in Hungary in a Norway Spruce stand during 1996–97 the net dry deposition (the difference of the dry deposition and the emission) is 1.8 gN m^{-2} yr^{-1}. As a consequence of the nitrous oxide and nitric oxide emission from the forest soil only a few percent of the deposited nitrogen compounds is released back to the atmosphere. The wet deposition amounts to approximately one half of the dry deposition, 0.9 gN m^{-2} yr^{-1}. The total dry+wet deposition is 2.7 gN m^{-2} yr^{-1}. From the difference between the measured dry deposition and the throughfall + stemflow measurements, it seems that one half of the deposited nitrogen compounds is taken up by stomata, the other half is leached to the forest soil.

Key-words: nitrogen balance, atmospheric wet and dry deposition, forest ecology, throughfall deposition.

1. Introduction

The role of atmospheric pollutants in forest health is well known. Acid deposition, especially near the densely populated regions of North-America and Europe, is accompanied by a certain amount of forest damage. The supply of nitrogen, phosphorus and other nutrients to the forest ecosystem mainly takes place from the atmosphere resulting in serious nutrient overloading at some places on the Earth (e.g., in The Netherlands).

During the intensive exchange processes of the trace materials between the atmosphere and the forest ecosystems, the forest (including the forest soil) may be a source of a certain group of compounds (e.g., nitric oxide, nitrous oxide, isoprene, terpenes). On the other hand, in the case of some materials, the atmosphere can also be an important source for the forest. Some of them provide nutrients (especially nitrogen compounds) to the plants, others are harmful to the vegetation (e.g., oxidants and acidic compounds).

The forest ecosystem may act as a source or a sink for nitrogen compounds as a function of the physical and chemical circumstances. Nitrogen compounds, e.g. nitric oxide, nitrogen dioxide, ammonia, nitric acid and particulate nitrates and ammonium also take part in the acidification and nutrient supply or loading. Through the decomposition of the organic matter content in the forest soil, as a result of denitrification processes, nitrous oxide is produced and emitted. The rate of nitrous oxide emission is proportional to the temperature, humidity and organic matter content of the soil (*Christensen et al.,* 1996). In certain circumstances the forest soil emits a substantially high amount of nitrous oxide, which may partly counterbalance the deposition of the other nitrogen compounds.

Nitrogen compounds, similarly to other pollutants, are deposited by turbulent diffusion motions followed by quasi-laminar, molecular diffusion. Reaching the surface of the vegetation, they are absorbed on the leaves or are taken up by the stomata. A limited amount of adsorption on the trunk and the soil surface is also possible. The materials taken up by cuticular adsorption are leached by the following precipitation event and appear in the throughfall precipitation samples. The results concerning the dry deposition of reactive nitrogen compounds in forests are compiled by *Hansson* and *Lindberg* (1991).

Nitrogen dioxide can be emitted from the surface of the canopy in special circumstances (*Bowden,* 1986). The nitric oxide emitted from the forest soil by bacterial activity is transformed by the chemical reaction with ozone into nitrogen dioxide that may modify the vertical profiles of nitrogen oxides in and above the canopy (*Duyzer,* 1991). Because the intensity of the solar radiation is relatively low below the canopy, the decomposition of nitrogen dioxide by photolysis into nitric oxide is limited there. The nitrogen dioxide produced by the reaction of ozone and nitric oxide is partly taken up by the canopy. If the concentration of nitrogen dioxide is higher below the canopy than above, upward flux is probable, otherwise downward flux, i.e. deposition can be detected. Because the two processes, namely the upward and downward flux, are in competition, the so-called net flux may be bi-directional above forests, i.e. both net deposition and emission can be observed. For example, nitrogen oxides are mostly deposited especially at high atmospheric concentrations and during intensive uptake of nitrogen by the vegetation.

As for the other important group, the reduced nitrogen compounds (ammonium and ammonia) can partly be emitted or deposited. Ammonia, produced by denitrification processes in the forest soil, can be emitted. The ammonia gas emitted from the soil is quickly taken up in the canopy. There is a so-called compensation point concentration of ammonia controlled by and in equilibrium with the canopy (*Farquhar et al.,* 1980). When the atmospheric ammonia level is higher than the compensation point, net deposition and in the opposite case emission is expected. According to recent measurements the rate of ammonia uptake is more substantial in the forest as was previously expected (*Duyzer et al.,* 1994; *Wyers et al.,* 1993).

It follows that the estimation of the nitrogen balance between the forest and the atmosphere is rather complicated. It requires the determination of the fluxes of both oxidised and reduced gas phase nitrogen compounds and particulate nitrate and ammonium. Beside that, the determination of the rate of the wet deposition of nitrogen compounds is also necessary. For the deposition estimation wet deposition, throughfall and stemflow measurements are also required. The measurement of the emissions of nitrogen compounds from the forest soil is also important.

A joint research program was started by the Forest Research Institute and the Hungarian Meteorological Service in 1988 to determine the rate of the acid deposition in forests. The investigations concentrated on nitrogen and sulphur compounds (*Führer* and *Horváth,* 1990, 1992; *Führer et al.,* 1994; *Horváth et al.,* 1993a, 1994a; *Horváth* and *Führer,* 1991). In these measurements the concentrations of the most important nitrogen and sulphur compounds and the rate of wet and dry deposition were determined. Dry deposition was estimated by using a simple inferential model taking into consideration average dry deposition velocity figures from the literature determined for surfaces different from the forest. This approximation involves some uncertainty in the estimation of dry deposition fluxes. Many results suggest that the dry deposition velocity of nitrogen compounds to the forest is substantially higher than was previously estimated, especially for nitrate and ammonium particles. On the other hand, in some cases (e.g., for nitrogen oxides) emission is also to be expected, which was not taken into account in our calculations before either. Therefore, the re-evaluation of the rate of dry+wet deposition of nitrogen compounds is necessary. In the frame of an international project (EUREKA, EUROTRAC, BIATEX) the dry deposition velocities of the ozone, nitrogen oxides and sulphur dioxide were determined in a Norway Spruce forest by the gradient method during field campaigns carried out in the four different seasons (*Horváth,* 1992, 1993; *Horváth et al.,* 1992, 1993b,c, 1994b,c,d; *Weidinger* and *Horváth,* 1994). It was found that the dry deposition velocity of nitrogen oxides strongly depends on meteorological circumstances. In some cases e.g., in the summer of 1993 and 1994 more emission than deposition was observed (*Horváth et al.,* 1995a,b, 1997).

For these reasons our hypothesis is that the nitrogen balance may be different from the figures that were previously determined. From the point of view of the acidification or for the determination of the nutrient loading, we need to know the nitrogen balance between the forest and the atmosphere more accurately.

The aim of our investigation is to determine the nitrogen balance between the atmosphere and the forest taking into account all nitrogen compounds existing both in reduced and oxidised forms in the gaseous or aerosol phase. The estimation of the nitrogen balance may also allow us to decide whether the deposited nitrogen compounds are being accumulated in the forest soil or that the emission processes are decreasing the effect of deposition partly or totally.

2. Measurements

For the estimation of the nitrogen balance between the atmosphere and the forest examined, we have to determine the dry and wet deposition rates of the different nitrogen compounds. In the case of the compounds being deposited or emitted the measurement of the rate of net flux is also necessary. The determination of the dependence of the rate of deposition on the meteorological conditions is also required.

Parallel with the determination of the dry flux of the nitrogen compounds, the difference between wet deposition and throughfall + stemflow measurements also has to be taken into consideration.

Flux measurements were carried out at the Forest Research Institute's measuring site in the Mátra Mountains (Nyírjes station, φ = 47°54'N; λ = 19°57'E; h = 600 m a.s.l.) in a Norway Spruce forest. The area of the forest is approximately 50 ha, the mean altitude is 600 m. The surrounding forests consist of mostly Pine and Beech species. The average height of the stand is about 16 meters, with a leaf area index of 3.3. Concentration measurements were carried out near the forest at an open place. During the year of 1996 the concentration of nitrogen compounds (ammonia, nitric acid, nitric oxide, nitrogen dioxide, ammonium and nitrate particles) as well as the ammonium and nitrate content of the precipitation water was measured for the determination of the wet deposition.

Gas and aerosol sampling was carried out by a three stage filter pack on the basis of 24 hour continuous sampling. The first Teflon filter captures the aerosol particles, the second and third Whatman filters prepared by basic and acidic materials collect the acidic (nitric acid) and alkaline (ammonia) gases, respectively. The sampling and analytical procedures were performed by the standard method proposed by the *EMEP* (1996) sampling and analysis protocol. The sampling of the precipitation water was carried out by a wet only precipitation sampler.

Concentrations of nitrogen compounds were determined as ammonium and nitrate ions by spectrophotometric and ion chromatographic methods, respectively. In the year of 1996 the concentration profile and the flux of ozone, nitric oxide and nitrogen dioxide below, in and above the canopy were continuously monitored. The flux measurements were carried out by the gradient method described in *Horváth et al.* (1998), by the tower shown on *Fig. 1.*

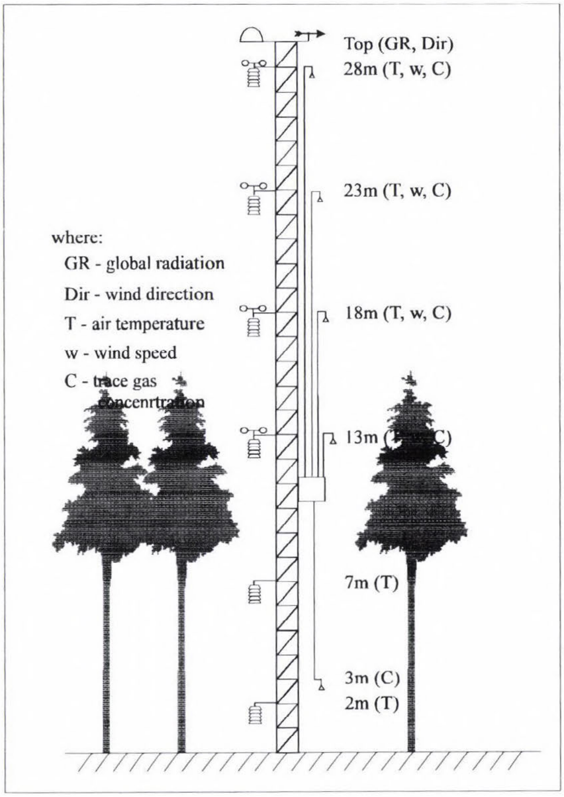

Fig. 1. The scheme of the measuring tower at Nyírjes station.

The gradient method is based on the parallel determination of the eddy diffusivity (K) and the vertical profile (gradient) of the concentration on the basis of the following expression:

$$F = -K\frac{\Delta C}{\Delta z}, \tag{1}$$

where the second term on the right denotes the gradient of the concentration.

The eddy diffusivity was calculated from the measured wind and temperature profiles on the basis of Monin-Obukhov's semi-empirical similarity theory (for details refer to *Horváth et al.,* 1998). The rate of eddy diffusivity depends on the roughness of the surface and the meteorological conditions, especially the stratification. In stable cases (mostly during the night-time hours), for energy reasons, the rate of exchange is low, when the eddy diffusivity is generally lower by one order of magnitude comparing with the unstable cases (daytime hours).

The concentration gradients were determined by sequential measurements at five different levels on the basis of five minute averaging (see on Fig. 1). The air was passed from the different levels to the HORIBA NO/NO_x gas monitor. The monitor was calibrated every two weeks.

The determination of nitrous oxide flux from the forest soil surface was carried out by the chamber method with a 10 cm diameter frame pressed 5 cm deep into the forest floor closed with a lid sealing 0.5 l of air during the measurement. In the chamber, installed on the forest soil, the accumulation of nitrous oxide was measured at 0, 15 and 30 minutes after closing. Samples were taken by evacuated tubes and were analysed by gas chromatography. The emission rate from the soil was calculated from the accumulation rate of the nitrous oxide in the chamber *(Ambus* and *Christensen,* 1995). Twenty four chambers were installed in the forest near the measuring tower in a net of 10 × 10 metres. Measurements were performed at three occasions on 15–16 May 1997. Simultaneously with the chamber measurements, five or ten replicate air samples were collected at the four heights from the tower immediately prior to and following the chamber measurements. Due to the low precision of the gas chromatograph when measuring atmospheric nitrous oxide gradients that require accuracy in the ppb range only data from the last of the three samplings with three replicate concentration measurements at each elevation will be reported. Other complementary measurements like wind direction, air humidity (at three levels), radiation balance and global radiation, soil moisture and humidity were also completed.

The data from sensors and the gas monitor was treated by a computer equipped data acquisition system. Five minute averages of the data have been stored.

3. The nitrogen balance

3.1 The flux of nitric oxide and nitrogen dioxide

On the basis of the concentration, wind and temperature profile measurements carried out during the year of 1996, the flux of nitric oxide and nitrogen dioxide was determined as described in Section 2, above the Norway Spruce forest, in the layer between 18 and 23 metres. This is the layer where the effect of deposition or emission processes can be detected. The main results are summarized in *Table 1*, where the average figures for the different quarters of the year can be seen separately for stable (positive Richardson number) and for unstable (negative Richardson number) stratification cases. During daytime hours when the energy balance for the surface is positive the stratification is generally unstable, while in night hours stable stratifications are expected. In the daytime, when the turbulent exchange processes are generally more intensive, a higher exchange rate (emission or deposition) can be observed in the table. The emission cases are marked by a negative sign. Because the emission and deposition processes take place in parallel for both nitric oxide and nitrogen dioxide, the so-called net flux can be detected during the measurements. In stable cases emission only is observed for nitric oxide (Table 1, 2nd column). This may be the consequence of the forest soil emission. Moreover, in stable stratification cases the stomata are closed therefore the NO uptake (deposition) is limited. For NO the only deposition form possible is stomatal uptake as it is practically insoluble in water, and thus the irreversible adsorption on the wet surface of the leaves is limited. In daytime hours, as a consequence of the photosynthetic active radiation, when the stratification is generally unstable, the deposition and emission processes are in competition, therefore both deposition and emission can be measured (Table 1, 3rd column).

Table 1. Flux of nitrogen oxides at Nyírjes monitoring station in ng m^{-2} s^{-1}

	NO flux		NO_2 flux	
Period	$R_i>0$	$R_i<0$	$R_i>0$	$R_i<0$
1st quarter	-2.1 (2 982)	-13.0 (771)	2.0 (3 239)	-21.7 (784)
2nd quarter	-1.4 (1 944)	-13.0 (845)	1.1 (2 763)	22.8 (1 336)
3rd quarter	-4.6 (1 172)	7.2 (734)	3.3 (2 204)	48.4 (1 162)
4th quarter	-6.0 (1 056)	12.4 (767)	14.4 (1 886)	52.3 (1 030)

$R_i>0$ and $R_i<0$ indicates stable and unstable cases, respectively. In brackets the number of cases are indicated, negative and positive signs denote the emission and deposition cases, respectively.

In the case of nitrogen dioxide mostly deposition can be observed. This is obvious since the forest soil is not the source of nitrogen dioxide. In some cases, however, on the surface of leaves chemical reactions take place leading to the release of nitrogen dioxide (*Bowden,* 1986). The emission figure observed in the first quarter of the year may be attributed to this phenomenon.

The profiles of nitric oxide and nitrogen dioxide are controlled not only by emission and deposition processes, but also by the chemical reaction of nitric oxide with ozone producing nitrogen dioxide and by the photolysis of the nitrogen dioxide. This may lead to the overestimation of the nitric oxide flux and the underestimation of the nitrogen dioxide flux, however, the estimation of the total flux (sum of nitric oxide and nitrogen dioxide flux) is probably correct.

On a yearly average nitric oxide emission and nitrogen dioxide deposition can be detected at the station.

3.2 The flux of ammonia/ammonium and nitric acid/nitrate

Concentrations of ammonia gas, nitric acid vapor, as well as nitrate and ammonium particles were continuously measured on the basis of 24 hour sampling at Nyírjes station. In contrast with nitrogen oxides, direct flux measurements were not carried out from a practical point of view. In the future by improving the measuring system the direct determination of dry deposition velocities of these components will be also available.

In the case of ammonia/ammonium and nitric acid/nitrate the dry flux can be inferred by using the concentrations if the average dry deposition velocities representative of the examined surface are known. The flux thus can be estimated by the $F = -v_d C$ expression, where v_d is the dry deposition velocity, C is the measured concentration.

The dry deposition velocity of ammonia gas to the spruce forest depends on the season. Because the ammonia is mostly taken up through stomata, the rate of the flux depends on the season i.e. on the open or closed state of the stomata. According to measurements above pine forest (*Andersen et al.,* 1993) the dry deposition velocity of ammonia ranges between -0.125 and 0.201 m s^{-1}, with an average of 0.026 m s^{-1}.

In the vegetation period when nitrogen uptake is at the maximum the average ammonia flux is 87 μgN m^{-2} h^{-1}, which refers to a 0.045 m s^{-1} deposition velocity at average concentration. The result of another investigation shows that the ammonia dry deposition velocity is in the range of 0.02–0.03 m s^{-1} at a yearly average in a spruce forest (*Duyzer et al.,* 1994).

The dry deposition velocity figures of the nitric acid determined for pine forests are extremely high, 0.07 m s^{-1} (*Janson* and *Granat,* 1997). There is no expressed difference between the daytime and night-time figures, which suggests that cuticular adsorption is the dominant deposition process in comparison with stomatal uptake. Probably there is no large difference between summer and winter figures in pine forests.

The aerosol particles are generally captured by the surface of leaves (cuticle) while the stomatal uptake has lower importance. Therefore the seasonal variation of the deposition velocity is not so expressed. Previously, the dry deposition velocity of particles was determined by theoretical calculations and by wind tunnel experiments, resulting in substantially lower deposition figures than were recently determined by experiments. In our previous calculations (*Horváth et al.,* 1993a) the lower figures were used in the calculation of the acid (sulphur and nitrogen) deposition at Nyírjes station. In recent years the contradiction has become obvious between the results of the two methods (*Ruijgrok et al.,* 1993; *Borrell et al.,* 1997). Different research groups agree that the figures determined experimentally are correct and they suggest >0.01 m s^{-1} dry deposition velocity for forests in the case of particles.

The dry fluxes of ammonia, nitric acid and nitrate, ammonium particles were determined by the recently determined deposition figures using the average concentrations in *Table 2*. The calculated dry fluxes can be seen in *Table 3*.

Table 2. The concentration of nitrogen compounds at Nyírjes monitoring station in $\mu g\ m^{-3}$

Period	Concentration					
	Nitric oxide	Nitrogen dioxide	Ammonia	Nitric acid	Ammonium	Nitrate
1st quarter	0.69	8.06	0.52*	1.51	0.42	0.54
2nd quarter	0.57	3.28	1.68*	0.50	0.56	0.50
3rd quarter	0.47	3.45	0.92*	1.50	0.70	0.59
4th quarter	0.62	3.98	0.41	1.87	0.86	1.39
1996	0.59	4.69	0.88	1.35	0.64	0.76

*In the cases marked by an asterisk there were no ammonia measurements for technical reasons. Data replaced by the results of another forestry station in Hungary (K-puszta).

3.3 The flux of nitrous oxide

On the basis of the methods described in paragraph 2, the nitrous oxide emission of the forest soil was measured in three series at the Nyírjes station in the Spring of 1997. In the majority of the installed cells emission can be detected with substantially high standard deviation (see *Fig. 2*). The average of the soil flux is $2.0 \pm 0.8\ \mu gN\ m^{-2}\ h^{-1}$. The atmospheric gradient of nitrous oxide at the last of the three sampling occasions was negative from the soil surface upwards prior to as well as following the gas sampling from the chambers. The values were -0.014 ppb N_2O m^{-1} (n.s.) and -0.068 ppb N_2O m^{-1} ($p<0.05$) when a linear model is used. This supports the conclusion that the soil emits nitrous oxide to the atmosphere as revealed by the chamber data.

Table 3. Summary of the dry deposition of nitrogen compounds at Nyírjes monitoring station

Period (quarter)	Dry deposition (emission) in mgN m^{-2}							
	Nitrous oxide	Nitric oxide	Nitrogen-dioxide	Ammonia	Nitric acid	Ammonium	Nitrate	Total dry depos.
1st	(-19.3)	-14.7	-6.2	87.6	185.0	25.7	9.6	268
2nd	(-19.3)	-18.0	19.6	489.0	61.1	34.2	8.9	576
3rd	(-19.3)	-0.4	45.2	268.0	183.0	42.8	10.5	530
4th	(-19.3)	6.2	88.7	69.0	232.0	52.6	24.7	454
1996	-77.2 ?	-26.9	147.3	913.6	661.1	155.3	53.7	1 828

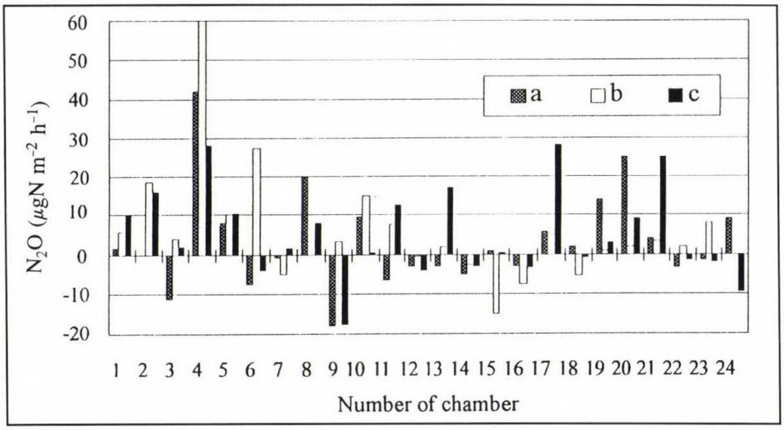

Fig. 2. Results of the three series (a, b, c) of measurements of dinitrogen oxide emission from the soil at Nyírjes station.

Because of the limited number of measurements the nitrous oxide emission for the whole year can not be estimated. The results concerning the dry spring period probably do not represent the yearly average. Therefore, the nitrous oxide emission has to be determined from figures from the literature. For spruce forest *Ambus* and *Christensen* (1995) found a 77 mgN m^{-2} yr^{-1} emission rate for nitrous oxide flux with a large spatial and temporal variation. This figure is 4.4 times higher (8.8 μgN m^{-2} h^{-1}) compared to the emission flux determined at Nyírjes station in Spring. In the calculation of the flux, as can be seen in Table 3, the data of the mentioned authors was used making the remark here that the estimation is somewhat uncertain because there could be differences between soil composition, humidity, etc. at the two places resulting in different emission rates.

3.4 Comparison of the determined dry deposition with the throughfall, stemflow deposition estimates

In dry periods the trace gases and particles are captured by the canopy partly on the surface of the leaves. The absorbed materials that are not taken up are leached by the following precipitation, which can be measured in the throughfall and in a small part in the stemflow samples. The nitrate and ammonium content generally increases, which can be measured in the wet only precipitation samples.

The dry deposition figures determined in paragraphs 3.1–3.3. are theoretically not comparable with the deposition estimated from the throughfall and stemflow measurements. One of the reasons is that the rate of net dry flux is the difference between deposition and emission terms. On the other hand dry deposition itself cannot be in relation with the deposition calculated by the throughfall estimation due to the following reason.

As mentioned, the flux of trace compounds can be characterised by the dry deposition velocity:

$$v_d(z) = \frac{-F_d}{C(z)}, \tag{2}$$

where $v_d(z)$ and $C(z)$ are the dry deposition velocity and concentration of the given compound at the height z, while F_d is the flux.

In the case of surfaces covered by vegetation, the dry deposition velocity can be described by the simple big leaf model as the result of the near surface resistances to the deposition. The effect of atmospheric turbulence can be characterised by the term r_a, as aerodynamic resistance. This term describes the rate of turbulent exchange processes i.e. the intensity of the turbulent transportation to the surfaces.

The turbulent processes are no longer effective from the displacement height. Below this in the so-called quasi-laminar layer, in the lack of regular turbulent motions, molecular diffusion and irregular motions transport the materials to the surface substantially slower than the turbulent motions. It is determined as r_b in the model.

The effect of the surface and the vegetation can be taken into account by the term r_c. This consists of different parts. When materials reach the level of leaves the uptake processes start immediately. Some of the materials like ozone, ammonia are mostly absorbed by stomata. This process can be described by r_{st} (stomatal) and r_{me} (mesophyll) resistances.

Other kinds of trace materials (like sulphur dioxide and nitric acid) are mostly adsorbed on the surface of the leaves (on the cuticle) remaining there until the following precipitation. This can be described as cuticular resistance,

r_{cu}. Beside these processes the trace materials can be adsorbed on the trunk (r_{tr}) and on the litter covered soil surface (r_{so}). The rate of surface adsorption processes strongly depend on the wetness of the surface.

The stomatal uptake of materials depends on, beside the meteorological circumstances, the physiological condition of the plants i.e. the open or closed state of stomata. The rate reaches its maximum during the daytime hours of the vegetation period, but at higher temperatures and low relative humidity it decreases. There is a strong relation between the photosynthetic active radiation and the open state of stomata until a given value where the relation is inverse.

As a result of the different surface resistances the dry deposition velocity can be described by the following expression:

$$v_d(z) = \frac{1}{(r_a + r_b + r_c)}, \tag{3}$$

where

$$\frac{1}{r_c} = \frac{1}{(r_{st} + r_{me})} + \frac{1}{r_{cu}} + \frac{1}{r_{tr}} + \frac{1}{r_{so}}. \tag{4}$$

According to this theory, during the direct measurement of the dry deposition flux (F_d) we have taken into consideration all of the terms of surface resistances $r_a+r_b+r_c$. However, in the dry deposition estimates calculated from the throughfall and stemflow figures the terms $r_{st}+r_{me}$ and r_{so} are not represented.

The directly measured dry deposition rates and the dry deposition calculated from throughfall measurements are equal only in the case when these three latter terms are negligible. The deposition onto the soil is generally negligible, but stomatal uptake is dominant for a group of compounds, like carbon dioxide and ozone. As for nitrogen compounds the stomatal uptake of ammonia is dominant, but the effectiveness of this process can not be excluded for other kinds of nitrogen compounds, also.

There are some other reasons for the limited applicability of the estimation of dry deposition from throughfall results, namely the contamination of insects, according to a group of experts.

In spite of this we have attempted to compare the deposition figures calculated from the two methods, because from the difference of these figures we can estimate the magnitude of the stomatal uptake. On the other hand, because the dry deposition calculated directly (D_d) is theoretically higher than the difference of throughfall and wet deposition (which is practically equal to D_d-D_{st}, where the latter term denotes the stomatal uptake) our theory is supported when the directly calculated deposition is higher.

The dry depositions calculated from throughfall and stemflow measurements are summarised in *Table 4*. The dry deposition without the stomatal uptake (and with the insect's contamination) can be seen in the last row. For the calculation of these figures the wet only deposition rate was subtracted from the sum of the throughfall and stemflow depositions. It seems from the data of the table that in the case of the nitrate ion, the substances leached from leaves cause only a 20 % increase compared to the wet deposition. For ammonium the increase is about 90 %, which is in agreement with the data in Table 3, where the deposition of ammonia and ammonium are much higher than that of nitric acid and nitrate. In the first quarter of the year the throughfall deposition gives a negative figure, which may be evidence for the limited applicability of throughfall estimations or indicates a possible nitrate and ammonium uptake from the precipitation by leaves through stomata.

Table 4. Wet deposition of nitrogen compounds and throughfall, stemflow data at Nyírjes monitoring station in the different quarters and during the whole year in mgN m^{-2}

Kind of precipitation samples	Nitrate deposition					Ammonium deposition					Total N deposition
	1st	2nd	3rd	4th	1996	1st	2nd	3rd	4th	1996	1996
Wet only	96.9	123.0	92.4	79.4	391.7	93.3	216.0	144.0	69.5	522.8	915
Bulk throughfall	43.8	173.0	98.7	86.3	401.8	80.9	380.0	321.0	153.0	934.9	1 337
Stemflow	0	41.0	19.3	5.5	65.8	0	32.6	27.6	3.6	63.8	130
D_d-D_{st}-D_w	-53.1	91.0	25.6	12.4	75.9	-12.4	196.6	204.6	87.1	475.9	552

(D_d-D_{st}-D_w) is the dry deposition without the stomatal uptake (difference of the sum of throughfall + stemflow and wet only results).

The directly measured dry deposition figures (Table 3), in accordance with the minimum of the throughfall estimation, is at a minimum in the first quarter. In *Table 5* the directly measured dry deposition can be compared with the estimated deposition from the throughfall measurements. It follows from the table that on a yearly basis only a small part of the gross dry deposition (the emission part is not involved), i.e. 28.6 % can be detected in the throughfall samples. This suggests that the dry deposition of nitrogen compounds mostly takes place through the stomata. The cuticular and trunk uptake (adsorption) amounts to only a smaller part (29 %) of the total deposition. In the case when biological (insect) contamination is not negligible this rate is lower, i.e. stomatal uptake is more effective.

Table 5. The nitrogen balance between the atmosphere and a spruce forest in 1996 at Nyírjes monitoring station in mgN m^{-2}

	Deposition		
Period	Dry	Wet	Total
1st quarter	268 (-66)	190	458
2nd quarter	576 (288)	339	915
3rd quarter	530 (231)	236	766
4th quarter	454 (100)	149	603
1996	1 828 (552)	914	2 742

In brackets are the dry deposition figures calculated from the difference of throughfall + stemflow and wet-only samples.

As a first approximation we may conclude that at least 71 % of the dry deposited nitrogen compounds, 1 380 mgN m^{-2} yr^{-1} are taken up by stomata and can not be detected in throughfall samples.

In the case when nitrate and ammonium uptake from the precipitation by the stomata is also effective the stomatal uptake can be calculated from the difference of the sum of dry and wet deposition (2 847 mgN m^{-2} yr^{-1}) and the throughfall+stemflow deposition (1 467 mgN m^{-2} yr^{-1}) leading to the same figure, 1 380 mgN m^{-2} yr^{-1}.

3.5. Estimation of the nitrogen balance

For the estimation of the nitrogen balance, the effects of the different deposition forms (dry+wet) need to be summarised. The dry+wet deposition for the year of 1996 and in the different quarters of the year together with the total deposition can be seen in Table 5. The dry deposition was calculated from the results of Table 3, while the wet deposition was estimated from the results of the wet only precipitation samples (Table 4). The table shows the net deposition figures also taking into account the emission.

From the results it can be concluded that in 1996, at the Nyírjes spruce forest, the nitrogen balance between the atmosphere and the forest ecosystem is 2.7 gN m^{-2} yr^{-1}, i.e. the different nitrogen compounds carry this amount of nitrogen to the forest from the atmosphere. Two thirds of the deposition is due to the dry deposition, which is higher than the previously estimated figure when lower deposition velocity figures (representative for other surfaces than forests) were applied (*Horváth et al.,* 1993a).

The reason for the difference can be explained by the fact that surface roughness for the forest is higher compared with other surfaces resulting in higher turbulent exchange as a consequence of the lower aerodynamical resistance (r_a). The canopy resistance r_c is also lower for forests because of the relatively dense surface characterised by the leaf area index.

Furthermore, it can be concluded that the emission processes from the soil are not in competition with the deposition, the nitrogen oxides emitted from the forest soil transport only a few percent of the deposited nitrogen into the atmosphere.

The nitrogen balance determined here has some uncertainty. The calculation of nitrous oxide emission was estimated by literature figures, which will probably will be modified with the results of measurement being carried out at present. The direct measurements of the dry deposition velocities of ammonia, nitric acid and ammonium, nitrate particles will also be required at Nyírjes station to avoid the error in estimation caused using literature data concerning forests with different climatic circumstances.

Hopefully, these investigations will be fulfilled in the future, but it seems from these results that the nitrogen balance will not differ substantially from the figures determined in this work.

The 2.7 gN m^{-2} yr^{-1} deposition figure refers to a 27 kgN ha^{-1} yr^{-1} rate, which is not negligible from the point of view of the forest ecosystem. It is probable that one half of the deposited nitrogen compounds are taken up by stomata partly as nutrients and partly causing damaging effects. The other half of the nitrogen compounds leach into the forest soil where they partly accumulate and partly run off with the soil water. To determine this division complex air chemistry, forestry and hydrological investigations are needed.

References

Ambus, P. and *Christensen, S.*, 1995: Spatial and seasonal nitrous oxide and methane fluxes in Danish forest-, grassland-, and agroecosystems. *J. Environmental Quality 24*, 993-1001.

Andersen, H.V., *Hovmand, M.F.*, *Hummelshoj, P.* and *Jensen, N.O.*, 1993: Measurements of ammonia flux to a spruce stand in Denmark. *Atmospheric Environment 27A*, 189-202.

Borrell, P., *Builtjes, J.H.*, *Grennfelt, P.* and *Hov, O.* (eds.) 1997: *Transport and Chemical Transformation of Pollutants in the Troposphere 10.* Photo-oxidants, acidification and tools: policy applications of EUROTRAC results. Springer. pp. 116.

Bowden, B.W., 1986: Gaseous nitrogen emissions from undisturbed terrestrial ecosystems: an assessment of their impacts on local and global budgets. *Biogeochem. 2*, 249-279.

Christensen, S., *Ambus, P.*, *Arah, R.M.*, *Clayton, H.*, *Galle, B.*, *Griffith, D.W.T*, *Hargreaves, K.J.*, *Klemedtsson, L.*, *Lind, A.-M.*, *Maag, M.*, *Scott, A.*, *Skiba, U.*, *Smith, K.A.*, *Welling, M.* and *Wienhold, F.G.*, 1996: Nitrous oxide emission from an agricultural field: comparison between measurements by flux chamber and micrometeorological techniques. *Atmospheric Environment 30*, 4183-4190.

Duyzer, J.H., 1991: The influence of chemical reactions on surface exchange of NO, NO_2 and O_3: results of experiments and model calculations. In *Precipitation Scavenging and Atmosphere-Surface Exchange 2.* (eds.: *S.E. Schwartz* and *W.G.N. Slinn*), Hemisphere Publ. Co., Washington, Philadelphia, London, 1105-1114.

Duyzer, J.H. Verhagen, H.L.M. and *Weststrate, J.H.*, 1994: The dry deposition of ammonia onto a douglas fir forest in the Netherlands. *Atmospheric Environment 28*, 1241-1253.

EMEP, 1996: *EMEP Manual for Sampling and Chemical Analysis*. EMEP/CCC-Report 1/95, NILU, Kjeller, Norway.

Farquhar, G.D., Firth, P.M., Wetselaar, R. and *Weir, B.*, 1980: On the gaseous exchange of ammonia between leaves and the environment: determination of the ammonia compensation point. *Plant Physiol. 66*, 710-714.

Führer, E. and *Horváth, L.*, 1990: Acid deposition in ecological basic terrain. *Proc. of "Acidification of Environment"* conference (Balatonfüred, 1990 November 14-16) (in Hungarian).

Führer, E. und *Horváth, L.*, 1992: Saure deposition in Ungarn (in Hungarian). *Agrokémia és Talajtan 41*, 90-94.

Führer, E., Baranka, Gy. and *Horváth, L.*, 1994: Quantity and variability of air pollution in ecological basic terrain (in Hungarian). *Erdészeti Lapok 129*, 308-310.

Hansson, P.J. and *Lindberg, E.L.*, 1991: Dry deposition of reactive nitrogen compounds: a review of leaf, canopy and non-foliar measurements. *Atmospheric Environment 25A*, 1615-1634.

Horváth, L., 1992: Measurement of dry deposition of nitrogen compounds and oxidants. In *EUROTRAC/BIATEX Annual Report*. EUROTRAC International Scientific Secretariat, Garmisch-Partenkirchen, 122-125.

Horváth, L., 1993: Gradient measurements of dry deposition flux of nitric oxide, nitrogen dioxide, ozone and sulfur dioxide above forest and low vegetation. Brief summary of the five field campaigns carried out in 1990-1993. *Air Pollution Research Report 47,* (eds.: *J. Slanina, G. Angeletti* and *S. Beilke*). CEC, Brussels, 183-187.

Horváth, L. and *Führer, E.*, 1991: Acid deposition in forest ecosystems. *Proc. Experttagung "Waldschadenforschung im östlichen Mitteleuropa und in Bayern" GSF-Forschungszentrum für Umwelt und Gesundheit (Bayern). Bericht* 24/91.

Horváth, L., Bozó, L., Haszpra, L., Kopacz, J., Molnár, Á., Nagy, Z., Führer, E., Sitkey, J. and *Weidinger, T.*, 1992: Gradient measurement of the dry flux of nitrogen dioxide and ozone over a Pine forest in Hungary. *Proc. of EUROTRAC Symposium '92* (ed.: *P.M. Borrell et al.*) 736-738. SPB Academic Publishing bv., The Hague, The Netherlands.

Horváth, L., Baranka, Gy. and *Führer, E.*, 1993a: Decreasing concentration of air pollutants and the rate of dry and wet acidic deposition at the three forestry monitoring stations in Hungary. *Időjárás 97*, 179-186.

Horváth, L., Nagy, Z., Kopacz, J., Führer, E. and *Weidinger, T.*, 1993b: Measurements of dry deposition velocities of trace gases over different surfaces (in Hungarian). *Proc. of Exhibition and Conference of Environment Protection in Veszprém* (1993. February. 2-11). Ipari és Kereskedelmi Minisztérium, 255.

Horváth, L., Weidinger, T., Nagy Z., Führer, E., Gyuricza, A., Kopacz, J. and *Lovas, K.*, 1993c: Gradient measurement of the dry flux of atmospheric trace gases over short vegetation and forest. *EUROTRAC/BIATEX Annual Report*. EUROTRAC International Scientific Secretariat, Garmisch-Partenkirchen, 116-121.

Horváth, L., Baranka, Gy. and *Führer, E. Gy.*, 1994a: Decreasing concentration of air pollutants and the rate of dry and wet acidic deposition at three forestry monitoring stations in Hungary. *Proc. of the Acid Rain Research Conference*, 10-12 October, 1994, 's-Hertogenbosch, The Netherlands, 477-482.

Horváth, L., Nagy, Z., Führer, E. and *Weidinger, T.*, 1994b: Field experiments for estimation of turbulent fluxes over different types of surfaces in Hungary. *Annales Geophysicae.* Supplement II to *Vol. 12*, C 335.

Horváth, L., Führer, E., Gyuricza, A., Lovas, K., Nagy, Z. and *Weidinger, T.*, 1994c: Gradient measurement of the dry flux of atmospheric trace gases over short vegetation and forest. *EUROTRAC/BIATEX Annual Report*. EUROTRAC International Scientific Secretariat, Garmisch-Partenkirchen, 94-96.

Horváth, L., Führer, E., Gyuricza, A., Lovas, K., Nagy, Z. and *Weidinger, T.*, 1994d: Gradient flux measurements of gases above short vegetation and forest. *The Proc. of EUROTRAC Symposium*

'94 (ed.: *P. Borrell*), SPB Academic Publishing bv. The Hague, The Netherlands, 477-478.

Horváth, L., Weidinger, T., Lovas, K., Nagy, Z., Führer, E., Labancz., K. and *Mészáros, R.*, 1995a: Deposition of ozone and nitrogen oxide to European forest. *Final Report for PECO Contract No. 94/2198/MW.7.*

Horváth, L., Nagy, Z., Weidinger, T., Artz, R., Luke, W.T., Valigura, R., Pinto, J. and *Womack, J.*, 1995b: Measurement of flux of trace gases (O_3, NO_x, SO_2, CO_2, HNO_3), particulate sulfate and nitrate and water vapor over short vegetation by gradient and eddy-correlation techniques in Hungary. *Annales Geophysicae,* Supplement II to *Vol. 13*, C 490.

Horváth, L., Weidinger, T., Nagy, Z. and *Führer, E.*, 1997: Measurement of dry deposition velocity of ozone, sulfur dioxide and nitrogen oxides above pine forest and low vegetation in different seasons by the gradient method. *Proc. of EUROTRAC Symposium '96* (eds.: *P.M. Borrell, T. Cvitas, K. Kelly* and *W. Seiler*). Computational Mechanics Publications, Southampton, 315-318.

Horváth, L., Nagy, Z. and *Weidinger, T.*, 1998: Determination of the dry flux of ozone and sulfur dioxide during the TRACT campaign. *Atmospheric Environment 32*, 1317-1322.

Janson, R. and *Granat, L.*, 1997: Dry deposition of HNO_3 to the coniferous forest. *Proceedings of EUROTRAC Symposium '96* (eds.: *P.M. Borrell, T. Cvitas, K. Kelly* and *W. Seiler*). Computational Mechanics Publications, Southampton, 351-355.

Ruijgrok, W., Nicholson, K.W. and *Davidson, C.I.*, 1993: Dry deposition of particles. In *Models and Methods for the Quantification of Atmospheric Input to Ecosystems.* Nordiske Seminar og Arbejdsrapporter 1993: 573. Nordic Council of Ministers, Copenhagen, 145-161.

Weidinger, T. and *Horváth, L.*, 1994: Analysis of dry deposition of trace gases in the frame of international projets on the modelling of near surface layer (in Hungarian). *Egyetemi Meteorológiai Füzetek 7*, 33-36.

Wyers, G.P., Otjes, R.P. and *Erisman, J.W.*, 1993: Dry deposition of ammonia onto a coniferous forest. *Air Pollution Research Report 47* (eds.: *J. Slanina, G. Angeletti* and *S. Beilke*). CEC, Brussels, 139-145.

Acknowledgements—Investigations were funded by the *PHARE TD&QM* (No. H 9305-02/1033) and K+F (No. 96-97-45-1047) projects through the contracts between the *National Committee for Technological Development* and the *Forest Research Institute,* Hungary, *Hungarian Higher Education Support Program* (FKFP 0168/1997), *OTKA* No. 026642 and *US-Hungarian Joint Research Fund,* No. 503.

IDŐJÁRÁS
Quarterly Journal of the Hungarian Meteorological Service
Vol. 103, No. 1, January–March 1999, pp. 19–36

The Penman-Monteith concept based land-surface model PMSURF

Ferenc Ács[1] and **Michael Hantel**[2]

[1]*Department of Meteorology, Eötvös Loránd University,*
H-1117 Budapest, Pázmány Péter sétány 1/a, Hungary,
e-mail: acs@nimbus.elte.hu

[2]*University of Vienna, Hohe Warte 38, A-1190 Vienna, Austria*

(Manuscript received 23 March 1998; in final form 24 July 1998)

Abstract—The land-surface model PMSURF, designed jointly at the Universities of Vienna and Budapest, is reviewed. PMSURF consists of one canopy layer and three soil layers. Prognosed state quantities are: stored water in the vegetation layer and soil moisture content in the soil layers. The forecast equations for these variables rest upon the budget laws for water substance. There is no temperature prediction, therefore net radiation or surface temperature is needed as input. This fact implies that in winter application snow and soil freezing/melting processes cannot be represented. Fluxes in the water equations comprise rain and rain interception, canopy drainage and infiltration, surface runoff, soil water diffusion, root water uptake, evapotranspiration, conductance of water through roots and stems and subsurface runoff. Energy and water fluxes are parameterized with the resistance concept.

PMSURF is tested on off-line mode for the Cabauw data set. The observed annual mean values and the seasonal changes of turbulent and water fluxes are satisfactorily reproduced. For example, the model yields latent and sensible heat fluxes of –38.0 and –4.1 W/m^2, evapotranspiration and runoff of –482 and 291 mm/year.

The sensitivity of model performance to the choice of turbulent heat flux parameterization concept is also studied by comparing PMSURF to the land-surface model PROGSURF (*Ács* and *Hantel*, 1998b). Sensitivity tests enable us to establish and to quantify the link between the model performance and the responsible mechanisms of turbulent heat flux parameterization concepts. The main results are as follows: PMSURF-calculated turbulent heat and water fluxes are somewhat closer to the observations than those calculated by PROGSURF. Further the course of evapotranspiration/soil moisture curve does not depend upon the turbulent heat flux parameterization concept.

The results are useful in optimizing evapotranspiration parameterization in land surface models. PMSURF presently serves to simulate observed surface fluxes for an atmospheric diagnostic model.

Key-words: parameterization of land-surface processes, turbulent heat parameterization concept, intercomparison of models.

1. Introduction

The *Project for Intercomparison of Land-surface Parameterization Schemes* (PILPS), which is part of the *World Climate Research Programme* (WCRP) under the auspices of the *Global Energy and Water Cycle Experiment* (GEWEX) and the *Working Group on Numerical Experimentation* (WGNE) tends to improve the understanding of land-surface models (LSM) with respect to their differences. The differences appear on three levels; according to this they can be classified into three categories:

(1) Differences in the parameterization of the parameters. The relevant parameters are radiation properties (reflexion, transmission and absorption) and all resistances and/or conductances in the soil-plant-atmosphere system. Among them the albedo and the surface resistances seem to be more important.

(2) Differences in the parameterization of the fluxes. The turbulent heat fluxes can be parameterized either by the Penman-Monteith's concept or by gradient laws. There are also many conceptual differences in the parameterization of water balance components. For instance, the transpiration can be parameterized by using three different concepts (*Mahfouf et al.*, 1996): the supply-demand approach, the canopy surface resistance concept and the moisture availability concept (ratio of actual and potential evapotranspiration). There are also basic differences in runoff parameterizations (*Wetzel et al.*, 1996).

(3) Differences in the application of prognostic equations. The type and the number of prognostic equations determine the model structure. The equations and their numerical implementation into the model can largely differ from model to model. These differences are often called as structural differences.

LSM with different structure, flux and/or parameter parameterizations were compared under diverse climatic conditions, e.g., at Caumont in Southern France (*Henderson-Sellers*, 1996), at Cabauw in the Netherlands (*Chen et al.*, 1997), or at Valdai in Russia (*Schlosser et al.*, 1997). These studies showed that there was considerable scatter between the PILPS models; further it was impossible to establish a link between the model's performance and the responsible mechanisms because most LSM differed in various aspects simultaneously (*Shao* and *Henderson-Sellers*, 1996).

The objective of this study is therefore twofold. First, we describe and validate the land-surface model PMSURF. The validation is performed using Cabauw data set. Second, we shall address the sensitivity issue studying and comparing model runs obtained by PMSURF and PROGSURF. PMSURF and PROGSURF models differ only in the parameterization of turbulent heat fluxes; so the sensitivity test reveals and quantifies the impact of turbulent heat flux parameterization concepts upon model performance.

2. *Model*

PMSURF (**P***enman*-**M***onteith's* **Sur***face* **F***luxes*) is based on previous work of *Ács* (1995, 1996) and *Ács* and *Hantel* (1998a, 1998b). It comprises one vegetation layer and three soil layers. The core of the scheme is a 3-layer diffusion type soil moisture prediction (*Sellers et al.*, 1986) in combination with *Penman-Monteith* (PM) concept for turbulent heat flux calculation. This means that there is no temperature prediction module, therefore net radiation or surface temperature is needed as input for its application. PMSURF is similar to *Dolman*'s (1993) model; its structure differs from SSiB-type models (e.g., *Ács*, 1994; *Xue et al.*, 1996) in the sense that PMSURF is designed to require only a minimum of soil vegetation parameters as input. Sub-gridscale variations of surface characteristics are not considered here.

The transport processes are quantified through the resistance formalism. *Fig. 1* shows the resistance system as implemented in PMSURF. The land is subdivided into a vegetated (*veg*) and a non-vegetated (bare soil) part (1 – *veg*). The vegetated land (terms *vegetation* and *canopy* will be used synonymously) is again subdivided into a wet vegetation (*wif*) and a dry vegetation part (1 – *wif*). Each of these subtypes is individually homogeneous. The specific surface characteristics are expressed via aerodynamic and surface resistances. In PMSURF we follow the convention to count all vertical fluxes positive if directed downwards. The consequence is that, e.g., evaporation and transpiration are practically always negative.

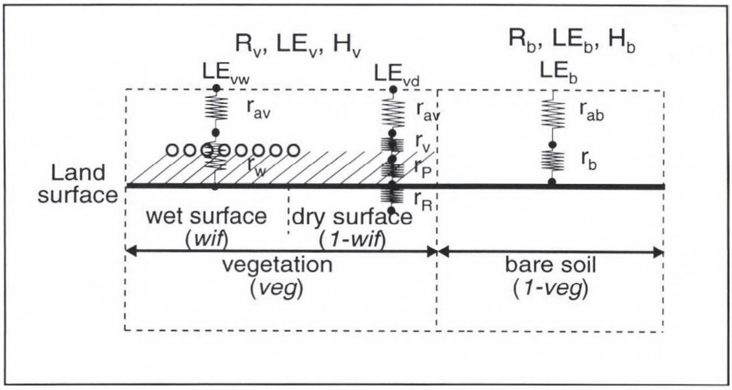

Fig. 1. The resistance system as implemented in PMSURF. Symbols: R_v, H_v, LE_v = net radiation, latent and sensible heat fluxes above vegetation; LE_{vw} and LE_{vd} = latent heat flux above wet and dry vegetation; R_b, H_b, LE_b: as before but for bare soil; r_{av} and r_{ab} = aerodynamic resistance above vegetation and bare soil; r_w, r_v, r_b = surface resistance of wet vegetation, dry vegetation, bare soil; r_P = plant resistance, r_R = soil resistance in root zone, *wif* = wet part of canopy surface; *veg* = vegetated part of land-surface.

In the following those parts of PMSURF are presented which deviate from PROGSURF. These are: the prognostic equations, the heat flux parameterization and the leaf water potential representation.

2.1 Prognostic equations

The model has four prognostic variables: intercepted water stored in vegetation layer M_v and soil moisture content in the 1st, 2nd and 3rd soil layer θ_i, for $i = 1,2,3$.

Water storage in the vegetation layer is predicted by:

$$\frac{\partial M_v}{\partial t} = P_v - D_v + E_{vw}, \tag{2.1}$$

where P_v is the interception of water by vegetation, D_v is the drainage of water from vegetation and E_{vw} is evaporation from wet parts of the vegetation ($E_{vw} < 0$) or dew formation ($E_{vw} > 0$).

Diffusion-type moisture prediction is applied in the soil layers. The prognostic equations for the three layers are:

$$\varrho_w \cdot D_1 \cdot \frac{\partial \theta_1}{\partial t} = P_{inf} - Q_1 + Q_{r0} - Q_{r1} + E_b - Q_{run1}, \tag{2.2}$$

$$\varrho_w \cdot D_2 \cdot \frac{\partial \theta_2}{\partial t} = Q_1 - Q_2 + Q_{r1} - Q_{run2}, \tag{2.3}$$

$$\varrho_w \cdot D_3 \cdot \frac{\partial \theta_3}{\partial t} = Q_2 - Q_3 - Q_{run3}, \tag{2.4}$$

where ϱ_w is water density, D_i is the depth of the *i*th soil layer, θ_i is the soil moisture content in the *i*th soil layer, P_{inf} is the water infiltrated into the soil, E_b is the evaporation from bare soil, Q_{r0} and Q_{r1} is the root water flux across surface and across bottom of the 1st soil layer, Q_1 and Q_2 is the water diffusion between adjacent layers, Q_3 is the gravitational drainage and Q_{runi} represents the lateral drainage from the *i*th layer. The gravitational and lateral drainage terms are positive representing outflow from the system.

2.2 Heat fluxes

The latent heat flux is parameterized using Penman-Monteith concept (*Monteith*, 1965):

$$L \cdot E_j = \frac{\Delta \cdot A_j + \varrho c_p \delta e / r_{aj}}{\Delta + \gamma (1 + r_j / r_{aj})}, \tag{2.5}$$

where L is the latent heat of vaporization, Δ is the slope of saturated vapor pressure curve at reference temperature T_r, A_j is the available energy of surface, ϱ is the air density, c_p is the specific heat of air at constant pressure. $\delta_e = e_S(T_r) - e_r$ is the vapor pressure deficit, $e_S(T_r)$ is the saturation vapor pressure at T_r and e_r is the vapor pressure at reference level. γ is the psychrometric constant, r_j and r_{aj} are the surface and aerodynamic resistance, respectively. The additional index j refers to the domains of vegetation ($j = v$) with relative coverage *veg*, and of bare soil with coverage $1 - veg$ ($j = b$, see Fig. 1). For bare soil $A_j = R_j - G_j$ but for vegetation $A_j = R_j$. R_j is the net radiation flux while G_j is the soil surface heat flux. The horizontal mean latent heat flux is:

$$L \cdot E \qquad \text{with} \qquad E = veg \cdot E_v + (1 - veg) \cdot E_b. \tag{2.6}$$

For vegetation we additionally distinguish between wet ($j = vw$) and dry ($j = vd$). The wet/dry distinction applies only to the surface resistance r_j. Thus $E_v = wif \cdot E_{vw} + (1 - wif) \cdot E_{vd}$. For simplicity, the vegetation resistances r_{vw}, r_{vd} will be abbreviated as r_w, r_v, respectively. *wif* is parameterized after *Sellers et al.* (1986).
The sensible heat flux is estimated as residual,

$$H_j = A_j - L \cdot E_j. \tag{2.7}$$

The weighted mean value is:

$$H = veg \cdot H_v + (1 - veg) \cdot H_b. \tag{2.8}$$

The soil surface heat flux under canopy G_v is assumed to be zero,

$$G_v = 0. \tag{2.9}$$

The bare soil heat flux is empirically estimated after *Nickerson* and *Smiley* (1975):

$$G_b = 0.15 \cdot R_b. \tag{2.10}$$

The horizontal mean soil heat flux is:

$$G = veg \cdot G_v + (1 - veg) \cdot G_b. \tag{2.11}$$

2.3 Calculation of leaf water potential

The leaf water potential Ψ_v is calculated using water flow continuity assumption in the soil-plant-atmosphere system; that is we suppose that the transpiration is equal to the root water uptake. Combining formulae for transpiration, root water uptake, canopy resistance and moisture availability, it is possible to get a quadratic equation for Ψ_v (see the Appendix):

$$a \cdot \Psi_v^2 + b \cdot \Psi_v + c = 0. \tag{2.12}$$

The coefficients *a, b* and *c* are given in the Appendix. Analyzing the order of magnitude of the quantities, it is possible to show that only one solution of the quadratic equation is physically based. The physically correct solution of Ψ_v is obtained by:

$$\Psi_v = \frac{-b + \left[b^2 - 4 \cdot a \cdot c\right]^{1/2}}{2a}. \tag{2.13}$$

2.4 Numerical implementation of the model

The sequence of calculations in a given time step is as follows: First, the radiation module calculates the net radiation of land-surface estimating separately the albedo for bare soil and vegetation. For the Cabauw data set according to PILPS 2a specifications, the vegetation and bare soil albedo is constant and therefore the corresponding albedo subroutines are not used.

Heat and water flux calculations follow the radiation module. The *vegetation module* calculates turbulent heat fluxes above vegetation, root water fluxes and water fluxes in vegetation layer. The *bare soil module* contains turbulent and soil heat flux parameterization above bare soil. In case of unstable stratification the flux/aerodynamic resistance relationship is iteratively calculated for both modules. The *ground module* calculates the soil heat flux of vegetation-ground system as weighted mean of its vegetated and non-vegetated components. Infiltration, surface runoff, soil water diffusion, lateral runoff and gravitational drainage are calculated without making such distinction.

At the end the prognostic equations (water and soil moisture storages in the vegetation and soil layers) are applied in a separate module. They are solved using an explicit time scheme. The time step used was 900 s.

3. Model validation

PMSURF has been extensively tested in off-line mode using the 1987 data from Cabauw, Netherlands. The well known dataset has been described and analyzed in detail by *Beljaars* and *Bosveld* (1997) and it is also used in PILPS project, phase 2a. In the numerical experiments PMSURF was always initialized as all PILPS participating models by saturating all liquid water stores. The variable and constant land-surface parameters are specified according to the specifications used in PILPS, 2a experiment (see Table A2, A3 and A4 in *Chen et al.*, 1997).

The model validation is performed by comparing simulated and observed surface fluxes. Among the results, the annual mean characteristics and seasonal changes of some heat and water balance components are presented and analyzed.

3.1 Annual mean characteristics and seasonal variations

The spinup time of the PMSURF model is 2 years, that is the equilibrium year is achieved in the 2nd year. The annual mean characteristics refer to the equilibrium year.

The annual mean sensible and latent heat fluxes obtained by PMSURF1 (standard PMSURF run) are presented on *Fig. 2* together with the other PILPS results (for details see Fig. 5 in *Chen et al.,* 1997). The results of PMSURF2 and PROGSURF will be discussed in Section 4. The sensible heat flux of PMSURF1 is –4.1 W/m^2, the latent heat flux is –38 W/m^2. The corresponding point on Fig. 2 is exactly located on the net radiation line; this is clear because the measured net radiation is used as input.

The annual runoff versus evapotranspiration is given on *Fig. 3*. (The figure is worth to compare to Fig. 10 in *Chen et al.*, 1997.) PMSURF1 yields –482 mm/year evapotranspiration and 291 mm/year runoff, while the corresponding observed fluxes were –525 and 250 mm/year. The annual mean soil water in the root zone obtained by PMSURF1 is 340 mm. Its estimated value (indirectly observed) is about 350 mm (*Chen et al.*, 1997).

The seasonal change of latent and sensible heat fluxes is presented on *Fig. 4*. The largest deviation between simulated and observed $L \cdot E$ values is about 15 W/m^2 and it appears in March and May. The largest deviation for H is about 10 W/m^2 and it appears in April and May.

PMSURF's performance can be understood in great extent analysing the evapotranspiration/soil moisture relationship $E(\theta)$ (for details see Section 4.3). Qualitatively, the two governing parameters of the $E(\theta)$-curve are the slope $S = \partial E(\theta)/\partial\theta$ in the transition region (i.e., region between water stressed and well watered conditions) and the saturation value $E(\theta_S)$; at Cabauw θ_S = 0.468 m^3/m^3. *Ács* and *Hantel* (1998a) showed that S is controlled by the parameterization of F_{ma}, while $E(\theta_S)$ is controlled by the parameterization of F_{ad} (see Eq. (A.4)). They also showed that the evapotranspiration for the Cabauw data set is predominantly controlled by the parameter $E(\theta_S)$; the parameter S is of minor influence at the Cabauw site.

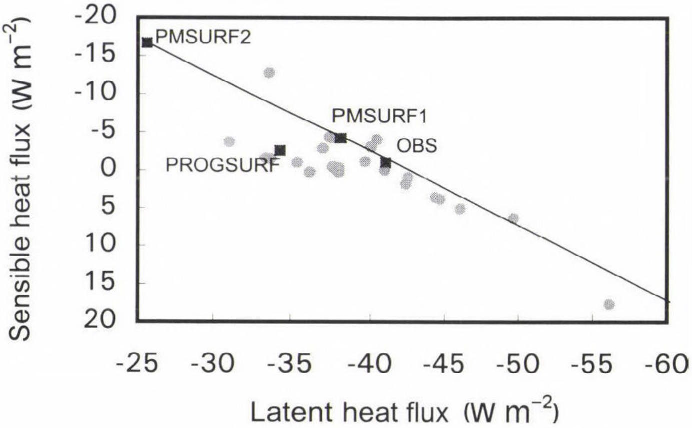

Fig. 2. Annually averaged sensible versus latent heat fluxes estimated by the different versions of PMSURF and PROGSURF (thick symbols) along with the equivalent PILPS phase 2a results (thin dots). "PMSURF1" = standard PMSURF run; "PMSURF2" = PMSURF run with latent heat flux parameterized by gradient formula "PROGSURF" = standard PROGSURF run; and "OBS" = observed value.

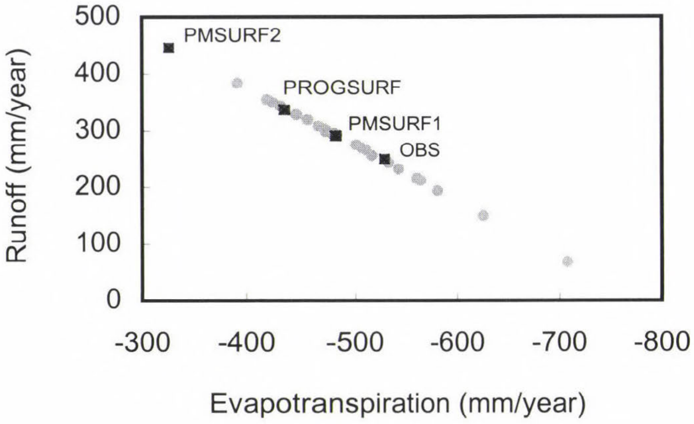

Fig. 3. Annual runoff versus evapotranspiration.

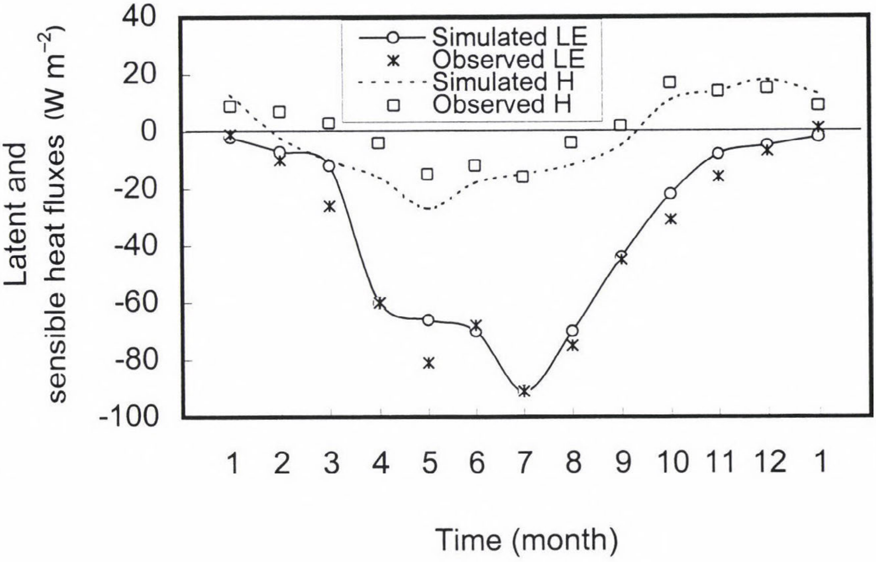

Fig. 4. Annual course of latent and sensible heat fluxes simulated by standard PMSURF.

4. Sensitivity tests

The sensitivity of model performance to the choice of turbulent heat flux parameterization concept is analysed. The sensitivity tests are carried out comparing two different modes of the PMSURF and the PROGSURF model.

In PMSURF the turbulent heat fluxes are parameterized using Penman-Monteith's concept. This implies the parameterization of soil and latent heat fluxes and the determination of sensible heat flux as the residual term from the energy balance equation. Therefore there is no surface temperature prediction, so net radiation and/or surface temperature are required as input. Soil heat flux is usually parameterized as the percentage of net radiation. The latent heat flux can be parameterized either by Penman-Monteith's combination equation (this is the common case) or by gradient formula. The former calculation mode for $L \cdot E$ represents the standard PMSURF referred to as PMSURF1. The latter calculation mode of $L \cdot E$ is not commonly used and it is referred to as PMSURF2.

In PROGSURF the turbulent heat flux parameterization is based on gradient law, that is latent and sensible heat fluxes are parameterized via gradient formulae independently from each other. This implies the soil surface temperature prediction, the parameterization of net radiation and the calculation of soil heat flux via heat conduction equation.

It is obvious that the two turbulent heat flux parameterization concepts are completely different. In PMSURF-approach the turbulent heat fluxes are diagnostically determined; whereas in PROGSURF-approach they are determined via gradient formulae which implies soil surface temperature prediction. But since there is no any other difference between the models, they can also be treated as two different modes of one model. Using this model architecture it is possible to study the link between the model's performance and the responsible mechanisms. So the PMSURF1/PMSURF2 comparison shows the deviations produced by the differences in the parameterization of latent heat flux (Penman-Monteith equation versus aerodynamic formula). The PMSURF2/PROGSURF comparison reveals the deviations in model performance produced by the application of force-restore method, while the PMSURF1/PROGSURF comparison quantifies the deviations produced by the differences in the turbulent heat flux parameterization concepts.

4.1 Annual mean characteristics

The annual mean sensible and latent heat fluxes obtained by PMSURF1, PMSURF2 and PROGSURF just introduced and the land-surface models participating in PILPS phase 2a have been presented on Fig. 2. The points of PMSURF1 and PMSURF2 lay on the observed net radiation line. This is clear since PMSURF uses observed radiation surface temperature as input. PMSURF1 is much more closer to the observation than PMSURF2. The PMSURF1/PMSURF2 deviation is very large. This deviation is caused by the differences in the parameterization of the latent heat flux. The Penman-Monteith-based latent heat flux parameterization (PMSURF1) uses indirectly the radiation surface temperature via net radiation. In spite of this, gradient formula based latent heat flux parameterization (PMSURF2) depends directly upon the radiation surface temperature. Obviously, the observed radiation surface temperatures seem to be too small, in the sense that the latent heat flux calculated by gradient formula (25.6 W/m^2) is far underestimated with respect to its observed value (about 41 W/m^2).

The PROGSURF-point deviates from the observed net radiation line. This indicates an error in the prediction of vegetation-ground temperature T_{vg}. The yearly mean of T_{vg} temperature (281.6 K) is somewhat overestimated with respect to the radiation surface temperature (280.7 K). This considerably improves the sensible and latent heat flux calculation but slightly underestimates the net radiation (the yearly mean of R is 37.9 W/m^2 instead of 42.3 W/m^2) as compared to PMSURF2. The PMSURF2/PROGSURF comparison shows the effect of force-restore method upon model performance. In spite of this, the PMSURF1/PROGSURF comparison indicates the effect of turbulent heat flux parameterization concept upon model performance. This effect seems to be not too significant though the results of PMSURF1 are in better agreement with observations than those of PROGSURF.

The annual runoff versus evapotranspiration has been presented on Fig. 3. The PMSURF1/PMSURF2 deviation caused by latent heat flux parameterization differences is the greatest. The difference in the evapotranspiration is about 160 mm. According to PMSURF2-results the observed radiation surface temperatures seem to be too small. The PMSURF2/PROGSURF deviation is great, but somewhat smaller than the PMSURF1/PMSURF2 deviation. The PROGSURF-results are much closer to the observation due to application of the force-restore method. The PMSURF1/PROGSURF deviation is the smallest. The difference in the evapotranspiration is about 50 mm. The PMSURF1-results are closer to the observation than the PROGSURF-results; in this sense the approach based on Penman-Monteith's concept seems to be more advantageous than the approach based on the gradient law.

4.2 Seasonal changes of energy and water balance components

Seasonal changes of soil heat flux obtained by PMSURF1, PMSURF2 and PROGSURF are presented on *Fig. 5*. The parameterization of soil surface heat flux in PMSURF1 and PMSURF2 is identical (see Eqs. (2.9) to (2.11)), so there is no difference between their courses. The course is unreal, it is represented by a constant close to zero. This fact is of no importance because

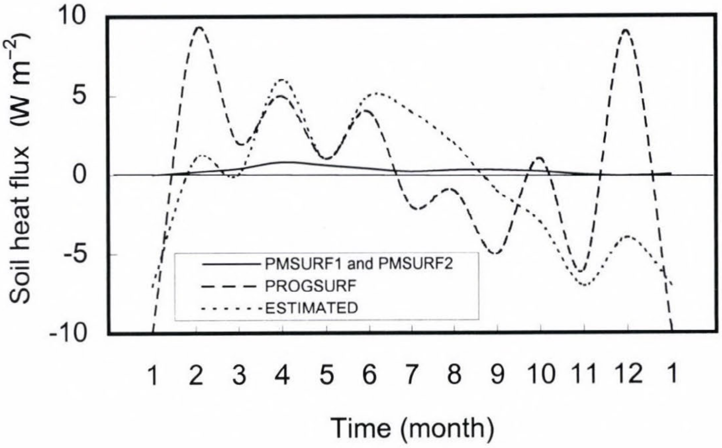

Fig. 5. Annual course of soil heat flux simulated by different modes of PMSURF and PROGSURF.

G is the least surface energy balance term. The estimated *G* on the basis of measured soil heat flux at 5 and 10 cm depth (*Beljaars* and *Bosveld*, 1997) is also small (not greater than 8 W/m^2) but it shows a yearly course. In PROGSURF the soil heat flux at 10 cm depth is parameterized by the heat conduction equation in conjuction with the force-restore method. The course obtained is much more real than PMSURF's course.

The annual course of evapotranspiration E obtained by the PMSURF modes and PROGSURF is presented on *Fig. 6*. The figure pictures strong seasonal changes of evapotranspiration. Note that at the specific site of Cabauw, *veg* is quite close to unity, i.e., evapotranspiration is practically equal to transpiration. PMSURF1, PROGSURF and PMSURF2 shows the greatest, the medium and the smallest annual amplitude, respectively. Both the PMSURF and the PROGSURF underestimate the absolute value of evapotranspiration with respect to observation. The greatest deviations of evapotranspiration are between PMSURF1 and PMSURF2. They are most pronounced in summer with maximum of almost 20 mm in July. The performance of PROGSURF is between PMSURF1 and PMSURF2, but much closer to PMSURF1.

The annual course of modeled total runoff for the PMSURF and PROGSURF runs (observations do not exist) is reproduced on *Fig. 7*. The greatest runoff is produced by PMSURF2. It changes between 40 and 50 mm/month in winter; in summer it is much smaller, but still greater than 10 mm/month. Q_{run} courses obtained by PMSURF1 and PROGSURF are very similar and close to each other. The greatest deviation between them appears in June and it amounts to about 10 mm/month. According to these runs there is no runoff in July and August, which is in accordance with the results of *Chen et al.* (1997).

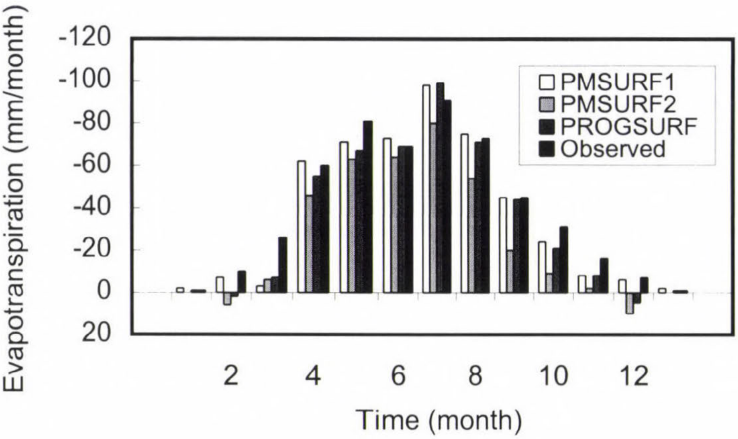

Fig. 6. Annual course of evapotranspiration simulated by different modes of PMSURF and PROGSURF.

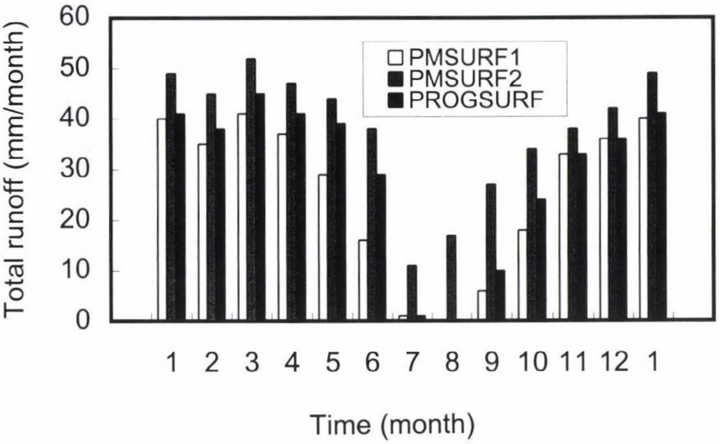

Fig. 7. Annual course of total runoff simulated by the different modes of PMSURF and PROGSURF.

4.3 Evapotranspiration/soil moisture relationship

The evapotranspiration/soil moisture relationship is a fundamental relationship in each model. It is determined by many factors; in this sense it can also be determined by the turbulent heat flux parameterization concept. Here this fact will be briefly controlled and discussed.

The $E(\theta)$ function (including the factor L) for standard PMSURF and PROGSURF is drawn on *Fig. 8*. The curves are obtained using the following data. Soil vegetation parameters are from the Cabauw data set. The vegetation-ground temperature used in PMSURF as input is the equilibrium temperature estimated by PROGSURF solving the energy balance equation of vegetation-ground system. In both runs the following atmospheric conditions were kept fixed: global radiation = 800 W/m^2, air temperature = 25.8°C, vapor pressure = 18 hPa, wind velocity = 6.0 m/s and precipitation = 0 mm. The height of reference level is 20 m.

There is practically no difference between the $E(\theta)$ curves obtained by the PMSURF1 and PROGSURF. This means that the turbulent heat flux parameterization concept does not affect the course of $E(\theta)$ curve when all other parameterizations and conditions are identical in PMSURF1 and PROGSURF. All these results and analyses suggest that at the Cabauw site the surface radiation temperatures seem to be too small, in the sense that the latent heat flux calculated by gradient formula using surface radiation temperature is far underestimated with respect to its observed values.

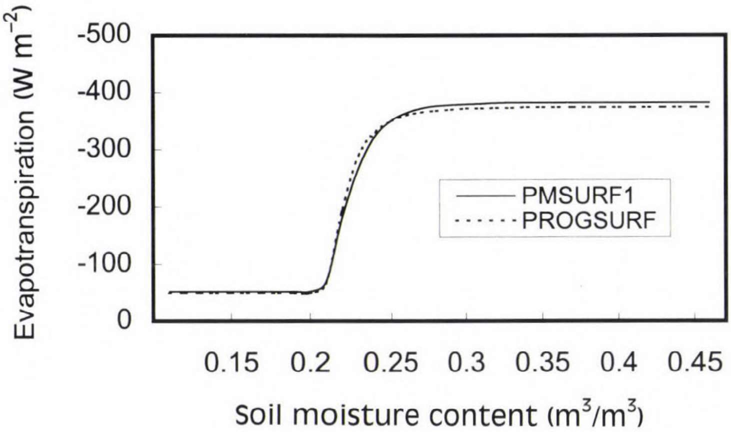

Fig. 8. Evapotranspiration versus root zone soil moisture simulated by the standard PMSURF and PROGSURF.

5. Conclusion

The land-surface model PMSURF has been briefly documented with respect to the land-surface model PROGSURF (*Ács* and *Hantel*, 1998a). PMSURF deviates from the PROGSURF as follows:

(1) net radiation or surface temperature is used as input,

(2) soil surface heat flux is calculated via net radiation,

(3) latent heat flux is parameterized via Penman-Monteith's combination equation (*Monteith*, 1965). This representation is implemented in both the aerodynamic resistance and leaf water potential calculations,

(4) sensible heat flux is estimated as the residual from the energy balance equation. These changes imply that in winter application snow and soil freezing/melting processes cannot be represented.

PMSURF has been tested in off-line mode for the Cabauw data set, using the same specifications that have been applied in the PILPS campaign (*Chen et al.*, 1997). The model reproduces satisfactorily both the observed annual mean values and the seasonal changes of turbulent and water fluxes. For example, the annual mean values of evapotranspiration and runoff are –482 and 291 mm, respectively. Nevertheless, soil surface heat flux is not satisfactorily reproduced.

The model sensitivity to the choice of turbulent heat flux parameterization concept has also been studied by comparing the standard PMSURF (referred to as PMSURF1), its modified version (referred to as PMSURF2) and the PROGSURF. The comparative analyses enable us to establish and to quantify the link between the model performance and the responsible mechanisms of turbulent heat flux parameterization concepts. The results can be summarized as follows:

(1) The PMSURF1/PMSURF2 comparison shows the model performance deviations produced by the differences in the parameterization of latent heat flux (Penman-Monteith equation versus aerodynamic formula). PMSURF2 underestimates significantly the evapotranspiration with respect to the observations and the simulation results of PMSURF1. This result suggests that the observed surface radiation temperatures seem to be too small to be successfully used in gradient formula.

(2) The PMSURF2/PROGSURF comparison reveals the deviations produced by the application of force-restore method. PMSURF2/PROGSURF comparison shows that the application of force-restore method improves considerably the turbulent heat flux calculation overestimating T_{vg} temperatures with respect to the observed temperatures. Note that the observed temperature is surface radiation temperature and the T_{vg} temperature is the equilibrium temperature of the vegetation-ground system.

(3) PMSURF1/PROGSURF comparison quantifies the deviations produced by the differences in the turbulent heat flux parameterization concepts. PMSURF1-calculated turbulent heat and water fluxes are somewhat closer to the observations than those calculated by PROGSURF. Further the course of $L \cdot E(\theta)$ curve does not depend upon turbulent heat flux parameterization concept.

This series of experiments allow us to qualify PMSURF as a PILPS-tested model (*Henderson-Sellers et al.*, 1993). It is hoped that the further intercomparison campaigns presently in preparation may be useful in optimizing evapotranspiration parameterization in land surface schemes. PMSURF is presently used to specify the boundary conditions (as substitute for observed fluxes of latent and sensible heat) for the software DIAMOD (*Hantel et al.*, 1993; *Haimberger et al.*, 1995) which is routinely used at the University of Vienna to diagnose the convective fluxes in the free atmosphere.

Acknowledgements—The authors wish to thank the *Österreichische Akademie der Wissenschaften* within the National Austrian Committee for the IGBP and the *Hungarian Ministry for Culture and Education* under grant FKFP No. 0168/1997 for the financial support of this study. We thank *Dr. L. Haimberger* and *Dr. M. Dorninger* for their helpful discussions and help in data transfer processing. The technical help provided by *Mr. Z. Barcza* and by *Mrs. B. Berger* has been very constructive.

APPENDIX

Parameterization of Ψ_v in PMSURF

Water transfer through plants is characterised by the transpiration and root water uptake. Both fluxes are parameterized using a resistance formalism in the soil-plant-atmosphere system:

$$E_{vd} = -\frac{1}{L} \cdot \frac{\Delta \cdot R_v + \varrho c_p [e_S(T_r) - e_r]/r_{av}}{\Delta + \gamma(1 + r_v/r_{av})} \tag{A.1}$$

and

$$Q_{r0} = -\varrho_w \frac{(\Psi_R - z_T) - \Psi_v}{r_R + r_P}, \tag{A.2}$$

where ϱ_w is the water density, Ψ_R is the soil moisture potential in the root zone and z_T is the vegetation source/sink height. It is well known, that the water storage in the plants is negligible with respect to water in- and outfluxes, so that it is reasonable to use a water flow continuity assumption (*Rutter*, 1975):

$$Q_{r0} = veg \cdot (1 - wif) \cdot E_{vd}. \tag{A.3}$$

At the same time both fluxes depend on leaf water potential Ψ_v: Q_{r0} explicitly, while E_{vd} implicitly via canopy resistance r_v. r_v is expressed through a multiplicative formula as follows:

$$r_v = \frac{r_{stmin} \cdot F_{ad}}{LAI \cdot GLF \cdot F_{ma}} \tag{A.4}$$

with

$$F_{ma} = \frac{\Psi_v - \Psi_{cr}}{\Psi_{SR} - \Psi_{cr}}. \tag{A.5}$$

Note that the notation used is as in *Ács* and *Hantel* (1998b). We see, that there are five equation with five unknowns: E_{vd}, Q_{r0}, r_v, F_{ma} and Ψ_v. All other terms either are constants or can be expressed independently from Ψ_v. Ψ_v is possible to get starting from Eq. (A.3). After some rearranging,

$$[(\Psi_R - z_T) - \Psi_v] \cdot [r_{av} \cdot (\Delta + \gamma) + \gamma \cdot r_v] \cdot L \cdot \varrho_w - RSP = 0, \tag{A.6}$$

where *RSP* is independent from Ψ_v, defined as

$$RSP = veg \cdot (1 - wif) \cdot \Delta \cdot R_v \cdot r_{av} \cdot (r_R + r_P) + \varrho c_p [e_S(T_r) - e_r] \cdot (r_R + r_P). \tag{A.7}$$

Replacing r_v, F_{ma} and introducing two new variables independent from Ψ_v, the Eq. (A.6) turns into the following equation:

$$[(\Psi_R - z_T) - \Psi_v] \cdot \left[AC + MF \cdot \frac{\Psi_{SR} - \Psi_{cr}}{\Psi_v - \Psi_{cr}} \right] - RSP = 0, \tag{A.8}$$

with

$$AC = r_{av} \cdot (\Delta + \gamma) \cdot L \cdot \varrho_w \tag{A.9}$$

and

$$MF = \gamma \cdot \frac{r_{stmin} \cdot F_{ad}}{LAI \cdot GLF} \cdot L \cdot \varrho_w . \tag{A.10}$$

Finally, multiplying Eq. (A.8) by $\Psi_v - \Psi_{cr}$ and rearranging it, we can get a quadratic equation for Ψ_v:

$$a \cdot \Psi_v^2 + b \cdot \Psi_v + c = 0, \tag{A.11}$$

where

$$a = 1, \tag{A.12}$$

$$b = -(\Psi_R - z_T) - \Psi_{cr} + \frac{MF \cdot (\Psi_{SR} - \Psi_{cr}) + RSP}{AC}, \tag{A.13}$$

and

$$c = \Psi_{cr} \cdot \left\{ (\Psi_R - z_T) - \frac{RSP}{AC} \right\} - \frac{MF \cdot (\Psi_R - z_T) \cdot (\Psi_{SR} - \Psi_{cr})}{AC}. \tag{A.14}$$

References

Ács, F., 1994: A coupled soil-vegetation scheme: Description, parameters, validation, and sensitivity studies. *J. Appl. Meteor. 33*, 268-284.

Ács, F., 1995: Simple surface flux model for use within diagnostic atmospheric models. *Proc. of the EGS XX General Assembly* (Supplements Issue of Annales Geophysicae, Part II., Supplement II to Volume 13, C470), Hamburg, 3-7 April.

Ács, F., 1996: Control of transpiration by soil moisture and atmosphere. *Proc. of the International Conference on Water Resources & Environmental Research: Towards the 21st Century* (Vol. I). Oct 29-31, 1996 Kyoto, Japan.

Ács, F. and *Hantel, M.*, 1998a: The land-surface flux model PROGSURF. *Global Planet. Change 19*, 19-34.

Ács, F. and *Hantel, M.*, 1998b: The land-surface hydrology parameterization in PROGSURF: Formulation and test results with Cabauw data. *Időjárás 102*, 109-127.

Beljaars, A.C.M. and *Bosveld, F.C.*, 1997: Cabauw data for the validation of land surface parameterization schemes. *J. Climate 10*, 1172-1194.

Chen, T.H., Henderson-Sellers, A., Milly, P.C.D., Pitman, A.J., Beljaars, A.C.M., Polcher, J., Abramopoulos, F., Boone, A., Chang, S., Chen, F., Dai, Y., Desborough, C.E., Dickinson, R.E., Dümenil, L., Ek, M., Garratt, J.R., Gedney, N., Gusev, Y.M., Kim, J., Koster, R., Kowalczyk, E.A., Laval, K., Lean, J., Lettenmaier, D., Liang, X., Mahfouf, J.-F., Mengelkamp, H.-T., Mitchell, K., Nasonova, O.N., Noilhan, J., Robock, A., Rosenzweig, C., Schaake, J., Schlosser, C.A., Schulz, J.-P., Shao, Y., Shmakin, A.B., Verseghy, D.L., Wetzel, P., Wood, E.F., Xue, Y., Yang, Z.-L. and *Zeng, Q.*, 1997: Cabauw experimental results from the project for intercomparison of land-surface parameterization schemes. *J. Climate 10*, 1194-1216.

Dolman, A.J., 1993: A multiple-source land surface energy balance model for use in general circulation models. *Agric. For. Meteorol. 65*, 21-45.

Haimberger, L., Hantel, M. and *Dorninger, M.*, 1995: A thermodynamic model for the atmosphere. Part III: DIAMOD with orography and improved error model. *Meteorol. Zeitschrift., N.F. 4*, 162-182.

Hantel, M., Ehrendorfer, M. and *Haimberger, L.*, 1993: A thermodynamic diagnostic model for the atmosphere. Part II: The general theory and its consequences. *Meteorol. Zeitschrift, N.F. 1*, 87-121.

Henderson-Sellers, A., Yang, Z.L. and *Dickinson, R.E.*, 1993: The project for intercomparison of land-surface parameterization schemes. *Bull. Amer. Meteorol. Soc. 74*, 1335-1349.

Henderson-Sellers, A., 1996: Soil moisture simulation: Achievments of the RICE and PILPS intercomparison workshop and future directions. *Global Planet. Change 13*, 99-115.

Mahfouf, J.-F., Ciret, C., Ducharne, A., Irannejad, P., Noilhan, J., Shao, Y., Thornton, P., Xue, Y. and *Yang, Z.-L.*, 1996: Analysis of transpiration from the RICE and PILPS Workshop. *Global Planet. Change 13*, 73-88.

Monteith, J.L., 1965: Evaporation and Environment. In *The State and Movement of Water in Living Organisms* (ed.: *G. Fogg*). Proc. 19th Symp. Soc. Exp. Biol., Cambridge, Cambridge University Press, pp. 205-236.

Nickerson, E.C. and *Smiley, E.V.*, 1975: Surface energy budget parameterizations for urban scale models. *J. Appl. Meteor. 14*, 297-300.

Rutter, A.J., 1975: The hydrological cycle in vegetation. In *Vegetation and the Atmosphere*. Vol. 1. *Principles* (ed.: *J.L. Monteith*). Academic Press, London, New York, 275 pp.

Schlosser, C.A., Robock, A., Pitman, A.J., Slater, A. and *Entin, J.*, 1997: Preliminary results from PILPS phase (2d): Analysis of modeled soil-water and snow processes for an 18-year period at a midlatitude grassland catchment. In *Proc. of the Joint Assemblies of IAMAS & IAPSO*. Jul. 1-10, 1997 Melbourne, Australia.

Sellers, P.J., Mintz, Y., Sud, Y.C. and *Dalcher, A.*, 1986: A simple biosphere model (SiB) for use within general circulation models. *J. Atmos. Sci. 43*, 505-531.

Shao, Y. and *Henderson-Sellers, A.*, 1996: Validation of soil moisture simulation in landsurface parameterization schemes with HAPEX data. *Global Planet. Change 13*, 11-46.

Wetzel, P.J., Liang, X., Irannejad, P., Boone, A., Noilhan, J., Shao, Y., Skelly, C., Xue, Y. and *Yang, Z.L.*, 1996: Modeling vadose zone liquid water fluxes: Infiltration, runoff, drainage, interflow. *Global Planet. Change 13*, 57-71.

Xue, Y., Zeng, F.J. and *Schlosser, C.A.*, 1996: SSiB and its sensitivity to soil properties- a case study using HAPEX-Mobilhy data. *Global Planet. Change 13*, 183-194.

IDŐJÁRÁS
Quarterly Journal of the Hungarian Meteorological Service
Vol. 103, No. 1, January-March 1999, pp. 37–65

Studies on the impact of global climate change on some environmental factors in Hungary

Á. Kertész[1], **D. Lóczy**[2], **J. Mika**[3], **S. Papp**[4], **T. Huszár**[1] and **A. Sántha**[5]

[1]Department of Physical Geography, Geographical Research Institute,
Hungarian Academy of Sciences, H-1061 Budapest, Andrássy út 62, Hungary;
E-mail: kertesza@helka.iif.hu; E-mail: thuszar@helka.iif.hu
[2]Department of Physical Geography, Janus Pannonius University,
H-7624 Pécs, Ifjúság útja 6, Hungary; E-mail: loczyd@ttk.jpte.hu
[3]Hungarian Meteorological Service,
H-1024 Budapest, Kitaibel Pál u. 1, Hungary; E-mail: mika@met.hu
[4]Department of Physical Geography, Eötvös Loránd University,
H-1083 Budapest, Ludovika tér 2, Hungary; E-mail: papps@ludens.elte.hu
[5]Bureau of Natural Protection, Authority for Nature Conservation, Ministry of Environment,
H-1121 Budapest, Költő u. 21, Hungary; santha.antal@ktmdom2.ktm.hu

(Manuscript received 30 September 1998; in final form 8 February 1999)

Abstract—Within the framework of the MEDALUS (Mediterranean Desertification and Land Use) Project funded by the European Union, authors investigate the impacts of global climate change on the physical environment of Hungary. The Danube-Tisza Interfluve was chosen as a test area.

Climate change in our region can be characterized by the term *aridification*. Trends of annual mean temperature and of annual precipitation give evidence of warming and drying during the last few decades. The average warming for the last 110 years is about 1 K per century and the change of precipitation is -0.91 mm per year. Because of the importance of the relationship between global and regional variations, regional scenarios were applied. Temperature and precipitation changes are in accordance with these scenarios.

The Danube-Tisza Interfluve is one of the most severely affected regions of Hungary as far as the drop of free groundwater levels and the depletion of confined groundwater reserves are concerned. 2 to 4 m drops in the annual mean groundwater level (compared to the average of the 1960s, the period, which most certainly preceeded the advent of aridification) are recorded. Soil moisture content also reduced during the first half of 1990s. The water level of ponds subsided as well. The dropping ground water level is, however, influenced by many factors so that it is not only the result of aridification.

Vegetation changes of the test area were investigated in detail. From the distribution of floral elements it is claimed that the continental group predominates but the proportion of the mediterranean group is very high (more than one third).

In four fixed cenological quadrates (represented by various subassociations of perennial *Festucetum vaginatae danubiale* of the Danube-Tisza Interfluve) classical cenological survey was supplemented with the study of plant species, which may show quantitative changes probably associated with climate change. Four plant species were selected: *Euphorbia seguierana, Artemisia campestris, Festuca vaginata* and *Stipa borysthenica*. The findings of this survey confirm aridification.

Investigations on soil dynamics revealed that in the most sensitive areas, with the gradual lowering of the water table in alkali ponds and with the complete desiccation of some of them, the direct contact between groundwater and salt-affected soils is interrupted, the solonchak soil dynamics ceases, helophile and hygrophile plant associations disappear.

The soda contents of solonchaks effected by a dry period have leached out from the whole profile. This is the most important indirect evidence for desalinization.

Impacts on soil moisture content were studied by applying the EPIC (Erosion Productivity Impact Calculator) model. The method of geographical analogy was applied, i.e. climate data of Pápa were selected as geographical analogues for the expected changes in the Pécsely basin.

Within the frame of a land capability analysis, environmental conditions were assessed for five major arable corps, taking decreasing precipitation amounts into account. The result was a significantly reduced land capability.

Key-words: climate scenarios, physical geography, desertification, land degradation, impacts on soils, soil moisture

1. Introduction

The ever increasing influence of human society on the physical environment may bring irreversible processes which are going to shape the setting for human life in the 21st century. At first, such processes probably occur in the atmosphere, where local and regional influences are most readily globalised, but — through transfers in the system of the physical environment — soon they are also to appear in less dynamic geospheres. Although the processes and consequences involved in global climate change have not yet been fully disclosed by international research, undeniable signs are described from various geographical environments. In the Mediterranean region, for instance, a desiccation tendency or locally even desertification cannot be questioned. In this region of marginal agricultural potential, land degradation has reached a critical stage.

Lying in the very heart of the Carpathian Basin, and on a low-lying flat terrain, Hungary may have to face severe ramifications. Like in other regions of Europe, the meteorological record for recent years in Hungary shows major deviations from long-term mean values. The transitional climate of the country with the three main (continental, mediterranean, and atlantic) climatic influences may easily be "diverted", rearranged into a new combination of climatic elements which resembles to the conditions of a neighbouring region (probably the Mediterranean) more closely. This involves a moderate warming and a relatively strong inclination to drought, which tendencies are running parallel with global warming processes, mostly likely connected with increasing greenhouse effect (*IPCC*, 1996).

Climate change is in interaction with geographical space and, consequently, it is within the scope of physical geography. A recent concept of geographical implication, i.e. the nature of response to the modification of climate, also supports this claim. It has been suggested that the change, starting from climate and affecting other environmental subsystems, does not simply cause a shift in geographical zones as it was conceived, for instance, when explaining the recolonisation of land liberated from ice-sheets in post-glacial times. It has been found that plant and animal species show variable adjustments, respond to different environmental thresholds and begin to "return" from their refuge areas at various dates (*Graham* and *Grimm*, 1990). Thus, instead of shifting of entire communities, diffuse dislocations are the rule.

Recalling that water availability is of major importance under the physical conditions of Hungary, the term *aridification* (*Kertész*, 1995) seems to be the most appropriate to describe ongoing processes. In authors' interpretation aridification means an increasing semiarid character manifested over a longer period in rising annual mean temperature, involving a rise in potential evaporation and in decreasing annual precipitation, leading to water deficit. Eventually, transformation of the physical environment ensues as a whole.

The expected impacts of global warming in the Mediterranean are studied comprehensively by the MEDALUS (Mediterranean Desertification and Land Use) project in international collaboration. Most of the research takes place in European countries since the project is financed by the European Union. Research is aimed at modelling predictable transformations in the physical and social environments and to found strategies for sustainable development. Investigations in Hungary constitute subproject MEDEAST (*Kertész et al.* 1997, 1998).

Main objectives of the Hungarian subproject are (see *Fig. 1*):

I. Climatological research to trace climate change in Hungary: is aridification justifiable from short- and medium-term climatic time series? What scenarios are valid for Hungary?

II. Research into the physical processes induced by aridification:

   (a) Changes in groundwater level — particularly in the most drought-stricken area.

   (b) The influence of climate change on natural vegetation.

   (c) Soil moisture dynamics and the impact of groundwater level changes on soil processes.

   (d) The control of aridification on geomorphological processes, e.g., soil erosion.

III. Land use adjustment to semiarid conditions: surveying and mapping changes and the investigation of land capability.

In our working hypothesis lowlands will show consequences different from those in mountains. Observations support the assumption that, along with the amount of atmospheric precipitation, its spatial and temporal patterns (distribution and intensity) also change to a considerable extent. In areas of high relief soil erosion conditions are modified, and more intense showers may remove larger amounts of soil. In lowlands, on the other hand, water deficit presents a major problem. In the present paper results from research on the Danube-Tisza Interfluve test area are dealt with.

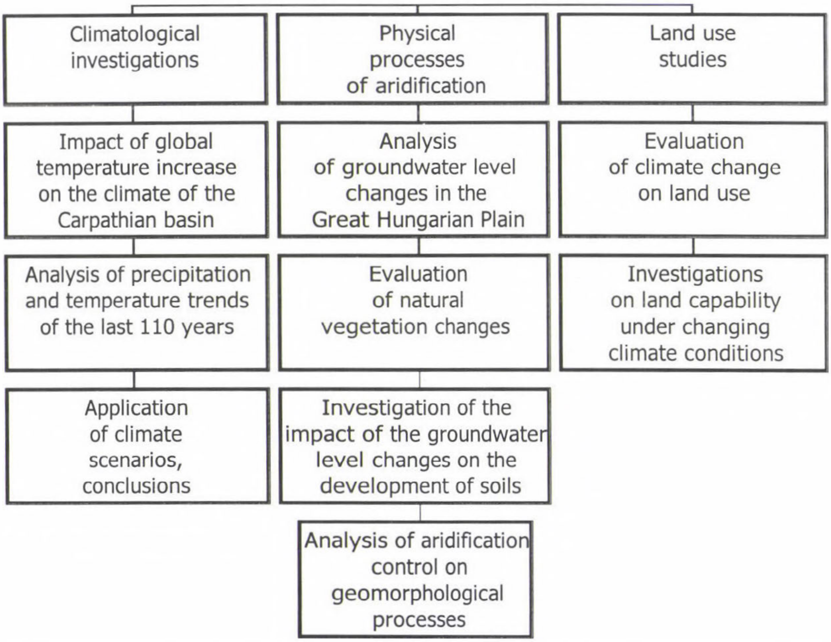

Fig. 1. Aridification research programme.

The response of each factor of the physical environment to global climate change takes place at different rates. The slowest response can probably be expected in the case of geomorphological processes, e.g., in the change of the erosion regime. The rate of vegetation change is rather quick, while soils are also modified relatively fast — although at a slower rate than vegetation. The main driving force in most environments is the reduced availability of water. In arid, semiarid and subhumid environments the concept of desertification is applied to characterize land degradation resulting from various factors, including climatic variations and human activities. Thus the changes of the physical environment described below can also be considered as components of the desertification process.

Taking the time scale of the processes into account, vegetation changes, changes in soil formation processes and in soil moisture will be discussed in detail below preceded by a short analysis of climate tendencies and of groundwater level changes as groundwater table fluctuations are the main driving force of environmental change in the Great Hungarian Plain. Another important aspect, i.e. land capability will shortly be dealt with as well.

2. Evidences for climate and ground water level change

We briefly overview how the past climate series and climate scenarios (based also on them) support this expectation.

2.1 Observed trends in the meteorological series

Data series for mathematical trend analysis are available for the past one-or-two centuries only. Systematic observations dating back for more than a century put meteorological data in a very favourable position compared with other environmental data (*Nemes* and *Szalai*, 1992). Reference stations to detect climate change of the time series and to represent changes of various climate elements in time and in space have been selected also in Hungary (*Ambrózy,* 1991).

Time series, however, must be free from inhomogeneities due either to local environmental effects or to the changes of measuring devices. Inhomogeneity means that data series characterising climate variations at the macroclimatic scale were influenced by mezo- or micro-climatic modifications around the site of observation or simply the place, instrumentation, or time of observations, etc. (e.g. *Heino,* 1994).

In Hungary the measurement frequency of temperature, air moisture, wind direction and wind velocity changed in the middle of the 1960-s which caused an error. This error could be corrected when calculating averages, but recent homogeneity analyses have indicated that the correction made for the climate data series was inappropriate, at least in the case of temperature (*Szentimrey*, 1994, 1997; *Szentimrey et al.,* 1998).

In the first study, *Szentimrey* (1994) considered temperature data of a meteorological station (Kremsmünster, Austria) as undistorted references in the mathematical breakpoint detection. Due to this homogeneity correction, the signals became identical at every station of Hungary.

Since *temperature* series have substantial inhomogeneities and the process of correction initiated at the Hungarian Meteorological Service is still in process, temperature analyses will not be dealt with here. According to the first experiences of homogenisation, an increasing trend (cca. 1 K/century) of the annual mean temperature can be observed (*Molnár,* 1995).

The warming tendency was clearly indicated by *Nemes* (1994), using yearly absolute minimum temperature values measured at any station of the country, as this parameter is being measured by different instruments (preserving the minimum measured value).

Precipitation series may have inhomogeneities because of changes in the instrumentation, too, but they mainly concern the data prior to 1901 (*Schirok-Kriston,* 1994). One of the mathematically best established calculation (*Koflanovits-Adámy* and *Szentimrey*, 1986) refers to seasonal precipitation data of 32 stations in the Carpathian basin between 1901–1984. The main results of this study are the maps of linear trends which are negative in spring and autumn, but non-significant (not even at the 90% level) for the rest of the year. Annual precipitation trends are negative everywhere, where significant.

Ambrózy et al. (1990) demonstrates how the standard 30-year averages varied between 1901 and 1988 at 162 precipitation stations in Hungary. The conclusion is that even the 30 years' averages varied substantially at a ten year time scale.

Half-year totals of winter precipitation after 1901 were approximated (*Nemes,* 1994) by a quadratic function with a maximum value in the thirties and decreasing afterwards. Ninety year trends of the summer half-year show a significant linear decrease.

17 stations between 1901–1989 were examined by *Molnár* (1995). The stations are mainly located in lowland areas, with the exception of Eger. The mean annual trend for the 17 stations was -0,9 mm/year.

The comparison of *precipitation* averages for the same 17 stations of the two periods (1900–1949 and 1950–1989; *Molnár,* 1995) demonstrates that there is a decrease in most of the months. In annual total, all stations show a decrease of precipitation in the second period (in some parts of the Great Hungarian Plain 10–15 mm, while in other parts 40–60 mm). As for the annual differences of precipitation changes, it is remarkable that there is no precipitation decrease in the summer. A strong increase is observed for June in the second period. Precipitation decline is very remarkable in the autumn months of the second period.

A somewhat different result was gained by *Schirok-Kriston* (1994) concerning precipitations exceeding the 30 mm/day threshold. The analysis of precipitation data between 1901–1990 only for the days above the threshold value does not show a significant trend of increase for Hungary. Precipitation frequency above the threshold was somewhat higher between 1931–60 than for 1901–1930, or for 1961–1990. From among the 30 years' averages prior to 1990, the highest mean temperature of the Northern Hemisphere (e.g. *Jones*, 1994) was reached in 1931–1960, which period was slightly warmer than the period of 1961–1990. This fact draws our attention to the relationship between global and regional variations. This approach is the basis of regional climate scenarios described in the next section. Principal problems of regional climate scenarios and some alternative approaches are dealt with in detail by *Mika* (1993).

2.2 Regional climate scenarios

The analysis of small (<1 K) changes of the hemispherical mean temperature was based on time series of instrumental measurements. A method of "slices" was introduced (*Mika*, 1988) to investigate the connections between regional climatic elements and two hemispherical temperature characteristics, i.e. average temperature ($<$T$>$) and air temperature contrast between continents and oceans (DT). The latter characteristic may be close to the optimum, as the first EOFs of CO_2-forced temperature change patterns (*Cubasch et al.*, 1992) show remarkable coincidence with the continent-ocean distribution map. Hemispherical mean temperature and continent-ocean contrast are derived from air temperatures above the continents by linear weighting according to the areas of the two domains. Correlation of the two hemispherical variables is negligible for all applied divisions of the investigated period, which makes it possible to avoid the problems of multi-collinearity of the physically plausible variables.

The essential point of the method is to divide the original time series into sub-periods of uniform length, and to perform a regression analysis between the time averages for the sub-periods. Namely

$$Y = b_0 + b_1 <T> + b_2 DT + e, \tag{1}$$

where Y is the mean value of the local variable; b_i is the regression parameters; $i = 0, 1, 2,$; $<T>$ is the average of the hemispherical mean temperature for the investigated period; DT is the average value of the hemispherical ocean-continents contrasts for the same period; e is the variable with normal distribution.

The aim of "slicing" is to quantify the non-significant relationships of the year-by-year resolution and to randomize the possible inhomogeneities of the series. In addition to the six (5, 9, 13, 17, 21 and 25 years long) sets of time-slices, a set of 13 years long "quasi-equilibrium" slices were defined with negligible air-temperature trends above the continents for the period 1881–1980.

With the method of slices it could be established that the 0.5 K hemispherical warming was accompanied with a 0.5–0.8 K temperature increase, a 7–14 percent decrease of precipitation and with a 20 percent increase in sunshine duration in the summer half-year during the last 100 years. There is a relationship between temperature and the continent-ocean temperature contrast in the winter half-year whereas precipitation and sunshine duration changes could be shown ambiguously. These changes correspond to 5–10 days increase in the vegetation period, about 60% increase in the frequency of dry months (with a soil humidity of less than 30% of available potential) and an 8–10% increase in global radiation at the surface.

The method of slices was also applied for temperature fields of the temperate Northern Hemisphere (*Mika*, 1992). In these computations, temperature in Greenland exhibits large relative sensitivity to hemispherical mean temperature variations. This fact was employed to prove the more general character of the relationships for different local variables in Hungary, using the measurements of the independent period 1981–1995, historical data from the period 1490–1779 and paleoclimatic reconstruction from 6000 to 1000 years BP.

Results of larger (> 1 K) global changes are described by *Mika* (1991). The verification of the above scenarios for recent independent periods will only be given here. The "slicing" method was applied for the 100 year period preceding 1980. The following 15 year period can be used as an independent period to validate the scenarios. For this purpose, 28 stations for temperature differences, with no inhomogeneities caused by the changes in the observation times and more than 300 stations for the precipitation differences were employed to determine the local anomalies in the later periods as compared to the 1951–1980 "baseline" climate.

Temperature and precipitation anomalies (*Figs. 2, 3*) in two independent periods after 1981 (1981–90 and 1991–95) broadly correspond to our expectations. This means that the anomalies have the same sign and order of magnitude as the product of the regression coefficients and hemispherical temperature anomalies of the recent periods (i.e. +0.21 K and ~0.35 K for $<T>$; 0.16 K and >0 for ΔT).

Winter half-year temperatures correspond to the scenario over most of the country (Fig. 2). The only exception is in East Hungary with a negative difference between the recent 10 and the preceding 30 years. In the summer half-year (Fig. 2) there are positive anomalies in the whole country for the last 10 years.

Precipitation changes are also in accordance with the scenarios (Fig. 3). Winter half-year precipitations decreased with the exception of a few small areas in western Hungary. In the summer half-year the strong decrease of precipitation is repeated, except in a few spots (Fig. 3). The largest drops are almost 100 mm (i.e., 25–30 per cent of the mean value of the previous 30 years).

It can be concluded that there are local anomalies for the 1981–1990 period corresponding to the scenarios based on statistical relationships from the previous century.

Since early 20th century, a number of evidence have been collected to support warming: winter half-year mean temperatures are rising, summers are ever hotter and the length of the growing season is expanding. Aridification is first of all manifested in the lower number of days with precipitation; rainfall intensity and, as a consequence, runoff probably increases; infiltration and groundwater table are reduced; soil moisture contents (particularly the moisture stored in the soil at the beginning of the growing season) drop and liability to drought grows. For three of the stations the autumn precipitation maximum seems to disappear entirely — in the very regions with marked mediterranean climatic influence.

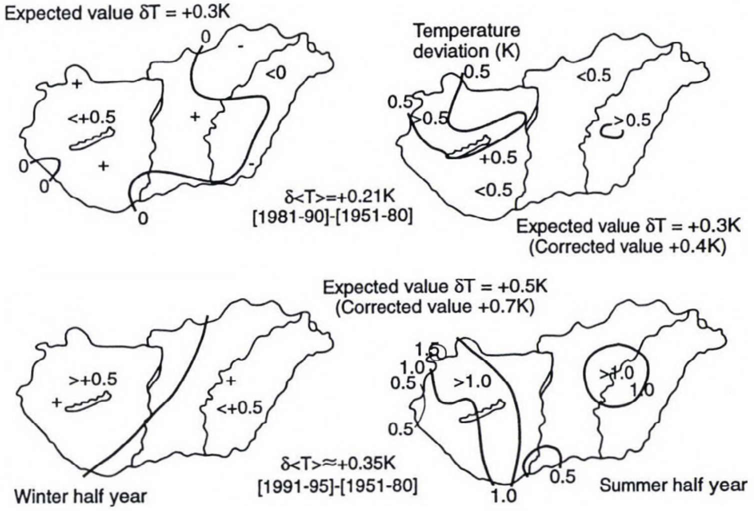

Fig. 2. Temperature deviations of the recent ten year (1981–1990) and five year (1991–1995) periods from the climate normal values of 1951–1980 in the winter half-year (October–March) and in the summer half-year (April–September).

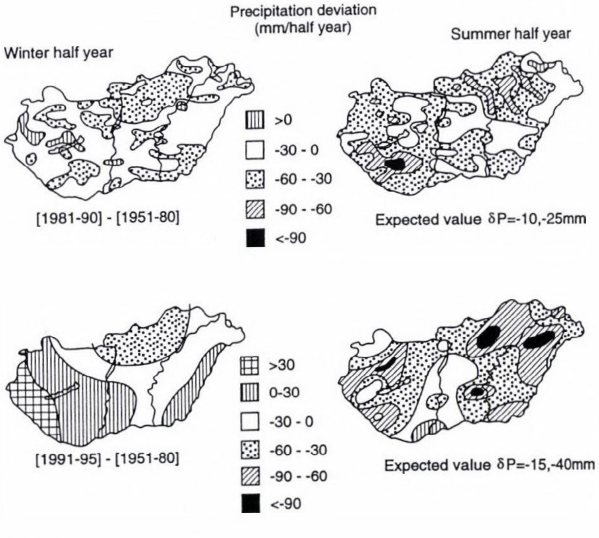

Fig. 3. Precipitation deviations of the recent ten year (1981–1990) and five year (1991–1995) periods from the climate normal values of 1951–1980 in the winter half-year (October–March) and in the summer half-year (April–September).

2.3 Groundwater level changes

The Danube-Tisza Interfluve (with a predominant sand soils) is one of the most seriously affected areas by droughts. Here the subsidence of groundwater table has been accompanying climatic tendencies since the 1970s embedded in the above outlined chain of processes. The most serious aspects of aridification here is the extremely reduced infiltration into the soils and the recharge of groundwater (*Szász*, 1987; *Huszár et al.*, 1996). In 1985–86 groundwater reached its lowermost recorded level (*Pálfai*, 1991, 1995). A lasting period of drought began in 1983 and since then the frequency of drought years is unprecedentedly high. In the past 15 years cumulative water deficit has amounted to more than 1000 mm. In the humid 1960s depths to groundwater table were recorded at 2 m below the surface with a seasonal range of 0.5 m, and most of the crops could be supplied with sufficient amounts of water (*Szalay et al.*, 1995). The recent shrinkage of free and confined (*Berényi* and *Erdélyi*, 1990) groundwater reserves, however, is endangering profitable cultivation in the region (*Varga-Haszonits*, 1988; *Major et al.* 1991).

As it was demonstrated, the first and most direct impact of aridification is found in the subsidence of the groundwater table. With dropping groundwater, *soil moisture* contents have been also reduced considerably during the 1990s (*Pálfai*, 1996). For instance, in the spring of 1990 in some sections of the Danube-Tisza Interfluve, the uppermost 1 m of soil had only 60 to 70 per cent soil-moisture reserves as opposed to the long-term average of 100 per cent of field capacity. In 1992 in the same area the 0 to 0.5 m topsoil contained less than 15 per cent moisture, which is below the wilting-point of most agricultural crops. Before the wet winter of 1995, the winter precipitation deficit had maintained a decreasing trend of relative moisture content in topsoil for 12–15 years.

The drought also involves water level drops of ponds. Confined groundwater reserves suffer from increased water intake for irrigation. Their level has sunk recently more than 20 m locally (*Berényi* and *Erdélyi*, 1990). The area affected is virtually the same as in the case of free groundwater. After the depletion of the Quaternary aquifer of the alluvial fan, the Pliocene aquifers follow and their pressure conditions are also on the decline.

It is debated whether global climate change is a major and sole driving force of dropping groundwater table on the Danube-Tisza Interfluve. Several authors sound opinions that human activities play an equally great part in the process (*Major* and *Neppel*, 1988; *Liebe*, 1993; *Pálfai*, 1996). It is well known that afforestation and deforestation influence local water budget. The percentage of the forested area on the Great Hungarian Plain has undergone an important change, i.e. from 25–30% around 1000 a.D. to 6% at the beginning of the 19th century (*Bartha*, 1993) and rising again to cca. 10% today. About two-thirds of the Great Hungarian Plain were covered constantly by water (swamp, or water surface) preceding drainage works of the 19th century. Drainage reduced the extension of seasonally inundated areas and swamps, and the water coming from the mountains was transported directly and exclusively by the rivers (*Nováky,* 1993). These changes induced by human activity during the last 150 years also contributed to increasing aridity of the Great Hungarian Plain. Human influence has been continuously very important since the drainage measures and thus it is difficult and complicated to separate the pure influence of global climate change from human impact. Anthropogenic influence does not only mean water regulation and land use change but it is also manifested in direct water intake, irrigation, amelioration measures and sewage production. Although water intake from confined groundwater for drinking and irrigation is growing steadily, the final cause of increased demand can be detected in the deficit of atmospheric precipitation and increased evaporation (driven by a 3–5 per cent growth in the mean temperature of the growing season). To the joint influence of these factors, groundwater levels dropped over a vast area (almost 9000 km^2). Although fluctuations of the groundwater level on the Danube-Tisza Interfluve have ever been observed during the last 100 years, groundwater level subsidence since the 1970s is extremely strong and it can be taken for a long-term trend connected with the above-mentioned human interventions and with global climate change. In the most susceptible areas, first of all in sand regions of the Danube-Tisza Interfluve 2–4 m drops of the mean annual groundwater level (compared to the average of the 1960s, the period preceding the beginning of aridification) are common (*see Fig. 4*). The subsidence of the groundwater level may locally reach 5–6 m.

A further depletion of groundwater resources on the Danube-Tisza Interfluve is expected in the wake of climate change. The shortage of soil moisture and groundwater is the main driving force of aridification in the region leading to the changes of the physical environment described below.

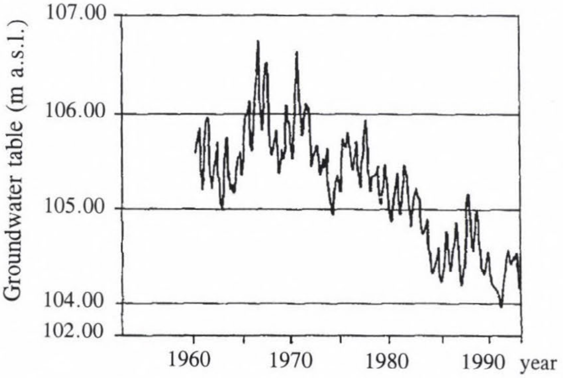

Fig. 4. Lowering of groundwater table (1952–1992) in the well of Ágasegyháza (Great Hungarian Plain)

3. *Changes in the physical environment*

3.1 Vegetation changes

Unfavourable hydrological changes induced by human intervention on the Danube-Tisza sand ridge were investigated in earlier research projects of the 1970s and 80s. Naturally, no mention of climate change was made at that time. With regard to the rather recent interest in this topic, research in Hungary including field botanical surveys, have not yet produced significant results. Very often the major task researchers are dealing with is the selection of appropriate methods of investigation and checking their applicability. Even in case of elaborating and employing the suitable methods — regarding the characteristics of the subject studied — findings to be evaluated and interpreted are only expected to be obtained in several years as far as floristic and vegetation surveys directed at aridification are concerned.

It is well-known that climate change is a major control of species distribution and abundance as well as the establishment of living communities (associations). Since naturally induced climate change is a very slow process and each species has a tolerance within broader or narrower limits, there is a certain time lag observed in the response of biota to climate change. Within a longer climatic period, short spells of climatic fluctuation are sometimes detected and their influence on biota is negligible.

According to the recent conception of Hungarian flora, the floral elements in the study area are shown on *Fig. 5.*

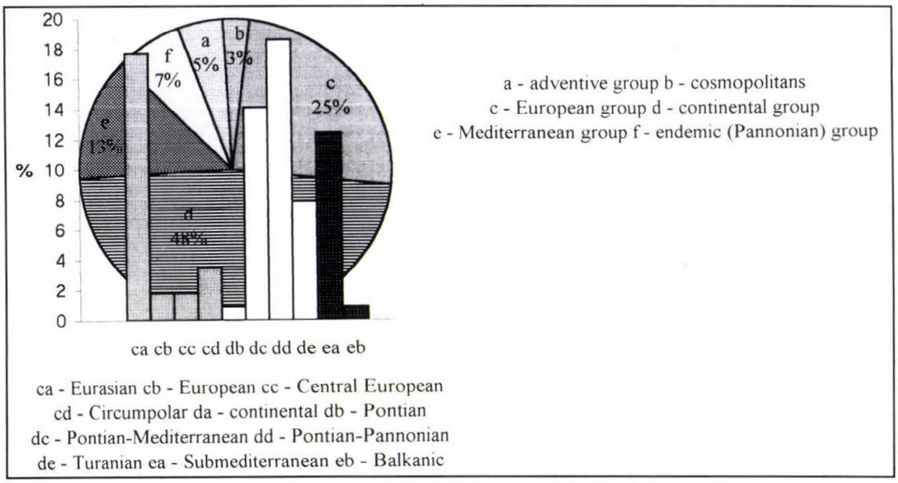

Fig. 5. Distribution of floral elements of the study area.

From the distribution of floral elements it is claimed that in the study area species of the continental group predominate, species of the European group are half of that number and somewhat more than one third belongs to the Mediterranean group. The ratio of Pannonian (endemic) species is relatively high, while adventives and cosmopolitans are not considerable. Mediterranean climatic influence is primarily characteristic in South-Transdanubia and along the south-central part of the Transdanubian Mountain Range. With regard to this, the expressly high frequency of Mediterranean species is of particular importance. In addition, if we consider the Pontian-Mediterranean elements classed with the continental group, the Mediterranean character is even more pronounced.

In the fixed cenological quadrates (represented by various subassociations of perennial *Festucetum vaginatae danubiale* of the Danube-Tisza Interfluve) classical cenological survey was supplemented with the study of plant species, which may show quantitative changes of specimen number probably associated with climate change, i.e. aridification of Hungarian climate. When identifying the sampling squares, a fundamental condition was the independence of the investigated vegetation type from hydromorphic influence.

Out of the selected four plant species two were dicotyledonous (*Euphorbia seguierana* and *Artemisia campestris*) and two are monocotyledonous graminaceous species (*Festuca vaginata* and *Stipa borysthenica*). The graminaceous species are association-forming, prevailing plants in the sand puszta grasslands.

Within the group of Borhidi's relative ecological indicators (*Borhidi,* 1995) according to the relative groundwater and soil moisture indicator (WB values) *Festuca vaginata, Stipa borysthenica* and *Euphorbia seguierana* are indicators of habitats with long drought periods (WB = 2), while *Artemisia campestris* represents xerophytes occasionally appearing at moist sites (WB = 3). Thus, the detection of specimen number changes of these four plants in sampling squares can be regarded a simple but effective method of providing evidence for climate change. Botanical observations in the field in recent years have supported the statement that in perennial open sand puszta grasslands *Stipa borysthenica* shows an increasing dominance in comparison to *Festuca vaginata.* There is an indirect relationship with the presumed aridification of the Carpathian Basin: the *Stipa borysthenica* has deeper root system reaching moister soil layers thus it better tolerates climatic aridification than *Festuca vaginata* with shallower rootage which finds support only in the topsoil.

Considering the above, the joint study of the mass conditions of the four plant species has to be accompanied by the relative quantitative changes of the species, with special regard to the *Stipa/Festuca* ratio.

The *Stipa/Festuca* mass ratio — probably related to aridification — has been investigated in sampling quadrats of summit position, i.e. independently of the microclimatic modification due to exposure. The data of specimen number and coverage point to an overwhelming dominance of *Stipa*: the number of specimens more than fourfold exceeds that of *Festuca.* In other sampling quadrats of the study area, where the reflecting mass ratios are typical of open perennial sand puszta swards, the ratio of the two species is just the opposite. The finding of this investigation seems to confirm aridification.

Last year the specimen numbers of the four plant species were surveyed from the ten quadrates of 25 m^2 area identified in five different microhabitats of the Fülöpháza test area (*Fig. 6*). Re-survey is performed every year.

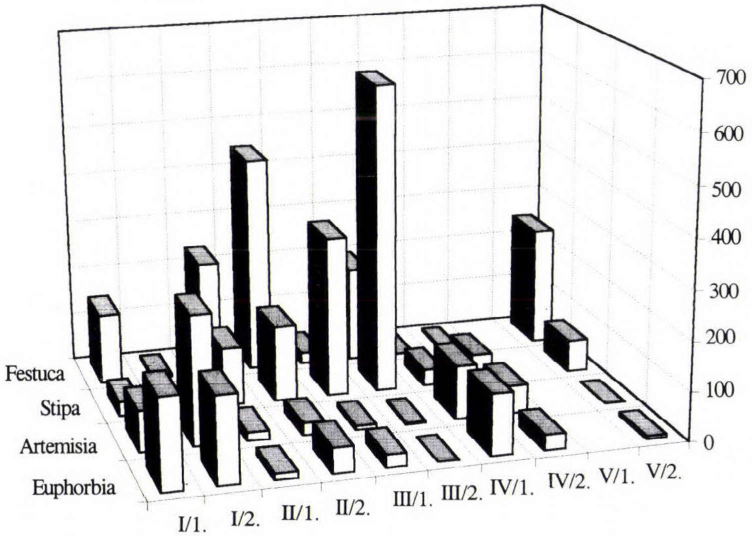

Fig. 6. Distribution of the individuals of the plant species investigated in detail (*Fetuca vaginata, Stipa borysthenica, Artemisia campestris, Euphorbia seguriana)* in the quadrates.

It has to be remarked, however, that in order to arrive at interpretable results from the botanical data series, long-term monitoring has to be achieved. This is supported by the properties of Hungarian climate. It suffices here to remind of the interruption of a dry period of 15 years by two humid years and it cannot be judged whether it continues in future or remains a short episode in the process of aridification accelerated by human intervention.

3.2 Soil formation processes

Climate change is mediated to the *soil subsystem* through the subsidence of groundwater table and reduction of soil moisture content (*Várallyay*, 1994). Alterations in water budget are reflected in soil formation with some decades of delay. The statement also applies to the sand soils over the topographic elevations of the Danube-Tisza Interfluve (dune summits and slopes) with extreme water budget in the first place. Solonchak soils, however, are exceptions and show an extraordinarily rapid seasonal dynamics manifested in the rearrangement of water-soluble potassium salts within the profile.

The investigation of the solonchak-type deposits of partially or totally desiccated alkali ponds is a particularly favorable opportunity to detect land degradation and aridification induced by natural trends (climate change) and human impacts (drainage, water intake, irrigation etc.). Communication between lowered groundwater table and capillary soil moisture is interrupted, soil dynamics towards solonchak formation ceases or even occasional leaching (desalinisation) occurs (*Kertész et al.,* 1998). As a consequence, a type of vegetation different from the previous one — more closed and poorer in halophytic species — can be established.

For the above outlined goals, monitoring has been extended to the immediate neighbourhood of the Danube-Tisza blown-sand area, the dry basin of the Szappan-szék pond. Its study was judged to supplement favorably the investigations into plant succession intended to detect the transformation of the sand region (see previous chapter).

Work began in autumn 1997 with on-the-spot and laboratory analyses of a base soil profile deepened in the most characteristic site of the Szappan-szék. Paradoxically, the soil pit left open the previous year was filled with rainwater during the humid spring and summer of 1998 and thus no sampling could take place. In order to record at least salt dynamics of the first year, samples were taken from an auger hole next to the pit. Both sampling had been preceded by a minimum one-week precipitation-free period.

Results of laboratory analyses of the 1997 and 1998 sampling experiments are presented in *Table 1* and the observed changes of soil properties (total salt and soda contents) are shown on *Fig. 7.*

Table 1. Laboratory analyses of base soli profile at Szappan-szék 1. Results indicate changes in the most mobile soil parameters

Depth	$CaCO_3$	Humus	Total salts %		Soda %		pH (H_2O)	
cm	%	%	1997	1998	1997	1998	1997	1998
0– 18	17.7	2.37	1.10	1.42	0.085	0.446	9.6	10.4
18– 38	14.2	0.21	0.90	0.33	0.080	0.166	9.6	10.2
38– 52	12.1	0.0	1.00	0.20	0.053	0.164	9.5	10.1
52– 71	10.8	0.0	0.80	0.19	0.048	0.144	9.4	10.1
71– 89	15.1	0.0	1.00	0.30	0.053	0.194	9.6	10.2
89–118	33.6	0.0	1.20	*	0.064	*	9.7	*

* Presence of groundwater made sampling impossible

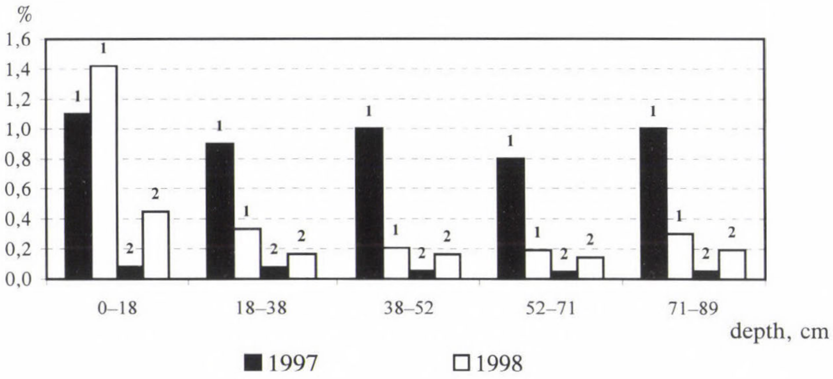

Fig. 7. Changes of the total salt (1) and sodium carbonate (2) content between 1997–1998. in base soil profile of Szappan-szék

The selected profile well represents solonchaks in Hungary with sodium salt content, developed under the influence of high-level groundwater table (obscure horizons, high $CaCO_3$ content, strongly alkalic soil reaction [$pH > 9$]), and — occuring on pond floor — shows more remarkable properties: salt contents including soda exceeds the limits established for this soil type in every horizon and at both measurement dates.

As conclusions it is claimed that:

(1) total salt contents of the soils — with the exception of the uppermost soil horizon — have reduced to one-third or one-fifth;

(2) soda contents have increased in each horizon and pH grew in parallel, by more than 0.5 (in the uppermost layer by almost 1);

(3) there is a gradual decrease in the above soil parameters to the depth of 70 cm and reduction is quite abrupt from the uppermost to the next horizon.

Among the above statements, a ready explanation is found for number 2: growth in soda content necessarily involves an increase in pH through alkalic hydrolysis.

Statements (1) and (3) may be related to the more abundant precipitation of the past year and, consequently, to the higher groundwater tables. (In September 1997 groundwater was recorded at 115 cm, while at 72 cm a year later.) In both cases the distribution of salts mentioned is a consequence of differences in salt re-solution and precipitating impacts between the higher groundwater table and the capillary zone above it. With high groundwater levels, most of the salts are dissolved and total salt amounts are reduced. The most easily soluble soda, which remains in solution the longest, was lifted into the soil profile by capillary processes. The extreme salt content of the uppermost horizon — as it has been shown by the mechanical analysis — is also partly due to the very great share of fine fraction.

A comparison was made between salt contents and salt profile curves of sodaic solonchaks in several dozens of kilometres distance, *surveyed in 1980*. It was assumed that the comparison may result in recognizing trends of soil dynamics over the almost two decades elapsed. Data from two profiles were described and analyzed by the staff of the Institute of Soil Science and Agrochemistry of the Hungarian Academy of Sciences (*Report*, 1980). The comparison seemed to be suitable (*Fig. 8*).

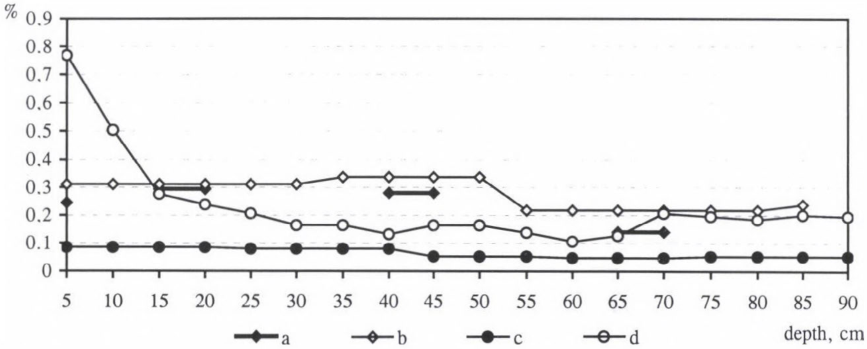

Fig. 8. Spatial and temporal comparison of total soda contents in the solonchak soils of the Danube-Tisza Interfluve. *a* and *b* = two different profiles described in 1980; *c* and *d* = values of profile az Szappan-szék 1 at two dates (1997 and 1998).

From the analyses of the figures, the following statements can be made:

(a) Total salt and soda contents are more or less gradually decreasing towards the deeper horizons in both profiles surveyed in 1980; the curves are running close to each other and this indicates similar salt conditions;

(b) The same parameters of the profile analyzed in 1997 — disregarding minor fluctuations deriving from layering — show similar distribution in the profile (the curves are similar); however, it is striking that curves of total salt and soda indicate much higher or much lower salt amounts than the average (i.e., in profiles described under (a));

(c) Salt profile curves for 1998 are substantially different from the previous ones: both total salts and soda contents show extremely high values in the uppermost 15–20 cm of the profile.

The following careful conclusions can only be drawn:

- for the time being, from only two profiles, it seems to be a law that salt contents and salt distributions of solonchak soils formed under similar conditions and not yet affected by aridification are largely similar (see (a)); this needs confirmation from the analyses of several further profiles;
- soda contents of solonchaks affected by a dry period of some length (one or two decades) have leached out from the whole profile and equally low in all horizons (see (b)); *this is the most important process and can be indirect evidence for desalinisation;*
- salt conditions developed in dry years can change radically in more humid years when the rising and subsequent lowering of the groundwater table and the reorganisation of the capillary zone — probably temporarily — leads to a concentration of salts in the upper soil horizons again (see (c)).

It is clear for us that measurements have to be performed more often than once a year in the future. Further analyses are necessary (adjusted to seasons, rainfall events, snow melting and considering ion distribution) to explain the processes observed more precisely. As a result, the other objective of research, i.e. to reveal the regularities of plant succession adjusted to salt budget, can also be realised.

3.3 Impacts on soil moisture content

The EPIC (Erosion Productivity Impact Calculator; *Sharpley* and *Williams*, 1990) is applied to estimate soil water content consequences of the expected regional climate changes in a typical subcatchment, the catchment of Örvényesi-séd, selected for study on the northern catchment of Lake Balaton, according to climate scenarios (*Mika*, 1988). The study is based on the soil hydrology parameters included in EPIC model, exhibiting relatively fast response to the climate variations. To specify regional climate scenarios for Hungary with a coarsely time resolution, two approaches are employed. The simpler one is the use of a geographical analogy which presumes correspondence of differences in monthly variance, and even the daily behaviour of the established differences corresponds to the scenario. Based on this concept, climate data of Pápa (north of Lake Balaton) were selected as geographical analogues for the expected changes in the Pécsely basin, considering the necessary similarities in the non-climatological conditions also. The second approach is a search for statistical connections between semiannual and monthly anomalies, and also between monthly anomalies and daily statistics within the same month. For generating daily weather sequences, the built-in generator of the EPIC is used. Results of the two approaches are compared. Climate differences generate considerable variation both in the soil water content and in transpiration. Another source of variation is crop-rotation, responsible for the half of standard deviations.

A small partial watershed of 0.3 ha area was selected for comparison. Its average altitude is 202 m, with a slope length of 123 m and a slope inclination of 6 per cent. The slope is covered by a typical, medium-eroded brown forest soil.

3.3.1 The EPIC model and its application

The EPIC was developed to predict the relationship between soil erosion and soil productivity. EPIC is physically based and capable of simultaneously and realistically simulating the processes involved in erosion by using readily available inputs.

Synthetic weather sequences are created by a weather generator. Currently these models are invariably stochastic. The precipitation components of the EPIC weather generator model are first-order two-state Markov chain types (*Richardson* and *Nicks*, 1990). There are two conceptual subcomponents: an event (or occurrence) submodel and an amount submodel. On each day of the simulation, the event submodel controls whether the day is wet or dry (a wet day is defined as one with at least 0.2 mm of rainfall; *Richardson* and *Nicks*, 1990). On any day of the simulation a probability for the occurrence of rainfall is chosen randomly. This probability is then compared with a threshold value (the "rainfall state probability"; if it exceeds the threshold then rainfall occurs. The threshold probability depends both on whether rainfall occurred on the previous day (although this is of course unknown for the first day of the simulation), and on the month. Because the occurrence of rainfall on this previous day depends on its turn on the occurrence of rainfall on the day preceding that, and so on, patterns of wet or dry spells extending over several days ("Markov chains") are built up. Only two states — wet or dry — are stipulated, and the submodel considers only one previous day's state in determining the threshold probability. It is, therefore, considered to be a first-order, two-state model. The quantity of precipitation on wet days is determined by the amount submodel.

3.3.2 Geographical analogy

Time resolution of the regional climate scenarios is generally insufficient to be directly applied in environmental (hydrological, agricultural, ecological, etc.) impact studies. Hence, down-scaling of the global climate model outputs in space has to be followed by downscaling of the scenarios in time. This task is tried to be solved by application of geographical analogy. This means to find another site, as a pair to the initial site in question (i.e. Mencshely in our case), where climate at present is similar to the one, expected by the scenario for the given time-slice of the future. The geographical analog is searched with respect to the scenario, described in Section 2.1.

Application of geographical analogy in this case means that diurnal statistical parameters of the meteorological variables at the initial station are introduced into the weather generator of the EPIC as those representing the 'present' climate at that site. Present statistical parameters derived at the geographical analog site are considered as characteristics of the "future" climate at the initial site.

Geographical analogs were derived using the following steps. Seasonal mean climate normal values were calculated for temperature and precipitation series at all stations of the country in the period 1951–1980. For all stations we computed the degree of analogy from the ratios (ANT = analogy of temperature, ANP = analogy of precipitation):

$$ANT = (T_{an} - T_{in}) / T_{ch} \qquad \text{and} \qquad ANP = (P_{an} - P_{in}) / P_{ch}, \tag{2}$$

where T_{an} and P_{an} are temperature and precipitation of the (possible) analogue to the corresponding values of the initial station (T_{in} and P_{in}), whereas T_{ch} and P_{ch} are the assessed (positive or negative) changes according to the scenario which correspond to 1 K global warming (*Mika*, 1988). The above values were calculated for the semiannual means (sums), separately.

For the application of geographical analogy and the evaluation of the method, a locality with geographical conditions, similar to those in the Pécsely Basin and meteorological parameters representing future climate had to be found. There were 42 meteorological stations with sufficient data included into this search. Naturally, the time series of the meteorological stations in the Great Hungarian Plain could not be considered since the evolution, structure, drainage and other landscape factors are entirely different in the two regions. After this further limitation, altogether 7 stations could be found to fulfil the above climatological criteria to be a geographical analog. Six of these stations, however, became further rejected due to geographical dissimilarities to the initial site, including erroneous mezo- or micro-scale effects on data quality.

The only selected analog, the area north of Pápa, the border region between the Bakony foothills and the Little Plain, largely corresponds to the geographical conditions of the Pécsely Basin as far as surface structure, landforms and partially soils are concerned. Differences in three main climate elements characterizing these two points for the investigated 1974–85 period, Mencshely (46°58'N, 17°42'E, 332 m a.s.l.) and Pápa (47°23'N, 17°23'E, 131 m a.s.l.) are presented in *Table 2*. Averaging these differences for the summer half-year i.e., for the growing season of maize in Hungary and also of soil drought, the differences are 0.5 K in temperature and -58 mm (-14% of the value in Mencshely) in precipitation. These differences, and also those for the winter half-year, are broadly consistent with the conditional forecasts concerning a 0.5 K increase of the hemispherical mean temperature, which is about 3–4 decades according to the global forecasts (*IPCC*, 1996).

Table 2. Average differences (Pápa–Mencshely) in monthly mean values of temperature (T) and precipitation (P), 1974–1985

	Jan	Feb	Mar	Apr	May	Jun	Jul	Aug	Sep	Oct	Nov	Dec
T (K)	0.7	0.8	0.9	0.6	0.6	0.5	0.6	0.6	0.4	0.3	0.8	0.8
P (mm)	-2	-13	-10	-8	-10	-18	-5	-11	-6	-5	-15	-13

The weather generator of the EPIC model is parameterized both for present (Mencshely) and "future" (Pápa: present) climate according to the 1974-85 period.

At the end of this paragraph we should mention that there is another, more direct way to apply the geographical analogy (*Erdős* and *Mika*, 1993). This is the way when the appropriate environmental characteristics are simply compared at the two sites and the difference between them is claimed to be a consequence of climate differences. This direct application requires high similarity of the non-climatic factors or good correspondence of their differences to those likely caused by gradual climate warming.

3.3.3 Results of soil moisture simulations

From the wide set of output parameters provided by the model, we selected those exhibiting fast response to the climate differences. The reason for this is that the design of the experiment, simulating present and future time slices, does not allow to simulate the transient modification of slowly varying soil parameters (e.g., mineralization and immobilization, chemical composition, pH, N and P cycling). The selected parameters are soil water content at the root zone and transpiration by the vegetation. The accuracy of EPIC in predictions was evaluated and gave satisfactory results for simulating of the water balance over a long period. Means, standard errors of the mean, ranges, probability distributions of evapotranspiration, runoff and growing season soil water depletion of observed and predicted values were very similar (*Steiner et al.*, 1990). Calibration in our case was restricted to tillage practice and crop parameters. Water content is calculated by the model according to the artificially generated weather, especially precipitation and thermal conditions of evapotranspiration. Soil moisture is computed in mm, with respect to the water demand of the plant canopy. It is analyzed in annual average and also in August, when generally the annual minimum occurs (*Table 3*).

Table 3. Basic statistical characteristics of the simulations with four-year crop rotation

mm	Annual transpiration		Annual soil-water content		Soil-water content in August	
	Average	Standard deviation	Average	Standard deviation	Average	Standard deviation
Pécsely	278	89	49	18	15	53
Pápa	262	90	39	19	12	48

With crop rotation, characteristic of the Pécsely basin, the soil water content exhibits quadriannual fluctuation both in August and in annual average. In more details, enhanced water demand of maize may explain the extremely negative values. Simulations run according to the recent crop rotation, with four year periodicity, transpiration exhibit similar cycles, but with shifted phase. Extreme minimum transpiration occurs in the 3rd year of rotation, which is largely produced by soil conditions, left bare for 3–4 months after harvesting the rape.

Considering these periodicities as disturbances of climatic differences, the simulations are repeated by assuming maize monoculture for the whole generated 30 years period (*Fig. 9*). Water demand of maize is the largest in July-August, that explains the experienced water deficit of 40–50 mm in the root zone. Of course, the expected monoculture for 30 years is an unrealistic assumption in practice. Our aim was only to cancel out the four-year fluctuation, to realise the climatical comparison.

Phase-out of this fluctuation was successful, since standard deviation of the simulated series decreased to its half in the annual soil water content, in its August value and in annual average transpiration, too (*Table 4*). So the difference in the soil water components caused by climatic differences between Pécsely and Pápa became more conspicuous.

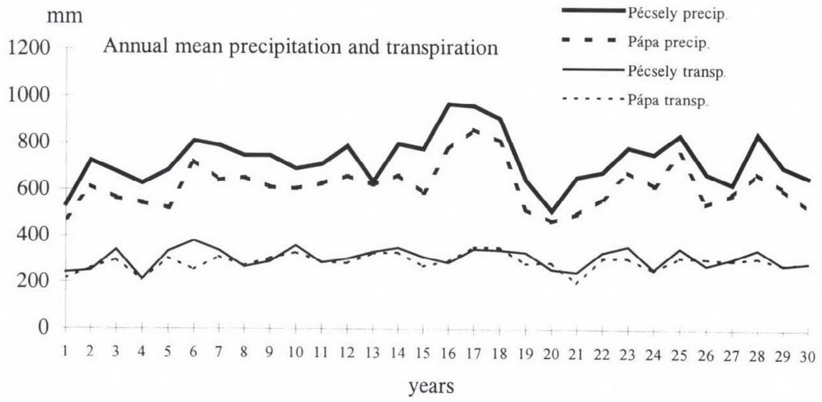

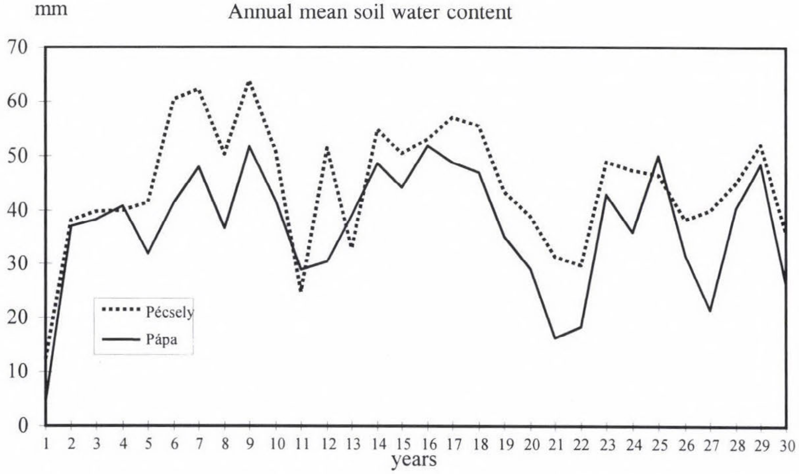

Fig. 9. Simulated annual mean precipitation and transpiration (upper part) and soil water content (lower part) at Pécsely and at its geographical analogue (Pápa) in case of the maize only experiment.

Table 4. Basic statistical characteristics of the simulations with maize monoculture

mm	Annual transpiration		Annual soil-water content		Soil-water content in August	
	Average	Standard deviation	Average	Standard deviation	Average	Standard deviation
Pécsely	306	42	45	12	-36	24
Pápa	289	37	37	11	-43	21

4. Agricultural implications

Through influencing the heat and water balances of landscapes, global warming may significantly affect the physical conditions of farming (*Szász*, 1987; *Hunkár et al.,* 1995). Even independently from global processes, the climate of Hungary shows liability to summer drought of variable length and the distribution of annual precipitation is irregular (*Szalóki*, 1994). In Hungary drought is the expression of relative rather than absolute water deficit (*Antal*, 1991). Drought does not only involve deleterious — occasionally even disastrous — impacts on agriculture when there is not sufficient precipitation but also when no rainwater reaches the root zones of crops (soil drought, or — in soils of poor water storage capacity — when the rainwater does not retained long enough there (physiological drought). Depending on the technology applied, water deficit could result in 10–15 per cent loss of yields.

4.1 Land capability analysis

The deterioration in the conditions of farming caused by reduced water availability have been attempted to be quantified by assessing *land capability* (*Lóczy*, 1988). As opposed to the usage of the term in Hungarian agricultural literature, land capability here refers to the range of agricultural crops successfully grown in a land area and their order of relative suitability. The agroecological studies in the Geographical Research Institute of the Hungarian Academy of Sciences (*Lóczy*, 1988; *Lóczy* and *Szalai*, 1993, 1994) parameterized water budget by topographic, climatic and soil parameters and portrayed ecological suitability through an ARC/INFO GIS. Environmental conditions were assessed for the five major arable crops (with the largest harvest area): winter wheat, maize, sunflowers, lucerne and sugarbeet. Since the input data incorporated mostly represent the period 1940–1970, the data base can be regarded to reflect conditions before the advent of the aridification trend.

It is assumed that land capability has been reduced by the lack of precipitation, dropping groundwater and lower soil moisture contents since then. In modelling of the changes, attempts to predict the impacts of climate change (e.g., in hydrology: *Szilágyi* and *Vorosmarty*, 1993; *Kozma-Tóth et al.,* 1995) have been taken advantage of. The geographical information system for land capability is able to estimate the extent environmental conditions which meet the requirements of crops or groups of crops in the case of dropping groundwater levels and decreasing precipitation amounts. The computer programme of assessment was run with reduced monthly precipitation inputs and evaluated the position of groundwater table relative to the root zones of crops.

4.2 Land use

As drought has long been a regular phenomenon over the Interfluve, land use has mostly adjusted to this situation by now. Plantations, primarily the orchards are gaining ground at the expense of arable land. Since the market demand higher is for fruit than for grain, this is an economically favourable tendency. The feedback to groundwater, however, may be positive since orchards — like forests (*Major* and *Neppel*, 1988) — further reduce groundwater table in their environs.

In general, the impact of forests on water budget needs a careful consideration before judgement. Water demands of arborous species range widely: from black pine (185 mm) to commercial poplar varieties (280 mm). On the long run, losses from the interception of leaves is largely counterbalanced by reduced evapotranspiration under a wetter microclimate. Although forestry experts tend to deny the responsibility of forests in sinking groundwater table, during in areas built up of deposits of low capillarity, forests may contribute to water deficit in neighbouring agricultural land and to reduced agricultural potential drought years without infiltration. Planted apricot and peach trees and vineyards with high summer water demands (*Szász*, 1995) may tap groundwater reserves even more heavily.

5. Discussion

Climate change impacts on soil and vegetation are in the focus of the present paper, preceded by a detailed description of climate trends and scenarios concerning Hungary. The main objective is to validate the hypothesis that climate change will cause drier soil conditions in the following decades.

This expectation was shared by various experts (e.g., *HCSD*, 1995). In the recent years there are some doubts about aridification mainly because of the last 3–4 years with normal, or wet conditions. The previous 10–15 years were characterized by dry summer half years corresponding to the warm hemisphere. It is therefore quite possible that 3–4 years ago a new cycle of normal or wet conditions began. We are not yet in the position to answer this question. Further research is needed to clarify whether it is a new cycle or we are facing only 3–4 years with values deviating from the average.

There is a discussion about precipitation change as well. According to several previous GCM outputs, a precipitation increase is projected for Hungary as a response to the CO_2 doubling (see *Mika*, 1991 for references). These GCMs were elaborated for 2–4 K temperature increase for which case the statistical methods applied by us were not applicable. This means that there is no contradiction between a drier climate for the 0–1 K global warming and a wetter climate in the case of a 2 K increase.

In a recent experiment performed by the OAGCM at Hadley center, the grid-point data for Hungary (as described by *Harnos,* 1998) gave -14% precipitation decrease for the summer half-year at a CO_2 level corresponding to a 0.7 K global warming. 1.8 K global warming was accompanied by a +8% precipitation increase.

In connection with the scenarios it should also be mentioned that for greater changes there is an *another approach* (*Bartholy et al.*, 1995; *Matyasovszky et al.*, 1995) which combines the frequency of diurnal mid-tropospheric circulation patterns with conditional autocorrelation of the investigated elements (precipitation, temperature and lake-evaporation) to synthesize their future values. These studies applied equilibrium (CO_2-doubling) atmospheric GCM-outputs only.

The method of geographical analogy, applied in Section 3.3 does not ensure a strictly established method, because modifications of the connections between elements or statistical moments in time could strictly be identical with their variations in space only if we approach climate change by a conservative shift of climate belts (regions) in space. This approach can only be validated if a better method (i.e., the method of slices which works well at longer time scales) could bring good results even at diurnal time scales. According to our first experiences, however, this is not the case. Hence geographical analogy remains a heuristic approach to the downscaling-in-time problem.

6. Conclusion

Global climate change is probably manifested in gradual aridification in the SE part of Central Europe. The physical processes triggered, however, are not so advanced as in the Mediterranean region. Aridification tendencies are detected in several environmental factors. The area most affected is the sand region of the Danube-Tisza Interfluve, where aridification — intertwined with human impacts — is expressed in dropping groundwater table, exhaustion of confined groundwater reserves and a slow modification of soil-forming processes. No major change is detectable in natural vegetation and land use.

Research of the consequences of climate change may promote the planning of preparatory measures and reduce environmental and economic damage.

Acknowledgement—The research for this paper was carried out as part of the MEDALUS III (MEditerranean Desertification and Land Use) collaborative research project. MEDALUS II was funded by the EC under its Environmental Programme, Contract Number EV5V0128/0166 and the support is gratefully acknowledged.

References

Ambrózy, P., 1991: Climatic reference stations (in Hungarian). *Légkör XXXVI.* No. 2.

Ambrózy, P., Koflanovits, E. and *Kövér, B.*, 1990: The temporal rearrangement of precipitation (in Hungarian). *Időjárás 94*, 156–167.

Antal, E., 1991: Impact of climate change on droughts in Hungary (in Hungarian). *Acta Geographica Debrecina 28-29,* 17-18.

Bartha, D., 1993: Development of holocene vegetation in the Great Hungarian Plain (in Hungarian). *Hidrológiai Közlöny 73*, 17-19.

Bartholy, J., *Matyasovszky, I.* and *Bogárdi, I.*, 1995: Effect of climate change on regional precipitation in Lake Balaton watershed. *Theoretical and Applied Climatology* 50, 237-250.

Berényi, P. and *Erdélyi, M.*, 1990: Sinking confined groundwater under the Danube-Tisza Interfluve (in HUngarian). *Vízügyi Közlemények 72,* 377-397.

Borhidi, A., 1995: Social behaviour types, the naturalness and relative ecological indicator values of the higher plants in the Hungarian Flora. *Acta. Bot. Hung. 39,* No. 1-2., 97-181.

Cubasch, U., *Hasselmann, K.*, *Hoeck, H.*, *Maier-Raimer, E.*, *Mikolajewicz, U.*, *Santer, B.D.*, and *Sausen, R.*, 1992: Time-dependent greenhouse warming computations with a coupled ocean-atmosphere model. *Climate Dynamics 8*, 55-69.

Erdős, L. and *Mika, J.*, 1993: Applying a new model to estimate effects of climate potential in yield. In *Proc. 16th Intern. Conf. on Carpathian Meteorology,* Smolenice, Slovakia, October 4-8, 1993, 200-210.

Graham, R.W. and *Grimm, E.C.*, 1990: Effects of global climate change on the patterns of terrestrial biological communities. *Trends in Ecology and Evolution 5,* 289-292.

Harnos, Zs., 1998: Expected climate tendencies and their impact on the production of some crops (in Hungarian). In *Climate change and consequences* (ed.: *Z. Dunkel*). Meteorological Scientific Days, November 20-21, 1997, Budapest, 55-65.

HCSD, 1995: *Hungary: towards strategy planning for sustainable development* (eds.: *Cs. Nemes* and *T. Faragó*). The Hungarian Comission on Sustainable Development, Budapest, 99 p.

Heino, R., 1994: Climate in Finland during the period of meteorological observations. *Finnish Meteorological Institute Contributions*, No. 12, Helsinki, pp. 209.

Hunkár, M., 1995: Assessment of impacts of climate change on the yields of wheat and maize. *WMO Report.*

Huszár, T., *Kertész, Á.*, *Lóczy, D.*, *Molnár, K.* and *Mika, J.*, 1996: Simulation of possible climate change effects on soil water content. *Proc. 'Climate Change' Conference, Visegrád.* Budapest, 171-176.

IPCC, 1996: Climate Change 1995. The Science of Climate Change. *Contribution of Working Group I to the Second Assessment Report of the IPCC* (eds.: *J.T. Houghton et al.*). Cambridge Univ. Press, 570 pp.

Jones, P.D., 1994: Hemispheric surface air temperature variations: a reanalysis and an update to 1993. *J. Climate 7,* 1794-1802.

Kertész, Á., 1995: Aridification in a region adjacent to the Mediterranean: Objectives and outline of a scientific programme. *MEDALUS Working Paper No 65*, King's College, London.

Kertész, Á., *Huszár, T.*, *Lóczy, D.*, *Mattyasovszky, I.*, *Mika, J.*, *Molnár, K.*, *Szalay, J.* and *Szalai, L.*, 1997: MEDEAST: The MEDALUS Programme in Eastern-Central Europe. In *MEDALUS II. Atlas of European Mediterranean Desertification: A Research Synthesis* (eds.: *J. Thornes* and *P. Mairota*). John Wiley, Chichester.

Kertész, Á., *Lóczy, D.*, *Molnár, K.* and *Szalai, L.*, 1998: Consequences of increasing aridity in the temperate zone: example Hungary. In *The Soil as a Strategic Reseource: Degradation Processes and Conservation Measures* (eds.: *A. Rodríguez Rodríguez, C.C. Jiménez Mendoza* and *M.L. Tejedor Salguero*). Goeforma Ediciones, Logrono, 287-303.

Koflanovits-Adámy, E. and *Szentimrey, T.*, 1986: The variations of the precipitation amounts in the Carpathian Basin during the present century. *Időjárás 90*, 206-216.

Kozma-Tóth, E., *Posza, I.* and *Tiringer, Cs.*, 1995: Water demand, actual transpiration and irrigation water demand. of arable crop stands (in Hungarian). *Orsz. Meteorológiai Szolgálat Éghajlati és Agrometeorológiai Tanulmányok 3*, 33-96.

Liebe, P. (ed.), 1993: Subsidence of groundwater levels on the Danube-Tisza Interfluve: reasons for the present situation and ways of improvement. *VITUKI, Hydrological Institute*, Budapest, 158 p.

Lóczy, D. (ed.), 1988: *Land Evaluation Studies in Hungary*. Akadémiai Kiadó, Budapest, 95 p.

Lóczy, D. and *Szalai, L.*, 1993: GIS application for land capability survey in Hungary. *Geografski zbornik, Zagreb, 33,* 53–56.

Lóczy, D. and *Szalai, L.*, 1994: Modernised verion of site assessment and agroecological zoning using GIS (in Hungarian). *Földrajzi Értesítő 44*, No. 1–2, 23–37.

Major, P. and *Neppel, F.*, 1988: Groundwater level subsidences in the Danube-Tisza Interfluve. *Vízügyi Közlemények LXX*, 605-626.

Major, G., *Major, P.* and *Vargay, Z.*, 1991: The effect of runoff conditions on groundwater level changes on the Danube-Tisza Interfluve. *Vízügyi Közlemények LXXIII,* 142-152.

Matyasovszky, I., *Bogárdi, I.*, *Bárdossy, A.* and *Duckstein, L.*, 1995: Local temperature estimation under climate change. *Theor. Appl. Climatology 50,* 1–14.

Mika, J., 1988: Regional features of global warming in the Carpathian Basin (in Hungarian). *Időjárás 92,* 178–189.

Mika, J., 1991: Predictable impacts of a major global warming in Hungary (in Hungarian). *Időjárás 95,* 265–278.

Mika, J., 1992: Method of slices to estimate regional features of the global warming at extratropical latitudes. *5th Int. Meeting on Statistical Climatology*, June 22-26, 1992, Toronto, 433-436.

Mika, J., 1993: Changes in the climate of the Great Hungarian Plain in relation to global climate change (in Hungarian). *Alföldi Tanulmányok, Békéscsaba, 15,* 11–29.

Molnár, K., 1995: Temperature and precipitation trends of Hungary. *MEDALUS Mediterranean Desertification and Land Use. Working Paper,* No. 67. July, 1995, King's College, London.

Nemes, Cs., 1994: Tendencies of several temperature characteristics in Budapest (in Hungarian). *Légkör XXXIX*, No. 4.

Nemes, Cs. and *Szalai, S.*, 1992: The long-time climatological series in Hungary. *Symposium Cracow*, June 1992, 81-85.

Nováky, B., 1993: Changes in the climate and in water budget of the Great Hungarian Plain. *Hidrológiai Közlöny 73*, No. 1, 20-23.

Pálfai, I., 1991: Drought in Hungary in 1990 (in Hungarian). *Vízügyi Közlemények 73,* 117–133.

Pálfai, I., 1995: Water management problems on the Danube–Tisza Interfluve and possible solutions (in Hungarian). *Vízügyi Közlemények 76,* 144–164.

Pálfai I., 1996: Changes of soil moisture and groundwater level in the Great Hungarian Plain (in Hungarian). *Vízügyi Közlemények 78,* 207–218.

Report, 1980: Report on activities for the Kiskunság National Park in 1979-80 (in Hungarian). *RISSAC, Hung. Acad. Sci.*, Budapest, 75+43 p.

Richardson, C.W. and *Nicks, A.D.*, 1990: Weather generator description. In *EPIC - Erosion/Productivity Impact Calculator: 1. Model Documentation* (eds.: *A.N. Sharpley* and *J.R. Williams*) *US. Dept. Agricult. Technical Bull.* No. 1768, pp. 93-104.

Schirok-Kriston, I., 1994: Temporal variation of the daily extreme high precipitation in Hungary. *Id-Időjárás 98,* 195-203.

Sharpley, A.N. and *Williams, J.R.*, (eds.), 1990: *EPIC - Erosion/Productivity Impact Calculator: 1. Model Documentation. US. Dept. Agricult.*, pp. 191-205.

Steiner, J.L., *Williams, J.R.* and *Jones, O.R.*, 1990: Evaluation of EPIC using a dryland wheat-sorghum-fallow. In *EPIC - Erosion/Productivity Impact Calculator: 1. Model Documentation* (eds.: *A.N. Sharpley* and *J.R. Williams*). *US. Dept. Agricult.*, pp. 191-205.

Szalóki, S., 1994: Consequences of dropping groundwater levels in crop cultivation (in HUngarian). In *Water management problems on the Danube–Tisza Interfluve* (ed.: *I. Pálfai*). Nagyalföld Foundation, Békéscsaba, 53–58.

Szalay, J. and *Lóczy, D.*, 1995: Some trends in groundwater level changes on the Danube–Tisza interfluvial region, Hungary. *MEDALUS Working Paper*, No. 57. King's College, London.

Szász, G., 1987: The role of climate in intensive development of agriculture. *Conf. on Climatic Changes*, Brno, 43-56.

Szász, G., 1995: Natural water utilisation of major crops in Hungary (in Hungarian). *OMSZ Éghajlati és Agrometeorológiai Tanulmányok 3,* Budapest, 11-31.

Szentimrey, T., 1994: Estimation of inhomogeneities in temperature data series of Hungary. *Climatol.*

and Agrometeorol. Papers N2. Hungarian Meteorological Service, 42 p.

Szentimrey, T., 1997: Statistical procedure for joint homogenization of climatic time series. *Proceedings of the Seminar for Homogenization of Surface Climatological Data*. Budapest, Hungary, pp. 47-62.

Szentimrey, T. et al., 1998: Homogeneity adjustments of *in situ* atmospheric climate data: a review. *International Journal of Climatology,* in print.

Szilágyi, J. and *Vorosmarty, C.*, 1993: Investigations on the causes of groundwater level subsidences on the Danube-Tisza Interfluve. *Vízügyi Közlemények LXXV,* 280-294.

Várallyay, Gy., 1994: Climate change, soil salinity and alkalinity. In *Soil Response to Climate Change* (eds.: *M.D.S Rounsevell* and *P.J. Loveland*). NATO ASI Series, Springer-Verlag, Heidelberg, Ser. I., Vol. 23, 39-54.

Varga-Haszonits, Z. and *Harnos, Zs.*, 1988: Effect of climate variability and drought on wheat and maize production. In *Identifying and coping with extreme meteorological events.* Országos Meteorológiai Szolgálat, Budapest, 138-166.

IDŐJÁRÁS

Quarterly Journal of the Hungarian Meteorological Service
Vol. 103, No. 1, January–March 1999, pp. 67–80

Investigation of the chemical composition of bulk precipitation in Tirana, Albania

M. Vasjari[1]*, **A. Cullaj**[1] and **E. Demiraj**[2]

[1]*Department of Chemistry, Tirana University, Tirana, Albania;*
E-mail: vasjari@fshn.tirana.al; Fax: +355 42 27625

[2]*Institute of Hydrometeorology, Tirana, Albania*

(Manuscript received 21 July 1998; in final form 16 December 1998)

Abstract–Precipitation samples were collected in Tirana, Albania during the period June 1995–May 1996, using a bulk precipitation sampler. The daily samples were analyzed for major ions (Ca^{2+}, Mg^{2+}, Na^+, K^+, NH_4^+, Cl^-, NO_3^-, SO_4^{2-}), trace metals (Pb^{2+}, Cd^{2+}, Zn^{2+}, Cu^{2+}, Fe^{3+}), conductivity, pH and alkalinity.

The mean pH value of the precipitation, calculated from the volume weighted H^+ concentration is found to be 6.789. Neutral or alkaline character of rain as a result of neutralization process is primarily caused by calcareous soil dust. Suspended soil contains Ca^{2+} ion, which accounts for 68% of the neutralization process. The neutralization factors of Ca^{2+}, NH_4^+ and Mg^{2+} explain their effect in the neutralization process.

In all raining samples SO_4^{2-} concentration exceeded the level of concentration of NO_3^- and Cl^-. If acidity is due to nss-SO_4^{2-}, nss-Cl^- and NO_3^- concentration, nss-SO_4^{2-} was found to be the dominant component during the whole period. The effect of NO_3^- and nss-Cl^- in acidity of rainwater compensated each other during the period of study.

Contribution of marine sprays to the total concentration of Ca^{2+}, SO_4^{2-} was very low. The two fractions were comparable to the level of Cl^- only.

The chemical composition data were elaborated taking into account meteorological variables (season of the year, precipitation type, air flow direction) to evaluate temporal variations and chemical source influence. Samples of precipitation arrived from the direction industrialised countries of Central Europe were characterized by the highest concentrations of NO_3^-, SO_4^{2-}.

The values of chemical components of Tirana rain samples analysed during this monitoring process were very close to those reported for Thessaloniki, Greece.

Key-words: wet precipitation chemistry, major ions, air trajectories.

---

* Corresponding author

1. Introduction

Environmental monitoring of precipitation has received particular attention because of the harmful effect of acid rains on the ecosystems and its role as a possible pathway to study the air pollution.

The chemical composition of rain is influenced by both natural and anthropogenic sources. It can not be regarded as a local phenomenon, because it is affected by emissions originated from large regions. Therefore the analysis of chemical composition of rain water connected with meteorological situation can provide a good information on air pollutants as well as on the effects of their long range transmission.

Precipitation chemistry in the Mediterranean area is characterized by a concentration level of main cations (Ca^{2+}, Mg^{2+}, Na^{+}, K^{+}) which is higher than the concentration of main anions (Cl^{-}, NO_3^{-}, SO_4^{2-}). It is related to the contribution of carbonate rich aerosols in the air masses travelling from northern Africa to this region. For the same reason, the pH values of precipitation of Southern Europe are higher than in the other parts of Europe. Nevertheless, as the recent studies have been explained, the damaging effects of acid rains were not alleviated even in the case of neutralization (*Avila*, 1996; *Al-Momani, et al.*, 1995; *Samara, et al.*, 1992). Adriatic Sea is considered to be the most polluted area of the Mediterranean region concerning sulphur compounds, bond nitrogen and heavy metals.

Economic structure of Albania consists of potentially polluting industrial branches as chemical industry, non-ferrous metallurgy, energetic, mechanic and paper industry, etc., emitting nearly all the pollutants reported by the other developed countries. Tirana is the largest city of Albania. The city has grown rapidly since 1991 enforcing too many environmental problems. Particularly the amount of pollutants is increased due to the specific conditions characterized by an uncommonly fast urbanisation. Some chemical and metallurgical industrial plants are situated at North and Southeast direction from Tirana that haven't worked continuously with full capacity during the period of this monitoring process. Tirana is surrounded by Dajti mountain on East. Situated in a field region, about 35 km from the seashore at the East of Adriatic Sea, Tirana is influenced by sea breeze all the year. Also it is influenced by air flow from Northwest to Southeast direction.

In this study one year monitoring data of the rain water of Tirana city are presented. Samples were analysed for Ca^{2+}, Mg^{2+}, Na^{+}, K^{+}, NH_4^{+}, Cl^{-}, NO_3^{-}, SO_4^{2-}, trace metals Pb^{2+}, Cd^{2+}, Zn^{2+}, Cu^{2+}, Fe^{3+}, conductivity, pH and alkalinity. The relationship between the chemical composition of rain and the meteorological conditions will also be discussed.

2. *Experimental*

2.1 Sampling and methods of analyses

Fifty one rain samples were collected during the period June 1995–May 1996, using a bulk precipitation sampler located very close to the centre of Tirana city. Each sample was collected over a 24 or 48 hour period. Samples were filtered through Whatman 41 filter paper and filtrates were subdivided into aliquots and properly conserved accordingly *APHA* (1985) recommendations. After each sampling event the collecting funnel was rinsed with distilled water. It was protected from the dry deposition during dry weather conditions.

Rain samples were analysed by standard methods *(APHA,* 1985). For pH and alkalinity measurements, a Radelkis OP-208/1 pH-meter with a Rose combination glass electrode and an automatic microburette Radelkis OP-930/1 were used. Conductivity measurements were carried out immediately after sampling with a Hanna instrument model HI 8633. Concentrations of NH_4^+ and Cl^- were determined by ionselective potentiometry using Radelkis ISE. NO_3^- and SO_4^{2-} concentrations were measured by UV-method and turbidimetry method receptively, using Pye-Unucam SP6-550 apparatus. Ca^{2+}, Mg^{2+}, Zn^{2+}, Na^+, K^+ were determined using a Pye-Unicam SP9 AAS. It does not meet the need for additives to suppress interference in rain samples. Other heavy metals have been determined by Electrothermal AAS using a Varian SPECTRAA 10/20 equipment.

Field blanks for wet deposition samples were collected. Approximately 200 ml of distilled deionized water was poured through the funnel and collected in the collection bottle like a rain sample. Sample handling and analytical procedures applied to rain water blanks were the same as those applied to samples.

2.2 Quality assurance program

This monitoring process consists of the following elements:

(1) Consistency checks *(APHA,* 1985; *Kulshrestha et al.,* 1995)

The consistency checks used the evaluation of ion balance, comparing the sum of anions and cations, and the estimation of conductivity calculated from the concentration of each ion multiplied by the equivalent ion conductivity.

(i) anion-cation balance

The control is based on the electroneutrality of rain water samples. Theoretically the sum of anions expressed in mequ L^{-1} must be equal exactly to the sum of cations, similarly expressed in any samples. A control chart was constructed to identify if the difference between the sums of the cations and anions falls between the control limits. The majority of samples was found to comply this requirement.

(ii) comparison between measured and calculated conductivity

An alternative way for data checking is the plot of measured versus calculated conductivity *(APHA,* 1985; *Samara et al.,* 1992). The linear correlation coefficient between them exceeds 0.913 (0.0000; n = 32).

(2) Quality control chart

Control performance (C/P) chart were use to ensure that quality of distilled water, pH, conductivity, alkalinity and Mg^{2+} were accurately determined. A further graphical presentation of the data was given using the modified Youden's plot (Q;D;T) *(Miller,* 1988; *Nadkarni*, 1991; *Meglen*, 1985). Firstly the control samples requested for each parameter were prepared, then control limits were calculated based on the firsts 20 measurements.

(3) Participation in the intercalibration exercises

"Aquacon-Med Bas-Subproject Nr. 6 Acid rain analysis" organised by Italian Institution of Hydrobiology during the period of study were used as an alternative way to evaluate the quality of analytical measurements (*AQUACON*, 1994; *AQUACON*, 1995).

3. Results and discussion

3.1 Chemical composition of rain

Table 1 presents the average composition of the rain water samples as well as the standard deviation values, minimum and maximum values to show the important annual variability.

The volume weighted mean is the best estimate of the average chemical composition of rain water for an annual period (*Samara et al.,* 1992; *Avila*, 1996; *Gatz et al.*, 1995a, 1995b; *Sequeira* and *Lung*, 1995). It was found to be lower than the arithmetic mean for all parameters. Similar relations have been reported in the other studies on rain water composition (*Samara et al.,* 1992). The values of geometric means for all parameters are lower than arithmetic means. This suggests that the log-normal approach is the best for the frequency distribution of these parameters. "Chi squared " test was used to check the distribution of all parameters (*Massart*, 1988). It was found that some parameters show bi-modal distribution (pH, conductivity, Ca^{2+}, Mg^{2+}, SO_4^{2-}, NH_4^+), perhaps indicating the presence of two classes of rain events.

Table 1. Chemical characteristics of rain (* μeq L^{-1}; ** pb)

Parameter	Mean	V. W. M^{+}	G. M.$^{++}$	S. D.	Range	n
pH	6.73	6.78	6.71	0.52	4.21-7.41	50
Alkalinity	0.13	0.13	0.12	0.07	0.04-0.39	48
Conductivity	45.24	41.83	41.66	18.49	17.8-99.4	50
(Na^{+})*	46.96	43.28	37.88	32.25	11-129	51
(K^{+})*	10.52	9.97	6.91	11.63	2-61	50
(Ca^{2+})*	233.78	219.44	212.92	105.44	76-644	51
(Mg^{2+})*	27.76	25.30	24.82	13.36	9-68	51
(NH_4^{+})*	68.08	76.87	44.15	61.70	5-211	34
(NO_3^{-})*	48.30	41.66	35.27	41.93	5-179	40
(Cl^{-})*	62.71	55.57	46.93	51.41	12-130	46
(SO_4^{2-})*	152.71	152.47	141.21	61.24	38-345	46
(Zn^{2+})**	56.07	48.94	47.21	36.44	20-160	51
(Cu^{2+})**	5.68	5.02	3.59	7.58	0.4-43.8	50
(Pb^{2+})**	1.06	0.94	0.71	1.08	0.1-6.4	49
(Cd^{2+})**	0.50	0.39	0.25	0.87	0.1-5.6	48
(Fe^{3+})**	76.40	76.90	60.45	57.84	20-310	47

+ Volume weight mean; ++ Geometric mean; S.D. Standard deviation

Table 2 shows that the means of all parameters of rainwater in Tirana are higher compared to that observed elsewhere in the Mediterranean countries. Particularly the closest values were measured in Greece. High values of Ca^{2+} suggest that neutralization is the major factor for the low acidity. The manual sampling methods have been affected by the value of Ca^{2+} which can be seen in the blank samples too.

According to this study the neutralization process is primarily due to Ca^{2+} concentration followed by NH_4^{+} and Mg^{2+}. The role of Ca^{2+}, NH_4^{+} and Mg^{2+} has been evaluated by calculating neutralization factors (NF) using the formula (*Kulshrestha et al.,* 1995):

$$NF_x = \frac{X}{NO_3^{-} + SO_4^{2-}}, \tag{1}$$

where X may be Ca^{2+}, Mg^{2+}, NH_4^{+} in mequ L^{-1}.

Table 2. The chemical composition of rain water in some Mediterranean countries (μeq L^{-1})

	France[(1)]	Spain[(2)]	Turkey[(3)]	Greece[(4)]	Italy[(5)]	Albania
pH	5.0	-	5.6	5.5	5.8	6.8
Alkalinity	-	13.5	-	-	-	134.0
Conductivity	46	-	-	40.2	-	41.8
Na^+	36	22.3	117	23.5	424	43.3
K^+	24	4.0	17	8.2	15	10.0
NH_4^+	70	22.8	43	54.6	20	76.9
Ca^+	101	56.6	81	219.0	154	219.4
Mg^+	19	9.7	101	21.2	115	25.3
Cl^-	71	28.5	117	35.6	474	55.6
NO_3^-	68	20.6	23	47.9	26	41.7
SO_4^{2-}	128	46.0	66	158.0	103	152.5
Site of sampling	Strasbourg	Monsteny	Izmir	Thessaloniki	Sardinia	Tirana
Sampling period	1991-1992	1983-1994	1993	1989-1990	1990-1991	1995-1996
Sampling	wet only	bulk	wet&dry	wet only	wet&dry	manual

(1) *Sanusi et al.*, 1996; (2) *Avila*, 1996; (3) *Al-Momani et al.*, 1995; (4) *Samara et al.*, 1992; (5) *Guerzoni et al.*, 1995

Fig. 1 shows the neutralization effect of these ions. It seems clearly that the contribution of NH_4^+ has a contrary tendency to contribution tendency of Ca^{2+}, meanwhile the effect of Mg^{2+} is constant during all the period. This situation means that acidity of samples was buffered on equal level. The values of pH ranged from 6.6 to 7.1 in 72% of the samples.

The concentration of SO_4^{2-} was higher than that of NO_3^- and Cl^-. A study in Thessaloniki gives similar results for these anions (*Samara et al.,* 1992).

Non sea salt fraction of SO_4^{2-} (nss-SO_4^{2-}) plays an important role in rain acidity due to the oxidation process of SO_2. NO_3^- and nss-Cl^- have an influence on rain acidity, too. The term non sea salt has been used in preference to non marine fraction. Assuming that all the sodium in rain water is derived from the sea nns-fractions were calculated for anions SO_4^{2-} and Cl^-, as follows:

$$x_i = X_i - C_{i,Na^+} \cdot R_d, \quad (2)$$

where x_i – nss-fraction of anion in sample *i*,
X_i – concentration of anion in sample *i*,
C_{i,Na^+} – concentration of Na^+ in sample *i*,
R_d – ratio of anion X to Na^+ in sea water.

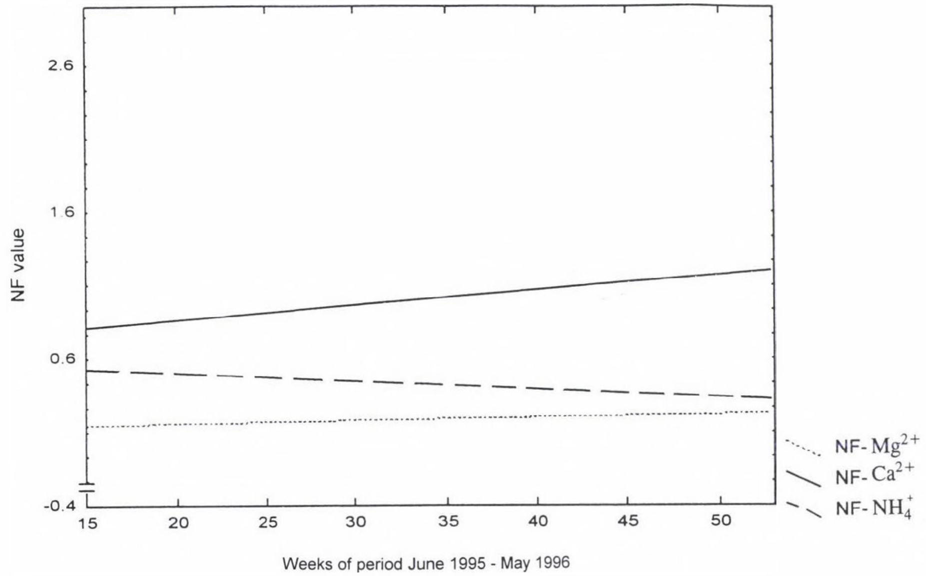

Fig. 1. Neutralization of rain water by Ca^{2+}, Mg^{2+} and NH_4^+.

Fig. 2 shows the contribution of anions during all the period. It seems that SO_4^{2-} has dominant role in the acidity of the rain water. The relative contribution of nss-Cl^- and NO_3^- to the acidity of rain water is variable but they compensate each other. If all the concentrations of nss-SO_4^{2-}, nss-Cl^- and NO_3^- in our samples were in respective acidic form, this would produce an average pH of 3.7 in the precipitation. Consequently, the high pH observed indicates a neutralization process caused by basic species incorporated in rain water.

The concentration of heavy metals in rain was lower than that of reported for the Mediterranean countries (*Amann et al.*, 1992).

The contribution of each ion to the sum of cation, anion and total ion mass in precipitation is shown on *Fig. 3*.

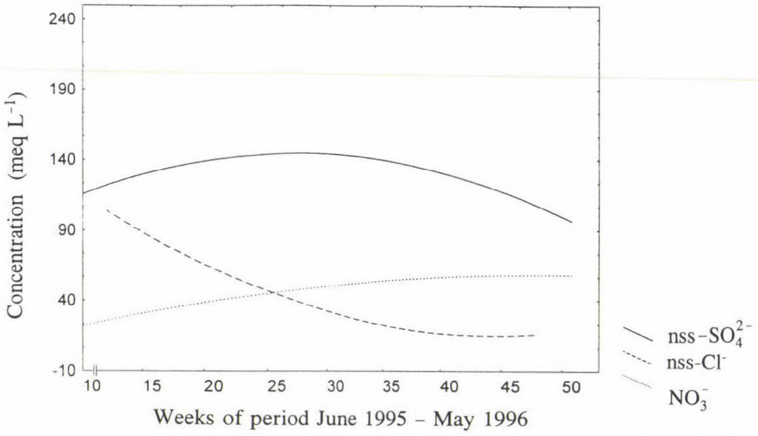

Fig. 2. Contribution of anions to the acidity of rain water.

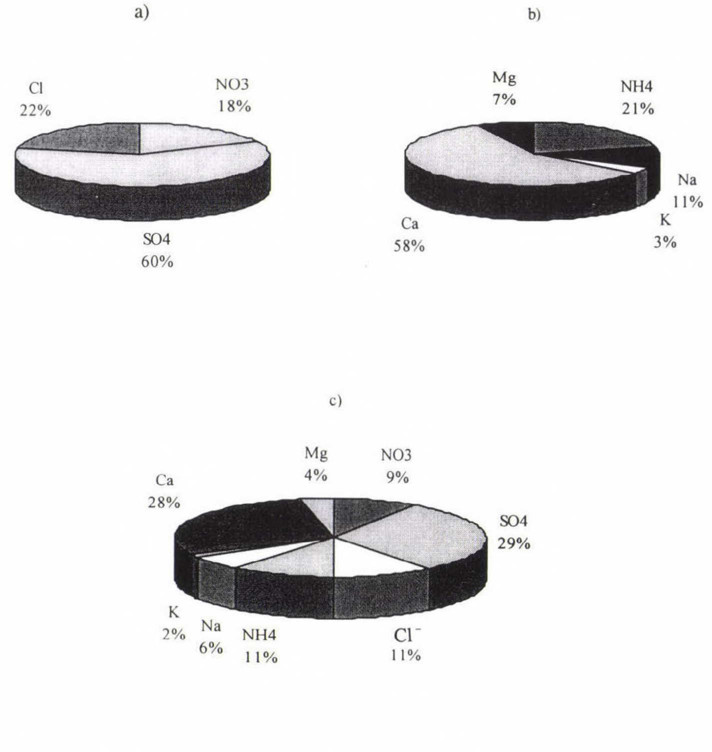

Fig. 3. Contribution of ions to chemical composition of rain water.

3.2 Sources of ions

Two methods were used to evaluate the sources of rain pollution. The most usual method of evaluating the contribution of sea salts to ion concentrations in rain water is to compare the ion/Na^- ratio in rain to that in sea water (*Samara et al.*, 1992). *Table 3* shows the ion/Na^- concentration ratios and the respective values in sea water.

Table 3. Ion/Na^+ concentration ratios in sea water and in our samples

Ion/Na^+ ratio	Ion/Na^+ concentration ratios			
	in sea water	in our samples		
		V.W.M.	G.M.	Mean
K^+/Na^+	0.02	0.28	-	0.28
Mg^{2+}/Na^+	0.22	0.72	0.66	0.74
Cl^-/Na^+	1.17	1.51	1.27	1.65
Ca^{2+}/Na^+	0.04	6.91	5.63	6.74
SO_4^{2-}/Na^+	0.12	4.95	3.85	4.60
SO_4^{2-}/NO_3^-	-	6.48	3.90	5.76

G.M. Geometric mean; V.W.M. Volume weight mean

Sea is considered to be the only source of sodium while the other ions may also be emitted from other industrial or natural sources. With this assumption we calculated the marine contribution of each ion that is incorporated in marine aerosols.

These contributions are graphically compared on *Fig 4*. It seems clearly that the nss concentrations are higher than the ss concentrations for every ions except Cl^-. Marine fraction of Cl^- is higher than non-marine fraction and has considerable value. Meanwhile for the other ions marine contribution is either weak or negligible.

Non-marine fraction of Ca^{2+} in rain is about 100 time higher than its marine fraction. A first explanation is the sampling method using a manual bulk precipitation sampler. The main source of atmospheric Ca^{2+} is believed to be the soil dust. It could be emitted by human activities such as traffic. In addition air masses originated from North Africa are rich in calcareous soil dust and may bring additional Ca^{2+} ions.

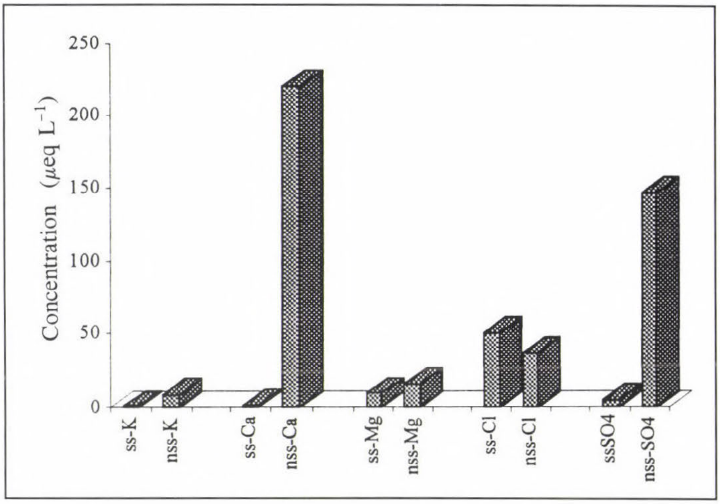

Fig. 4. Sea-salt and non-sea-salt concentrations.

The concentration of SO_4^{2-} in precipitation can be attributed to the oxidation process of SO_2 emitted from the local industry, and to the long-range transport from the industrialized countries.

Correlation analysis was used to obtain additional information on the sources of ions in the rain samples.

Na^+ and Cl^- ions are correlated with a coefficient of 0.6309 (44;0.0000) due to their common marine source. Most of the crustal elements, namely Ca^{2+}, Mg^{2+} are also correlated with each other with a coefficient of 0.7653 (47;0.0000). Their non-marine fractions (nss-Ca^{2+}, nss-Mg^{2+}) have better correlation (0.8225;43;0.0000). The Mg^{2+} ion is also correlated with Na^+ (0.7346;48;0.0000), indicating that a fraction of this element can be accounted for by sea salt.

Good correlations were found between SO_4^{2-} and Ca^{2+} (0.6689;44;0.0000), and SO_4^{2-} and Mg (0.6621;45;0.0000) which support the assumption that solid air particles may be potential sources for SO_4^{2-} in precipitation.

As shown from the inspection of the correlation matrix there is no correlation between NO_3^- and any other ions. This suggests that NO_3^- in rain originates from ionisation of nitrate salts which are produced by neutralization processes.

The quite good correlation of heavy metals (Cu^{2+}-Pb^{2+}; Zn^{2+}-Cd^{2+}; Cu^{2+}-Cd^{2+}; Pb^{2+}-Cd^{2+}; Cu^{2+}-Zn^{2+}) with linear correlation coefficients from 0.66 to 0.87 (47;0.0000) indicates their common anthropogenic sources.

3.3 Effects of meteorological variables

3.3.1 Seasonal effects

The chemical composition of precipitation varies in different seasons. While the conductivity (VWM) is constant during spring, a seasonal pattern is shown for other measured parameters in summer and autumn.

Concentration of ions that are dominant in chemical composition of rain (Ca^{2+}, SO_4^{2-}) appears to be constant almost through the year without any seasonal tendency. Their concentrations vary from 200 to 400 μeq L^{-1}, and from 100 to 250 μeq L^{-1} for Ca^{2+} and SO_4^{2-} in most of the rain events. The parameters that show wide range of variability are K^{2+}, Cl^- and Na^+.

Parameters, which are naturally coupled like pH and alkalinity show the same trend with the highest values in summer. Ca^{2+} content also shows its highest values in summer due to the influence of the warm and dry weather. The influence of weather conditions is reflected in contribution of soil dust, too. In calm weather conditions Ca^{2+} content exceeds 60.2% and 50.8% in spring and summer, respectively. Thus in spring, when calm weather conditions are more frequent, the contribution of soil dust in the concentration of these cations in the atmosphere of Tirana city is larger.

Ions, primarily originating from marine aerosols (Na^+, Cl^-) appear with lower values during the spring and achieve the highest level of their concentrations in winter. This allows to suggest that during the warm and dry summer the atmosphere is richer in marine aerosols that is reflected in increased value of ion (Na^+ and Cl^-) concentrations in the following seasons.

Fig. 5 shows VWM concentrations of SO_4^{2-}, NO_3^-, NH_4^+ and Ca^{2+} ions in March, April and May when fertilizers are mostly used (*Al-Momani et al.,* 1995). SO_4^{2-}, NO_3^- and NH_4^+ ions have a trend similar to that of the constituents of fertilizers, which suggests that fertilizers play an important role in the composition of rain water in this period. Meantime, Ca^{2+} ion shows a different temporal variation as expected.

There were not any significant differences in the seasonal concentrations of heavy metals.

3.3.2 Effects of wind directions

Meteorological variables such as air mass trajectories play an important role in the distribution of air pollution. The air flow direction in the higher level of the atmosphere influences the wind direction in the lower atmospheric layers. Surface winds measured in every hour were taken into account to relate rain composition to rain pollution origin. Frequency distribution of wind direction is given on *Fig. 6*, which shows that the chemical composition of rain during the period of study was strongly affected by NW direction and less strongly by SE, SW wind directions.

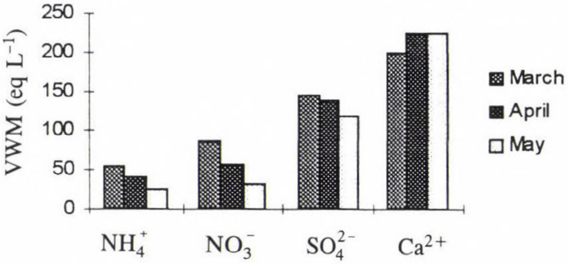

Fig. 5. Role of fertilizers in chemical composition of rain.

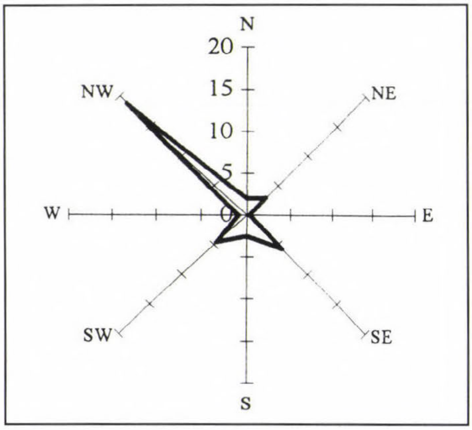

Fig. 6. Wind frequency direction (June 1995–May 1996). Q = 67.3%.

Rain samples are classified into six classes according to wind sectors. Rain samples effected by NW wind direction contained high concentrations of SO_4^{2-} and NO_3^-. It is likely due to the influence of long-range transport of SO_2 and NO_x from industrialised countries of Central Europe. The emissions of local industry are also transported. Their pH, due to the neutralization process extend to the level of the other classes.

Rain samples influenced by SE, SW were characterized by relatively high value of pH. This alkalinity can be attributed to the calcareous soil dust transported from North Africa, or from shorter distances.

The VWM concentrations of Na^+ and Cl^- do not show any trend according to wind direction as it can be expected. This indicates that Tirana region is effected by sea breeze during the whole period investigated.

Rain events are classified into rain and storm. The influence of marine aerosols presented by Na^+ and Cl^- concentrations was the highest in rain cases and the lowest in storm cases, probably due to the fact that most storms did not come from the sea direction. NO_3^- showed similar picture. The other parameters did not show significant variations with precipitation type.

Concentration of chemical parameters of Tirana rain samples analysed during this monitoring process were higher than those of reported for some Mediterranean countries, but were very close to those reported for Thessaloniki (Greece).

4. Conclusions

Monitoring of chemical composition of precipitation in Tirana was carried out according to a one year monitoring program based on standard analytical methods and quality assurance programs. The main features of the precipitation chemistry were:

(1) Rain samples showed neutral pH values, similar to those reported for some other Mediterranean countries.

(2) Neutralization process was attributed primarily to high concentration of Ca^{2+} ion (68%) followed by NH_4^+ (24%).

(3) The concentration of SO_4^{2-}, was higher than that of nitrates and chlorides. Nss-SO_4^{2-} plays the dominant role in acidifying the rain water.

(4) SO_4^{2-} and Ca^{2+} ions make the highest contribution to the chemical composition of rain. They account for 29% and 28% of the total mass of ions.

(5) The concentrations of heavy metals in rain were low, particularly Pb^{2+} and Cd^{2+} (0.1–7 ppb) were lower than those reported for other Mediterranean areas; whereas the level of Zn^{2+} (20–160 ppb) is closer to them.

(6) Concerning the sources of ions in the chemical composition of rain, the contribution of sea was found to be important on the level of Cl^-, whereas for other ions marine effect is negligible.

(7) During warm and dry summer conditions the atmosphere is mostly influenced by soil dust, and the concentration of crustal elements (Ca^{2+}, K^+, Mg^{2+}) and the parameters that are connected to them (pH, alkalinity) had their highest values.

(8) The rain samples influenced by the air flow originating from industrialized countries of Central Europe were distinguished by high concentrations of NO_3^- and SO_4^{2-}. At the same time, a good linear

correlation between SO_4^{2-}-Ca^{2+} and SO_4^{2-}-Mg^{2+} could be explained by the influence of solid air particles in the SO_4^{2-} concentration in composition of rain water.

(9) Chemical composition of precipitation varies seasonally. Spring is characterized by more calm weather situations, thus the contribution of soil dust to the concentration of these cations in the atmosphere of Tirana city is larger.

(10) Chemical composition of the rain water is also affected by the constituents of fertilizers (SO_4^{2-}, NO_3^-, NH_4^+) particularly during the period of their application.

References

Al-Momani, I.F., Ataman, O.Y., Anwari, M.A., Tuncel, S., Kose, C. and *Tuncel, G.*, 1995: Chemical composition of precipitation near an industrial area at Izmir, Turkey. *Atmospheric Environment 29*, 1131-1143.

Amann, M., Bertok, I., Cafala, J., Klaasse, G. and *Schopp, N.*, 1992: *Status Report: Strategies for Reducing Sulphur Dioxide Emissions in Europe*. IIASA, Laxenburg, Austria.

APHA, AWWA, WPCF, 1985: *Standard Methods for the Examination of Water and Wastewater*. 16th ed. American Public Health Association, Washington, D.C. 20005.

AQUACON, 1994: MedBas-Subproject No. 6: "Acid Rain Analysis". Intercomparison 1/93. In *Documenta dell´Instituto Italiano di Idrobiologia*, No. 47.

AQUACON, 1995: MedBas-Subproject No. 54: "Acid Rain Analysis". Intercomparison 1/95. In *Documenta dell´Instituto Italiano di Idrobiologia*, No. 47.

Avila, A., 1996: Time trends in the precipitation chemistry at a mountain site in northeastern Spain for the period 1983-1994. *Atmospheric Environment 30*, 1363-1373.

Gatz, D.F. and *Smith, L.*, 1995a: The standatd error of weighted mean concentration-I. Bootstrapping vs other methods. *Atmospheric Environment 29*, 1185-1193.

Gatz, D.F. and *Smith, L.*, 1995b: The standard error of weighted mean concentration-II. Estimating confidence intervals. *Atmospheric Environment 29*, 1195-1200.

Guerzoni, S., Cristine, A., Caboi, R., Le Bolcoch, O., Marras, I. and *Rundeddu, L.*, 1995: Ionic composition of rainwater and atmospheric aerosols in Sardenia, Southern Mediterranean. *Water Air and Soil Pollution 85*, 2077-2082.

Kulshrestha, U.C., Sarkar, A.K., Srivastava, S.S. and *Parashar, D.C.*, 1995: Wet-only and bulk deposition studies at New Delhi (India). *Water, Air and Soil Pollution 4*, 2137-2142.

Massart, D.L., Vandeginste, B.G.M., Deming, S.N., Michotte, Y. and *Kaufman, L.*, 1988: *Chemometrics: A Text Book*. Elsevier, Tokyo.

Meglen, R.R., 1985: A quality control protocol for the analytical laboratory. In *Environmental Applications of Chemometrics*. American Chemical Society, pp. 251-270.

Miller, J.C., 1988: *Statis. for Anal. Chem.* Second edition. New York.

Nadkarni, R.A., 1991: The quest for quality in the labortaory. *Analytical Chemistry 63*, 675A-682A.

Samara, C., Tsitouridou, R. and *Balafoutsis, C.*, 1992: Chemical composition of rain in Thessaloniki, Greece, in relation to meteorological conditions. *Atmospheric Environment 26B*, 359-367.

Sanusi, A., Wortham, H., Millett, H. and *Mirabel, P.*, 1996: Chemical composition of rainwater in eastern France. *Atmospheric Environment 30*, 59-71.

Sequeira, R. and *Lung, F.*, 1995: A critical data analysis and interpretation of the pH, ion loadings and electrical conductivity of rainwater from the territory of Hong Kong. *Atmospheric Environment 29*, 2439-2447.

ATMOSPHERIC ENVIRONMENT

an international journal

To promote the distribution of Atmospheric Environment *Időjárás* publishes regularly the contents of this important journal. For further information the interested reader is asked to contact *Prof. P. Brimblecombe*, School for Environmental Sciences, University of East Anglia, Norwich NR4 7TJ, U.K.; e-mail: atmos_env@uea.ac.uk

Volume 33 Number 1 1999

G.C.K. Lam, D.Y.C. Leung, M. Niewiadomski, S.W. Pang, A.W.F. Lee and *P.K.K. Louie:* Street-level concentrations of nitrogen dioxide and suspended particulate matter in Hing Kong, 1-11.

J.P. Kunsch: Critical velocity and range of a fire-gas plume in a ventilated tunnel, 13-24.

I.V. Patroescu, I. Barnes, K.H. Becker and *N. Mihalopoulos:* FT-IR product study of the OH-initiated oxidation of DMS in the presence of NO_x, 25-35.

D.M. Holland, P.P. Principe and *J.E. Sickles, II:* Trends in atmospheric sulfur and nitrogen species in the eastern United States for 1989-1995, 37-49.

R.H. Grant and *Ka-Lam Wong:* Ozone profiles over a suburban neighborhood, 51-63.

R.C. Musselman and *W.J. Massman:* Ozone flux to vegetation and its relationship to plant response and ambient air quality standards, 65-73.

T. Salthammer, A. Schwarz and *F. Fuhrmann:* Emission of reactive compounds and secondary products from wood-based furniture coating, 75-84.

H. Kaupp and *M.S. McLachlan:* Atmospheric particle size distributions of polychlorinated dibenzo-*p*-dioxins and dibenzofurans (PCDD/Fs) and polycyclic aromatic hydrocarbons (PAHs) and their implications for wet and dry deposition, 85-95.

R. Vecchi and *G. Vali*: Ozone assessment in the southern part of the Alps, 97-109.

N. Moschonas, D. Danalatos and *S. Glavas:* The effects of O_2 and NO_2 on the ring retaining products of the reaction of toluene with hydroxyl radicals, 111-116.

K. Koeltzsch: On the relationship between the Lagrangian and Eulerian time scale, 117-128.

J.L. Collett, Jr, K.J. Hoag, D.E. Sherman, A. Bator and *L. Willard Richardson:* Spatial and temporal variations in San Joaquin Valley fog chemistry, 129-140.

G.L. Hutchinson, W.X. Yang and *C.E. Andre:* Overcoming humidity dependence of the chromium trioxide converter used in luminol-based nitric oxide detection, 141-145.

Volume 33 Number 2 1999

B.R.T. Simoneit, J.J. Schaurer, C.G. Nolte, D.R. Oros, V.O. Elias, M.P. Fraser, W.F. Rogge and *G.R. Cass:* Levoglucosan, a tracer for cellulose in biomass burning and atmospheric particles, 173-182.

A. El-Hussein, A. Mohammed and *A.A. Ahmed:* Radon exhalation and ultrafine fraction of radon progeny in closed room air, 183-190.

P.-L. Leung and *R.M. Harrison:* Roadside and in-vehicle concentrations of monoaromatic hydrocarbons, 191-204.

N.V. Heeb, A.-M. Forss and *C. Bach:* Fast and quatitative measurements of benzene, toluence and C_2-benzenes in automotive exhaust during transient engine operation with and without catalytic axhaust gas treatment, 205-215.

T.G.M. Demmers, L.R. Burgess, J.L. Short, V.R. Phillips, J.A. Clark and *C.M. Wathes:* Ammonia emissions from two mechanically ventilated UK livestock buildings, 217-227.

F. Sauer, C. Schäfer, P. Neeb, O. Horie and *G.K. Moortgat:* Formation of hydrogen peroxide in the ozonolysis of isoprene and simple alkenes under humid conditions, 229-241.

D. Blaha, K. Bartlett, P. Czepiel, R. Harriss and *P. Crill:* Natural and anthropogenic methane sources in New England, 243-255.

Y.F. Li, Y.J. Zhang, G.L. Cao, J.H. Liu and *L.A. Barrie:* Distribution of seasonal SO_2 emissions from fuel combustion and industrial activities in Shanxi province, China, with 1/6°x1/4° longitude/latitude resolution, 257-265.

R.A. Hashmonay, M.G. Yost and *C.-Fu Wu:* Computed tomography of air pollutants using radial scanning path-integrated optical remote sensing, 267-274.

P.N. Price: Pollutant tomography using integrated concentration data from non-intersecting optical paths, 275-280.

A. Mauriiizi and *F. Tampieri:* Velocity probability density functions in Lagrangian dispersion models for inhomogeneous turbulence, 281-289.

B.L. Duffy, P.F. Nelson, Y. Ye and *I.A. Weeks:* Speciated hydrocarbons profiles and calculated reactiviiities of exhaust and evaporative emissions from 82 in-use light-duty Australian vehicles, 291-307.

R.M. Harrison, M. Jones and *G. Collins:* Measurements of the physical properties of particles in the urban atmosphere, 309-321.

D.R. Hastie, J. Narayan, C. Schiller, H. Niki, P.B. Shepson, D.M.L. Sills, P.A. Taylor, Wm. J. Moooroz, J.W. Drummond, N.Reid, R. Taylor, P.B. Roussel and *O.T. Melo:* Observational evidence for the impact of the lake breeze circulation on ozone concentrations in Southern Ontario, 323-35.

Volume 33 Number 3 1999

R.M. Koerner, D.A. Fisher and *K. Goto-Azuma:* A 100 year record of ion chemistry from Agassiz Ice Cap Northern Ellesmere Island NWT, CANADA, 347-357.

A. Rodrigo, A. Avila and *A. Gómez-Bolea:* Trace metal contents in *Parmelia capelia* (L.) Ach. compared to bulk deposition, throughfall and leaf-wash fluxes in two holm oak forests in Montseny (NE Spain), 359-367.

C.L. Blanchard, F.W. Lurmann, P.M. Roth, H.E. Jeffries and *M. Korc:* The use of ambient data to corroborate analyses of ozone control strategies, 369-381.

R.S. Gabruk, R.I. Sykes, C. Seigneur, P.Pai, P. Gillespie, R.W. Bergstrom and *P. Saxena:* Evaluation of thc reactive and optics model of emissions (ROME), 383-399.

D. Wang, S.R. Yates, J. Gan and *J.K. Knuteson:* Atmospheric volatilization of methyl bromide, 1,3-dichloropropene, and propargyl bromide through two plastic films: transfer coefficient and temperature effect, 401-407.

W.K. Jo and *K.H. Park:* Commuter exposure to volatile organic compounds under different driving conditions, 409-417.

A. Samecka-Cymerman and *A.J. Kempers:* Bioindication of heavy metals in the town Wroclaw (Poland) with evergreen plants, 419-430.

D.A. Winner and *G.R. Cass:* Modeling the long-term frequency distribution of regional ozone concentrations, 431-451.

W.J. Massmann: Molecular diffusivities of Hg vapor in air, O_2 and N_2 near STP and the kinematic viscosity and thermal diffusivity of air near STP, 453457.

M. Jang and *R.M. Kamens:* Newly characterized products and composition of secondary aerosols from thc reaction of a-pinene with ozone, 459-474.

C.F. Clement and *I.J. Ford:* Gas-to-particle conversion in thc atmosphere: I. Evidence form empirical atmospheric acrosols, 475-487.

C.F. Clement and *I.J. Ford:* Gas-to-particle conversion in the atmosphere:II. Analytical models of nucleation bursts, 489-499.

C. Duneñas, M.C. Fernández, S. Cañete, J. Carretero and *E. Liger:* ^{222}Rn concentrations, natural flow rate and the radiation exposure levels in the Nerja Cave, 501-510.

Volume 33 Number 4 1999

M.R. Heal, M.A. O'Donoghue and *J.N. Cape:* Overestimation of urban nitrogen dioxide by passive diffusion tubes: Overestimation of urban nitrogen dioxide by passive diffusion tubes: a comparative exposure and model study, 513-524.

T. Etzkorn, B. Klotz, S. Sørensen, I.V. Patroescu, I. Barnes, K.H. Becker and *U. Platt:* Gas-phase absorption cross sections of 24 monocyclic aromatic hydrocarbons in the UV and IR spectral ranges, 525-540.

C.J. Halsall, B. Gevao, M. Howsam, R.G.M. Lee, W.A. Ockenden and *K.C. Jones:* Temperature dependence of PCBs in the UK atmosphere, 541-552.

G. Buzorius, K. Hämeri, J. Pekkanen and *M. Kulmala:* Spatial variation of aerosol number concentration in Helsinki city, 553-565.

K. von Salzen and *K.H. Schlunzen:* A prognostic physico-chemical model of secondary and marine inorganic multicomponent aerosols I. Model description, 567-576.

B. Hall, C. Claiborn and *D. Baldocchi:* Measurement and modeling of the dry deposition of peroxides, 577-589.

S.M. Aschmann and *R. Atkinson:* Atmospheric chemistry of 1-methyl-2-pyr-olidinone, 591-599.

I. Mori, Y. Iwasaka, K. Matsunaga, M. Hayashi and *M. Nishikawa:* Chemical characteristics of free tropospheric aerosols over the Japan Sea coast: aircraft-borne measurements, 601-609.

B. Lighthart: An hypothesis describing the general temporal and spatial distribution of alfresco bacteria in the earth's atmospheric surface layer, 611-615.

G.M. Lovett, A.W. Thompson, J.B. Anderson and *J.J. Bowser:* Elevational patterns of sulfur deposition at a site in the Catskill Mountains, New York, 617-624.

D.L. MacTaggart, S.O. Farwell, J.R. Burdge, Z.T. Cai, T.J. Haakenson and *W.L. Bamesberger:* A continuous monitor-sulfur chemilumin-escence detector (CM-SCD) system for the measurement of total gaseous sulfur species in air, 625-632.

J.A. van Aardenne, G.R. Carmichael, H. Levy II, D. Streets and *L. Hordijk:* Anthropogenic NO_x emissions in Asia in the period 1990-2020, 633-646.

J.P. Putaud, B.M. Davison, S.F. Watts, N. Mihalopoulos, B.C. Nguyen and *C.N. Hewitt:* Dimethylsulfide and its oxidation products at two sites in Brittany (France), 647-659.

A. Scaperdas and *R.N. Colvile:* Assessing the representativeness of monitor data from an urban intersection site in central London, UK, 661-674.

NOTES TO CONTRIBUTORS OF *IDŐJÁRÁS*

The purpose of the journal is to publish papers in any field of meteorology and atmosphere related scientific areas. These may be

- reports on new results of scientific investigations,
- critical review articles summarizing current state of art of a certain topic,
- shorter contributions dealing with a particular question.

Each issue contains "News" and "Book review" sections.

Authors may be of any nationality, but the official language of the journal is English. Papers will be reviewed by unidentified referees.

Manuscripts should be sent to

Editor-in-Chief of IDŐJÁRÁS
P.O. Box 39
H-1675 Budapest, Hungary

in three copies including all illustrations. One set of illustrations has to be of camera ready quality, the other two might be lower quality.

Title part of the paper should contain the concise title, the name(s) of the author(s), the affiliation(s) including postal and E-mail address(es). In case of multiple authors, the cover letter should indicate the corresponding author.

Abstract should follow the title, it contains the purpose, the data and methods as well as the basic conclusion.

Key-words are necessary to help to classify the topic.

The text has to be typed in double spacing with wide margins. Word-processor printing is preferred. The use of SI units are expected. The negative exponent is preferred to solidus. Figures and tables should be consecutively numbered and referred to in the text.

Mathematical formulas are expected to be as simple as possible and numbered in parentheses at the right margin. Non-Latin letters and hand-written symbols should be indicated and explained by making marginal notes in pencil.

Tables should be marked by Arabic numbers and printed in separate sheets together with their captions. Avoid too lengthy or complicated tables.

Figures should be drawn or printed in black and white, without legends, on separate sheets. The legends of figures should be printed as separate list. Good quality laser printings are preferred as master copies.

References: The text citation should contain the name(s) of the author(s) in Italic letter and the year of publication. In case of one author: *Miller* (1989), or if the name of the author cannot be fitted into the text: *(Miller,* 1989); in the case of two authors: *Gamov* and *Cleveland* (1973); if there are more than two authors: *Smith et al.* (1990). When referring to several papers published in the same year by the same author, the year of publication should be followed by letters a,b etc. At the end of the paper the list of references should be arranged alphabetically. For an article: the name(s) of author(s) in Italics, year, title of article, name of journal, volume number (the latter two in Italics) and pages. E.g. *Nathan, K.K.,* 1986: A note on the relationship between photosynthetically active radiation and cloud amount. *Időjárás 90*, 10-13. For a book: the name(s) of author(s), year, title of the book (all in Italics except the year), publisher and place of publication. E.g. *Junge, C. E.,* 1963: *Air Chemistry and Radioactivity.* Academic Press, New York and London.

The final version should be submitted on diskette altogether with one hard copy. Use standard 3.5" or 5.25" DOS formatted diskettes. The preferred word-processors are WordPerfect 5.1 and MS Word 6.0.

Reprints: authors receive 30 reprints free of charge. Additional reprints may be ordered at the authors' expense when sending back the proofs to the Editorial Office.

More information: gmajor@met.hu
Information on the last issues:
http://www.met.hu/firat/ido-e.html

Published by the Hungarian Meteorological Service

Budapest, Hungary

INDEX: 26 361

HU ISSN 0324-6329

IDŐJÁRÁS

QUARTERLY JOURNAL
OF THE HUNGARIAN METEOROLOGICAL SERVICE

CONTENTS

****

http://www.met.hu/firat/ido-e.html

VOL. 103 * NO. 2 * APRIL–JUNE 1999

IDŐJÁRÁS

Quarterly Journal of the Hungarian Meteorological Service

Editor-in-Chief
G. MAJOR

Executive Editor
M. ANTAL

Editorial Office: P.O. Box 39, H-1675 Budapest, Hungary or
Gilice tér 39, H-1181 Budapest, Hungary
E-mail: gmajor@met.hu or *antal@met.hu*
Fax: (36-1) 290-7387

Subscription by

mail: IDŐJÁRÁS, P.O. Box 39, H-1675 Budapest, Hungary;
E-mail: gmajor@met.hu or *antal@met.hu*; *Fax: (36-1) 290-7387*

IDŐJÁRÁS
Quarterly Journal of the Hungarian Meteorological Service
Vol. 103, No. 2, April–June 1999, pp. 85–91

New results on the chemical composition of aerosol particles in the atmosphere. Are cloud condensation nuclei produced by the biosphere?

Ernő Mészáros

Department of Earth and Environmental Sciences,
University of Veszprém
H-8201 Veszprém, P.O. Box 158, Hungary
e-mail: meszaros@anal.venus.vein.hu

(Manuscript received 18 February 1999; in final form 7 May 1999)

Abstract—It is generally accepted that cloud condensation nuclei (CCN) consist of the water soluble fine aerosol particles with size below about 1 μm. Former results about the chemical composition of inorganic aerosol particles indicated that water soluble compounds were mostly composed of ammonium sulfate, ammonium bisulfate or sulfuric acid as a function of ammonia available in the air. Under continental conditions nitrate can also be found in the particles in a smaller quantity. On this basis it was postulated that CCN were sulfate particles formed in the air by chemical reactions. Under oceanic conditions the precursor gas is dimethyl sulfide, while over the continents sulfate particles originate from sulfur dioxide. Since this gas is mostly of anthropogenic origin, one concluded that continental CCN are mainly due to human activities. Owing to the spectacular progress in analytical chemistry, during the last years the organic part of the atmospheric aerosol has also been studied. The results obtained are of interest in particular when the water soluble fraction of organic compounds is also investigated. These new research efforts resulted in the following findings. Firstly, under continental conditions the organic carbon concentration is comparable to that of sulfate ions. Secondly, at least half of the mass of organic carbon can be found in compounds soluble in water. Finally, an important part of water soluble organic carbon consists of macromolecular compounds. The aim of this paper is to summarize the results of these recent studies, including those carried out in Hungary. On the other hand, the significance of the new information is discussed from the point of view of water vapor condensation. It is speculated, but not proved, that we cannot exclude the possibility that, beside sulfates, organic substances also provide active cloud condensation nuclei.

1. Introduction

The chemical composition of atmospheric aerosol particles is of interest for many problems in environmental science. For atmospheric research the particle composition is important in particular for understanding the phase transition of water in the air. Thus, cloud droplets form on aerosol particles called cloud condensation nuclei (CCN). Thermodynamic calculations show that water soluble particles are very active in this process. For this reason many programs have been carried out to study the size and nature of water soluble substances. This is understandable since the number of CCN active at a given supersaturation determines the structure of clouds (the concentration and diameter of cloud droplets). This means that they control, among other things, the precipitation forming ability and albedo of the clouds.

Studies done in this field indicated that the number of coarse particles (with diameter above 1 μm), formed by the desintegration of the Earth surface, is too low compared to the concentration of cloud droplets. This implies that the sizes of CCN are in the fine particle size range consisting of particles with diameter below the above value. *Junge* (1963) was the first who demonstrated that in continental environment water soluble particles in the size range of $0.2 < d < 2.0$ μm (where d is the particle diameter) are composed of ammonium sulfate, ammonium bisulfate or sulfuric acid as a function of gaseous ammonia available. Later it was found (*Mészáros*, 1968) that particles smaller than 0.2 μm contain about half of the mass of sulfate and ammonium ions This means that, on a number basis, the great majority of sulfate particles have a diameter below the above value. Further, the study of the morphology of fine aerosol particles collected under oceanic conditions made it evident that sulfate particles are predominant in the fine size range even in air above the sea surface (*A. Mészáros* and *Vissy*, 1974; *Butor,* 1976). These sulfate particles form by the condensation of the reaction products of dimethyl sulfide emitted by the oceanic biota (*Charlson et al.*, 1987). On the other hand, *Twomey* (1968) pointed out on the basis of the volatility of CCN that they consists of sulfate particles. This conclusion was confirmed by several authors using different measuring techniques. Consequently, it was concluded that continental clouds form on sulfate particles of anthropogenic origin (*Twomey*, 1991; *Hudson*, 1991). This raised the question: how did continental clouds form before the industrial revolution (*Mészáros*, 1992). Anyway, it seemed that something is still needed to explain the formation of clouds at least under continental conditions.

2. New findings on the chemical composition

One possible explanation of the formation and structure of continental clouds without human activities is to suppose that CCN are also due to particle production by vegetation. This possibility was raised over three decades ago by *Went* (1960). He postulated that the blue-haze formed over forested areas in summer, during sunny, calm periods, is the result of the reactions of volatile organic compounds released by vegetation. Unfortunately this promising proposition has not been considered in detail after the publication of that paper.

This situation was partly due to analytical difficulties. The second problem was the fact that, before analyses, aerosol samples were generally dissolved in organic solvents. As an example, *Rogge et al.* (1993) leached the samples by hexane and a mixture of benzene/isopropanol and analyzed the liquids obtained by up-to-date gas chromatographic and other techniques. They found that in polluted air in southern California (U.S.A.) 45% of total fine aerosol mass is due to carbonaceous particles. One third of this quantity is elemental (black) carbon, while two thirds is organic carbon. *The ratio of organic carbon to sulfate* (measured parallel) *is larger than unity*. In spite of the fact that the authors cited identified more than 80 organic compounds, the mass of the species identified constituted only 10% of the total carbon mass. The compounds identified were mostly *organic acids* like aromatic polycarboxylic acids, aliphatic dicarboxylic acids and n-alkanoic acids.

On the basis of their samplings at remote Californian and oceanic sites, *Simoneit* and *Mazurek* (1982) stated that higher plant waxes constituted the predominant natural component of the aerosol. These waxes consist mostly of *lipids* with much higher concentrations at continental sites. The materials extractable from lipids by the solvent dichloromethane are composed primarily of n-alkanes (and other hydrocarbons), fatty acids and fatty alcohols. In the air, *carboxylic acids* (simpler than fatty acids) are also ubiquitous. These species have low molecular weights and high polarity. Consequently they are soluble in atmospheric waters. Thus, formic and acetic acids were detected in precipitation samples collected under different conditions. Their concentrations were substantial particularly in the tropics (*Keen et al.*, 1983). Further studies also indicated that carboxylic acids can also be identified in aerosol samples. These studies show that oxalic acid is the most important carboxylic acid in the atmospheric aerosol. The size distribution of oxalate ions is very similar to that of sulfate, which makes it possible that they form internally mixed particles with sulfate ions (*Mészáros et al.*, 1997).

In the atmosphere the natural solvent is water, and lead to phenomena like haze, fog and clouds. For this reason, a new era in the study of organic substances was begun when water soluble substances were also extracted from aerosol samples. *Mukai* and *Ambe* (1986) did not use water, but leached the samples by an alkaline solution. By analyzing aerosol samples collected in rural Japan, they obtained in this way a brownish liquid with characteristics very similar to those of *humic acids* common in the soil. This finding was in agreement with the results of *Likens et al.* (1983) indicating that in precipitation samples dissolved macromolecules (molecular mass above 1000) can be found in relatively high concentration. However, Mukai and Ambe reported low concentrations of macromolecular humic-like substances in the atmospheric aerosol.

In Europe, macromolecules in aerosol samples were first identified by *Havers et al.* (1998) in Germany. According to their publication humic-like substances made up a significant part of organic carbon. These substances consist mainly of polysaccharides and aliphatic substructures. This finding was essentially confirmed by *Zappoli et al.* (1999) on the basis of the analyses of fine aerosol samples collected in Sweden, Hungary and Italy. This international group also demonstrated that an *important part* (half on an average) *of humic-like macromolecules is soluble in water*. The comparison of the thermograms of aerosol particles collected in Hungary and humic acid standards also showed (*Gelencsér et al.*, 1999) that humic-like substances cannot be found in the coarse size range. This means that the formation of the particles containing these materials is different from the simple disintegration of the surface. Recent analyses by pyrolysis gas chromatography-mass spectrometry (*Gelencsér*, unpublished material) also indicate that macromolecules in the fine size range are composed of polysaccharides, lignins, proteins and lipids very similarly to major soil compounds.

The carbon thermograms of fine aerosol particles collected in rural air over Hungary are characterized by two peaks (*Gelencsér et al.*, 1999). The first peak at lower temperature refers to more volatile and/or more easily oxidizable organic compounds, while the considerably larger second peak represents less volatile and/or less oxidizable species (and a lesser extent elemental carbon). Humic acid standards produced only the second peak at the higher temperature. This indicates that humic acid-like, macromolecular substances constitute the second peak. On the other hand one can speculate that the first peak is mostly due to low molecular mass carboxylic acids. By accepting this concept, which needs further confirmation, one can state that in Hungary the concentration of macromolecular species is much higher than that of carboxylic acids. However, identical analyses of fine aerosol particles sampled in the Swiss Alps (*Krivácsy*, unpublished material) indicate that in cleaner tropospheric air carboxylic acids account for a higher fraction of organic carbon compared to macromolecular species. This is in agreement with the results obtained recently in very clean Arctic air, according to which water soluble organic species are composed mainly of carboxylic acids (*Kawamura et al.*, 1998).

3. Discussion: the possible composition of CCN

On the basis of the above results one can conclude that an important fraction of fine organic particles is soluble in water. *The water soluble organic species consist either of carboxylic acids* with low carbon number *or of macromolecular substances* that behave like humic acids. Although carboxylic acids can be formed by chemical reactions in the atmosphere, it is improbable that macromolecular compounds are created in this way. The soil does not produce macromolecular aerosol compounds by mechanical desintegration. This is proved by the fact that no macromolecules were identified in the coarse size range. Secondly, biomass burning is not substantial in Hungary. For this reason one has to postulate that macromolecular organics in the aerosol are attributed to primary biogenic sources.

It is to be noted that the possibility that natural vegetation emits CCN under tropical and intertropical conditions was proposed several years ago. *Désalmand et al.* (1982) found in the Ivory Coast that in the dry season CCN are due to biomass burning, while in the rainy season high relative humidities, favorable for the bacterial decomposition of plants, result in higher CCN concentrations. Désalmand and her coworkers did not measure the particle composition. However, other studies on the elemental composition carried out in the Amazon basin show that primary biogenic particles constitute 55–95% of the mass of fine particles (*Artaxo* and *Hansson*, 1995). On the basis of the material presented in this paper we can raise the question whether *organic particles give an important part of CCN even at mid-latitudes*. Considering the large water soluble organic fraction of the atmospheric aerosol we cannot exclude that the answer is positive. Thus, we have to take into account seriously this possibility.

It would be difficult to compare the importance of organic water soluble substances in condensation relative to that of sulfate particles. For example, in rural air over Hungary about one third of the mass of fine particles is composed of sulfate. Organic carbon also constitutes about 30% of the total mass concentration. However, this fraction is expressed as *elemental* carbon and not an organic *compound*. As we have seen above, macromolecular species are present in a rather high proportion. For this reason we can suppose with caution that carbon concentration must be multiplied by two, as a first approximation, to obtain the concentration of carbon compounds as a whole. This speculation results in organic mass two times greater than that of sulfate ions. Since only half of the organics is soluble in water (see above), one receives in this way that *the mass concentration* of water soluble organic species is approximately equal to that of sulfate. One has to note in this respect that *Saxena et al.* (1995) measured the hygroscopic growth of particles in Arizona (U.S.A.) by using a special measuring technique. They also determined the size distribution of ammonium sulfate and organic particles. At the same time they calculated, by a thermodynamic approach, the hygroscopic particle growth due to ammonium sulfate alone. They found that at high relative humidities the water quantity measured was twice the calculated value. Since the organic mass fraction correlated well with the excess water, the American authors concluded that the half of the liquid water on aerosol particles is caused by the presence of water soluble organic compounds. This conclusion is in surprisingly good agreement with the results of our chemical measurements.

One has to also mention that recent fog studies in Po Valley, Italy, demonstrate (*Facchini et al.,* 1999) that the partitioning of organic compounds between fog water and interstitial aerosol depends on the water solubility of particles. Thus, *polar water soluble species* constituting the major fraction of total carbon *can be found mostly in droplet phase,* while insoluble carbon is detected preferentially in interstitial particles. This study also show water soluble organic species are scavenged by fog droplets similarly to inorganic ions. This important finding also points in the direction that CCN consist at least partly of water soluble organics.

For further considerations it would be necessary to have some information on the size distribution of macromolecular compounds, since size plays an important part in the control of the condensation activity of aerosol particles. Another problem is whether CCN have a sufficient size (mass) to be detected by chemical analyses of fine particles. Anyway we note that there is some indication that organic species constitute smaller particles than sulfate ions (*Novakov* and *Penner*, 1993). This means that the *number concentration* of organic particles is higher than the number of sulfate particles if their mass concentrations are equal. This would point in the direction that organic particles give more CCN than sulfate aerosols. However, the solubility of the humic acid-like species is an open question. Although this is not proved, one can speculate that the affinity of sulfate to water is stronger than that of soluble organic species. This means that sulfate particles are active in condensation at lower supersaturations than organic particles.

Finally, we can state that during the last years much new information has been obtained concerning the chemical composition of aerosol particles in the air. This information makes it possible to consider the problem of CCN in a new perspective. However, many new questions have arisen. Thus, it goes without saying, that before drawing a final conclusion on the nature of CCN, further studies are needed. It seems to be particularly important to link direct measurements of CCN with chemical analysis of the organic fraction of the atmospheric aerosol.

References

Artaxo, P. and *Hansson, H.C.*, 1995: Size distribution of biogenic aerosol particles from the Amazon basin. *Atmospheric Environment 29*, 393-402.

Butor, J.F., 1976: Application des techniques de la microscopie électronique à l'étude de aérosol fin. Thèse 3e cycle, Brest, *Rapport C.E.A.R.O.* 4709.

Charlson, R.J., Lovelock, J.E., Andreae, M.O. and *Warren, S.G.*, 1987: Oceanic phytoplankton, atmospheric sulfur, cloud albedo and climate. *Nature 326*, 665-661.

Désalmand, F., Baudet, J. and *Serpolay, R.*, 1982: Influence of rainfall on the seasonal variations of cloud condensation nuclei concentrations in a subequatorial climate. *J. Atmospheric Sci., 39*, 2076-2082.

Facchini, M.C., Fuzzi, S., Zappoli, S., Andracchio, A., Gelencsér, A., Kiss, Gy., Krivácsy, Z., Mészáros, E., Hansson, H.-C., Alsberg, T. and *Zebühr, Y.*, 1999: Partitioning of the organic aerosol component between fog droplets and interstitial air. Submitted to *Journal of Geophysical Research.*

Gelencsér, A., Hoffer, A., Molnár, A., Krivácsy, Z., Kiss, Gy. and *Mészáros, E.*, 1999: Thermal behaviour of carbonaceous aerosol from a continental background site. Submitted to *Atmospheric Environment.*

Havers, N., Burba, P., Lambert, P. and *Klokow, D.*, 1998: Spectroscopic characterization of humic-like substances in airborne particulate matter. *J. Atmospheric Chem. 29*, 45-54.

Hudson, J.G., 1991: Observation of anthropogenic cloud condensation nuclei. *Atmospheric Environment 25A*, 24449-2451.

Junge, C.E., 1963: *Air Chemistry and Radioactivity*. Academic Press. New York and London.

Kawamura, K. Legrand, M. and *Cachier, H.*, 1998: Organic matter in polar aerosol, snow and ice. *IGAC Newsletter 14*, 12-15.

Keen, W.C., Galloway, J.N. and *Holden, J.D. Jr.*, 1983: Measurements of weak organic acidity in precipitation from remote area of the world. *J. Geophysical Res. 88*, 5122-5130.

Likens, G.E., Edgerton, E.S. and *Galloway, J.N.*, 1983: The composition and decomposition of organic carbon in precipitation. *Tellus 35B*, 16-24.

Mészáros, A. and *Vissy, K.*, 1974: Concentration, size distribution and chemical nature of atmospheric aerosol particles in remote oceanic areas. *J. Aerosol Sci. 5*, 101-110.

Mészáros, E., 1968: On the size distribution of water soluble particles in the atmosphere. *Tellus 20*, 443-448.

Mészáros, E., 1992: Structure of continental clouds before the industrial era: a mystery to be solveo. *Atmospheric Environment 26A*, 2469-2470.

Mészáros, E., Barcza, T., Gelencsér, A., Hlavay, J., Kiss, Gy., Krivácsy, Z., Molnár, A. and *Polyák, K.*, 1997: Size distribution of inorganic and organic species in the atmospheric aerosol in Hungary. *J. Aerosol Sci. 28*, 1163-1175.

Mukai, A. and *Ambe, Y.*, 1986: Characterization of humic like-acid brown substance in airborne particulate matter and tentative identification of its origin. *Atmospheric Environment 20*, 813-819.

Novakov, T. and *Penner, J.E.*, 1993: Large contribution of organic aerosol to cloud-condensation-nuclei concentration. *Nature 365*, 823-826.

Rogge, W.F., Mazurek, M.A., Hildeman, L.M. and *Cass, G.R.*, 1993: Quantification of organic urban aerosol at molecular level: identification, abundance and seasonal variation. *Atmospheric Environment 27A*, 1309-1330.

Saxena, P., Hildeman, L.M., Mc Murry, P.H. and *Seinfeld, J.H.*, 1995: Organics alter the atmospheric behavior of hygroscopic particles. *J. Geophys. Res. 100*, 18755-18770.

Simoneit, B.R.T. and *Mazurek, M.A.*, 1982: Orgonic matter of the troposphere–II. Natural background of biogenic lipid matters over the rural western United States. *Atmospheric Environment 16*, 2139-2159.

Twomey, S., 1968: On the composition of cloud nuclei in the north-eastern United States. *J. Rech. Atmosphérique 4*, 281-285.

Twomey, S., 1991: Aerosol, clouds and radiation. *Atmospheric Environment 25A*, 2435-2442.

Went, F.W., 1960: Blue haze in the atmosphere. *Nature 187*, 641-643.

Zappoli, S., Andracchino, A., Fuzzi, S., Facchini, M.C., Gelencsér, A., Kiss, Gy., Krivácsy, Z., Molnár, A., Mészáros, E., Hansson, H.C. and *Rosman, K.*, 1999: Inorganic and organic macromolecular components of fine aerosol in different areas of Europe in relation to their water solubility. *Atmospheric Environment 33*, 2733-2743.

IDŐJÁRÁS
Quarterly Journal of the Hungarian Meteorological Service
Vol. 103, No. 2, April–June 1999, pp. 93–105

Measurements of atmospheric carbon dioxide at a low elevation rural site in Central Europe

László Haszpra

Hungarian Meteorological Service
H-1675 Budapest, P.O. Box 39, Hungary; e-mail: haszpra@met.hu

(Manuscript received 4 January 1999; in final form 20 April 1999)

Abstract–The atmospheric mixing ratio of carbon dioxide has been measured since 1981 at K-puszta (Hungary) as part of the WMO BAPMoN/GAW program. The data show remarkable daily and seasonal variations due to the activity of the surrounding vegetation. The mean daily amplitude is 43 ppm in July and 5 ppm in January. Considering only the spatially more representative daytime values the annual amplitude of the mixing ratio is 28 ppm. The trend and the temporal course of the growth rate of the daytime mixing ratio are similar to those observed at Mauna Loa, Hawaii, Point Barrow, Alaska, or at monitoring sites in Germany. The overall trend during 1981–1998 is 1.51 ppm/year with a short term fluctuation between –4.3 and +7.0 ppm/year.

Key-words: trends in the composition of the atmosphere, carbon dioxide, diurnal variation, seasonal variation.

1. Introduction

The atmospheric mixing ratio of carbon dioxide has been increasing for at least 200 years due to human activity (see ice core measurements of e.g. *Barnola et al.* (1995) or *Etheridge et al.* (1996), and the direct atmospheric measurements of e.g. *Beardsmore* and *Pearman* (1987), *Keeling et al.* (1989), *Keeling* and *Whorf* (1994), *Thoning et al.* (1994) or *Levin et al.* (1995)). This increase may enhance the greenhouse effect of the atmosphere generating global climatic change (*IPCC*, 1996). Recently, several papers based on atmospheric measurements and model calculations (e.g. *Keeling et al.*, 1989; *Tans et al.*, 1989; 1990; *Enting* and *Mansbridge*, 1991; *Musselman* and *Fox*, 1991; *Tans*, 1991; *Quay et al.*, 1992; *Sarmiento* and *Sundquist*, 1992; *Sundquist*, 1993; *Dixon et al.*, 1994; *Hesshaimer et al.*, 1994; *Ciais et al.*, 1995; *Denning et al.*, 1995; *Taguchi*, 1996) concluded that there should be a large CO_2 sink in the northern hemisphere. A number of these papers suggest that this "missing sink" is the terrestrial biosphere in the northern temperate latitudes. The characterization and quantification of the "missing sink" needs additional monitoring sites in this region (*Tans*, 1991) and the evaluation of the data measured by the stations already in operation. However, most of the existing monitoring sites are located on high mountains or on the sea shore, while the majority of the area of the continents is of low elevation, close to vegetation and far from the sea.

Inverse modelling techniques (e.g. *Enting et al.*, 1995; *Law et al.*, 1996), among others, combining general circulation models, existing mixing ratio measurements and known source data are used for estimating the location and strength of the "missing sink". Data series obtained at continental monitoring sites show special features due to local conditions, which have to be taken in account before their inclusion in a global study. The diurnal variation in CO_2 mixing ratios may give information about the spatial representativeness of the data, and may suggest a data selection technique, as will be seen in this paper. The amplitude, relative phase and temporal variation of the seasonal cycle may reflect the location, strength and evolution of the sources and sinks. The average mixing ratio, its trend, and its changes relative to those at other monitoring sites may indicate the areas and factors influencing the global atmospheric carbon budget. This paper presents the 17-year long time series and its characteristic features from a low elevation, continental station located in one of the suspected regions of the "missing sink", for those, who intend to use the data in global models.

2. Sampling site and instrumentation

K-puszta regional background air pollution monitoring station is located at 46°58'N, 19°33'E, 125 m above mean sea level, on the Hungarian Great Plain, in the middle of the Carpathian Basin (*Fig. 1*). The station is located in a big (approx. 0.3 km^2) clearing in a forested area where the immediate surroundings of the station are kept undisturbed by human activity. The nearest public road and settlements (a few hundred inhabitants) are about 3 km to the east/southeast of the station (*Fig. 2*). At the station there is no notable local anthropogenic source (electric heating, no local generator, the staff only consists of a part-time observer). K-puszta is as free from direct pollution as it is possible in highly industrialized, densely populated Central Europe.

The biggest pollution source in this region is Budapest (1.9 million inhabitants), approximately 80 km NNW from K-puszta. The second largest city is Kecskemét (100 thousand inhabitants), located 20 km to the southeast of the station. The prevailing wind in this region is northwesterly and the average wind speed is only 1.9 m/s.

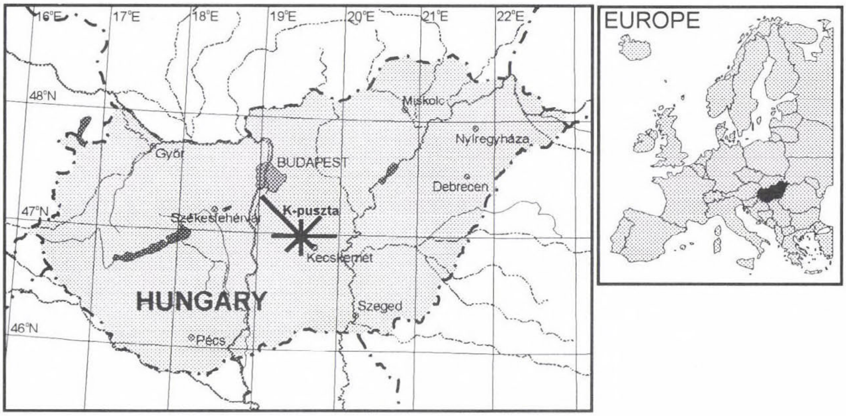

Fig. 1. Geographical location of K-puszta and major cities (more than 100 thousand inhab.), as well as the frequency distribution of the wind direction at K-puszta.

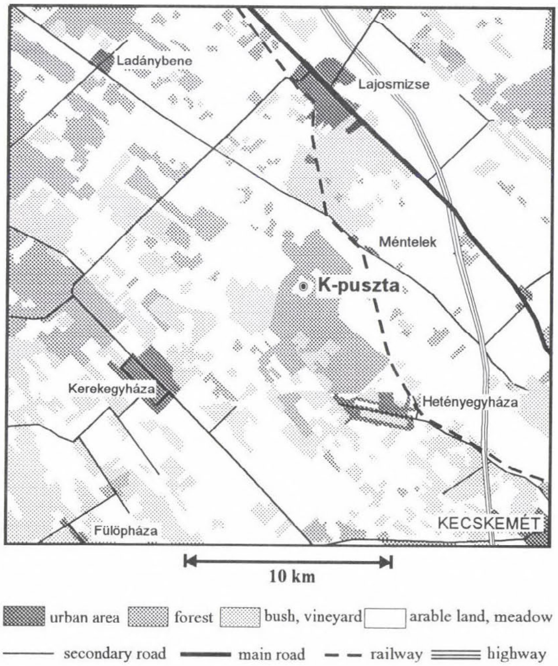

Fig. 2. Region of K-puszta.

At K-puszta the Institute for Atmospheric Physics of the Hungarian Meteorological Service has been operating a SIEMENS ULTRAMAT 3 CO_2 analyzer since July 1981, for the BAPMoN/GAW program of the World Meteorological Organization. The air inlet of the instrument is at 10 m above grass-covered, sandy ground. Before 1993 the instrument was calibrated against CO_2-in-nitrogen standards provided by the Scripps Institution for Oceanography, U.S.A. (*Haszpra*, 1995). During that time a linear response function was determined on the basis of three standard gases. Since 1993 four CO_2-in-air standards obtained from the National Oceanic and Atmospheric Administration (NOAA-U.S.A.) have been used. For the determination of the mixing ratio quadratic response functions are used. Between two calibrations the response function is linearly interpolated. The pre-1993 data have been corrected against pressure broadening effect *after* the 1992 WMO Round-Robin Inter-laboratory Intercomparison (*Pearman*, 1993). The data presented in this paper are expressed on the WMO Manometric Scale.

3. Data selection and averaging

In order to characterize the carbon dioxide content of the lower troposphere in most of our studies the mixing ratios measured only in the early afternoon hours (12-16 h, local standard time [LST]) are used, when the vertical mixing of the atmosphere is the most intensive (see also Chapter 4.1). For data selection the commonly used clean air sector method (sector from which no anthropogenic influence is expected) cannot be applied because such a sector can hardly be defined: the concentration field is fairly isotropic (*Fig. 3*). It may be the result of the more or less evenly distributed sources and sinks around the station and the large scale mixing in the Carpathian Basin. A similar result was obtained for pollution by anthropogenic non-methane hydrocarbons (*Haszpra et al.*, 1994) which could indicate the direction of the major anthropogenic source areas, like Budapest. As the region is climatologically calm, data selection based on the wind speed (e.g. *Levin et al.*, 1995) is hardly applicable either. Therefore, only the technically false data are rejected. The data are available at the WMO World Data Center for Greenhouse Gases, Tokyo, Japan, and at the Carbon Dioxide Information Analysis Center, Oak Ridge, Tennessee, U.S.A.

The raw data are the 30 minute averages. The 'daily average' mixing ratio of the early afternoon hours is calculated if at least four 30 minute averages are available. The daily average for the whole day is calculated only if 50% of the data is available for both the daytime hours (10–18 h LST) and nighttime hours (21–05 h LST). A monthly average is calculated from the daily averages if at least 10 daily averages are available for the calculation.

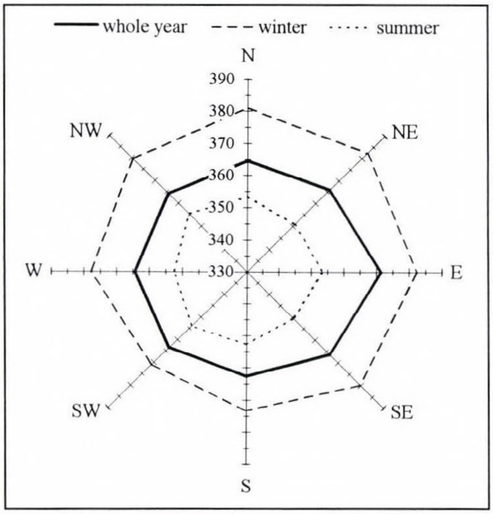

Fig. 3. Sectorial distribution of the atmospheric mixing ratio (ppm) of carbon dioxide at K-puszta in winter (Dec–Feb), in summer (Jun–Aug) and in the whole year of 1997 in the early afternoon hours (12–16 h LST), when the wind speed is higher than 0.5 m/s. When the wind speed is less than 0.5 m/s the average mixing ratios are 363.7 ppm, 375.4 ppm and 351.8 ppm for the whole year, winter and summer, respectively.

4. Data analysis

Fig. 4 shows the time series of the daily average mixing ratios based on the early afternoon (12–16 h) measurements. The data gaps in the 90's are caused by the long delivery time for spare parts of the instrument and the station reconstruction in 1992, while in the earlier years even obtaining a tank of reference gas was problematic. The average availability of the data between 1989 and 1997 is 72%, including the data gaps in late 1990, 1992 and 1996.

4.1 Diurnal cycle

The station is surrounded by vegetation and located in a flat, low elevation, climatologically calm region, where a shallow nocturnal boundary layer forms frequently. Carbon dioxide emitted by the vegetation and soil accumulates in that layer, where the nighttime mixing ratio may exceed 500 ppm on certain summer nights. The average daily variation relative to the daily average is presented in *Fig. 5* for one month in each of the four seasons. The average daily amplitude is as high as 43 ppm in July, while it is negligible (less than 5 ppm) in January. A similar feature can be observed at other low elevation continental sites like at Waldhof, Germany (53°N, 11°E, 73 m a.s.l.) (*Levin et al.*, 1995). For the interpretation of the diurnal variations of the mixing ratio the average daytime and nighttime depth of the mixed layer are also presented in *Fig. 6*.

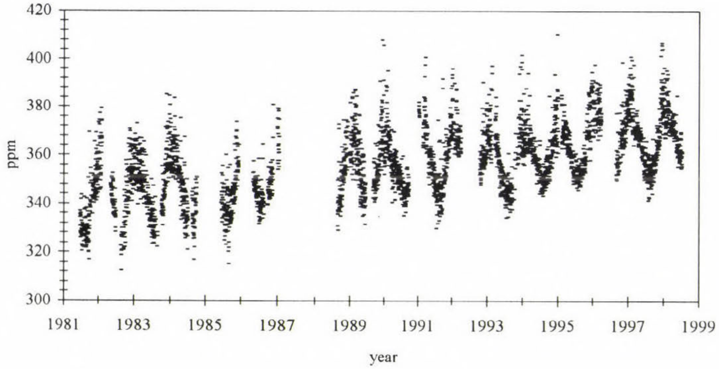

Fig. 4. Daily average atmospheric mixing ratio of carbon dioxide at K-puszta, based on the early afternoon (12–16 h LST) measurements.

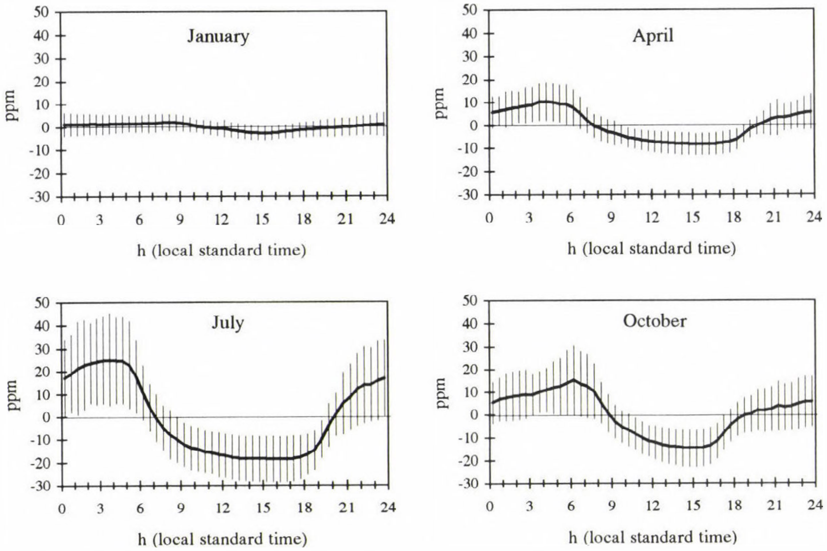

Fig. 5. The average diurnal cycle of CO_2 mixing ratio at K-puszta relative to the daily average (error bar = $\pm\sigma$).

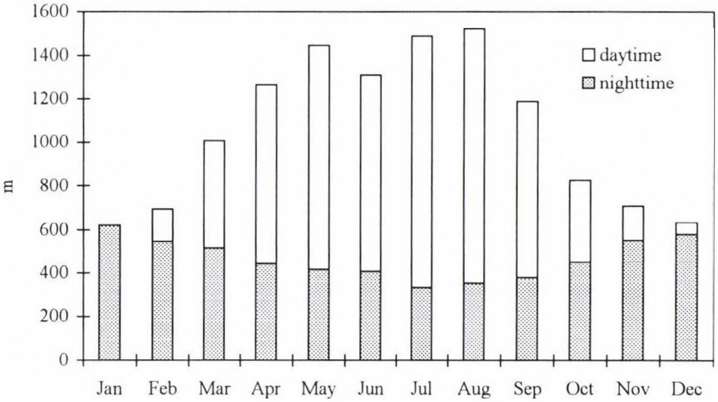

Fig. 6. The average daytime and nighttime depth of the mixed layer between 1987 and 1992 in a suburb of Budapest, 70 km from K-puszta based on the data and method of *Matyasovszky* and *Weidinger* (1998).

The respiration depends strongly on the characteristics of the soil and vegetation, therefore it may be site specific. Consequently, the high nighttime concentrations formed in the shallow stable boundary layer may have much lower spatial representativeness than the early afternoon ones when the mixing processes homogenize a deep layer of the atmosphere. For the regional characterization of the carbon dioxide content of the lower troposphere *we use only the data measured between 12 h and 16 h local standard time.* The tall tower measurements in the U.S.A. (*Bakwin et al.*, 1995) and the analysis of the data of the German monitoring stations at different elevations (*Levin et al.*, 1995) show that such a data selection criterion may underestimate somewhat CO_2 concentration of the lower troposphere in summer due to CO_2 uptake by the vegetation at the surface, and might overestimate it a bit in winter due to the anthropogenic emission trapped in the shallow boundary layer. More concrete values of the potential bias will be obtained from the Hungarian tower measurements started recently (*Haszpra* and *Nagy*, 1997; *Haszpra*, 1998).

4.2 Seasonal cycle

The mixing ratio measured at K-puszta shows a pronounced seasonal variation (*Fig. 7*). The average annual amplitude is about 28 ppm based on the monthly averages. This value would be decreased to 15 ppm if the 'whole-day' values were used for the calculations, mainly due to the increased monthly averages in summer (high nighttime concentrations). The potentially significant difference should be considered in the analysis of the data measured in the continental region applying different data selection techniques.

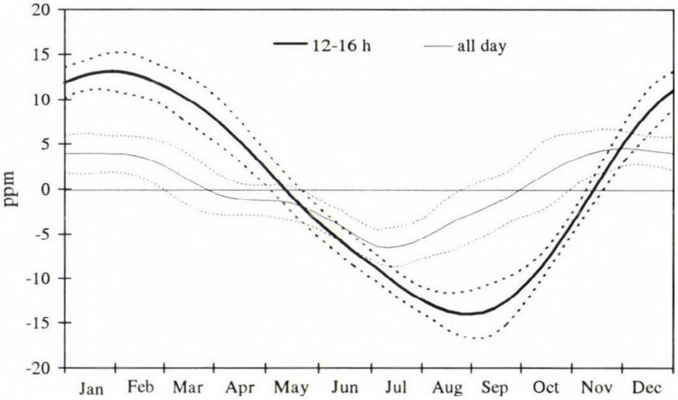

Fig. 7. The average seasonal cycle of CO_2 mixing ratio at K-puszta calculated from the detrended monthly averages (*Thoning et al.*, 1989) with $\pm\sigma$ intervals.

The CO_2 surplus season lasts from early November to mid-May. The minimum concentration is reached at the end of August, while the maximum can be observed in late January. As an additional argument for using only the early afternoon mixing ratio values Fig. 7 also presents the seasonal cycle for the 'whole-day' values. This curve shows not only a smaller annual amplitude but also a different shape of the seasonal cycle. It is caused by the special climatology of the Carpathian Basin. In winter cold air may fill up the basin causing limited vertical mixing. The more or less stable air mass breaks up in early spring causing a drop in the concentration that is not attributed to any source or sink.

4.3 Trend

Fig. 8 shows the trend of the atmospheric mixing ratio of carbon dioxide measured at K-puszta. The smoothed curve and the time dependent trend were calculated using the algorithm developed by *Thoning et al.* (1989). From the beginning of the measurements period the mixing ratio has increased from 343 ppm to almost 369 ppm (mid-1998). These values are very similar to the mixing ratios measured at the Northern Hemispheric baseline stations Mauna Loa, Hawaii, and Point Barrow, Alaska, or at the German regional monitoring sites (*WDCGG*, 1998). If the 'whole-day' values were considered, the corresponding values would be 11 ppm higher at K-puszta, almost uniformly for the whole period.

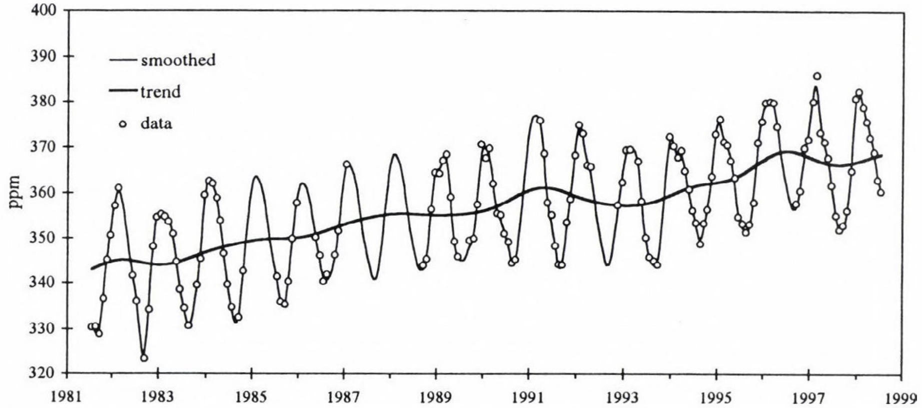

Fig. 8. Trend of atmospheric carbon dioxide mixing ratio at K-puszta.

The overall trend for the 17 years of the measurements is 1.51 ppm/year. However, similar to the baseline stations mentioned above, the growth rate of the mixing ratio calculated from the time dependent trend was not constant during the period covered. It shows significant fluctuations (*Fig. 9*). The fluctuation at K-puszta is more pronounced than at the other stations. At the same time the temporal variation of the growth rates also shows — at least qualitative — similarities. The growth rate is higher than average at each station in 1983, (1985–1986), 1990 and 1993–1995, while it is lower in 1982, (1984–1985) and 1991–1992 (see also *Conway et al.*, 1994). Most of these fluctuations may be triggered by the occurrences of El Niño events in the South Pacific Ocean while the big drop in the growth rate in 1991–1992 might be caused by the climatological consequences of the extreme eruption of Mt. Pinatubo (*Lambert et al.*, 1995). Omitting the period of the long data gap at K-puszta in 1987–1988 the cross-correlations were calculated for the growth rates observed at K-puszta, Mauna Loa and Point Barrow as the functions of lag-time (*Fig. 10*). The maximums of the time dependent cross-correlation of the growth rates are 0.67 for Point Barrow and 0.70 for Mauna Loa, respectively. The high correlation proves that, in spite of the 'noise' generated by the nearby vegetation and anthropogenic sources, the global changes are clearly recognizable even in the middle of a continent.

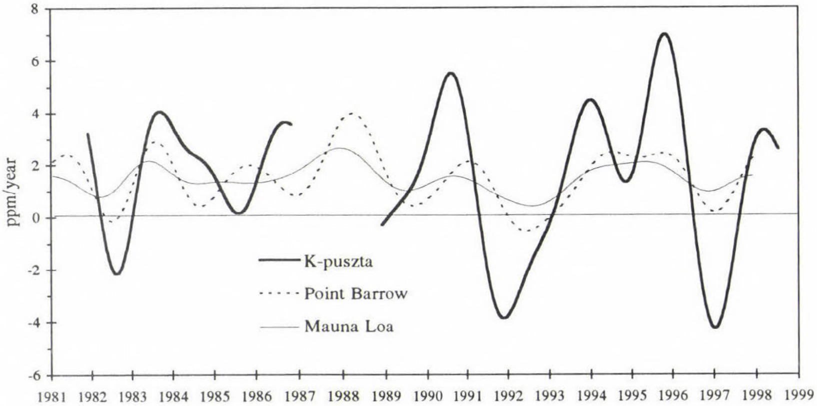

Fig. 9. The growth rate of the atmospheric carbon dioxide mixing ratio.

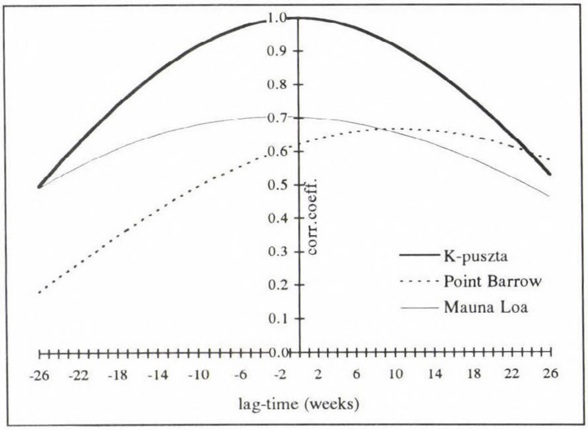

Fig. 10. Cross-correlations of the growth rates as functions of lag-time.

Although El Niño is a phenomenon of the South Pacific Ocean, its climatological effect can also be traced in Europe (*Pongrácz* and *Bartholy*, 1998). These climatological changes may influence the CO_2 emission/uptake of the vegetation/soil which result in higher fluctuation in the growth rate of the atmospheric CO_2 content over the continent. However, the verification of this hypothesis needs further studies.

5. Summary

The data presented here prove that the global characteristics like the trend, the growth rate fluctuation of the carbon dioxide content of the atmosphere can also be observed at low elevation sites in the middle of a continent. The surrounding vegetation and the climatological calmness of the region results in pronounced diurnal and seasonal cycles of the CO_2 mixing ratio. In this paper we call attention to the importance of the data selection technique at stations under similar environmental conditions that may influence, at least, the average concentrations reported and the characteristics of the seasonal cycle significantly. The "missing sink" question demands continental measurements in spite of their methodological problems. Further research is needed to solve these, usually site specific, problems to get a database suitable for the modeling of the global carbon budget.

Acknowledgement—The author thanks NOAA CMDL for the data presented in this paper for comparison, and *Kirk W. Thoning* (NOAA CMDL) for the software used for the trend and growth rate calculations. The author especially appreciates the discussions with *Pieter P. Tans* (NOAA CMDL) and his suggestions. This project was supported by the U.S.–Hungarian Scientific and Technological Joint Fund (J.F. No. 162 and 504) and by the Hungarian National Scientific Research Fund (T7282 and T23811).

References

Bakwin, P.S., Tans, P.P., Zhao, C., Ussler, W., III, and *Quesnell, E.*, 1995: Measurements of carbon dioxide on a very tall tower. *Tellus 47B*, 535-549.

Barnola, J.M., Anklin, M., Porcheron, J., Raynaud, D., Schwander, J. and *Stauffer, B.*, 1995: CO_2 evolution during the last millennium as recorded by Antarctic and Greenland ice. *Tellus 47B*, 264-272.

Beardsmore, D.J. and *Pearman, G.I.*, 1987: Atmospheric carbon dioxide measurements in the Australian region: data from surface observatories. *Tellus 39B*, 42-66.

Ciais, P., Tans, P.P., Trolier, M., White, J.W.C. and *Francey, R.J.*, 1995: A large northern hemispheric terrestrial CO_2 sink indicated by the $^{13}C/^{12}C$ ratio of atmospheric CO_2. *Science 269*, 1098-1102.

Conway, T.J., Tans, P.P., Waterman, L.S., Thoning, K.W., Kitzis, D.R., Masarie, K.A. and *Zhang,N.*, 1994: Evidence for interannual variability of the carbon cycle from the National Oceanic and Atmospheric Administration/Climate Monitoring and Diagnostics Laboratory Global Air Sampling Network. *J. Geophysical Research 99D*, 22831-22855.

Denning, A.S., Fung, I.Y. and *Randall, D.*, 1995: Latitudinal gradient of atmospheric CO_2 due to seasonal exchange with land biota. *Nature 376*, 240-243.

Dixon, R.K., Brown, S., Houghton, R.A., Solomon, A.M., Trexler, M.C. and *Wisniewski, J.*, 1994: Carbon pools and flux of global forest ecosystems. *Science 263*, 185-190.

Enting, I.G. and *Mansbridge, J.V.*, 1991: Latitudinal distribution of sources and sinks of CO_2: results of an inversion study. *Tellus 43B*, 156-170.

Enting, I.G., Trudinger, C.M. and *Francey, R.J.*, 1995: A synthesis inversion of the concentration and $\delta^{13}C$ of atmospheric CO_2. *Tellus 47B*, 35-52.

Etheridge, D.M., Steele, L.P., Langenfelds, R.L., Francey, R.J., Barnola, J.M. and *Morgan, V.I.*, 1996: Natural and anthropogenic changes in atmospheric CO_2 over the last 1000 years from air in Antarctic ice and firn. *J. of Geophysical Research 101D*, 4115-4128.

Haszpra, L., 1995: Carbon dioxide concentration measurements at a rural site in Hungary. *Tellus 47B*, 17-22.

Haszpra, L., 1998: On the representativeness of carbon dioxide measurements. *Abstracts of the Joint International Symposium on Global Atmospheric Chemistry, August 19-25, 1998, Seattle, U.S.A.*, p. 105.

Haszpra, L. and *Nagy, Z.*, 1997: Vertical concentration profile measurements of carbon dioxide at a rural site in Hungary. *Extended Abstracts of the 5th International Carbon Dioxide Conference, Cairns, 8-12 Sept., 1997*, 31-32.

Haszpra, L., Gyuricza, A. and *Szilágyi, I.*, 1994: Preliminary statistical analysis of non-methane hydrocarbon measurements at TOR Station 15 (K-puszta, Hungary). In: *Proc. of EUROTRAC Symposium '94, Garmisch-Partenkirchen, 11-15 April, 1994* (eds.: *P.M. Borrell, P. Borrell, T. Cvitaš* and *W. Seiler*). SPB Academic Publishing bv, The Hague. 421-424.

Hesshaimer, V., Heiman, M. and *Levin, I.*, 1994: Radiocarbon evidence for a smaller oceanic carbon dioxide sink than previously believed. *Nature 370*, 201-203.

IPCC, 1996: *Climate change 1995. The science of climate change* (eds.: *J.T. Houghton, L.G. Meira Filho, B.A. Callander, N. Harris, A. Kattenberg* and *K. Maskell*). University Press, Cambridge.

Keeling, C.D. and *Whorf, T.P.*, 1994: Atmospheric CO_2 records from sites in the SIO air sampling network. In *Trends '93: A Compendium of Data on Global Change*. ORNL/-CDIAC-65. (eds.: *T.A. Boden, D.P. Kaiser, R.J. Sepanski* and *F.W. Stoss*). CDIAC, Oak Ridge National Laboratory, Oak Ridge, Tennessee, U.S.A., 16-26.

Keeling, C.D., Bacastow, R.B., Carter, A.F., Piper, S.C., Whorf, T.P., Heimann, M., Mook, W.G. and *Roelffzon, H.*, 1989: A three-dimensional model of atmospheric CO_2 transport based on observed winds; 1, Analysis of observational data. In *Aspects of climate variability in the Pacific and Western Americas. Geophys. Monogr. Ser. 55.* (ed.: *D.H. Peterson*). Washington, D.C., pp. 165-236.

Lambert, G., Monfray, P., Ardouin, B., Bonsang, G., Gaudry, A., Kazan, V. and *Polian, G.*, 1995: Year-to-year changes in atmospheric CO_2. *Tellus 47B*, 53-55.

Law, R.M., Rayner, P.J., Denning, A.S., Erickson, D., Fung, I.Y., Heimann, M., Piper, S.C., Ramonet, M., Taguchi, S., Taylor, J.A., Trudinger, C.M. and *Watterson, I.G.*, 1996: Variations in modeled atmospheric transport of carbon dioxide and the consequences for CO_2 inversions. *Global Biogeochemical Cycles 10*, 783-796.

Levin, I., Graul, R. and *Trivett, N.B.A.*, 1995: Long-term observations of atmospheric CO_2 and carbon isotopes at continental sites in Germany. *Tellus 47B*, 23-34.

Matyasovszky, I. and *Weidinger, T.*, 1998: Characterizing air pollution potential over Budapest using macrocirculation types. *Időjárás 102*, 219-238.

Musselman, R.C. and *Fox, D.G.*, 1991: A review of the role of temperate forests in the global CO_2 balance. *J. Air Waste Management Assoc. 41*, 798-807.

Pearman, G.I., 1993: Survey of the results of the 1991-1992 round-robin inter-laboratory intercomparison. In *Report of the seventh WMO meeting of expert on carbon dioxide concentration and isotopic measurement techniques, Rome, Italy, 7-10 September 1993* (eds.: *G.I. Pearman* and *J.T. Peterson*). *WMO GAW Report No. 88.*

Pongrácz, R. and *Bartholy, J.*, 1998: ENSO related NAO signal comparison. *Proc. of European Conference on Applied Climatology, 19-23 October, 1998, Vienna.*

Quay, P.D., Tilbrook, B. and *Wong, C.S.*, 1992: Oceanic uptake of fossil fuel CO_2: Carbon-13 evidence. *Science 256*, 74-79.

Sarmiento, J.L. and *Sundquist, E.T.*, 1992: Revised budget for the oceanic uptake of anthropogenic carbon dioxide. *Nature 356*, 589-593.

Sundquist, E.T., 1993: The global carbon dioxide budget. *Science 259*, 934-941.

Taguchi, S., 1996: A three-dimensional model of atmospheric CO_2 transport based on analyzed winds: Model description and simulation results for TRANSCOM. *J. Geophysical Research 101D*, 15099-15109.

Tans, P.P., 1991: An observational strategy for assessing the role of terrestrial ecosystems in the global carbon cycle: Scaling down to regional levels. In *Scaling processes between leaf and landscape levels* (eds.: *J. Ehleringer* and *C. Field*). Academic Press, San Diego.

Tans, P.P., Fung, I.Y. and *Takahashi, T.*, 1990: Observational constrains on the global atmospheric CO_2 budget. *Science 247*, 1431-1438.

Thoning, K.W., Tans, P.P. and *Komhyr, W.D.*, 1989: Atmospheric carbon dioxide at Mauna Loa Observatory 2. Analysis of the NOAA GMCC data 1974-1985. *J. Geophysical Research 94D*, 8549-8565.

Thoning, K.W., Tans, P.P. and *Waterman, L.S.*, 1994: Atmospheric CO_2 records from sites in the NOAA/CMDL continuous monitoring network. In *Trends '93: A Compendium of Data on Global Change*. ORNL/CDIAC-65. (eds.: *T.A. Boden, D.P. Kaiser, R.J. Sepanski* and *F.W. Stoss*). CDIAC, Oak Ridge National Laboratory, Oak Ridge, Tennessee, U.S.A. 28-40.

WDCGG, 1998: *WMO WDCGG CD-ROM No. 4*. Japan Meteorological Agency - World Meteorological Organization, Tokyo - Geneva.

IDŐJÁRÁS
Quarterly Journal of the Hungarian Meteorological Service
Vol. 103, No. 2, April–June 1999, pp. 107–121

Near surface ozone concentration evaluation and prediction in Budapest

Györgyi Baranka

Institute for Atmosheric Physics
H-1675 Budapest, P.O. Box 39, Hungary
e-mail: baranka@met.hu

(Manuscript received 5 March 1999; in final form 10 May 1999)

Abstract—In Budapest near surface ozone levels have been measuring at three points. One of them is representative for the air quality of a large area of the city, for this reason it was choosen for prediction. During the time period (May 1–July 30, 1997) the meteorological parameters and ozone levels were examined as well. It is found, that temperature and wind speed have an influence on ozone values. An increase by leaps and bounds of temperature causes an increase of ozone concentration. A combination model consisting of a deterministic (OZIPR) and a statistical model were used for forecasting the ozone maximum the next 10 hours. To improve the results coming from the photochemical model a regression analysis was applied which was based on meteorological condition and emissions in Budapest. The verification of the forecast shows that the obtained results are better than using a persistency model.

Key-words: urban ozone concentration, forecasting system, photochemical transport model, multiply regression analysis, model evaluation.

1. Introduction

At the Ministerial conference in London, May 1996 a Technical Working Group (TWG) on Data Exchange and Forecasting for Ozone Episodes was formed to develop a co-ordinated system for data exchange and forecasting air pollution episodes in Europe. The exchanged data are made directly available to the public, for instance via a world wide web page, to emphasise the transboundary nature of ozone episodes in Europe.

The Working Group concluded that a central system operating at the regional scale is needed. A joint European forecast system will provide information on larger spatial scales which will improve the insights during the build-up and further development of actual ozone episodes. The results of such a causal model will form essential inputs to national systems. It is judged that national models, in particular statistical models, based on local conditions and local inputs will have better performance than a European-scale model. Consequently, using a national ozone forecasting model is indispensable to an adequate ozone prediction and for extending the forecast period to 2 or more days. For this purpose, a Hungarian ozone forecasting system has been under development. Moreover, when the current national forecast models are used in combination with the results of a large-scale photochemical model, better performance might be obtained.

Near surface ozone is commonly perceived to be a regional pollutant. For this reason in many European countries ozone prediction models are used on the regional scale. However, smog problems can arise in big cities like Budapest where the density of population is quite high.

In this paper a smog forecasting system has been used for Budapest to predict the maximum ozone concentration for the next 10 hours. This system consists of a deterministic and a statistical model. The deterministic model is the photochemical transport model developed for the U.S. Environmental Protection Agency (EPA) called OZIPR, OZIPR (R for research) is a research-oriented version of EPA's OZIPP (Ozone Isopleth Plotting Package) computer modeling program. This air quality simulation model, in conjuction with the Empirical Kinetics Modeling Approach (EKMA), relates ozone concentration to levels of organic and nitrogen oxide (NO_x) emissions. A statistical model has been developed for emissions and meteorological conditions in Budapest. This forecasting system was tested here for the summer period in 1997.

2. Data evaluation for 1997's summer period

Spatial variations in O_3 concentrations occur on the macro- and microscales, as well. These variations are relevant for exposure assessments and for understanding and controlling the photochemical formation of O_3. Ozone concentrations differ between urban and rural areas, between urban and remote sites, and even between rural and remote sites, as a function of space and travel time of plumes, in addition to other factors. For exposure assessments, however, it is important to note that fairly significant intra-city and intra-airshed variations in O_3 concentrations can occur.

O_3 concentrations are often higher in some suburban or even rural areas downwind of urban areas than in the urban areas themselves. The time required for the development of photochemical reactions, transport of the urban plume, and the absence of fresh NO emissions as the plume travels, are key factors in producing higher concentrations in some downwind areas.

There are three ozone measurement sites in Budapest. The first one (Laborc Street) is situated in the north-west part of the city, the second one (Baross Square) is in the downtown area (these ozone values are lowest), and the third ("Fodor József" National Centre of Public Health, National Institute of Environmental Health, NIEH) is located in south-east part of Budapest. The prevailing wind direction is from north-west, and these stations are located along this direction crossing the town. Daily average ozone data coming from these stations have been compared to the regional background concentrations, which are measured at the K-puszta station 70 kms from Budapest (in the east-south direction), as *Fig. 1* shows. The data covers the period from March to July in 1997, when relatively high ozone concentrations were measured. In August measurements were not available in Budapest from the NIEH station so that only three months of 1997' summer period ozone data were examined at the urban and in rural sites. The highest values can occur at K-puszta station and an appreciable intracity gradient in O_3 concentrations can develop across the city. For the prediction of ozone concentration the NIEH data were chosen, because this monitoring site is located in the downwind area of the city, and its location is quite high (20 m above ground-level) so higher values can occur.

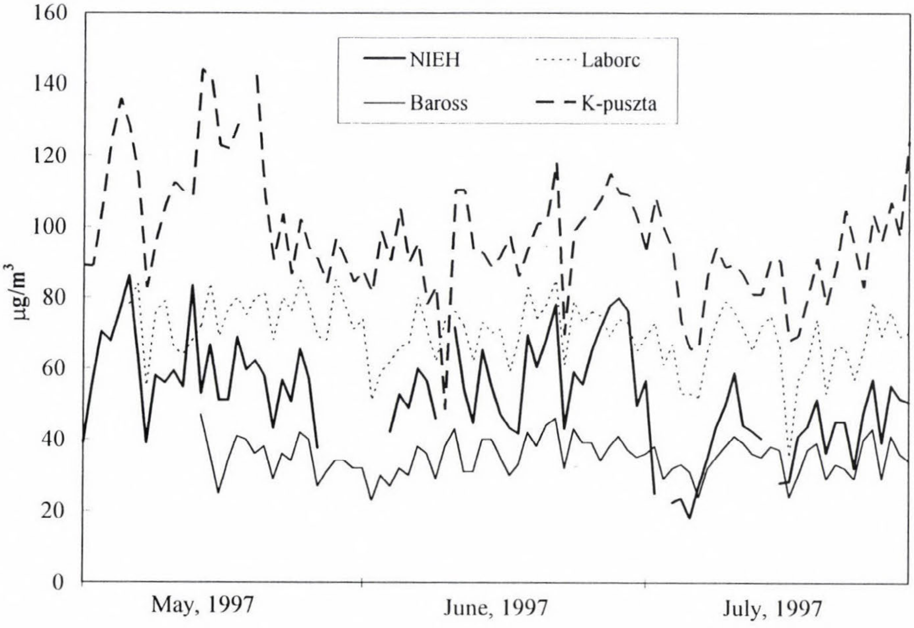

Fig. 1. Daily average ozone concentrations at four monitoring sites.

It can be seen in Fig. 1 that ozone episodes are not only a local, but a regional phenomenon. At the beginning of May, and at the end of June the ozone level was elevated at K-puszta, and at the same time high values were detected at the NIEH station.

The development of ozone concentrations at the NIEH station is displayed in two time scales in *Fig. 2*. This allows the diurnal variation and the development of an ozone episode over several days to be shown independently. Elevated concentrations occur, in general, between 10 a.m. and 8 p.m. Ozone levels higher than 100 $\mu g/m^3$ can be observed at the beginning and at middle of May, and at beginning and at the end of June. A temporary decrease can be seen in July.

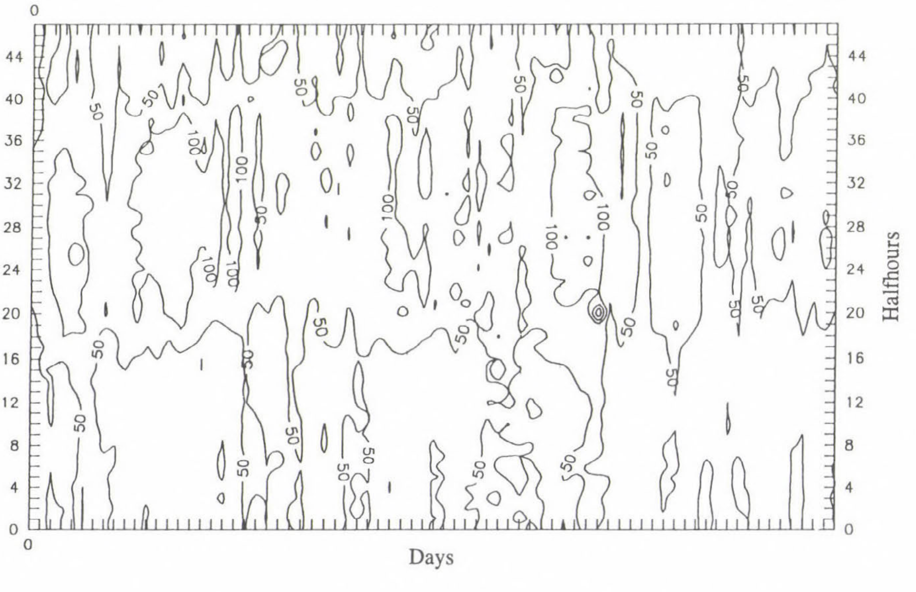

Fig. 2. Half-hour mean values of ozone concentration observed in Budapest during the time period from 1 May to 31 July, 1997.

3. Meteorological conditions

When the ozone concentration was high, during the time period from 1 May to 30 June, 1997 hourly values of ozone concentration, air temperature, wind velocity and wind direction have been monitored in Budapest. *Fig. 3 a-c.* shows that NW and SE directions are preferred in frequency, and NW winds are the strongest. These strong NW winds may represent the weather fronts of an anticyclone passing from NW to SE. Interestingly, the highest concentrations in ozone are associated with westerly winds. This fact can be explained by the position of the monitoring station that is situated in the eastern part of Budapest and is affected by the urban plume of the city.

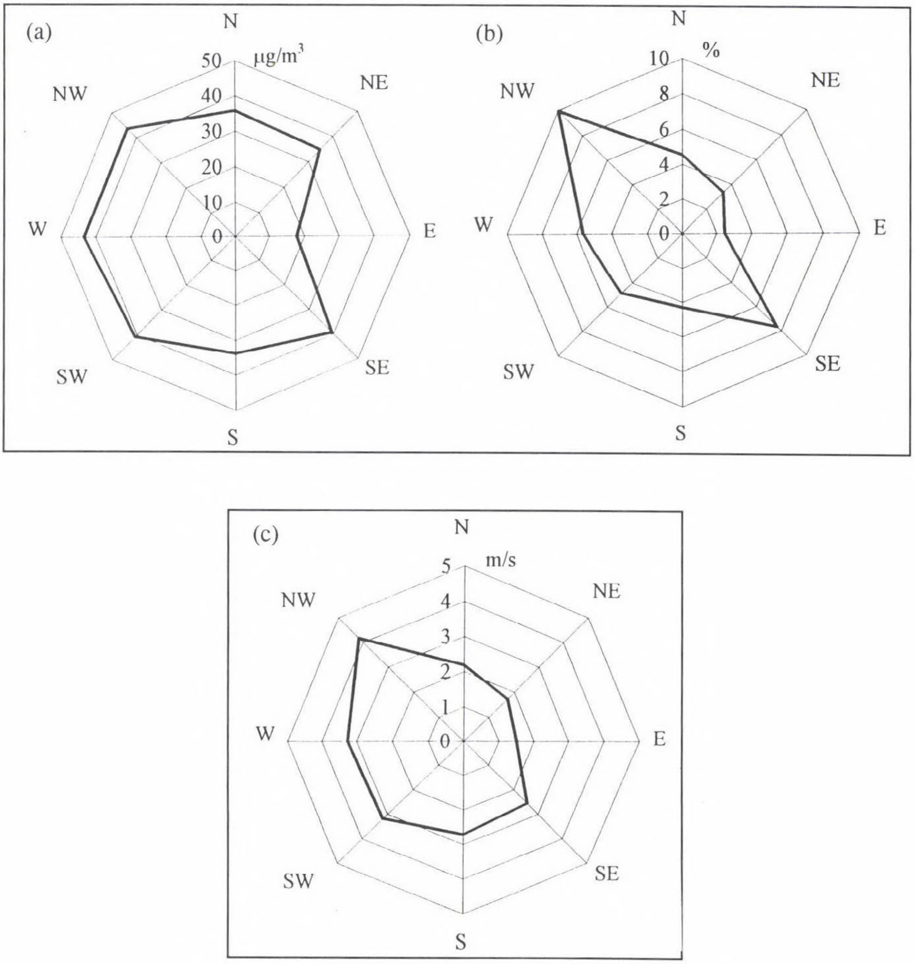

Fig. 3. (*a*) Windrose for ozone concentration, (*b*) wind frequency and (*c*) wind velocity.

Tropospherical ozone is formed in photochemical reactions. The chemical equilibrium of

$$NO_2 + O_2 + h\nu \leftrightarrow NO + O_3 \tag{1}$$

is disturbed by the presence of CO and/or non-methane hydrocarbons. Such substances 'catch' NO and, thus, shift the equilibrium Eq. (1) towards ozone production (*Graedel* and *Crutzen*, 1993). In this manner, the concentration of precursors and the strength of the solar radiation determine the amount of the ozone that is produced. Besides this, the temperature influences the efficiency of the reaction (1). Apart from air-mass convection, air temperature is an indicator for the strength of solar radiation.

Ozone concentration and air temperature are displayed simultaneously in *Fig. 4*. The peaks temperature and ozone concentration coincide, which means that the ozone concentration increases with temperature. Generally, the ozone concentration depends on the intensity of the UV radiation. Often the rise of the temperature coincides with a rise of UV-radiation. It follows, that ozone concentration should be correlated with air temperature. This way, the hypothesis that ozone concentration is associated with changes in temperature could be established here.

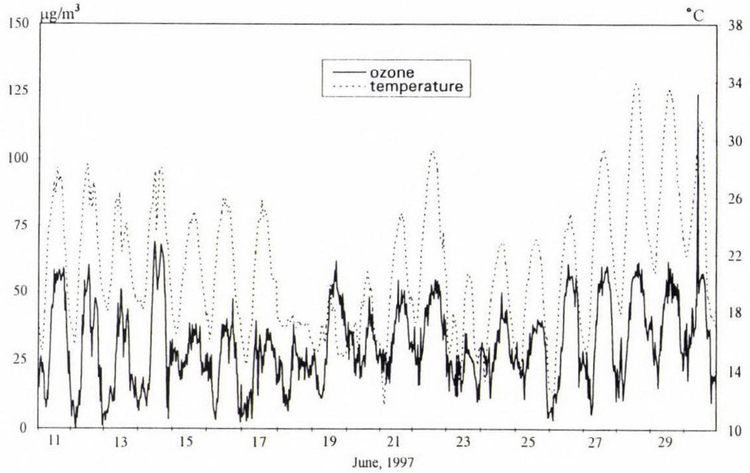

Fig. 4. Ozone concentration (solid line) and temperature (dashed line).

In order to study the impact of air movement on ozone accumulation, ozone concentration is plotted parallel to observed wind speed and direction in *Fig. 5* and *6*. Fig. 5 compares the ozone concentration with the wind speed. It is possible to see an association between both variables as the plots of wind speed looks nearly similar to the plot of ozone concentration. Often the peaks occur at the same time. Sometimes there are also exceptions, for instance on 14. 06. 1997 about midday where the wind speed is relatively low and the ozone concentration is high.

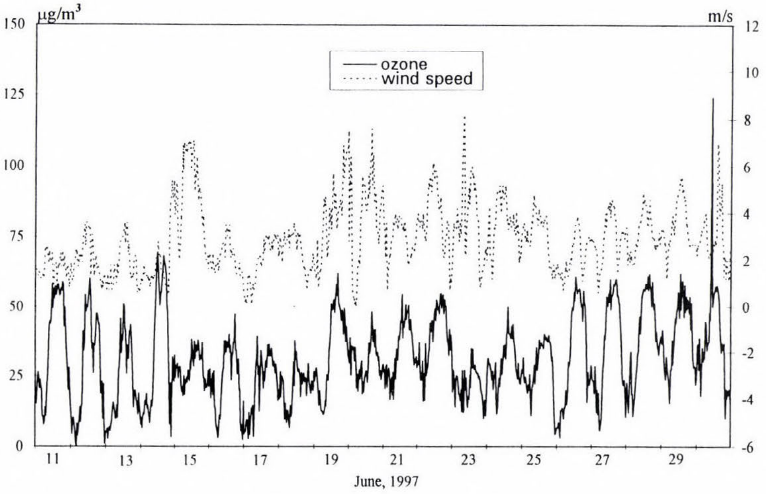

Fig. 5. Ozone concentration (solid line, left axis) compared with wind speed (dashed line).

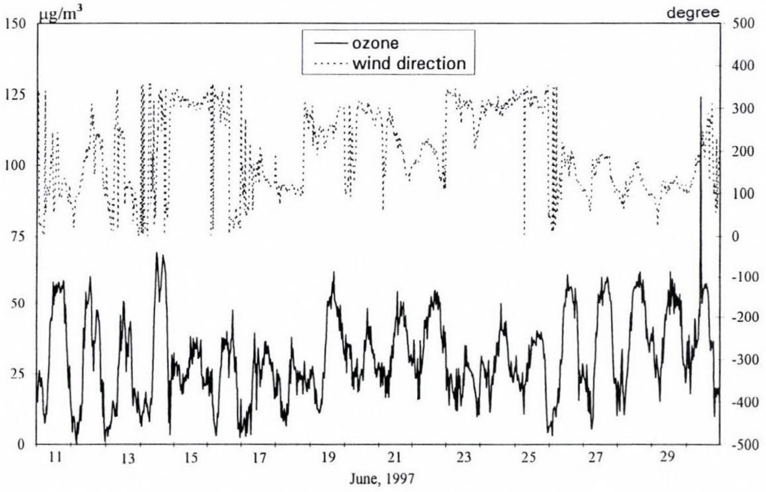

Fig. 6. Ozone concentration (solid line, left axis) compared with wind direction (dashed line).

In Fig. 6 the ozone concentration and direction of wind are not synchronous, that means that the times of peaks do not coincide and that the plot of wind direction has a structure different from the plot of ozone concentration.

In summary, it is found that temperature and wind speed have an influence on ozone concentration. It also seems that the direction of wind has no influence on ozone concentration, but this conclusion must be studied in more detail.

4. Forecasting

Episodes of photochemical air pollution are periods of some days to some weeks with calm, warm, sunny weather, in which atmospheric photochemical reactions of nitrogen oxides and volatile organic compounds lead to a host of mostly noxious air pollutants. Ozone is considered to be the most important of these in view of its concentrations and its effects on human health.

A hybrid model for the prediction of the ozone episodes at one point, the NIEH station, was developed. This system consists of a deterministic and two statistical models. In the deterministic model, the concentration is calculated from emissions of ozone precursors (volatile organic compounds and nitrogen oxides) and forecasted meteorological conditions in Budapest taking into account relevant atmospheric processes such as dispersion, transport, chemical conversion and deposition. The statistical model is based on a multiple linear regression analysis.

4.1 Deterministic model

OZIPR a new trajectory-type, air quality simulation model based on EPA's Ozone Isopleth Plotting Program (OZIPP) Model (*Gery* and *Crouse*, 1996), which was established for regulatory purposes but contains improved and expanded capabilities that make the model useful for research purposes. OZIPR serves the dual purpose of providing: (1) a simple trajectory model capable of utilizing complex chemical mechanisms, emissions, and various meteorological parameters, (2) procedures through which the Empirical Kinetics Modeling Approach (EKMA) can be implemented for calculation of emission reductions needed to achieve compliance with the National Ambient Air Quality Standard for ozone. While these capabilities were included in earlier versions of OZIPP, the new OZIPR contains major improvements that increase the program's ability to input, utilize, and output a much larger range of information.

The OZIPR simulates complex Chemical and Physical processes of the lower atmosphere through use of a trajectory model. The model incorporates the Carbon Bond 4.0 (CBM-IV) chemical mechanism (*Whitten* and *Gery*,

1986) which are complex chemical mechanisms used to describe the chemical processes that occur within the modelled air mass. The chemical mechanism in the model is based on the Carbon Bond Mechanism IV (CBM-IV) and contains 37 compounds and about 80 chemical reactions for the numerical solution of the chemistry and the application of the chemical mechanism). The physical representation is a well-mixed column of air extending from the ground to the top of the mixed layer. So the determination of the mixing height is a very important parameter. This idealized air column moves with the wind (along the wind trajectory, but cannot expand horizontally). Emissions from the surface are included as the air column passes over different emission sources, and air from above the column is mixed in as the inversion height rises during the day.

OZIPR model input parameters along the trajectories are: co-ordinates; time zone; date of the day (year, month, day), the starting hour and the end of the simulation. The model required meteorological and air quality inputs are shown in *Table 1*.

Table 1. Meteorological and air quality inputs of OZIPR model

Meteorological inputs	Predicted values	Measured values	Average values
Height of mixing layer at 8 a.m.			✓
Maximum height of mixing layer		✓	
Surface temperature	✓		
Relative humidity		✓	
Atmospheric pressure		✓	
Dry deposition velocity			✓
Air quality inputs			
O_3, NO_x, VOC and CO concentrations at 8 a.m.		✓	
Aloft of O_3, NO_x, VOC and CO con.			✓
NO_2/NO_x ratio at 8 a.m.		✓	
Reactivity of VOC			✓

The height of mixing layer is one of the fundamental parameters to characterize its structure and is required in dispersion models. Note that the maximum values of the mixing height are determined by midnight radiosonde measurements using Holtzworth's method. The other essential input parameters are emission values estimated from values in U.S. cities and adapted to the sources condition of Budapest.

OZIPR model provides a 10-hour ozone forecast each morning at 8 a.m., that is to say the expected maximum value of the ozone concentration of the afternoon for one ozone monitoring site in Budapest.

4.2 Statistical models

Most of the national ozone forecasting systems use statistical (multiple regression) models. Temperature and previous day's ozone levels are commonly used as independent variable. In more recently developed systems, neural networks are frequently used. Output of the system is tomorrow's maximum ozone level, that is a forecast span of less than 24h; forecasts for 48h are given by one or two systems only.

We have established a statistical model for improvement of the deterministic model results. This calculation is based on a multiple linear regression involving only one ozone measuring site (NIEH) in Budapest. The maximum ozone concentration for 10 hours ahead is the output. Temperature and the previous day's ozone levels are used as independent variables.

The maximum ozone concentration for the actual day is calculated by using the max. O_3 concentration coming from the OZIPR model (max O_3 model), the temperature maximum for the actual day coming from weather forecasting (max Tact), as well as the maximum ozone concentration of the previous day (max O_3 prev), and the temperature maximum of the previous day (max T prev). The two latest independent variables are based on measured data. These inputs are coupled by the following equation are provide the maximum ozone concentration prediction for the next 10 hours:

$$\begin{aligned} \max O_3\, prog &= k + a\,(\max O_3\, model) + b\,(\max Tact) + \\ & c\,(\max O_3\, prev) + d\,(\max T prev), \end{aligned} \tag{2}$$

where *k, a, b, c, d* are regression coefficients. Statistical parameters of the regression model are summarized in the *Table 2*.

Using this method we can obtain more adequate results than when only running a deterministic model, but extreme events (situation far from averages) can not be predicted well. This phenomenon is a feature of the statistical model. If not only the temperature, but other meteorological parameters which have an influence on ozone formation, are included in the model, more reliable results can be obtained. Moreover the long-range transport, which affects ozone levels has not been taken into account.

Table 2. Statistical parameters of the linear regression model

Abbreviation	Definition	Values
k	The constant of the linear regression	-405.567
a	The regression coefficient of the first independent variable	0.229
b	The regression coefficient of the second independent variable	0.680
c	The regression coefficient of the third independent variable	-0.050
d	The regression coefficient of the fourth independent variable	0.826
se_k	The standard error value for the constant k	210.952
se_a	The standard error value for the coefficient a	0.225
se_b	The standard error value for the coefficient b	0.877
se_c	The standard error value for the coefficient c	0.129
se_d	The standard error value for the coefficient d	0.852
r^2	The coefficient of determination	0.119
se_y	The standard error for the y estimate	19.741
F	The F statistic	2.326
df	The degrees of freedom	69.000
ss_{reg}	The regression sum of squares	3625.621
ss_{resid}	The residual sum of squares	26890.080

5. Evaluation of the results

Air-quality models are evaluated by comparing their predictions with ambient observations. For validation of the forecast procedure independent data, that is, data not used in the development of the (statistical) model is needed, and it is desirable to have several years of data available for evaluating model performance. If this is not feasible an alternative procedure might be followed, in which skill parameters are introduced.

For quality information, the skill of forecast system can be tested by using a binary system for comparison of forecast and observed occurrence of air quality classes, that is using a standard contingency table of the type displayed in *Table 3*, where N is the total number of data points and defining: f = total number of forecast exceedances, m = total number of observed exceedances, a = number of correctly forecast exceedances. The other matrix elements in Table 3 can be expressed in N, m, f, and a. This method are proposed by TWG (*van Aalst* and *de Leeuw*, 1997) as well.

Table 3. Contingency table used for verification of ozone forecast

	Observed		
Forecast	Yes	No	Total
Yes	a	f – a	f
No	m–a	N + a – m – f	N – f
Total	m	N – m	N

For this kind of evaluation the ozone threshold values are needed. Nowadays the following threshold values are valid in Budapest: for 24 h it is 100 $\mu g/m^3$, for one half-hour it is 110 $\mu g/m^3$. A smog event is defined as a day with maximum one-half-hour ozone concentration exceeding 110 $\mu g/m^3$.

Using these definitions, various skill parameters can be defined:

— fraction of correct forecast smog events (probability of detection)

$$SP = a/m\ 100\% . \tag{5}$$

Note that the fraction of "unexpected events" is given by (100 - SP)%;

— fraction of actual forecast smog events

$$SR = a/f\ 100\% . \tag{6}$$

Note that the fraction of "false alarm" is given by (100 - SR)%. Both SP and SR range from 0 to 100 with a best value of 100.

In an overall assessment of the forecast skill for all four matrix elements have to be considered. The weighting of each of the four elements in the total skill might depend on the objectives of the forecast system. When the main objective is the warning of sensitive population groups the number of unexpected smog events should be minimal. In cases where the forecast is used as a trigger for short-term abatement measures (e.g., traffic ban) the "false alarms" should be minimal in view of the high costs involved in taking this kind of measures. A high false alarm rate will also reduce the confidence of the general public in the system.

— Assuming an equal weight to the correct forecasting of smog events and of non-smog events, the scoring parameters SP and SR can be combined to form a success index, SI, ranging from –100 to 100 with a best value of 100:

$$SI = \left(\frac{a}{m} + \frac{N + a - m - f}{N - m} - 1 \right) \cdot 100\% . \tag{7}$$

For evaluating of the numerical output of a forecast (sub)-system the following skill parameters, each evaluating different aspects of the system, can be considered:

— the fractional bias, FB, between averaged values for forecast and observation

$$FB = 2\,\frac{(\overline{P} - \overline{M})}{(\overline{P} + \overline{M})}, \tag{8}$$

where P is the forecast value and M is the observed value. FB will detect any systematic difference between observation and forecast. FB ranges between -2 and +2 with the best value of 0;

— the skill score, S defined as:

$$S = 100\left\{1 - \frac{\sum (P_{i+1} - M_{i+1})^2}{\sum (M_i - M_{i+1})^2}\right\}, \tag{9}$$

where P_i and M_i are forecast, respectively observed values at day i. The score S includes the persistency model as reference model. A value $S<0$ indicates that the forecast model is worse than the persistency model. A score $S = 100$ indicates the perfect model;

— the hit score, H, can be defined as:

$$H = 100\,\frac{1}{N}\sum \frac{2r - \Delta}{2r}, \tag{10}$$

where $\Delta = \min(|P - M|, 2r)$ and r is an uncertainty range around the forecast and observed value. The uncertainty in the observed value will depend on, e.g. uncertainties in the measurements but more importantly on the spatial variability of M within the study area. The uncertainties in forecast value will result from the model concept. When these uncertainties are not known, the hit score may provide a simple estimate of their impact on forecast performance. The hit score H indicates the overlap between the interval ($P \pm r$) and ($M \pm r$). H ranges between 0 and 100 with a best value of 100. Disadvantage of H is that it assumes a uniform distribution of P, M within the interval $\pm r$ and it assumes equal ranges around both P and M. The hit score, H, has been evaluated with a range $r = 10\ \mu g/m^3$.

In the evaluation of skill parameters a reference model should be included. The persistency model is recommended as the reference model. The persistency model is an extremely simple model assuming that the forecast situation equals the present situation. In view of the phenomenology and average duration of ozone smog episodes the persistency model will be reasonably successful; the skill of the forecast system should be better. In practice this means that the forecast should be able to predict abrupt changes in air quality levels.

When skill parameters are all scaled between 0 and 100 summarising graphs like *Fig. 7* can be made. Using such a figure, a direct comparison between the forecast model and the reference (persistency) model can be made. The figure and *Table 4* show that the developed hybrid model for 10-hour ozone prediction provides better results than the persistency model. So it can be used operationally.

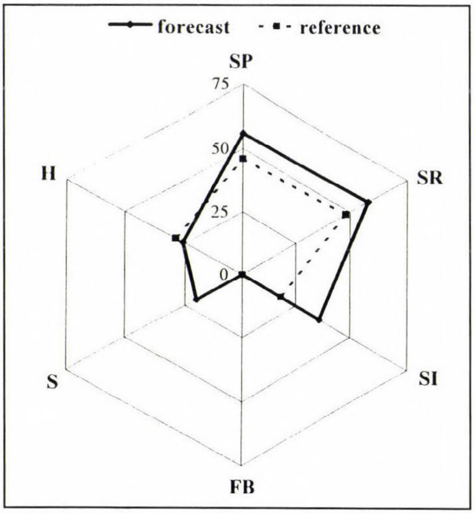

Fig. 7. Summary of evaluation of the ozone forecast system for Budapest in summer 1997.

Table 4. Evaluation of the ozone forecast of summer 1997 (May 1–July 31) made for Budapest

	Observed		
Forecast	Yes	No	Total
Yes	14	10	24
No	11	39	50
Total	25	49	74
Number	**Skill parameters**	**Ozone forecast**	**Persistency model**
1	SP	56	46
2	SR	58	48
3	SI	36	18
4	FB	0	0
5	S	20	n.a.
6	H	26	29

The prediction of ozone concentration is not so easy because oxidant formation seemed to be very episodic, and episodes appear to be of two types: local/mesoscale and transport (*Schjoldager,* 1981). This approach does not consider the mesoscale and long-range transport episodes. The aim of the future research is to extend the output for the whole area of Budapest, and to place uncertainties on the output values. The updating of emission data will be investigated as well.

6. Conclusions

In summary, the following conclusions are drawn:

- Ozone can accumulate when there are high temperatures and stagnant air in Budapest.
- A trajectory-type ozone simulation model and a statistical model were used to predict the expected maximum concentration of the next 10 hours for one monitoring site of Budapest.
- Advantages of forecasting system are ease of use due to small number of predicted input parameters, and ability to deal with transport phenomena when the changes of local precursor emissions are known.
- Better results are obtained by using the forecast model than by relying on persistency.

References

Gery, M.W. and *Crouse, R.R.*, 1996: *User's Guide for Executing OZIPR.* No 9D2196 NASA.

Graedel, T.E. and *Crutzen, P.J.*, 1993: *Atmospheric Change. An Earth System Perspective.* W.H. Freeman and Company, New York.

Hertel, O., Berkowitz, R., Christensen, J. and *Hov, Ø.*, 1993: Tests of two numerical schemes for use in atmospheric transport-chemistry models. *Atmospheric Environment 27A*, 2591-2611.

Schjoldager, J., 1981: Ambient ozone measurements in Norway 1975-1979. *Journal of Air Pollut. Control Assoc. 31*, 1187-1191.

van Aalst, R.M. and *de Leeuw, F.A.A.M.* (eds.), 1997: *National Ozone Forecasting Systems and International Data Exchange in Northwest Europe.* Technical Report No. 9. European Environment Agency, Copenhagen.

Whitten, G.Z. and *Gery, M.W.*, 1986: *Development of the CBM-X Mechanisms for Urban and Regional AQSMs.* EPA-600/3-86-012. U.S. Environmental Protection Agency, Office of Mobile Sources, Ann Arbor Mich.

IDŐJÁRÁS

Quarterly Journal of the Hungarian Meteorological Service
Vol. 103, No. 2, April–June 1999, pp. 123–136

The effect of alginite on the production and water use of maize

Angéla Anda[*1] and **Márta Hunkár**[2]

[1]*Pannon Agricultural University of Keszthely,*
H-8361, Keszthely, Hungary; e-mail: and5536@ella.hu
[2]*Hungarian Meteorological Service, Agrometeorological Research Station,*
H-8361 Keszthely, Hungary; e-mail: h11260hun@ella.hu

(Manuscript received 25 January 1999; in final form 16 April 1999)

Abstract—Bioproduction and environment-friend agriculture need non-toxic, natural materials to improve soil conditions for maintaining the production on a reasonable level. Alginite is originated from the Pliocene age located at the site of the past Pannon Sea. The aim of our investigation was to determine the effect of alginite on the production level and water use of different maize hybrids as well as the mechanism of its influence. The hybrids were Norma 370 SC a water stress tolerant hybrid and MVK-480 SC which was bred for irrigated conditions. Experiments were carried out in 1996 and 1997 at Keszthely, Hungary (46°46'N, 17°14'E, 128 m a.s.l). Treatments were as follows: (1) C: Control (without alginite and nitrogen fertiliser); (2) A: Alginite 5 kg m^{-2} (8 g kg^{-1} soil), no nitrogen fertiliser; (3) N: No alginite, 300 kg ha^{-1} fertiliser (10 g m^{-2} N, 8 g m^{-2} P, 12 g m^{-2} K fertilisers); (4) A+N: Alginite 5 kg m^{-2} (8 g kg^{-1} soil), 300 kg ha^{-1} fertiliser (10 g m^{-2} N, 8 g m^{-2} P, 12 g m^{-2} K fertilisers). The plants were grown in evapotranspiration pots 4 m^2 each in three replications. The responses of hybrids to alginite were slightly different. Leaf area increase due to alginite was more expressive in the case of Norma than in MVK-480 especially in treatments without nitrogen application. Alginite caused significant depression in water use in the case of cv. MVK-480 comparing treatment A and C as well as in treatments A+N and N. In the case of cv. Norma differences were not significant because of the leaf area response. In the beginning of the growing season an increased stomatal resistance could be measured in the alginite treatments in accordance with decreased water loss at that time. The effect of alginite as a nutrient is more expressive without nitrogen fertilisation. In 1996 there was 7% and 10% more yield in treatments. A comparing to control C in MVK-480 and Norma, respectively. In the second year, 1997 the effect was stronger (30% and 74%). Reason of difference between the individual treatments might have been on the one hand the nutrient effect of alginite on crop production and on the other hand the change in soil hydrophysics, that could result a humid-warm microenvironment which has a feedback to the evapo-transpiration processes.

Key-words: alginite, evapotranspiration, micro environment, plant production.

---

[*] Corresponding author

1. Introduction

Agriculture is often blamed for contaminating land with chemicals. The importance of environment friend farming has been growing fast in past decades. Searching for materials which are suitable from this point of view began in the eighties. The alginite as a substitute of artificial fertilisers satisfies the most rigorous laws and requirements of bioproduction technologies avoiding the excess use of chemicals. For this reason it is an agent much in demand, especially on areas where environmental control has top priority. Alginite is the local resource of strictly protected region, the Lake Balaton catchment area, where the investigations had been carried out and this natural material would be applied. The most important advantages of alginite are decreasing nutrient infiltration and lake eutrophysation. For this reason we could not give up its use in our surroundings, mainly in the closest fields to the lake.

After the volcanism of Pliocene time, the Pannonian lakewater infiltrated through the pores and fissures of the tuff-ring and formed a deepwater (50 to 120 m) crater lake extremely enriched with nutrients (*Nagy*, 1978; *Hargitai*, 1985). The wealth of mineral and organic nutrients led to a marked growth of green algae (*Botrycoccus braunii*). When dead, they would settle at the lake-bottom to accumulate as an alginite bed, that may be taken to be a fossil biomass (*Knutson et al.*, 1986). Superimposed on an organic rich layer, a thin layer of carbonate rich sediments (lime, dolomite, diatomite) was laid down in an arid growing season. Process was repeated several times producing pairs of laminae composed of algae on the one end and clay, lime and diatoms on the other one (*Ravasz* and *Solti*, 1987). This mixed material is called alginite. Because of its special composition, it is suitable for complex soil melioration, for the structure of the soil, its water and nutrient regime and humus content can be simultaneously improved (*Russel*, 1992). Due to the composition of alginite, huge amount of literature introduced it as a substitute of fertilisers (*Solti*, 1985, 1985a, 1987; *Solti* and *Szabó*, 1985; *Solti et al.,* 1985). Chemical compounds of the alginite are presented in *Table* 1.

Table 1. Chemical compounds in g kg^{-1} of alginite of Hungarian origin

N Total	N Hydrolysable	P	K	Ca	Mg	Organic matter
3-5	0.12-0.2	5-6	6-9	100-300	8-10	200-300

In spite of the relatively high nitrogen, phosphorous and potassium (NPK) content of alginite, the soluble mineral rate of macroelements is low. In case of N the ratio of hydrolysable N is only 4%. Therefore the alginite can not be taken as a complete nutrient source. Size of yield increase depends on applied dose. Beside that alginite may be a crop nutrient supplement, its high water retaining capacity has of primary importance in dry seasons (*Russel,* 1992).

Our experimental field is located on highly protected recreational area of Hungary, on Lake Balaton catchment area where decrease of nutrient leaking into the ground- and lake water is very important. Since alginite is a non toxic environ-ment friend natural material, satisfying the most rigorous environmental laws and restrictions, it could be applied in crop growing of bioproduction. The alginite is a local resource of Lake Balaton region, therefore transportation expenses are low when it is used close to the mine.

The aim of our investigations was to determine the changes in yield and water regime of two different maize hybrids due to alginite treatment. Possible explanation of alterations in plant and environmental factors resulted from alginite application are discussed as well.

2. Materials and methods

At the Agrometeorological Research Station of Keszthely, Hungary there are 24 Thornthwaite type compensation evapotranspirometers (ET-pots) with a surface of 4 m^2 and a depth of 1 m each. This apparatus provides unlimited water supply from below the pots. Water consumption of the soil-plant system can be measured on a daily basis. Actual evapotranspiration is calculated using the values of water uptake and potential evapotranspiration. In this study we used to estimate the daily values of potential evapotranspiration according to local formula of *Antal* (1968). The soil in the pots is a Ramann type brown forest soil with mean bulk density of 1.5 Mg m^{-3} in the top 1 m of the profile and a field capacity of 290 mm m^{-1}. The pH of the soil and alginite were 6.3 and 6.9, respectively.

Experiments were conducted in 1996 and 1997. Maize hybrids were studied; namely Norma 370 SC which is a water stress tolerant hybrid and MVK-480 SC which was bred for irrigated conditions. Both of them are commercial varieties in Hungary. Treatments were as follows:

(1) C: Control – without alginite and nitrogen fertiliser.

(2) A: Alginite 5 kg m^{-2} (8 g kg^{-1} soil), no nitrogen fertiliser.

(3) N: No alginite, 300 kg ha^{-1} fertiliser (10 g m^{-2} N, 8 g m^{-2} P, 12 g m^{-2} K fertilisers).

(4) A+N: Alginite 5 kg m^{-2} (8 g kg^{-1} soil), 300 kg ha^{-1} fertiliser (10 g m^{-2} N, 8 g m^{-2} P, 12 g m^{-2} K fertilisers).

A randomised complete block design with three repetitions was used. Alginite and fertiliser were incorporated in the upper 40 cm soil layer at the end of April, 1996, just before planting. Seeds were sown on 30th of April, 1996 and 15th of May, 1997. The plants emerged on 12nd and 29th of May, respectively. There were 28 plants in each ET-pot, i.e., a plant density of 7 plants m^{-2}, or 70 000 plants/ha. The pots were surrounded with maize having the same density.

Assimilatory surface was characterised by leaf area index (LAI) measured weekly using LI-3000 type portable leaf area meter (LI-COR, Lincoln, NE). Leaf area of the same 10 plants per pot was measured during the entire growing season.

On a few sample days yearly, air temperature and relative humidity within the canopy were registered at three levels (ground-, cob-, and top levels of plants) with psychrometers connected to a LI-COR Model LI 1000-32 datalogger. The sensors were shaded to remove the effect of direct radiation.

Soil temperature was sensed remotely on the same days when stomatal resistance was also measured. An infrared thermometer of Raynger II Model (Raytek, Santa Cruz, CA) was used with a 20 field of view and an 8–14 μm spectral band filter. Emissivity of soil was assumed to be 0.9 (*Anda*, 1993). Average soil surface temperature was measured by walking along the rows for 60 seconds holding the instrument at 0.1 m, just above the soil surface.

At the end of the growing season, cobs were harvested. Fresh weight was measured and a sample of three cobs per pot was ovendried at 60°C for 48 hours to obtain moisture content of the cobs. Data were analyzed using combined analysis of variance across the years.

3. Results and discussion

3.1 Weather of the experimental seasons

The growing season 1996 began with a warm and rainy period (*Table 2*). It was favorable for germination and early development of the plants. A longer dry period started at the end of May and continued in June. The temperature in the middle of June was above the long term average. The second dry period occurred between July and the 2nd pentad of August. During this time temperatures were rather cool. September was extremely wet and cold. The spring of 1997 was very dry until the 4th pentad of May. Heavy rains provided sufficient water for development until the end of July. August and September were dry again with rather cool temperature.

Table 2. Monthly mean temperature (T, °C) and amount of precipitation (P, mm) in the growing season of 1996 and 1997 at Keszthely, Hungary

		Apr	May	Jun	Jul	Aug	Sept
1996	T	10.1	16.4	19.7	18.9	19.5	12.3
	P	84.0	79.1	38.2	56.8	82.6	171.6
1997	T	7.7	16.6	19.3	19.5	19.9	14.8
	P	10.9	75.0	93.7	111.0	27.2	21.5

3.2 Assimilatory surface (LAI)

Seasonal variation of leaf area index is shown in *Fig. 1a* and *1b*. Maximum leaf area was reached middle of July 1996 and early August 1997, respectively. Both alginite and nitrogen caused some increase in LAI. Compared to treatment C, treatment A had a 30–50% ($P<0.01$) greater LAI in the case of cv. Norma and a 5–13% ($P<0.05$) increase occurred in the case of MVK-480. The well known nitrogen effect on LAI was also demonstrated in our experiments. When alginite was applied together with nitrogen, the differences in LAI between the treatments A+N and N were not significant for both cultivars.

Senescence of leaves in plant stands grown without N was always faster than in canopies with additional N fertiliser.

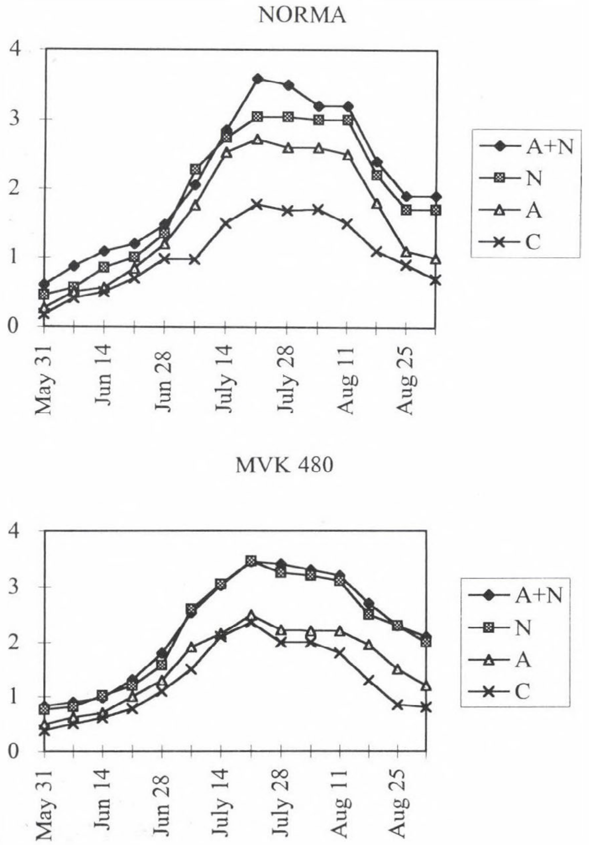
NORMA

MVK 480

Fig. 1a. Seasonal variation in leaf area index of maize during 1996.

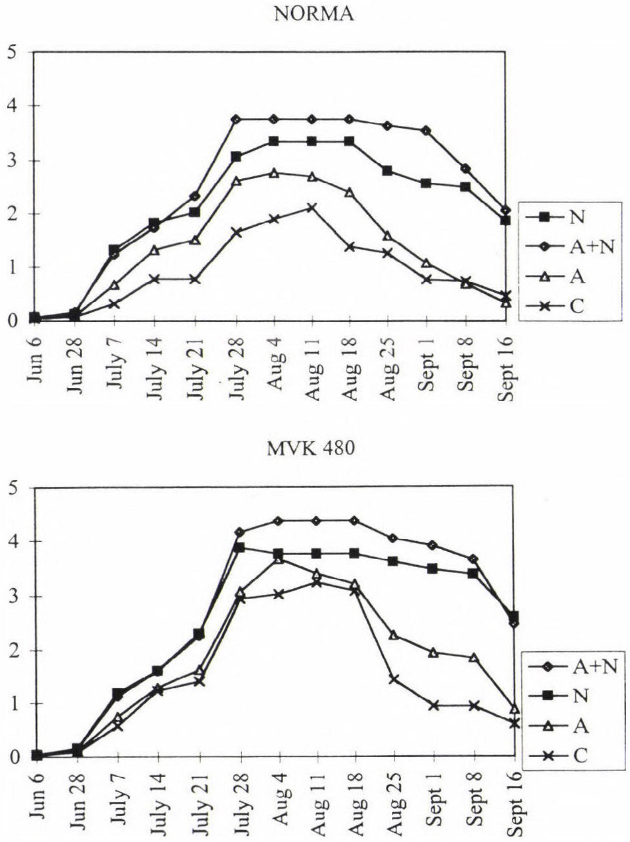

Fig. 1b. Seasonal variation in leaf area index of maize during 1997.

3.3 Evapotranspiration

Accumulated evapotranspiration from emergence until maturity is presented in *Table 3*. In both N fertilisation cases evapotranspiration is greater than the value of control case by 85–115 mm. Evapotranspiration was less when alginite was applied. Differences were 6.5–5.8% ($P<0.01$) with N and 5.7–4.0% ($P<0.05$) without N. In the case of cv. Norma differences were not significant. It suggests that the two hybrids response differently to alginite. While leaf area of cv. Norma became larger due to alginite, there was no significant increase in evapotranspiration. This indicated that alginite decreased transpiration rate in cv. Norma. Evapotranspiration water demand of MVK-480 was 6.4–8.1% ($P<0.05$) higher than for cv. Norma in treatment C.

Table 3. Means of accumulated evapotranspiration (ET, mm) in 1996–97 for treatments and cultivars

	Cultivars		
Treatments	MVK-480	Norma	LSD $_{0.05}$
A+N	428.6	434.4	72.0 NS
N	450.7	439.6	4.3 *
LSD $_{0.05}$	17.0 *	59.3 NS	
A	337.4	343.1	4.1 *
C	359.5	335.1	9.2 *
LSD $_{0.05}$	7.1 *	12.3 NS	

* — significant at the 0.05 probability level; NS — non significant

Analyzing the evapotranspiration on daily basis showed that differences between treatments altered in time with and without alginite. Especially when the evaporative demand of the air was high, treatments with alginite had significant less evaporation, as it occurred during the first half of June in 1996 (*Fig. 2*). On 21 June 1996 a rainy period started and the differences in daily evapotranspiration between treatments were not so clear.

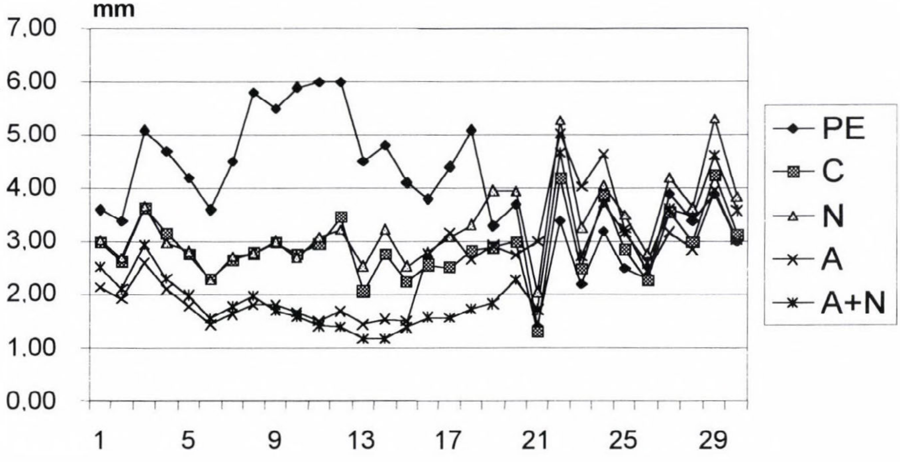

Fig. 2. Potential and actual daily evapotranspirations (mm) of cv. MVK-480 in different treatments (June 1996, Keszthely, Hungary).

3.4 Stomatal resistance

Stomatal resistance was measured at different phenological stages in 1997. In the beginning and the end of the season the daily means of stomatal resistance were about two times higher than in the middle of the vegetation period (*Fig. 3*). Minimum values were measured in the first half of August just after tasseling. At that time in daily course the values in the morning were between 3 and 4 s cm^{-1}, which felt down to 0.8–1.1 s cm^{-1} around solar noon and then increased again up to 2–3 s cm^{-1} in the afternoon.

In 1997 seasonal means of stomatal resistance of MVK-480 were 11.9–17.7% ($P<0.05$), lower than averages of Norma in different treatments. Highest deviation was measured between control treatments. When N was also supplied, stomatal resistance values were closer to each other.

Significant increase in stomatal resistance between treatments A and without A was measured in the beginning of the growing season in accordance with decreasing water loss at that time. (This change ceased in seasonal average resistance of Norma but manifested in MVK-480.)

The nitrogen decreased the stomatal resistance in each treatment. Seasonal average resistance of Norma and MVK-480 with N were 24.6 and 20.5% ($P<0.05$), less than in treatment C. When alginite and nitrogen were applied together, the size of change in mean stomatal resistance moderated in 14.8 and 9.0% (not significant) in Norma and MVK-480, respectively.

3.5 Microenvironment

Microenvironment in our terms means the characteristics of soil and air very close to the plants. We do not use the technical term of microclimate because of the small size of our experimental plots for developing a microclimate which differs from the macroclimate needs large homogeneous crop stand. Nevertheless any kind of physical or chemical interference may cause change in energy exchange inside plant canopy, which might be observed by measuring surface and air temperatures and humidity very close to the heat and water sources. Energy exchange is controlled mainly by radiation balance which is depending on the leaf area index. Therefore showing any other effect than the size of LAI is possible only when LAI is more or less the same. In our experiment it was the situation in cv. MVK-480, in both of the years in the treatments N and A+N. Therefore the alteration in microenvironment as a result of alginite application was more expressed in MVK-480, than those in variety of Norma. Daily course of the characteristics of the microenvironment is presented by values measured on 15 July of 1996. (Meteorological data for the sample day were as follows: 30.6°C maximum temperature; 13.6°C minimum temperature; 27.78 MJ m^{-2} global radiation; 5.0 mm potential evapotranspiration. LAI in the treatments were as follows: A+N: 3.02; N: 3.04; A: 2.15; C: 2.1.) This day was a typical day considering analysis of the other days as well.

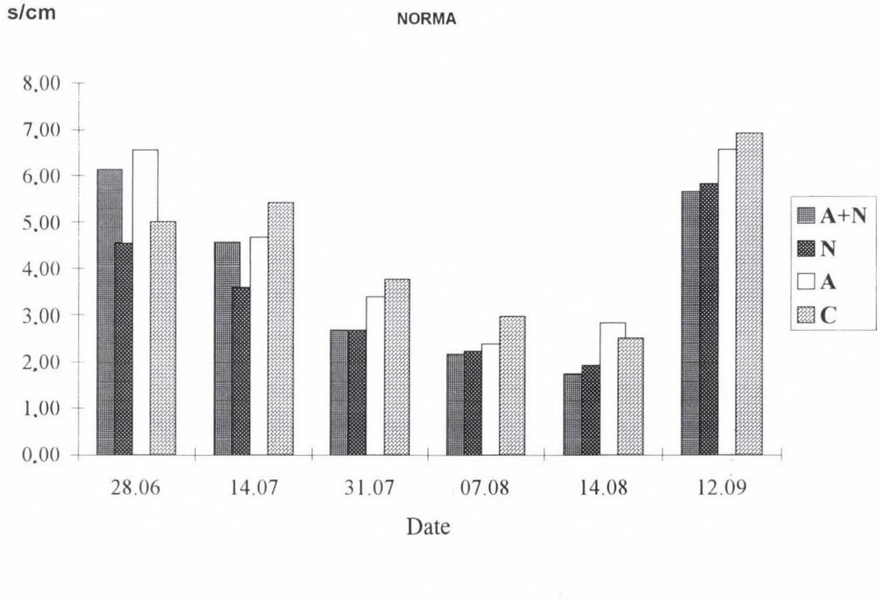

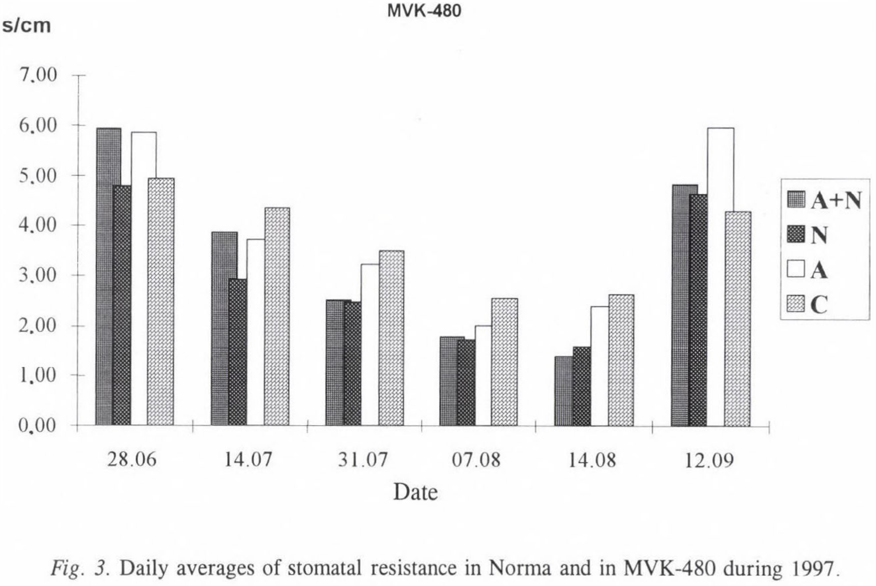

Fig. 3. Daily averages of stomatal resistance in Norma and in MVK-480 during 1997.

Soil surface temperatures did not differ between N and A+N. Differences were observed only between A and C, where the shadowing leaf area differed as well. Before 2 p.m. soil surface of A was cooler, but later in the afternoon A was the warmer treatment by some degrees (*Fig. 4*).

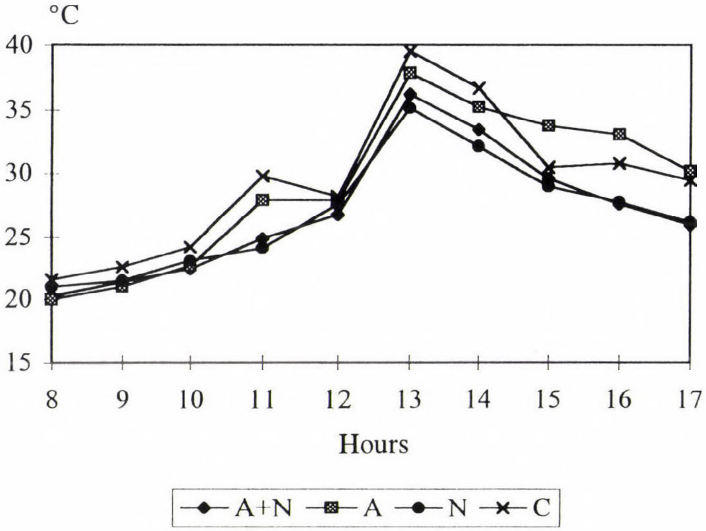

Fig. 4. Diurnal variation in soil surface temperature (15 July 1996).

The warmest air temperature was measured in the control treatment, independently on radiation angle of incidence (*Fig. 5*). In the morning (8.30–9.30 a.m.), closely to the soil surface the alginite decreased the air temperature in treatments A and A + N by 1.9°C and 0.6°C, compared to C and N, respectively. Later on, at higher solar angles treatment A caused the highest air temperature of all (4.6–5.1°C in different levels of the canopy), but the absolute value of its air temperature never exceeded the air temperature of control plots. It seems that both the warming and cooling processes derived from the soil are slower due to alginite application.

Air humidity was expressed by vapor pressure (hPa). The alginite increased the vapor pressure in each level of plant height (*Fig. 6*). The possible process which results this kind of profiles in temperature and humidity is the evapotranspiration, the sum of soil evaporation and plant transpiration. Parallel with growing LAI, the ratio of evaporation is decreasing. In spite of that we did not find significant differences in stomatal behaviour between the treatments — except of the beginning of the seasons —, the alginite decreases the transpiration of plants. This physiological influence might have been the reason of the changes of microenvironment conditions: higher air temperature is a result of the increased sensible heat flux derived from the surface to the ambient air. It is in accordance with a lower transpiration rate. Only the soil surface can provide excess humidity to the air within the canopy, because of the alginite content of the upper soil layer.

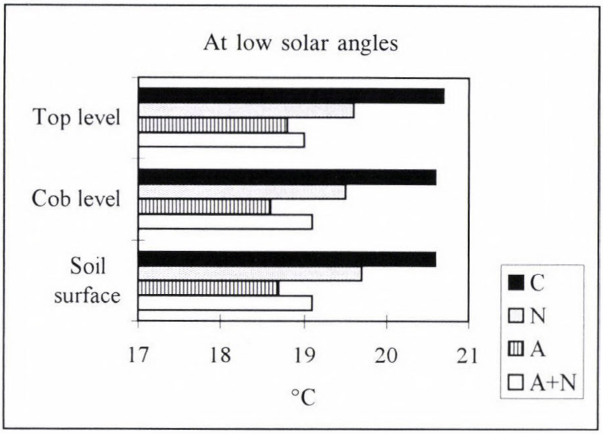

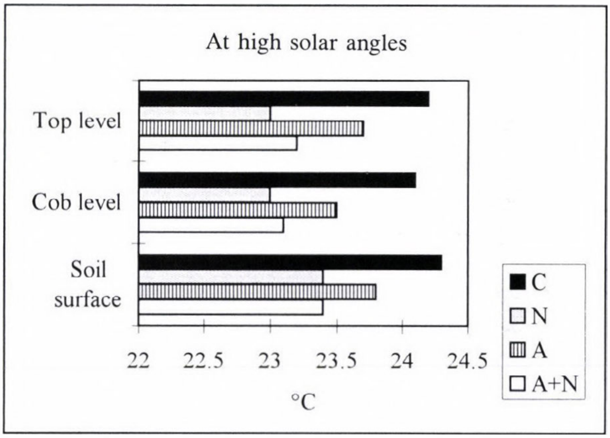

Fig. 5. Representative profiles of air temperature at low and high solar angles on the 15th July 1996.

3.6 *Yield*

MVK-480 produced more yield in both years and all treatments (*Table 4*). The differences compared to cv. Norma were between 23% and 75% depending on the treatment ($P<0.05$). In the first year of the experiment there was no significant difference between the treatments N and A+N, but in the second year alginite increased cob yield by 13.4% ($P<0.01$) and 36.7% ($P<0.05$) in MVK-480 and Norma, respectively. The effect of alginite was more pronounced when no N was applied. In 1996 there was 7% ($P<0.01$) and 10% ($P<0.01$)

more yield in treatment A than in C for MVK-480 and Norma respectively. In 1997, A and C differed by 30% ($P<0.05$) and 74% ($P<0.05$), with yield levels that were less than in 1996. The higher differences in yield between A and C treatments in the second year might be caused by the gradual decreasing level of natural fertility of the soil because of no N application.

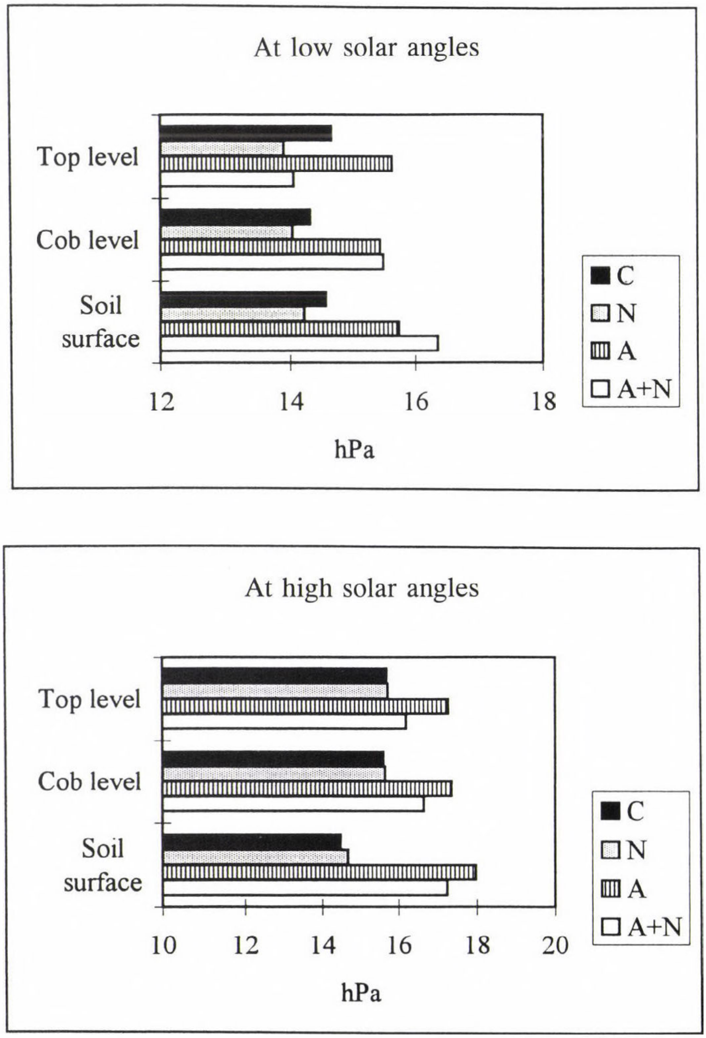

Fig. 6. Representative profiles of vapor pressure at low and high solar radiations on the 15th July 1996.

Table 4. Cob yield (g/m^2) in ET pots for different hybrids in different treatments

	Cultivars		
Treatments	MVK-480	Norma	LSD$_{0.05}$
A+N	1271	998	352.0 NS
N	1194	845	365.5 NS
LSD$_{0.05}$	328.9 NS	316.1 NS	
A	566	378	485.9 NS
C	495	289	374.1 NS
LSD$_{0.05}$	94.6	206.4 NS	

4. Conclusions

In spite of high macroelement content of alginite, its available nutrient rate is relatively low. For this reason the alginite can not be taken into account as a complete nutrient source. The alginite is never suitable to substitute for fertilisers.

Considering the mixing ratio, the actual pH of the soil supplied with alginite has not been changed significantly.

The hybrids of maize MVK-480 and Norma are different in their water relations. Norma is taken to be a water stress tolerant variety while MVK-480 is sensitive to water shortage. Under well watered conditions the productivity of MVK-480 is greater than Norma as it was demonstrated by our experiments. The response of that two varieties to alginite treatment is also different. Alginite has a nutrient effect which is more effective in the case of Norma than in MVK-480, the increase in production and leaf area due to alginite is more expressive in Norma than in MVK-480. The effect of alginite on water relations manifested itselves mainly in cv. MVK-480 where LAI did not change due to alginite while the evapotranspiration decreased.

Evapotranspiration consists of soil evaporation and plant transpiration. Stomatal resistance characterises the ability of plant for transpiring water through stomata. The actual evapotranspiration however depends on environmental factors as humidity and temperature of ambient air. Whilst we did not find unambiguous differences in stomatal behaviour resulted from alginite application between the individual treatments, the changes in air humidity as well as in soil and air temperatures indicate that physical conditions of evaporation has been modified because of alginite. Alginite is mixed in the upper soil level and makes changes in water capacity and conductivity through retaining water in this soil layer. This “wet sponge” provides a humid air inside the plant canopy which slows the soil heating processes. It has a feedback to the actual evapotranspiration especially when the potential evapotranspiration, calculated from climatological characteristics is extremely high.

The yield excess resulted from alginite supply is moderate. Considering the aim of the alginite application, use of environment friend agricultural technology on protected areas, alginite should therefore be regarded as a local mineral source of the Lake Balaton catchment area.

References

Anda, A., 1993: Surface temperature as an important parameter of plant stand. *Időjárás 97*, 259-267.

Antal, E., 1968: *Irrigation Timing by Using Meteorological Data* (in Hungarian). PhD Thesis, Budapest.

Hargitai, L., 1985: Agrochemistry of alginites and their possible use (in Hungarian). *Földtani Kutatás*, 1-2, 29-33.

Knutson, C.F., Dana, G.F., Macaulay, G. and *Hutton, A.C.*, 1986: Developments in oil shale (alginite). *The Amer. Assoc. of Petroleum Geologist Bull. 70,* 1638-1642.

Nagy, E., 1978: Palynological investigations of alginites in Hungary. *Journal of Palynology 14,* 94-100.

Ravasz, C. and *Solti, G.*, 1987: Genetic types of oil shales in Hungary (in Hungarian). In *Magyar Állami Földtani Intézet Évkönyve* (ed.: *D. Solti*), LXX. Budapest, Hungary, 609-615.

Russel, P.L., 1992: *Oil Shales of the World, Their Origin, Occurrence and Exploitation*. Pergamon Press, U.S.A., 413-450.

Solti, G., 1985: Agricultural utilisation of Neogene minerals raw materials in Hungary. In *Neogene Mineral Resources in the Carpathian Basin*. VIIIth RCMNS Congress, Budapest, Hungary, 519-530.

Solti, G., 1985a: Prospection and utilisation of alginite in Hungary. In *Neogene Mineral Resources in the Carpathian Basin*. VIIIth RCMNS Congress, Budapest, Hungary, 503-517.

Solti, G., 1987: Role of alginite and other geological products in improving soil fertility (in Hungarian). *Talajtermékenység javítása,* 358 pp.

Solti, G. and *Szabó, V.*, 1985: Possibilities for the agricultural use of the oil shales overlying the coal seam at Várpalota (in Hungarian). *Földtani Kutatás,* No. 1-2, 59-71.

Solti, G., Szabó, V. and *Papp, K.*, 1985: Examination of possibilities for the agricultural use of Maroccan, Yugoslav and Swedish oil-shales (in Hungarian). *Földtani Kutatás*, No. 1-2, 73-93.

NEWS

The WMO Norbert Gerbier - MUMM International Award winners in 1999

The fiftieth session of the WMO Executive Council conferred the Norbert Gerbier - MUMM International Award for 1999 on two Hungarian climate researchers, *Ms. Katalin Molnár* and *Mr. János Mika*. Both PhDs are presently affiliated at the Hungarian Meteorological Service.

The institution of the Norbert Gerbier - MUMM International Award was approved during the 39th session of the Executive Council, after the decease of Mr. Norbert Gerbier, the internationally appreciated French expert in agricultural meteorology. The purpose of the Award is to encourage and reward annually an original scientific paper on the influence of meteorology in a particular field of the physical, natural or human sciences, or conversely, the influence of one of these sciences on meteorology. The award aims at stimulating interest in such research, in support of WMO programmes.

Nomination for the Award is the right of all Permanent Representatives of Members of WMO, in response to the announcement annually distributed by the Secretary-General of the WMO, concerning papers published during the previous 18 months. The selection of the award winner is made by the selection committee, specially constituted for this purpose for a four-year period, that consists of not more than two members of the Executive Council and ex officio, the president of the Commission of Agricultural Meteorology. This decision is based on the preliminary assessment performed by three distinguished scientists in the field of meteorological applications.

The Award is presented annually and consists of a diploma, a medal bearing a likeness of Mr. Norbert Gerbier and a prize of 50.000 French francs.

The year 1999 Award was conferred on the authors for the paper entitled "Climate as a changing component of landscape: recent evidence and projections for Hungary" which was published in *Zeitschrift für Geomorphologie, N. F.,* Suppl.-Bd 110, (Berlin, Stuttgart), August, 1997.

The Award Ceremony took place during the fifty-first session of the Executive Council on 27 May 1999. Participants of the Award Ceremony were addressed by *Dr. J. Zillman,* President of the WMO; *Prof. G. O. P. Obasi*, Secretary-General of the WMO; *Mrs. G. Guiard-Gerbier,* France and *Mr. O. Brun,* representative of the MUMM Foundation, France. The Award was acknowledged by Katalin Molnár on behalf of the two winners who were accompanied by their spouses on this prominent occasion.

Summary of the
Norbert Gerbier – MUMM International Award '99
winner scientific paper
(The study was originally published in Zeitschrift für Geomorphologie
Neue Folge, Suppl.- Bd. 110, 1997, pp. 185-195, with 5 figures and 2 tables)

Climate as a changing component of landscape: recent evidence and projections for Hungary

Katalin Molnár and *János Mika*

Summary. Recent and expected future changes of temperature (corrected for inhomogeneities) and precipitation in Hungary are investigated, also in connection with the global climate tendencies. These factors are generally assessed in long-term averages, an approach with conceptual difficulties if global climate really changes. Two periods (1900–1949 and 1950–1989) are identified to compare monthly temperature and precipitation averages for the two periods. Differences are considerable for both elements. In the second part of the paper, an attempt is made to describe the climatic conditions modified according to a presumed regional climate change scenario for the 230 micro-regions of Hungary. Mean temperatures for the summer and winter half-years as well as annual precipitation are first analysed for the period 1951–1980. Maps of future areal distribution of winter, summer and annual temperature and precipitation have been produced, assuming 0.5, 1, 2 and 4 K increase in the annual mean temperature of the Northern Hemisphere. Regional scenarios related to small (0.5 and 1 K) hemispherical changes, are based on the method of 'slices' which establishes bilinear regressions between local and hemispherical variations, after a special filtering. Consequences of larger global changes are derived from General Circulation Model (GCM) outputs and paleoclimatic analogues. An independent comparison of the 10 years (1981–1990) and 30 years (1951–1980, i.e., the reference period of the previous maps) is also presented to demonstrate that the regional climate of recent decade is not in contradiction with the scenarios fully based on data from the previous time periods. These maps also show that for studying geomorphologic processes characterised by time-scales not much longer than a decade, the precise derivation of climate averages is even more crucial.

Present address of the authors:
Hungarian Meteorological Service, H-1525 Budapest, P.O. Box 38, Hungary
e-mail: *molnar.katalin@met.hu* and *mika@met.hu*

ATMOSPHERIC ENVIRONMENT

an international journal

To promote the distribution of Atmospheric Environment *Időjárás* publishes regularly the contents of this important journal. For further information the interested reader is asked to contact *Prof. P. Brimblecombe*, School for Environmental Sciences, University of East Anglia, Norwich NR4 7TJ, U.K.; e-mail: atmos_env@uea.ac.uk

Volume 33 Number 5 1999

Fast-track

D.J. Fish, D.E. Shallcross and *R.L. Jones:* The vertical distribution of NO_3 in the atmospheric boundary layer, 687-691.

P. Wolkoff, P.A. Clausen, C.K. Wilkinson, K.S. Hougaard and *G.D. Nielsen:* Formation of strong airway irritants in a model mixture of (+)-α-pinene/ozone, 693-698.

Papers

J. Kildesø, J. Vallarino, J.D. Spengler, H.S. Brightman and *T. Schneider:* Dust built-up on surfaces in the indoor environment, 699-707.

M.W. Gardner and *S.R. Dorling:* Neutral network modelling and prediction of hourly NO_x and NO_2 concentrations in urban air in London, 709-719.

E.D. Pellizzari, C.A. Clayton, C.E. Rodes, R.E. Mason, L.L. Piper, B. Fort, G. Pfeifer and *D. Lynam:* Particulate matter and managanese exposure in Toronto, Canada, 721-734.

R.A. Hashmonay, M.G. Yost, Y. Mamane and *Y. Benayahu:* Emission rate apportionment from fugitive sources using open-path FTIR and mathematical inversion, 735-743.

A.S. Ansarei and *S.N. Pandis:* Prediction of multicomponent inorganic atmospheric aerosol behavior, 745-757.

E.J. Highwood, K.P. Shine, M.D. Hurley and *T.J. Wallington:* Estimation of direct radiative forcing due to non-methane hydrocarbons, 759-767.

P.E. Padgett, E.B. Allen, A. Bytnerowicz and *R.A. Minich:* Changes in soil inorganic nitrogen as related to atmospheris nitrogenous pollutants in southern California, 769-781.

M. Fang, M. Zheng, F. Wang, K.L. To, A.B. Jaafar and *S.L. Tong:* The solvent-extractable organic compounds in the Indonesia biomass burning aerosols — caracterization studies, 783-795.

W.O. Siegl, R.H. Hammerle, H.M. Herrmann, B.W. Wenclawiak and *B. Luers-Jongen:* Organic emission profile for a light-duty diesel vehicle, 797-805.

J.D. Shannon: Regional trends in wet deposotion on sulfate in the United States and SO_2 emissions from 1980 through 1995, 807-816.

G.A. Allen, J. Lawrence and *P. Koutrakis:* Field validation of a semi-continuous method for aerosol black carbon (aethalometer) and temporal patterns of summertime hourly black carbon measurements in southwestern PA, 817-823.

J.A. Lind and *G.L. Kok*: Emission strenghts for primary pollutants as estimated from an aircraft study of Hong Kong air quality, 825-831.

S.E. Conell and *T.D. Jickells:* Water-soluble organic nitrogen in atmospheric aerosol: a comparison of UV and persulfate oxidation methods, 833-840.

Volume 33 Number 6 1999

H. Zhuang, C.K. Chan, M. Fang and *A.S. Wexler:* Size distributions of particulate sulfate, nitrate, and ammonium at a coastal site in Hong Kong, 843-853.

J.P. Greenberg, A. Guenther, P. Zimmermann, W. Baugh, C. Geron, K. Davis, D. Helmig and *L.F. Klinger:* Tethered balloon measurements of biogenic VOCs in the atmospheric boundary layer, 855-867.

M.D. Moulik and *J.B. Milford:* Factors inlfluencing ozone chemistry in subsonic aircraft plumes, 869-880.

T.C.W. Tung, C.Y.H. Chao and *J. Burnett:* A methodology to illvestigate the particulate penetration coefficient though building shell, 881-893.

A. Kasper-Giebl, M.F. Kalina and *H. Puxbaum:* Scavanging ratios for sulfate, ammonium and nitrate determined at Mt. Sonnblick (3016 m a.s.l.), 895-906.

L.W.A. v. Hove, M.E. Bossen, F.A.M. de Bok and *C.A.M. Hooijmaijers:* The uptake of O_3 by poplar leaves: the impact of a long-term exposure to low O_3-concentrations, 907-917.

E.G. Pavelin, C.E. Johnson, S. Rughooputh and *R. Toumi:* Evaluation of pre-industrial surface ozone measurements made using Schönbein's method, 919-929.

P.A. Ariya, H. Niki, G.W. Harris, K.G. Anlauf and *D.E.J. Worthy:* Polar sunrise experiment 1995: hydrocarbon measurements and tropospheric Cl and Br-atoms chemistry, 931-938.

I. Mavroidis, R.F. Griffiths, C.D. Jones and *C.A. Biltoft:* Experimental investigation of the residence of contaminants in the wake of an obstacle under different stability conditions, 939-949.

S. Parat, A. Perdrix, S. Mann and *P. Baconnier:* Contribution of particle counting in assessment of exposure to airbone microorganisms, 951-959.

J.S. Fuglestvedt, T.K. Bernsten, I.S.A. Isaksen, H Mao, X.-Z. Liang and *W.-C. Wang:* Climatic forcing of nitrogen oxides through changes in tropospheric ozone and methane; global 3D model studies, 961-977.

E. Dupont, L. Menut, B. Carissimo, J. Pelon and *P. Flamant:* Compatison between the atmospheric boundary layer in Paris and its rural suburbs during the ACLAP experiment, 979-994.

U. Kuhm, C. Amman, A. Wolf, F.X. Meixner, M.O. Andreae and *J. Kesselmeier:* Carbonile sulfide exchange on an ecosystem scale: soli represents a dominant sink for atmospheric COS, 995-1008.

Technical Note

X. Li-Jones, C. McCormick and *H.B. Maring:* Zero offset in computer-recorded analog data in measuring aerosol scattering coefficient: a "threshold" or a "blank"? 1009-1013.

Volume 33 Number 7 1999

A.T. Buckland and *D.R. Middleton:* Nomograms for calculating pollution within street canyons, 1017-1036.

R.M. Harrison, J.P. Shi and *M.R. Jones:* Continuous measurements of aerosol physical properties in the urban atmosphere, 1037-1047.

J.G. Vasiliou, D. Sorensen and *P.H. McMurry:* Sampling at controlled relative humidity with a cascade impactor, 1049-1056.

R.D. Saylor, W.I. Chameides and *M.E. Chang:* Demonstrating attainment in Atlanta using urban airshed model simulations: impact of boundary conditions and alternative forms of the NAAQS, 1057-1064.

B. Eklund: Comparison of line- and point-source releases of tracer gases, 1065-1071.

D.J. Luecken, G.S. Tonnesen and *J.E. Sickles, II:* Differences in NO_y speciation predicted by three photochemical mechanisms, 1073-1084.

M. Kahn, Y.J. Yang and *A.G. Russell:* Photochemical reactivitics of common solvents: comparison between urban and regional domains, 1085-1092.

A. Venkatram, D. Fitz, K. Bumiler, S. Du, M. Boeck and *C. Ganguly:* Using a dispersion model to estimate emission rates of particulate matter from paved roads, 1093-1102.

C. Treviño and *F. Méndez:* Simplifed model for the prediction of ozone generation in polluted urban areas with continuous precursor species emissions, 1103-1110.

Y. Andersson-Sköld and *D. Simpson:* Comparison of the chemical schemes of the EMEP MSC-W and IVL photochemical trajectory models, 1111-1129.

C. Zellweger, M. Ammann, P. Hofer and *U. Baltensperger:* NO_y speciation with a combined wet effluent diffusion denuder-aerosol collector coupled to ion chromatography, 1131-1140.

I.J. Simpson, G.C. Edwards and *G.W. Thurtell:* Variations in methane and nitrous oxidel mixing ratios at the Southern boundary of a Canadian boreal forest, 1151-1158.

M.A.K. Khailil and *R.A. Rasmussen:* Atmospheric chloroform, 1141-1158.

C.M. Mitic, W.J. Massman, P.H. Schuepp and *J.L. Collett Jr.:* Structural analysis and flux associations of CO_2, H_2O, heat and ozone over cotton and grape canopics, 1159-1173.

Volume 33 Number 8 1999

M. Glasius, M.F. Carlsen, T.S. Hansen and *C. Lohse:* Measurements of nitrogen dioxide on Funen using diffusion tubes, 1177-1185.

D.J. Hall, S. Walker and *A.M. Spanton:* Dispersion from courtyards and other enclosed spaces, 1187-1203.

Z. Guo, J.C.S. Chang, L.E. Sparks and *R.C. Fortmann:* Estimation of the rate of VOC emissions from solvent-based indoor-coating materials based on product formulation, 1205-1215.

H.N. Knudsen, U.D. Kjaer, P.A. Nielsen and *P. Wolkoff:* Sensory and chemical characterization of VOC emissionss from building products: impact of concentration and velocity, 1217-1230.

A. Feilberg, R.M. Kamens, M.R. Strommen and *T. Nielsen:* Modeling theee formation, decay, and partitioning of semivolatile nitro-polycyclic aromatic hydrocarbons (nitronaphthalenes) in the atmosphere, 1231-1243.

J.M.F. Diaz, M.A.R. Braña, B.A. Garcia, C.G.-P. Muñiz and *P.J.G. Nieto:* Difficulties inherent to the use of analytic solution of the condensation-evaporation equation for multicomponent aerosols, 1245-1259.

L. Morawska, S. Thomas, D. Gilbert, C. Greenaway and *E. Rijnders:* A study of the horizontal and vertical profile of submicrometer particles in relation to a busy road, 1261-1274.

M.E. Jenkin and *G.D. Hayman:* Photochemical ozone creation potentials for oxygenated volatile organic compounds: sensitivity to variations in kinetic and mechanistic parameters, 1275-1293.

E. Smet, H.V. Langenhove and *I.D. Bo:* The emission of volatile compounds during the aerobic and the combined anaerobic/aerobic composting of biowaste, 1295-1303.

M.A.K. Khailil and *R.A. Rasmussen:* Atmospheric methyl chloride, 1305-1321.

Technical Note

A. Kasper-Giebl and *H. Puxbaum:* Deposition of particulate matter in diffusion tube samplers for the determination of NO_2 and SO_2, 1323-1326.

M. Sharan, A.K. Yadav, M.P. Singh and *S. Gupta:* Accounting for the source strength in the solution of the diffusion equation: Alternative mathematical formulations, 1327-1330.

Volume 33 Number 9 1999

NOTES TO CONTRIBUTORS OF *IDŐJÁRÁS*

The purpose of the journal is to publish papers in any field of meteorology and atmosphere related scientific areas. These may be

- reports on new results of scientific investigations,
- critical review articles summarizing current state of art of a certain topic,
- shorter contributions dealing with a particular question.

Each issue contains "News" and "Book review" sections.

Authors may be of any nationality, but the official language of the journal is English. Papers will be reviewed by unidentified referees.

Manuscripts should be sent to

Editor-in-Chief of IDŐJÁRÁS
P.O. Box 39
H-1675 Budapest, Hungary

in three copies including all illustrations. One set of illustrations has to be of camera ready quality, the other two might be lower quality.

Title part of the paper should contain the concise title, the name(s) of the author(s), the affiliation(s) including postal and E-mail address(es). In case of multiple authors, the cover letter should indicate the corresponding author.

Abstract should follow the title, it contains the purpose, the data and methods as well as the basic conclusion.

Key-words are necessary to help to classify the topic.

The text has to be typed in double spacing with wide margins. Word-processor printing is preferred. The use of SI units are expected. The negative exponent is preferred to solidus. Figures and tables should be consecutively numbered and referred to in the text.

Mathematical formulas are expected to be as simple as possible and numbered in parentheses at the right margin. Non-Latin letters and hand-written symbols should be indicated and explained by making marginal notes in pencil.

Tables should be marked by Arabic numbers and printed in separate sheets together with their captions. Avoid too lengthy or complicated tables.

Figures should be drawn or printed in black and white, without legends, on separate sheets. The legends of figures should be printed as separate list. Good quality laser printings are preferred as master copies.

References: The text citation should contain the name(s) of the author(s) in Italic letter and the year of publication. In case of one author: *Miller* (1989), or if the name of the author cannot be fitted into the text: *(Miller,* 1989); in the case of two authors: *Gamov* and *Cleveland* (1973); if there are more than two authors: *Smith et al.* (1990). When referring to several papers published in the same year by the same author, the year of publication should be followed by letters a,b etc. At the end of the paper the list of references should be arranged alphabetically. For an article: the name(s) of author(s) in Italics, year, title of article, name of journal, volume number (the latter two in Italics) and pages. E.g. *Nathan, K.K.,* 1986: A note on the relationship between photosynthetically active radiation and cloud amount. *Időjárás 90,* 10-13. For a book: the name(s) of author(s), year, title of the book (all in Italics except the year), publisher and place of publication. E.g. *Junge, C. E.,* 1963: *Air Chemistry and Radioactivity.* Academic Press, New York and London.

The final version should be submitted on diskette altogether with one hard copy. Use standard 3.5" or 5.25" DOS formatted diskettes. The preferred word-processors are WordPerfect 5.1 and MS Word 6.0.

Reprints: authors receive 30 reprints free of charge. Additional reprints may be ordered at the authors' expense when sending back the proofs to the Editorial Office.

More information: gmajor@met.hu

Information on the last issues:
http://www.met.hu/firat/ido-e.html

Published by the Hungarian Meteorological Service

Budapest, Hungary

INDEX: 26 361

HU ISSN 0324-6329

IDŐJÁRÁS

QUARTERLY JOURNAL
OF THE HUNGARIAN METEOROLOGICAL SERVICE

CONTENTS

****

http://www.met.hu/firat/ido-e.html

VOL. 103 * NO. 3 * JULY–SEPTEMBER 1999

IDŐJÁRÁS

Quarterly Journal of the Hungarian Meteorological Service

Editor-in-Chief
T. PRÁGER

Executive Editor
M. ANTAL

Editorial Office: P.O. Box 39, H-1675 Budapest, Hungary or
Gilice tér 39, H-1181 Budapest, Hungary
E-mail: prager@met.hu or *antal@met.hu*
Fax: (36-1) 290-7387

Subscription by

mail: IDŐJÁRÁS, P.O. Box 39, H-1675 Budapest, Hungary;
E-mail: prager@met.hu or *antal@met.hu*; *Fax: (36-1) 290-7387*

EDITORIAL

Dear Reader,

On April 1, 1999 there was a change in the position of the Editor-in-Chief of IDŐJÁRÁS. *Prof. G. Major,* Member of the Hungarian Academy of Sciences, who has been the Editor-in-Chief in the last four years, retired from this position due to several other obligations he has to fulfil. From January 1999 he was appointed to serve as the Chairman of the Scientific Council of Hungarian Meteorological Service (HMS), and, of course, he continues to be the Head of the Satellite Research Laboratory.

The President of the HMS, the organization which owns the IDŐJÁRÁS, has nominated me as Editor-in-Chief. It is a great honour for me to greet you in my new position, and, please allow me to introduce myself shortly and also to say some words about my ideas concerning the journal.

I graduated from mathematics and meteorology at the Eötvös Loránd University in Budapest in 1974, and begin my scientific work at the HMS. After one year work in the field of numerical weather prediction I obtained a Ph. D. (or more exactly C. Sc.) fellowship in Moscow at the Hydrometeorological Scientific Research Centre of the previous Soviet Union, one of the leading scientific institutions in meteorology at that time. I spent three years in Moscow working on my thesis, the subject of which was the development of a limited area nested grid NWP model. There I had opportunity to meet and learn from famous scientists, like *Prof. L. S. Gandin*, *Prof. G. I. Marchuk* and others.

After successfully defending my C. Sc. thesis I returned home and began to work at the Department of Meteorology of the Eötvös Loránd University as associate professor. Here I worked out the training plan of some new subjects in meteorologists' training, like Dynamical Models of the Atmosphere and Numerical Weather Prediction, and also participated in writing of university textbooks. From 1987, keeping my position at the university in half-stage, I returned to the HMS and began to work as the head of Section for Atmospheric Dynamics at the Institute for Atmospheric Physics under the directorship of *Prof. E. Mészáros*. The scientific profile of the section was climate modeling, in which we got special support and valuable scientific supervision from *Dr. G. Götz*, deputy director of the Institute at that time.

In 1989 I was granted a one year postdoctoral position at the National Center for Atmospheric Research (Boulder, U.S.A.). Here my research work was concentrated on the sensitivity analysis of some climate and NWP models with the application of the adjoint technique. During this time I had scientific cooperation with outstanding scientists like *Dr. D. Williamson*, *Dr. E. Kalnay* and others, whom I owe a debt of gratitude for supporting my work. My scientific cooperation with scientists working in the field of adjoint applications and variational data assimilation continued after my returning home in 1990. In 1994 I headed the local organizing committee of the Second Workshop on Adjoint Applications in Meteorology.

Unfortunately the political change which took place in Hungary in 1989 has found the Meteorological Service in a rather bad shape concerning its ability to adapt itself to the new economic circumstances. In this situation a new leadership was nominated and I took the position of the head of Department for Atmospheric Observations. In this capacity my task was to supervise the countrywide meteorological observation network, including upper-air and meteorological radar observatories, and environmental measuring sites. In the period 1991–1997 with the substantial help of my colleagues we succeeded in reconstructing the main components of the observing system, enhancing both their quality and cost-efficiency.

In the beginning of this year research and development activities of the HMS, that were largely hindered in the past years by financial restrictions were brought together in the frame of a Research and Development Department, and I was nominated as its head. As you can see, I have already tried almost every possible field of activity which is given inside our science and dare hope, that wide-range experience will help me in the editorial work.

Now, some words about my intended editorial policy. I do not plan significant changes in the profile of the journal. Repeating the words from the editorial comments written by my predecessor, *Prof. Major* four years ago: "the basic purpose of the journal is to publish high quality articles from any field of the atmospheric sciences written in English", and — in my view — both he and *Prof. Mészáros* before him did an excellent job to fulfil this task. While encouraging and highly appreciating papers from the "traditional" fields of the journal in the future, I try to put more stress in its profile on meteorological scientific subjects, which — in my judgment — were somehow under-represented in the journal until now, like weather forecasting including NWP or scientific results with new observational techniques, etc.

The regions from which we especially intend to attract publications are countries with economies in transition and developing countries, where, in our thinking, significant scientific potential not always matches the possibilities of publication, or, in other words, it is not always an easy task for scientists from this regions to make their high level results available for the global scientific community. Of course, absolutely no formal geographical limitation exists when choosing our authors. Another baseline of our publishing strategy is to choose reviewers for the papers from the circle of the most widely known and recognized experts of the field in question. I am absolutely convinced that the above goals can be met only with a high level Editorial Board, where good balance of geographical representation and uniform scientific excellence are both present. Since the previous Editorial Board well exhibited these features, we plan only a few changes, mainly in the direction to include outstanding young scientists in its rows.

Closing my comments I wish to express my sincere thanks to authors, readers and all who contributed in the past and hopefully will continue to contribute in the future in the publication of the 103 years old IDŐJÁRÁS. I will try to serve in accordance with the traditions of the journal.

Sincerely,

Dr. Tamás Práger
Editor-in-Chief

IDŐJÁRÁS

Quarterly Journal of the Hungarian Meteorological Service
Vol. 103, No. 3, July–September 1999, pp. 145–160

Energy budget components in a forest clearcut: analysis of measurement results

T. Weidinger[1], **F. Ács**, **R. Mészáros** and **Z. Barcza**

Department of Meteorology, Eötvös Loránd University,
H-1117 Budapest, Pázmány Péter sétány 1/A, Hungary

(Manuscript received 25 March 1999; in final form 22 June 1999)

Abstract—Energy budget components were measured over a big forest clearcut during a 2 week period in June and July, 1995 in the framework of NOPEX (**No**rthern Hemisphere Land Surface Climate **P**rocesses **Ex**periment) CFE-2 (Second Concentrated Field Effort) to analyze the energy budget residue and its relation to energy budget components. The energy budget residue can be interpreted as the uncertainty of energy budget calculation, which consists of the measurement error, the differences between the source areas of radiation and energy balance components, the effects of advection, surface inhomogeneity, etc. It was determined as the residual of land-surface energy balance equation. The energy budget components were measured independently of each other. The values of turbulent fluxes were determined using eddy correlation technique.

The main measurement results are as follows: the daily mean values of the energy budget residue are between 2–28 W m^{-2}; the 2 week average value is 15 W m^{-2}, the corresponding standard deviation is 40 W m^{-2}. The order of magnitude of the energy budget residue is as great as the total soil heat exchange. The investigation has shown that the residuum is mainly not caused by instrumental problems.

Modellers always find closure of the energy balance because they use the energy balance equation to determine the soil temperature. Closure is obtained by iterating while allowing the soil temperature to vary. This method can result poor soil and surface temperature forecasts in case of significant energy budget residue.

Key-words: NOPEX, clearcut, surface energy budget, energy budget residue, eddy correlation technique.

1. Introduction

The basic object of NOPEX (**No**rthern Hemisphere Land Surface Climate **P**rocesses **Ex**periment) is to estimate the regional scale surface fluxes for boreal ecosystems (*Lundin,* 1995). The project has started in 1991 by long-term and

---

[1] Corresponding author. E-mail: weidi@ludens.elte.hu

special measurements performed in different areas of NOPEX-region (Central-Eastern Sweden). The long-term measurements were extended by special observations in CFE1 and CFE2 (Concentrated Field Efforts). The dataset is completed with remote sensing, hydrological and climatological observations. Field experiments with specific biophysical observations representative for patch scale have a special role in NOPEX (*Halldin et al.,* 1995). They provide both specific and basic information for scaling up the fluxes from patch to region (*Chehbouni et al.,* 1995). A specific surface type of NOPEX region is the forest clearcut. To know the daily variation and uncertainty of energy budget components above the different surface types is important for upscaling the fluxes from local to regional scale.

There are a few reasons why the energy budget studies above forest clearcuts are important.

(1) Clearcut and its microclimate completely differ from the surrounding forest (*Ghuman* and *Lal.,* 1986; *Chen et al.*, 1993). Its characteristics are studied by measurements and/or modelling. During the growing season the daily averages of air and soil temperatures, wind velocity and solar radiation are consequently smaller, air and soil moisture are larger inside a forest than in a clearcut (*Chen et al.*, 1993). The clearcut's albedo parameter is larger than the albedo in a forest area. The runoff is faster, the soil heat flux is larger. As the microclimate of a clearcut differs from the microclimate of a forest thus the turbulent exchange also alters over clearcuts. These effects are important for planning of reforestation.

(2) The basic energy balance characteristics of forest clearcuts are not known well. The surface energy and water budgets completely differ in a clearcut and inside a forest; they are influenced by the differences between the source areas of radiation and energy balance components (*Schmid*, 1997), by surface inhomogeneities (vegetation, soil and water content heterogeneities, direction dependent fetch), local advection and many other edge-caused effects.

(3) Model experiments and field observations are necessary to describe the properties of evapotranspiration, diurnal and seasonal variations of the surface and soil parameters, and to predict their values. Most of the studies are based on the energy balance equation describing one or more specific properties of a clearcut. However, most of the measurements performed have difficulties in the closure of the energy budget; they only deal with some of its components. Evapotranspiration and surface conductance above a clearcut were considered by *Adams et al.* (1991), where the analysis was based on eddy correlation measurements of sensible heat flux and additional measurements of soil heat flux and net radiation. Our measuring concept is similar to that of described by *Adams et al.* (1991). Unlike in *Adams et al.* (1991) study we measure the latent heat flux separately instead of calculating it from the energy balance equation. In order to estimate evapotranspiration in a forest clearcut *Flint* and *Childs*

(1991) have used the Priestley-Taylor equation. This method also requires the measurement of all terms of the energy budget. They have estimated their components with Bowen-ratio technique. Some microclimatic elements (soil and air temperature, soil moisture and saturation deficit) were also analyzed by *Groot* and *King* (1993) using soil-atmospheric model and field observation of energy budget components together with the use of the Bowen-ratio method. It was found that the prediction of atmospheric variables over a clearcut is more erroneous than the prediction of soil state variables due to the surface heterogeneities. *Stathers et al.* (1985) have shown that over clearcuts the soil temperature is quite sensitive to solar radiation, wind speed and surface roughness, but relatively insensitive to air temperature, lower boundary soil temperature and soil thermal properties. All these studies concentrate on one or few components of the energy balance equation; that is one component is always determined as a residual in the energy balance equation. Thus, there is no energy budget error estimate whatsoever represented in these studies.

The aim of this study is therefore twofold: first of all, the determination of daily courses of the energy balance components, and the investigation of some aspects of energy budget closure.

First, we review the measurement of energy balance components over a large forest clearcut near Siggefora during a two week period in summer 1995 in the frame of NOPEX CFE2 (Second Concentrated Field Effort). The results obtained are important because the surface type is very specific and there are only a few similar measurements published in the literature. Compared to former studies we performed more detailed measurements; each energy balance component has been measured independently, which made it possible to evaluate the energy budget residue (Δ). This term can be interpreted as

$$R_n - LE - H - G_{st} - G_c = \Delta \neq 0 , \qquad (1)$$

where R_n is the net radiation, LE and H is the latent and sensible heat flux, respectively; G_{st} is the heat storage of 8 cm depth surface soil layer and G_c is the heat conductance into the deeper soil. The total soil heat exchange (G) is the sum of the heat storage and the heat conductance term ($G = G_{st} + G_c$).

Second, we analyze the relationship between the energy budget residue (Δ) and energy balance components to prove the reliability of measurement results. Energy must be conserved at the earth's surface. This statement of the first law of thermodynamics is used in all weather and climate models as one of the basic equations. The discrepancy between the available energy ($R_n - G$) at the surface and the consumption of energy by turbulent fluxes ($H + LE$) is well-known for about 10 years and widely accepted in recent years. The "unclosure" of about 10–30% of the available energy is presently a "number" to characterise and to compare field experiments (*Foken* and *Oncley*, 1995). In most cases the absolute values of available energy (R_n - G) have exceeded the turbulent fluxes (H + LE) (*Panin* and *Tetzlaff*, 1999).

In the 1980s, significant progress was made in methods to measure sensible and latent heat fluxes so it was no longer necessary to determine one part of the energy balance equation (mostly the latent heat flux) as the residuum of all the other parts. However, using these measurements, many land surface experiments were unable to demonstrate that the sum of all terms of the energy balance equation is zero. In fact, differences of 50 W m^{-2} were common and values even up to 200 W m^{-2} were observed. Fundamental problems may exist in our understanding of the energy exchange between atmosphere and surface (*Foken* and *Oncley*, 1995; *Oncley*, 1999).

Nevertheless, the closure problem did not result in significant effort to determine its cause. There are two reasons for this lack of research effort.

(1) Many experimentalist use the so-called Bowen-ratio method to measure fluxes. With this method, a surrogate for the ratio H/LE (Bowen ratio) is measured and the sum $H + LE$ is determined from measurements of R_n, G_{st}, G_c and the energy balance equation. With the sum and ratio of H and LE, it is trivial to determine their values.

(2) Even if both fluxes were measured, the energy budget residue (Δ) is sometimes used to correct their values.

Of course, modellers always find closure of the energy balance because they use the energy balance equation to determine the soil temperature. Closure is obtained by iterating while allowing the soil temperature to vary. This method can result in poor soil and surface temperature forecasts. This problem can also affect the fluxes of chemical species, such as carbon dioxide, since similarity relations are often used to compute these fluxes from the turbulent energy fluxes (*Oncley*, 1999).

Recently, the problems of Global Climate Change focused our interest on the water cycle (GEWEX, IGBP) and the carbon cycle (EUROFLUX, AMERIFLUX, JAPANNET and others) not for a qualitative overview but for a highly accurate quantitative determination (*Hutjes*, 1998). Therefore the discussion of the residuum of closure of energy balance is important above different surface types.

In the present study site description is presented first and methodology of measurement is demonstrated. Next, the calculation of momentum, latent and sensible heat flux is reported. Then properties of surface heterogeneity in the source region, the daily courses of all energy budget components and the energy budget residue (Δ) are discussed. Finally, a section for conclusions is provided.

2. *Micrometeorological measurements*

2.1 Site description

The experimental site is located in a large clearcut of a boreal pine forest within the NOPEX area, about 40 km far from Uppsala, Sweden. The forest was cut over a few years ago, therefore direct forest degradation effect is already not visible in the site. The shape of the clearcut and the meteorological conditions (precipitation, temperature, wind direction, momentum flux and frontal overpasses) during the measuring period are presented in *Fig. 1*. The characteristic size of the clearcut is 0.5 km × 1.5 km. The mean slope angle is approximately 1.5°.

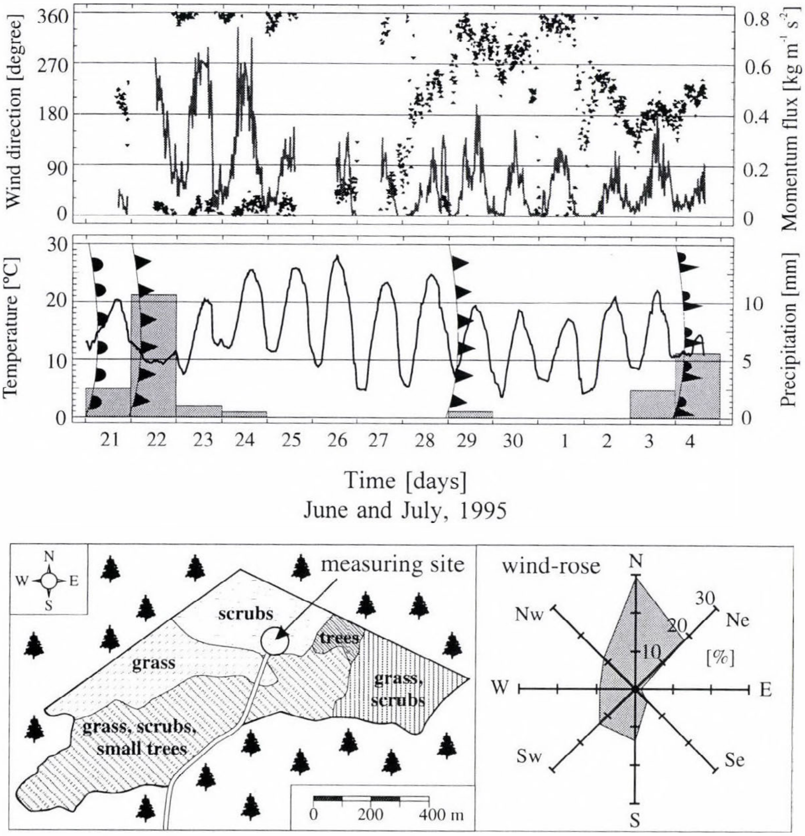

Fig. 1. Site characteristics and meteorological conditions during the measurement period.

The measuring equipment were mounted in the middle, slightly sloping part of the field. The fetch was approximately 200 m long at the beginning of the expedition for mainly northern wind (June 22–26, 1995) and on July 3–4 for mainly southern wind. In other cases the fetch was about 300–800 m long. About 80% of the field was covered by shrub and grass with 0.2–0.6 m height, by stumps of the cut trees and sparsely by young pines and some other type of trees. Among vegetation different size granite stones were scattered in grant numbers, which modified the surface albedo and roughness of the area. The wet soil surface was partly covered by smaller or greater puddles. At the beginning of the expedition there was frontal precipitation (Fig. 1). Then the soil was saturated. In that time about 3–5% of the surface was covered by puddles. The water disappeared from the pits at the end of June. Site values of soil moisture content is obtained by interpolation of measurements performed at different locations every 3 days. Precipitation was taken from *in situ* measurements. The soil water table was approximately at 0.6 m depth near the measurement tower. The average density of the upper 8 cm soil was 1.65×10^3 kg m^{-3}. Values of soil moisture content were obtained by gravimetric measurements; it was 0.35×10^3 and 0.26×10^3 kg m^{-3} at saturation and under dry conditions, respectively. The specific heat capacity of wet soil varied between 1400 and 1580 J kg^{-1} K^{-1} depending on soil moisture content. During the measurement period the soil heat capacity change was greater than 10% of the initial value. The estimated leaf area index (LAI) and roughness length was 1.3–1.8 m^2 m^{-2} and 5 cm, respectively.

2.2 Measurements of state variables and fluxes

Air temperature, dew point temperature and the temperature of the upper 8 cm soil layer were measured in every 20 minutes. The soil heat storage term was calculated from the averaged soil temperature values obtained by 4 sensors installed on wet and dry soil surfaces using the spatially averaged soil density. Soil heat flux was measured in 8 cm depth at two locations on 0.5 m distance. The heat flux plates were situated in a dry and a wet location. The solar radiation was measured by Schenk pyranometer, the photosynthetically active radiation (PAR) by LI-COR sensor, and the net radiation by REBS Q-6 net radiometer. The radiation components together with other meteorological elements were collected by a Campbell 21X datalogger. The solar radiation and PAR sensors were calibrated in Hungary. In other cases the manufacturing calibration was used. The measurement error of net radiation, caused by neglecting wind speed corrections for REBS Q-6 net radiometer, were between 2–4% according to the manual of new type REBS Q-7 net radiometer.

Wind speed, wind direction, momentum, sensible and latent heat fluxes were determined, using the eddy-correlation measurement technique applying a Solent three-axis research ultrasonic anemometer (GILL-1012) and a KH-20

Krypton Hygrometer (Campbell Scientific, Ltd) using 20 minute averaging periods. This equipment was mounted on a 5.5 m height mast. Data were sampled at 21 Hz. The reference moisture for the determination of moisture fluctuations was given by the dew point temperature measurement. In cool nights (e.g., on the 27th of June and the 2nd of July) the condensed dew at the iron body of the KH-20 Krypton Hygrometer could cause errors in the latent heat flux estimation.

When eddy correlation measurements are missing, the sum of sensible and latent heat flux ($H + LE$) are calculated using the correlation between R_n and ($H + LE$). Missing 20 minute average wind speed data (U) is estimated from its daily average courses.

2.3 *Determination of turbulent fluxes*

The turbulent fluxes are determined after *McMillen's* methodology (1988) using 20 minute averaging time. The coordinate system is rotated to the main wind direction. The wind speed, temperature and moisture datasets are detrended for calculation of the time series of fluctuations (actual value – mean value) by moving averages technique using 400 s time window for the estimation of mean values.

The sonic temperature was calculated according to *Kaimal* and *Gaynor* (1991) as:

$$T_s = T(1 + 0.32 e/p) = \frac{c_{vm}}{c_{pm} R_m} c^2, \tag{2}$$

where c_{vm}, c_{pm} are the specific heat capacities of moist air at constant volume and pressure, respectively; R_m is the specific gas constant of moist air; c, T, T_s are the measured sound speed, air temperature and the sonic temperature, respectively; p and e are air pressure and the water vapor pressure, respectively. The sensible heat flux (H) was calculated from

$$H = c_{pm} \rho_m \overline{w'T'} = c_{pm} \rho_m (\overline{w'T_s'} + 0.1 \overline{w'e'}), \tag{3}$$

where ρ_m is the density of moist air, w', T_s', T', e' are the fluctuation of vertical wind speed, sonic temperature, air temperature and water vapor pressure (in hPa), respectively.

Flow distortion by sonic anemometer is eliminated by applying the manufacturer's wind speed calibration (Gill calibration). This seemed to be an adequate available tool for our measurements. The matrix calibration method proposed by *Grelle* and *Lindroth* (1994) is more precise than Gill's one, but the deviation between them in the case of latent and sensible heat fluxes is only up to 2–4%. This deviation produces slight underestimation of H and LE. The matrix calibration was not applied because the rough dataset from sonic anemometer was collected using the option of manufactory calibration.

On the other hand, the calculation error of temperature fluctuation may cause a few percent overestimation of sensible heat fluxes after *Kaimal* and *Gaynor*, 1991. They have suggested a wind speed correction for sonic anemometers with three pairs of sensors that are orthogonal to each other. Since the sensors of Gill sonic anemometer are not orthogonal, we did not apply this correction. Negligence of the above mentioned two corrections partly compensated each other.

The latent heat flux is calculated according to *Tanner et al.* (1993) using both the equipment-dependent oxygen-correction and the corrections of latent and sensible heat fluxes (*Webb et al.,* 1980):

$$LE = LE_m (1 + K_0)(1 + K_E + K_H), \tag{4}$$

where L is the latent heat of vaporization, E_m is the measured water vapor density flux; K_0, K_E and K_H are the correction terms of oxygen, latent and sensible heat flux, respectively.

The KH-20 Krypton Hygrometer works on both 123.58 nm and 116.49 nm wavelengths. The absorption of energy due to the presence of oxygen has also to be taken into account. The voltage output of the hygrometer depends upon fluctuations of the two gases and can be approximated by

$$V = V_0 e^{-x k_w \rho_v} e^{-x k_0 \rho_0}, \tag{5}$$

where ρ_v and ρ_0 are the densities of water vapor and oxygen in g m^{-3}, respectively; x is the path length between source and detector (x = 1.32 cm), k_w and k_0 are the extinction coefficients of water vapor and oxygen respectively, while V_0 and V are the base and the output voltages in mV, respectively.

Using the logarithmic form of Eq. (5) combined with Eq. (4) the uncorrected latent heat flux is:

$$LE_m = -\frac{L}{x k_w} \overline{(\ln V)' w'}, \tag{6}$$

where $(\ln V)'$ is the deviation of logarithmic voltage from its average. The extinction coefficient k_w is found to be 0.138 m^3 g^{-1} cm^{-1} $< k_w <$ 0.152 m^3 g^{-1} cm^{-1} using the factory calibration based on 20 minute average of water vapor density.

Neglecting pressure fluctuations with respect to the fluctuations of temperature, the oxygen fluctuation corrections implemented into the Bowen-ratio (β) can be expressed as:

$$K_0 = 0.23 \frac{k_0}{k_w} \frac{L}{T} \beta \, , \tag{7}$$

where k_0 is 8.5×10^{-3} m^3 g^{-1} cm^{-1} according to *Tanner et al.* (1993). The oxygen correction (K_0) of the rough latent heat flux is 10% of the value of LE_m for $\beta = 1$, which is a relatively large value. K_E and K_H in Eq. (4) were calculated after *Webb et al.* (1980) from

$$LE = LE_m (1 + K_0)\,(1 + rm)(1 + s \frac{\beta}{c_{pm} T}) \, , \tag{8}$$

where r is the average mixing ratio, s is the specific moisture and $m = 1.607$ is the ratio of dry air molecule weight to water molecule weight. After *Tanner et al.* (1993) $K_H/K_E \approx 5$ and typical values of K_E are between 0.01 and 0.02.

3. Results

First, the surface homogeneity of the measurement site is considered. Further, the effect of soil wetness variations upon soil heat conductance term (G_c) is analyzed. At last, daily courses of energy budget components and the energy budget residue (Δ) are analyzed with more attention.

The effect of local surface heterogeneity in the source region can be characterized by a correction factor k (*Panin et al.*, 1996) as:

$$k = \frac{\sum\limits_i ((R_n)_i - G_i)}{\sum\limits_i (H_i + LE_i)} \, , \tag{9}$$

where $G_i = (G_{st})_\mathrm{i} + (G_c)_i$ is the total soil heat exchange. The factor k is determined for the 10 day measurement period between June 24–July 3, 1995. The ratio of available energy ($R_{ni} - G_i$) and the turbulent fluxes ($H_i + LE_i$) is calculated for every 20 minutes ($i = 1, 2, \dots 10 \times 24 \times 3$). The mean value of k is 1.24 which is practically equal with LINEX experiment ($k_{LINEX} = 1.25$; *Foken,* 1997). According to *Foken's* (1997) criterion, the experimental location can be classified as slightly heterogeneous.

Daily courses of turbulent fluxes (H, LE) with the energy budget residue (Δ) in measuring period are presented in *Fig. 2*. According to the convention used the turbulent fluxes are positive upwards.

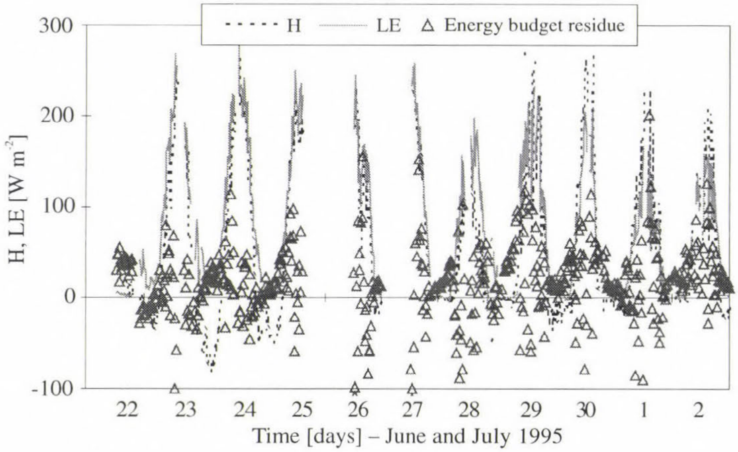

Fig. 2. Daily variation of turbulent fluxes and closure term in the measuring period.

At the beginning of the measuring period H and LE are approximately equal; their maximum values are between 250 and 300 W m^{-2}. The absolute value of Δ is usually – excepting some rare situations – below 100–150 W m^{-2}. In the last days of the measuring period – when the soil surface layer was much more dry – H exceeds LE and the scatter of Δ is somewhat larger.

Mean values (m) and standard deviations (σ) of net radiation (R_n), sensible (H) and latent (LE) heat flux and the soil heat conductance at 8 cm depth (G_c) are presented in *Table 1* for 9 days, when the eddy covariance system worked well (594 measurement periods for 9 days).

Table 1. Main values (m) and standard deviations (σ) of net radiation (R_n), sensible (H) and latent heat flux, and the soil heat conductance at 8 cm depth (G_c) for 9 days, when the eddy covariance system worked well (W m^{-2})

	R_n	H	LE	G_c
m	151	48	63	6.5
σ	187	78	59	14

The mean values and standard deviations of energy budget components for this period are not deviate considerably from the values for the whole measurement period (not presented here). The values of standard deviations are grater than the means. It is clear because the daily variation of energy budget components is higher than the mean values. For instance, the difference between the minimal and maximal net radiation is approximately 650 W m^{-2} (-55 W m^{-2}< R_n < 590 W m^{-2}).

The daily course of soil heat conductance at 8 cm depth, measured by REBS heat flux plates located on wet (plate I.) and dry (plate II.) areas, are shown in *Fig. 3*. The accuracy of the soil heat plates is good because their registrations are the same during the frontal precipitation time period of 22 June. There is an expressed deviation between the amplitudes measured in wet and dry locations; they exceeded 25 W m^{-2} in the afternoon of 25 June, when the areal mean value is close to 40–45 W m^{-2}. In the second half of the measuring period the deviations were smaller due to soil water content decrease. The greatest G_c values appeared in wet soil at about 15 LT (Local Time); in dry soil between 17 and 18 LT. In the energy budget analysis areally averaged soil heat conductance is used. Wet and dry areas are taken into account by 80% and 20%.

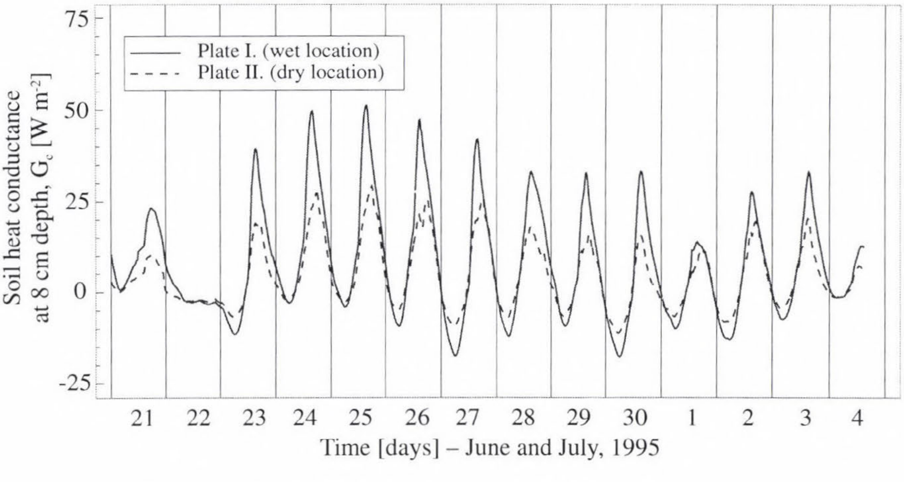

Fig. 3. Soil heat conductance (G_c) at 8 cm depth measured by plates on wet and dry locations.

Daily courses of all energy budget components for 30 June and 1 July are presented in *Fig. 4*. General features are as follows: all energy budget components show large fluctuations. The largest, medium and smallest terms are net radiation, turbulent fluxes and soil heat flux with the energy budget residue, respectively. The soil heat exchange and the energy budget residue are smaller than the turbulent fluxes but the difference is not irrelevant.

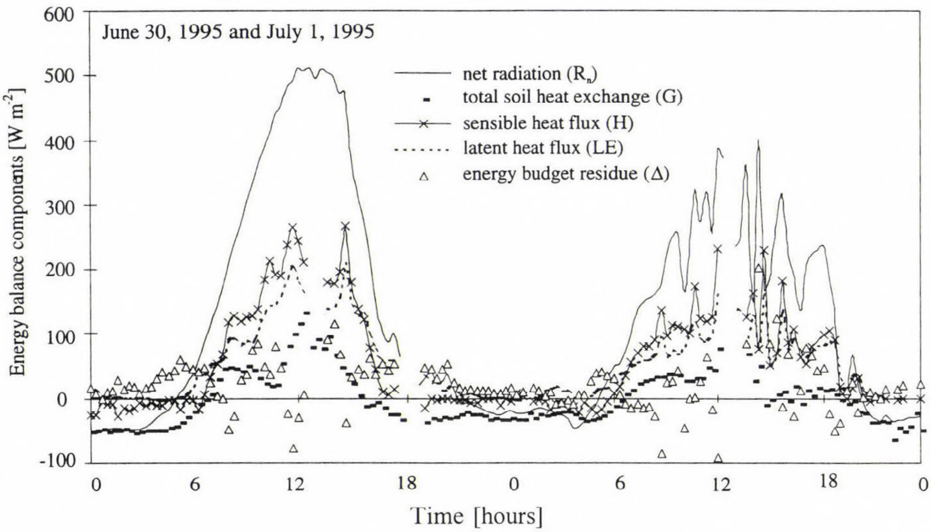

Fig. 4. Daily variation of energy budget components and closure term on 30 June and 1 July.

The two days chosen are different. 30 June is a sunny day with much insolation while 1 July is cloudy with weaker insolation. On 30 June the daily average of net radiation and the energy budget residue is 148 W m^{-2} and 22 W m^{-2}, respectively. On 1 July the averages are 109 W m^{-2} and 8 W m^{-2}, respectively. Δ shows large fluctuations similarly to all energy budget components. Δ is mostly positive in both days. It depends largely upon net radiation fluctuations. Inspecting Fig. 4 we see that the order of magnitude of G is as great as that of Δ. The standard deviation of Δ is about 30 W m^{-2} and 50 W m^{-2} on 30 June and 1 July, respectively.

The day-time ($R_n > 0$) and night-time ($R_n < 0$) averages of the energy budget residue (Δ) are presented in *Fig. 5*. The main characteristics are as follows:

(i) The energy budget residue (Δ) differs from zero but it is always smaller than 35 W m^{-2}.

(ii) $\Delta > 0$ except of the night-time period of 22–23 June. 11 and 1 mm precipitation is observed in day- and night-time period, respectively.

(iii) At night (from 22 to 06 LT) Δ is between −12 W m^{-2} and 13 W m^{-2}, which is a relatively large value as compared to energy budget components. The corresponding standard deviation of Δ is 15 W m^{-2}.

(iv) The larger the day-time mean net radiation is, the greater the Δ is and vice versa. For instance Δ is smaller than 10 W m^{-2} on 28 June, 1 July and on 3 July when average day-time net radiation is between 190 W m^{-2} and 210 W m^{-2}. Reversed Δ is about 30 W m^{-2} on 29 and 30 June and on 2 July when average day-time net radiation is between 250 W m^{-2} and 275 W m^{-2}. The standard deviation of the energy budget residue for day-time during the whole measurement period is about 45 W m^{-2}.

(v) The energy budget residue depends on wind speed and wind direction. For instance $|\frac{\Delta}{R_n}| < 0.2$ for $U > 2$ m s^{-1} and $-0.2 < \frac{\Delta}{R_n} < 0.4$ for $U < 2$ m s^{-1} when $R_n > 100$ W m^{-2} and the wind direction is between north and northeast (see Fig. 1).

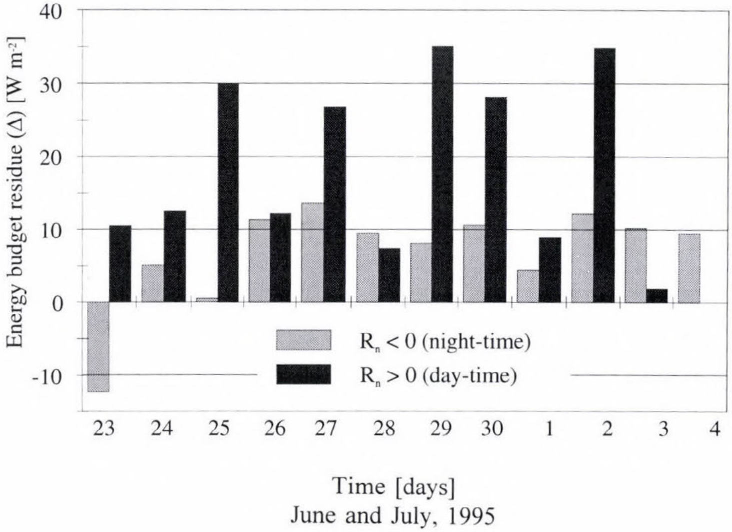

Fig. 5. Day-time ($R_n > 0$) and night-time ($R_n < 0$) averages of energy budget residue.

4. Conclusions

Daily variations of energy budget components over a big forest clearcut have been estimated by measurements to analyze the energy budget residue (Δ) and its relation to energy budget components. The energy budget components were independently measured from each other as accurately as possible. Turbulent fluxes were determined using the eddy correlation technique.

An energy deficit was observed, which means that the sum of turbulent fluxes were less than the available energy. Those are experienced by many field experiments (e.g., *Foken*, 1997; *Panin et al.*, 1998). The accuracy of our measurements for energy budget components (as H, LE, R_n, G_c) was below 5–10% and there was not any detected systematic error. Recent investigation has shown that the energy budget residue, which in the day-time period may grow up to 150 W m^{-2} is not caused mainly by instrumental problems but

(i) by methodological problems associated with uncertainties of estimation of flux time series (*Foken* and *Wichura*, 1996; *Weidinger* and *Matyasovszky*, 1998),

(ii) by neglecting the effect of density fluctuations for calculation of turbulent fluxes and

(iii) by differences between the source areas of radiation and energy balance components (*Schmid*, 1997),

(iv) by effect of surface heterogeneity, since the standard method to describe the turbulent fluxes requires stationarity and horizontal homogeneity which are not realised between the horizontally inhomogeneous land surface and atmosphere (*Panin* and *Tetzlaff*, 1999),

(v) by horizontal advection (*McNaughton*, 1976),

(vi) by effect of convective-scale flux components (*Laubach* and *Teichmann*, 1999), and

(vii) by effects of the additional terms of energy budget like the photosynthetic heat flux density, the heat storage for the vegetation and for the air, etc.

The energy budget residue is quantified and the possible reasons are qualified in this paper. The results are as follows:

(1) The maximum values of turbulent fluxes change between 150 and 300 W m^{-2}. At the beginning of the measurement period H and LE are close to each other, while at the end of the measurement period H usually exceeds LE.

(2) The deviations between the soil heat conductance measured at two different locations at 8 cm depth can exceed 25 W m^{-2} in the afternoon; this is considerably large with respect to the areal mean of G_c, which is up to 40–45 W m^{-2}.

(3) The daily mean of the energy budget residue is between 2–28 W m^{-2}. Its average value in the measurement period is 15 W m^{-2}. It shows large fluctuations which are governed by changes of net radiation. Therefore the time averaged value of standard deviation is more than 40 W m^{-2}. The order of magnitude of Δ is as large as G. In extreme cases their values can exceed 150 W m^{-2}. The energy budget residue depends on net radiation, wind speed and wind direction.

(4) The surface heterogeneity factor k introduced by *Panin et al.* (1996) is 1.24 for the experimental site chosen. According to *Foken's* (1997) criterion, the site can be characterized as slightly heterogeneous.

Acknowledgments–The authors wish to thank the Hungarian Scientific Foundation OTKA T-016183 and OTKA F-026642, and the Hungarian Higher Education Support Program FKFP-0168/1997 and U.S.-Hungarian Research Joint Found No. 503 for the financial support of this study.

References

Adams, R.S., Black, T.A. and *Fleming, R.L.*, 1991: Evapotranspiration and surface conductance in a high elevation, grass-covered forest clearcut. *Agric. For. Meteorol. 56,* 173-193.

Chehbouni, A., Njoku, E.G., Lhomme, J.-P. and *Kerr, Y.H.*, 1995: Approaches for averaging surface parameters and fluxes over heterogeneous terrain. *J. Climate 8,* 1386-1393.

Chen, J., Franklin, J.F. and *Spies, T.A.*, 1993: Contrasting microclimates among clearcut, edge, and interior of old-growth Douglas-fir forest. *Agric. For. Meteorol. 63*, 219-237.

Flint, A.L. and *Childs, S.W.*, 1991: Use of the Priestley-Taylor evaporation equation for soil water limited conditions in a small forest clearcut. *Agric. For. Meteorol. 56,* 247-260.

Foken, Th. and *Oncley, S.*, 1995: Workshop on industrial and methodological problems of land surface flux measurements. *Bull. Amer. Meteorol. Soc. 76*, 1191-1193.

Foken, Th. and *Wichura, B.*, 1996: Tools for quality assessment of surface-based flux measurements. *Agric. For. Meteorol. 78,* 83-105.

Foken, Th. (Copyeditor), 1997: Results of the LINEX-96/2 experiment. *Deutscher Wetterdienst Forschung und Entwicklung, Arbeitsergebnisse Nr. 48,* 37 pp.

Ghuman, B.S. and *Lal, R.*, 1986: Effects of partial clearing on microclimate in a humid tropical forest. *Agric. For. Meteorol. 40,* 17-29.

Grelle, A. and *Lindroth, A.*, 1994: Flow distortion by a Solent sonic anemometer: wind tunnel calibration and its assessment for flux measurements over forest and field. *J. Atmos. Oceanic Technol. 11,* 1529-1542.

Groot, A. and *King, K.M.*, 1993: Modeling the physical environment of tree seedlings on forest clearcuts. *Agric. For. Meteorol. 64*, 161-185.

Halldin, S., Gottschalk, L., van de Griend, A., Gryning, S.-E., Heikinheimo, M., Högström, U., Jochum, A. and *Lundin, L.-C.*, 1995: Science plan for NOPEX. *NOPEX Technical Reports, Technical Report* No. 12, 38 pp.

Hutjes, R.W.A., 1998: BACH revised science agenda for 1998-2001. *BACH NEWS 6*, BAHC International Project Office, Potsdam, Germany, 3-7.

Kaimal, J.C. and *Gaynor, J.E.*, 1991: Another look at sonic thermometry. *Boundary-Layer Meteorol. 56*, 401-410.

Laubach, J. and *Tichmann, U.*, 1999: Surface energy budget variability: A case study over grass with special regard to minor inhomogeneities in the source area. *Theor. Appl. Climatol. 62*, 9-24.

Lundin, L.-C., 1995: Long-term investigations of climate and hydrology within the NOPEX project. *Annales Geophysicae, Supplement II to Vol. 13,* C 343.

McMillen, R.T., 1988: An eddy correlation technique with extended applicability to non-simple terrain. *Boundary-Layer Meteorol. 43,* 231-245.

McNaughton, K.G., 1976: Evaporation and advection II: evaporation downwind of a boundary separating regions having different surface resistances and available energies. *Quart. J. Roy. Meteorol. Soc. 102,* 193-202.

Oncley, S., 1999: Scaling up heat and water measurement, during the energy balance experiment (EBEX), NCAR, *Working Paper*.

Panin, G.N., Tetzlaff, G., Raabe, A., Schönfeldt, H.J. and *Nasonov, A.E.*, 1996: Inhomogeneity of the land surface and the parameterisation of surface fluxes — a discussion. *Wiss. Mitt. Inst. f. Meteorol. Univ. Leipzig & Inst. f. Troposphärenforsch. Leipzig*, 4, 204-215.

Panin, G.N., Tetzlaff, G. and *Raabe, A.*, 1998: Inhomogeneity of the land surface and parameterisation problems of surface fluxes in natural conditions. *Theor. Appl. Climatol. 60*, 163-178.

Panin, G.N. and *Tetzlaff, G.*, 1999: A measure of inhomogeneity of the land surface and prameterisation of turbulent fluxes under natural conditions. *Theor. Appl. Climatol. 62*, 3-8.

Schmid, H.P., 1997: Experimental design for flux measurements: matching scales of observations and fluxes. *Agric. For. Meteorol. 87*, 179-200.

Stathers, R.J., Black, T.A. and *Novak, M.D.*, 1985: Modelling soil temperature in forest clearcuts using climate station data. *Agric. For. Meteorol. 36*, 153-164.

Tanner, B.D., Swiatek, E. and *Greene, J.P.*, 1993: Density fluctuations and use of the krypton hygrometer in surface flux measurements. *Proc. of the 1993 National Conference on Irrigation and Drainage Engineering, Irrigation and Drainage Division, American Society of Civil Engineers*, 21-23 July, 1993, Park City, Utah, ASCE, New York.

Webb, E.K., Pearman, G.I. and *Leuning, R.*, 1980: Correction of flux measurements for density effects due to heat and water vapour transfer. *Quart. J. Roy. Meteorol. Soc. 106*, 85-100.

Weidinger, T. and *Matyasovszky, I.*, 1998: Estimating turbulent fluxes using an optimal averaging method. *Annales Geophysicae, Supplement II to Vol. 16*, C 617.

IDŐJÁRÁS
Quarterly Journal of the Hungarian Meteorological Service
Vol. 103, No. 3, July–September 1999, pp. 161–176

Connection between vine production and meteorological variables on the Great Hungarian Plain

Károly Tar[1] and **Edit Hajdu**[2]

[1] *Department of Meteorology, University of Lajos Kossuth*
H-4010 Debrecen, P.O. Box 13, Hungary
E-mail: tark@tigris.klte.hu

[2] *Research Institute for Viticulture and Enology*
H-6001 Kecskemét, P.O. Box 25, Hungary; E-mail: tark@tigris.klte.hu

(Manuscript received 20 November 1998; in final form 7 June 1999)

Abstract—The effect of the weather type of different years on the production of two varieties of vine grape has been investigated. One of the varieties (*Zenit*) has short growing period, the other (*Jubileum 75*) has long growing period. Phenological and production data altogether with meteorological ones were collected in 1982–1987 at Kecskemét-Miklóstelep, the centre of the Great Hungarian Plain. Statistical relationships has been looked for between the characteristics of the grape and vine at one side and the yearly temperature and precipitation characteristics at the other side. It is found, that the effect of the weather type is much smaller on the phenology and the production of the short growing grape variety than on that of the long growing one.

Key words: growing period, cluster yield and weight, berry weight and diameter, sugar degree and acid content, mean temperature, amount of precipitation.

1. Introduction

Extreme meteorological elements of the continental climate represent stress effect on the life of vine, and influence the effectiveness of its cultivation. Besides the producing area and varieties, year is a quite important factor. Effect of the year is basically determined by sunshine duration and precipitation. Production of vine highly depends on the year because it is a plant requiring much light and warmth. However, depending on their genotype, the different vine varieties respond to environmental effects (such as year) in different ways.

In the Research Institute for Viticulture and Enology, Kecskemét-Miklóstelep (Hungary), wine-grape varieties of short and long growing period were chosen for our study. The purpose was to attempt to reveal the role of temperature and precipitation as meteorological elements determining their production. This kind of study was performed in connection with a breeding experiment with new variety candidates (*Füri et al.*, 1991).

2. Experimental conditions, variety characteristics

On the basis of meteorological and experimental data from the period 1982-1987, the varieties *Zenit* of short growing period and *Jubileum 75* of long growing period were studied. According to *Csepregi* and *Zilai* (1988) they can be described as follow:

Zenit (Ezerjó × Bouvier) has early maturity. It ripens in early September with a sugar degree above 17 Mm°. The cluster is middle large (100 g), the berries are little (1.7 g). This variety is not too susceptible to rot, however, it is sensitive to frost and drought. It produces well (11-14 t ha^{-1}). Its wine has excellent quality.

Jubileum 75 (Ezerjó × Szürkebarát) is a slowly ripening variety; it ripens in early October. The cluster is middle large (150 g), the berries are little (2.4 g), and they are not susceptible to rot. It tolerates frost as low as -21°C. It requires high nutritive supply. Yield is moderate (10-12 t ha^{-1}). Its wine is fine: a table wine that is poor in extracts.

The experimental plantation is on sand, in arid environment and lives on its own root. The vine-stocks are cultivated by high cordon with Sylvoz dressing. The vegetation area is big, in a twin-stock design.

3. Aim of the study

On the basis of the six years of observations, notices and measures, the following features of the above mentioned vine varieties were available: *sprouting day, harvest day, length of the growing period, cluster yield, cluster weight, berry weight, berry diameter, sugar degree and titrated acid content of the must and sugar free solids content of the wine.*

The following features were obtained from daily mean temperatures and daily amounts of precipitation: *annual mean temperature and precipitation amount, annual accumulated temperature above 10°C, annual number of wet days, annual intensity of precipitation,* as well as *mean temperature, precipitation amount, accumulated temperature above 10°C, number of wet days and intensity of precipitation in the growing period.*

Aim of our study was to determine the main statistical characteristics of above mentioned features, and to reveal the stochastic connection between the selected meteorological elements and the two vine varieties.

4. Results

As it will be seen from the detailed results, the extreme climate of the Great Hungarian Plain is well represented by the selected six years.

4.1 Meteorology of the area in the studied period

First, the main characteristics of observed temperature and precipitation amounts measured in Katonatelep and Miklóstelep during 1982–87 were compared to the longer-term climate conditions in Katonatelep. Since the meteorological measurements are not continuously available in Miklóstelep, the observed values of the two variables were compared to the climate of Katonatelep. Miklóstelep lies 18 km to the SW of Katonatelep. In Katonatelep a 35 year long dataset is available from 1962 to 1996. Measured values suggest that Miklóstelep was slightly warmer and wetter than Katonatelep during the given period (1982–87): annual mean temperature was 0.6°C higher and annual mean precipitation was 30 mm more in Miklóstelep. The highest temperature differences occurred in January and July, while maximum precipitation differences were observed in August. These results permit an assumption that the simplified Walter-Lieth climate diagram (*Justyák*, 1995) for Katonatelep (*Fig. 1*) can be applied to Miklóstelep as characteristic climate of the period 1962–96. According to the diagram all the months are humid. *Fig. 2* shows annual climate diagrams derived from monthly mean temperature and precipitation amounts during the six year long observation period. This figure suggests that climate of the tentative area is favourable for vineyard; spring and two summer months are wet, autumn is dry. Annual climate diagrams result in the following wet-dry relation. During the 1982–87 period 18 months were arid, that is 25% of all possible months, while 42% of all the summer and autumn months were arid (15). The period between March and October is the most important part of the year (for vineyards); humid conditions occurred in 28 months, that is 58% of all possible cases.

Table 1 shows the annual values, their mean and standard deviation and the variation coefficient (relative standard deviation = standard deviation/mean). The values of the table show, that 1983 and 1985 were the warmest and the coldest years, respectively. The coldest year was the most humid one and 1986 was the most arid year (as Fig. 1 also suggests). The highest number of wet days occurred in the most humid year, while the number of them was the lowest in 1983. Consequently, the highest and the lowest precipitation intensity happened in 1985 and in the most arid year (1986), respectively. However, the difference is only 1 mm day^{-1}. Values of the variation coefficient show that the annual precipitation amount and number of wet days have the highest, and the annual mean temperature has the lowest variation in the experimental plantation which represents the wine districts of the Great Hungarian Plain well.

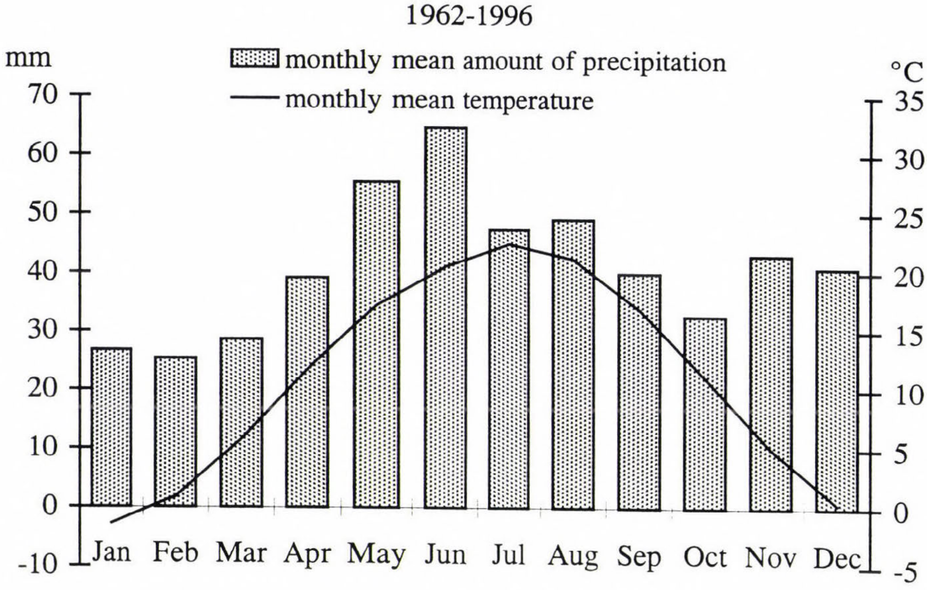

Fig. 1. Climate diagram of Kecskemét-Katonatelep on average of 35 years.

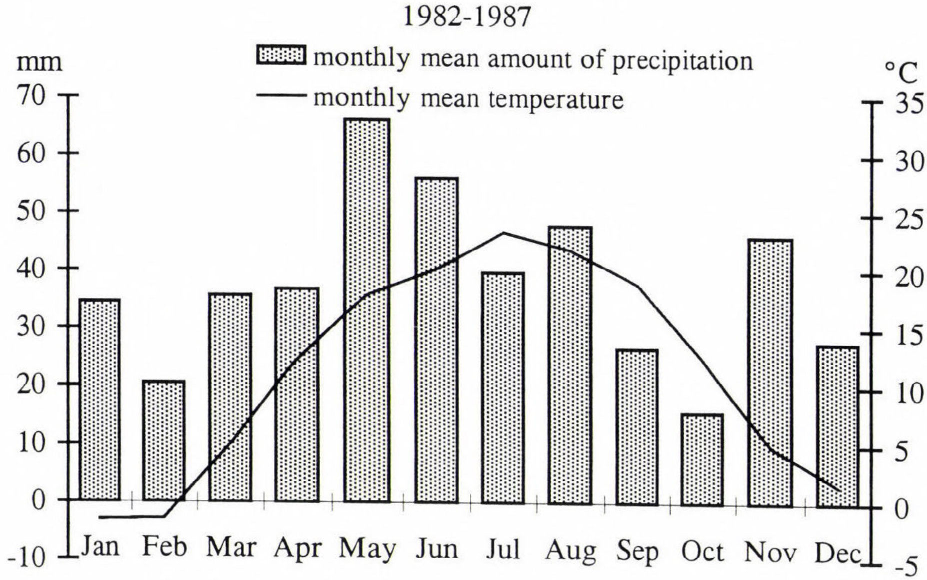

Fig. 2. Climate diagram of Kecskemét-Miklóstelep on the average of six years.

Table 1. Annual values and most important statistical parameters of meteorological elements of the study (Kecskemét-Miklóstelep)

Year	Yearly mean temperature (MTY, °C)	Yearly accumulated temp. > 10°C (TSY, °C)	Yearly amount of precipitation (PSY, mm)	Yearly number of wet days (PDY)	Yearly intensity of precipitation (mm day^{-1})
1982	11.7	1854.0	406.9	81	5.0
1983	12.3	1950.2	405.4	78	5.2
1984	11.2	1651.8	462.6	101	4.6
1985	10.6	1685.5	540.8	110	4.9
1986	11.6	1944.5	369.5	89	4.2
1987	10.8	1723.2	532.0	109	4.9
Mean	**11.4**	**1801.5**	**452.9**	**94.7**	**4.8**
Standard deviation	0.6	132.1	71.3	14.0	0.4
Coeff. of variation	0.055	0.073	0.157	0.148	0.078

Table 2 contains sprouting and harvest days and the length of the growing period (difference of sprouting and harvest days) of the two vine varieties as well as some meteorological features of this period for each year. Some statistical parameters were also calculated.

The growing period of *Jubileum 75* is generally 23 days longer than that of *Zenit*. The highest difference (40 days) was in 1985, and the lowest (3 days) in 1986, in the most arid year. Variation around the mean value (standard deviation) of the length of the growing period is 14 in the case of *Jubileum 75*, and it is higher by half than that of *Zenit*. Difference between the mean temperatures of their growing periods does not dramatically differ: it ranges from 0.5°C (1984) to 0.1°C (1983, 1987). Therefore, there is no characteristic difference between the mean values and standard deviations of the six years. Maximum values of the accumulated temperature above 10°C can be found in 1983 (the warmest year) for both varieties. In the case of *Jubileum 75*, however, the minimum values happened in 1983, the second coldest year, and not in the coldest one. In general, the growing period of this variety begins six days later and takes almost 30 days longer. This fact can explain that the accumulated temperature above 10°C is higher by 200°C on an average than that of *Zenit*. On the other hand, the late sprouting is advantageous for it to survive late spring frosts. Precipitation amount of the growing period is also higher (by 25 mm on an average) for this variety except 1986, the most arid year. Maximum of the precipitation amount was in 1985, the most humid year, for both varieties. However, its minimum was in the most arid year for *Jubileum 75* only. In the case of *Zenit*, the minimum occurred in 1983, the warmest year. That year the low amount of precipitation had a negative effect on acid content of the must and extract content of the wine in *Zenit*. Number of wet days of the growing period follows the same pattern for this variety. However, in the case of *Jubileum 75*, the maximum is in 1984, a year when the temperature and the precipitation were more or less normal. On the other hand, mean temperature of the growing period of this variety is the lowest in this year. Contrary to the annual precipitation intensity, the precipitation intensity in the growing period is always over 5 mm day^{-1} for both varieties. It must be noticed that in the case of *Jubileum 75* the maximum is in the warmest year, while the minimum occurred in 1984 for both varieties.

Table 2. Yearly values and most important statistical parameters of the growing period and phenological features of the vine varieties

Year	The growing period's							
	beginning (sprouting day)	end (harvest day)	length (day)	meteorological features				
				mean temperature (MTV, °C)	accumulated temp. > 10°C (TSV, °C)	amount of precip. (PSV, mm)	number of wet days (PDV)	intensity of precip. (mm day^{-1})
				Zenit				
1982	122	245	123	21.4	1417.3	204.5	31	6.6
1983	102	251	149	20.9	1646.4	187.1	30	6.2
1984	110	249	139	19.1	1285.8	209.7	42	5.0
1985	112	241	129	19.7	1266.7	266.3	45	5.9
1986	112	251	139	21.3	1575.7	205.8	31	6.6
1987	120	251	131	20.2	1345.8	241.2	35	6.9
Mean	**113**	**248**	**135**	**20.4**	**1423.0**	**219.1**	**36**	**6.2**
Standard deviation	7.2	4.1	9.2	0.9	156.5	29.0	6.4	0.7
Coeff. of variation	0.064	0.017	0.068	0.046	0.110	0.133	0.179	0.111
				Jubileum 75				
1982	127	284	157	21.0	1733.5	231.7	38	6.1
1983	110	271	161	21.0	1777.5	239.9	32	7.5
1984	118	296	178	18.6	1550.5	261.2	52	5.0
1985	120	289	169	19.4	1599.8	288.1	50	5.8
1986	118	260	142	21.3	1617.7	205.8	31	6.6
1987	121	264	143	20.3	1488.0	242.7	36	6.7
Mean	**119**	**277**	**158**	**20.3**	**1627.8**	**244.9**	**40**	**6.3**
Standard deviation	5.5	14.5	14.2	1.1	109.5	27.8	9.0	0.9
Coeff. of variation	0.046	0.052	0.090	0.053	0.067	0.114	0.227	0.137

According to the variation coefficients concerning meteorological features, the number of wet days in the growing period shows the highest, while mean temperature the lowest variation for both varieties. The order between these values, however, depends on the varieties. As the standard deviation shows, distribution of the sprouting day is more uniform for *Jubileum 75* and the two other phenological parameters for *Zenit*, respectively. The time of ripening of *Zenit* is in a period of the year when the climate is generally not too extreme and fluctuating.

In *Table 3* annual meteorological elements and meteorological elements in the growing period are compared: difference of the mean temperatures (MTV-MTY), ratio of accumulated temperatures above 10°C, precipitation amount and number of wet days (TSV/TSY, PSV/PSY, PDV/PDY) are calculated. Mean temperatures of the growing period are higher by 9.1 and 8.9°C on an average than the annual mean temperature for *Zenit* and *Jubileum 75*, respectively. The difference between the mean temperatures of the two periods is the lowest in 1984 and the highest in 1986 (the most arid year) for both varieties. The growing period represents 79 and 90% of the annual accumulated temperature above 10°C in the cases of *Zenit* and *Jubileum 75*, respectively, obviously because of the longer growing period of the latter variety. It can also be noticed that the minimum of these ratios was in 1985 (the coldest and the most humid year) for *Zenit*, however, the maximum of them was in the same year for *Jubileum 75*. Values of the variation coefficients are always higher in the case of *Jubileum 75*.

Table 3. Parameters containing the annual and the growing period meteorological elements (symbol as in Table 1 and 2)

Year	MTV-MTY (°C)	TSV/TSY (%)	PSV/PSY (%)	PDV/PDY (%)
		Zenit		
1982	9.8	76.4	50.3	38.3
1983	8.6	84.4	46.2	38.5
1984	7.8	77.8	45.3	41.6
1985	9.1	75.2	49.2	40.9
1986	9.7	81.0	55.7	34.8
1987	9.4	78.1	45.3	32.1
Mean	**9.1**	**78.8**	**48.7**	**37.7**
Standard deviation	0.7	3.4	4.0	3.6
Coeff. of variation	0.080	0.043	0.083	0.096
		Jubileum 75		
1982	9.3	93.5	56.9	46.9
1983	8.7	91.1	59.2	41.0
1984	7.3	93.9	56.5	51.5
1985	8.8	94.9	53.3	45.5
1986	9.7	83.2	55.7	34.8
1987	9.5	86.4	45.6	33.0
Mean	**8.9**	**90.5**	**54.5**	**42.1**
Standard deviation	0.9	4.7	4.8	7.2
Coeff. of variation	0.097	0.052	0.087	0.171

4.2 Production of the vine varieties in the studied period

Differences were studied in the harvest values of these two varieties at the meteorological conditions characterised above. *Table 4* lists features concerning production, must and wine of these varieties as well as their most important statistical indices for each year.

Table 4. Annual values and most important statistical parameters of production features of the vine varieties.

Year	Cluster yield (kg stock^{-1})	Cluster weight (g)	Berry weight (g)	Berry diameter (mm)	Sugar degree of the must (Mm°)	Acid content of the must (g l^{-1})	Solids content of the must (g l^{-1})
				Zenit			
1982	2.13	132	1.80	13.85	17.2	8.1	–
1983	2.60	148	2.30	14.00	17.6	6.6	17.8
1984	2.29	96	1.20	12.75	19.6	8.5	18.7
1985	4.16	112	1.30	12.85	17.3	8.4	18.0
1986	2.70	88	1.40	13.95	21.8	8.0	24.7
1987	0.68	100	1.50	13.85	19.2	9.5	21.6
Mean	**2.43**	**112.7**	**1.58**	**13.54**	**18.8**	**8.2**	**20.2**
Standard deviation	1.1	23.1	0.4	0.6	1.8	0.9	3.0
Coefficient of variation	0.462	0.205	0.257	0.043	0.095	0.115	0.147
				Jubileum 75			
1982	5.46	188	2.00	15.70	17.6	6.1	16.7
1983	4.89	190	2.20	15.70	19.5	6.0	22.0
1984	3.69	76	2.20	14.95	19.8	7.2	19.3
1985	3.54	148	1.80	13.60	18.8	8.3	18.5
1986	2.65	120	2.10	15.05	20.6	5.1	17.4
1987	0.31	80	1.70	14.70	18.3	7.0	–
Mean	**3.42**	**133.7**	**2.00**	**14.95**	**19.1**	**6.6**	**18.8**
Standard deviation	1.8	50.4	0.2	0.8	1.1	1.1	2.0
Coefficient of variation	0.533	0.377	0.105	0.052	0.057	0.169	0.104

Maximum of the cluster yield was in 1985 (the coldest and most humid year) and 1982, for *Zenit* and *Jubileum 75*, respectively. The secondary maximum, however, is in 1983 (the warmest year) for the latter variety. The maximum is in 1987 (the second coldest and most humid year having the most wet days) for both varieties. It can be noticed, however, that 1986/87 winter was extremely cold (with an absolute radiation minimum temperature of -29,6°C), and both varieties suffered significant frost damage. The mean value, the standard deviation and the variation coefficient are higher for *Jubileum 75*.

Maximum of the cluster weight was in the warmest year for both varieties, however the minimum value was in the most arid year for *Zenit*; this suggests that this variety is susceptible to the lack of water. The minimum was in 1984 for *Jubileum 75*. Accumulated temperature above 10°C was the lowest in this year. This experience supports observations that this variety requires much warmth. Mean, standard deviation and variation coefficients are also higher for this variety.

Berry weight of *Zenit* is extremely high in the warmest year (1983). In the case of *Jubileum 75*, however, there are the same maximum values in this year and in 1984 (the year having the lowest accumulated temperature above 10°C). At the same time, the maximum value of berry weight of *Zenit* was obtained in this year, too. *Jubileum 75* also had a high value in 1986, the most arid year. In the case of this variety mean value is higher but standard deviation and variation coefficient is lower than those of *Zenit*. Time pattern of the berry weight well shows the susceptibility of *Zenit* and tolerance of *Jubileum 75* to drought.

Time pattern of berry *diameter* is similar to that of berry weight. Values of the statistical parameters are higher for *Jubileum 75*.

Sugar degree of the must was the highest in 1986 (the most arid year with a minimum precipitation intensity and with an accumulated temperature above 10°C near the maximum), and the lowest in 1982. It is interesting that in 1982 mean temperature in the growing period of *Zenit* was maximum, and that of *Jubileum 75* also was high. The mean value was also higher, however, the two other parameters were lower for this variety.

Time pattern of the *acid content of the must* is also characteristic for the given varieties. The minimum content was in the warmest and in the most arid year for *Zenit* and *Jubileum 75*, respectively. *Jubileum 75* has its maximum in the coldest and most humid year. However, *Zenit* reaches the maximum value in the second coldest and most humid year. Mean value is higher, standard deviation and variation coefficient is lower in the case of *Zenit*.

Because of lacking data, statistical parameters for *solids content of the wine* can be compared only. These are higher for *Zenit*.

According to the variation coefficient, the cluster yield shows the highest, and berry diameter the lowest variation. The order between these limits depends on the varieties.

4.3 Connection between the features of the vine varieties and meteorological elements

The above mentioned analyses and comparisons show that different features of the must and wine of these two varieties are in stochastic relationship with the studied meteorological elements. If this relationship is supposed to be linear, then in the $y = bx + a$ regression equation y means the different production features of the vine varieties and x means the meteorological elements. Closeness of the relationship is shown by the linear correlation coefficient. Its value is theoretically zero if there is no (even a stochastic) connection between the studied random variables. Therefore, a statistical test calculated from a sample of random variables is necessary to decide when its value can be regarded to be significantly different from zero. The point is that an r_p critical value depending on the element number of the sample and the significance level can be determined, and r correlation coefficients of absolute value higher than r_p significantly differ from zero. In our case at $p = 0.05$ significance level $r_{0.05} = 0.814$, and at $p = 0.10$ significance level $r_{0.10} = 0.7239$. Regarding the solid content of the wine, the correct values are $r_{0.05} = 0.8783$ and $r_{0.10} = 0.8054$ since the number of elements is less by one.

Table 5 lists linear correlation coefficients between phenological features and production of the vine varieties as well as meteorological elements, that are suitable for the above mentioned test and can be evaluated (they are higher than 0.6, but are not significant at the above mentioned levels).

The table shows that the number of the correlation coefficients suitable for above mentioned criteria are 32 and 26 for *Jubileum 75* and *Zenit*, respectively. Number of significant cases of $p = 0.05$ probability providing a very close connection is 11 and 7, that of $p = 0.10$ probability is 9 and 6 for the above mentioned varieties. The numbers of the coefficients, which are valuable but not significant, are almost equal (13 and 12). Therefore, production of *Jubileum 75* is more climate dependent than that of *Zenit*.

The number of correlation coefficients, which are significant at the probability levels 0.05 and 0.10, is 13 and 20 for *Zenit* and *Jubileum 75*, respectively. About 50% (6 and 11) coincides with meteorological elements of the growing period. Therefore, the climate of a year influences production and phenological features of the given vine varieties as much as the climate of the growing period.

There is no significant relation between the phenological features and the meteorological elements for *Zenit*. Length of the growing season of *Jubileum 75* seems to be in relation with wet days, mean temperature and amount of precipitation of this season. It is strange that length and mean temperature of the growing period does not show strong negative correlation (increase in one implies decrease in other). This can be explained by the growing period being prolonged by autumnal days of lower mean temperature. Of course,

Table 5. Values of linear correlation coefficients between phenological and production features of vine varieties and meteorological elements.

Meteorological elements	Phenological features									
	Lenght of growing period	Sprouting day	Harvest day	Cluster yield	Clusree weight	Berry weight	Berry diameter	Sugar degree of the must	Acid content of the must	Solids content of the wine
				Zenit						
Annual mean temperature						*0.7844*			**-0.8483**	
Annual accumulated temperature >10°C						0.7009	**0.8305**		-0.7103	
Mean temp. of growing period						0.6117	**0.8773**			
Accumulated temp. >10°C of growing period	0.6251					*0.7353*	*0.7865*		*-0.7607*	
Annual amount of precipitation									0.6577	
Annual number of wet days					-0.6257	*-0.7674*	-0.6275		*0.8021*	
Annual intensity of precipitation					**0.8564**	0.6540		**-0.9270**		-0.7854
Growing period amount of precipitation			-0.6070						0.6634	
Growing period number of wet days						-0.7115	**-0.9554**			
Growing period intensity of precipitation							**0.8460**			0.6021
				Jubileum 75						
Annual mean temperature				0.6092		*0.7839*	**0.8816**		*-0.7664*	
Annual accumulated temperature >10°C			-0.6456		0.6135		0.6648		**-0.8763**	
Mean temp. of growing period	*-0.7810*		*-0.7787*						*-0.8086*	
Accumulated temp. >10°C of growing period					**0.9365**		0.6186			
Annual amount of precipitation				**0.8538**		*-0.7652*	*-0.7831*		**0.9109**	
Annual number of wet days					-0.7142	-0.6820	**-0.8762**		*0.7785*	
Annual intensity of precipitation				-0.6979				-0.6930		
Growing period amount of precipitation	*0.7375*		0.7252				-0.6973		**0.9675**	
Growing period number of wet days	**0.8279**		**0.8976**						**0.8280**	
Growing period intensity of precipitation	-0.6486		**-0.8158**							

(It is significant on **p = 0.05** or *p = 0.10* sigificance level.)

date of the harvest day shows similar connection with meteorological elements since it is one (partly subjective) of the determinative factors. Its strong negative correlation with precipitation intensity in the growing period can be explained by the fact that prior to the late date of harvest there are early autumnal days of low precipitation. Of course, these results are not surprising, but, strangely enough, *Zenit* does not show them.

Cluster yield is not correlated with any meteorological element in the case of *Zenit*. It has very strong positive relation with the accumulated temperature above 10°C in the growing period in the case of *Jubileum 75*. Correlation of the *average cluster weight* is in similar connection with the accumulated temperature above 10°C in the growing period. The average cluster weight is in the closest connection with the annual precipitation intensity in *Zenit*. Probably, this variety can utilise water when there is higher precipitation. The berry weight has the strongest correlation with the annual mean temperature for both varieties; it is followed by negative correlation with the number of wet days and the annual accumulated precipitation for *Zenit* and *Jubileum 75*, respectively. Berry diameter significantly depends on four meteorological elements in *Zenit*, first of all on the number of wet days in the growing period. This connection, however, is negative similarly to the annual wet days for *Jubileum 75*.

Sugar degree of the must is in significant and valuable negative correlation with annual precipitation intensity for *Zenit* and *Jubileum 75*, respectively. It is obvious that correlation of sugar degree with precipitation is negative. The fact that this was experienced only at precipitation intensity can be explained that it represents both accumulation of precipitation and length of the humid period. *Acid content of the must* is in negative connection with temperature variables, and shows positive correlation with precipitation ones for both varieties. The closest negative correlation is found with the annual mean temperature and the annual accumulated temperature above 10°C for *Zenit* and *Jubileum 75*, respectively. The latter variety shows a very close positive correlation with the annual accumulated temperature and the accumulated temperature in the growing period. It is not so close with the number of wet days in the growing period.

According to above mentioned data, there is no significant correlation between the same variables at the level $p = 0.05$ at the same time for both varieties. If both levels are allowed, the common combinations are the following: berry weight–annual mean temperature, acid content of the must–annual mean temperature, acid content of the must–annual number of wet days. This is less than 10% of the total events (33), consequently, features of the varieties have a significant effect on the closeness of the studied connections.

When correlation is significant (i.e., can be considered real) at the level $p = 0.05$, it is reasonable to calculate constants of the regression line.

Knowing the meteorological elements, approximate values of a given limit of error for the phenological and production feature can be calculated by the equation $y = bx + a$. Perhaps, it is more important that b regression coefficient represents susceptibility of these features to the given meteorological element: it shows how a unit change of the latter modifies values of the phenological and production features on an average.

Fig. 3 and *Fig. 4* show the observed values and regression lines at the level $p = 0.05$ in cases that are interesting from a viticultural point of view on the basis of Table 5. Therefore, susceptibility can be concluded from the equation of the lines. For instance, 1 mm/day increase in annual precipitation intensity results in 53 g increase in cluster weight on an average according to the equation $y = 53.03\ x - 141.44$ giving the connection between cluster weight and annual precipitation intensity in the case of *Zenit*. Another example: 1°C increase in accumulated temperature above 10°C in the growing period results in an increase of 0.4 g in the cluster weight of *Jubileum 75*. The other figures can be analyzed similarly.

Connection of the phenological and production features with the parameters representing annual and vegetation seasonal meteorological elements listed in Table 3 was also studied. In the case of *Zenit*, only a negative significant correlation between berry diameter and the PDV/PDY ratio can be obtained at the level $p = 0.10$: $r = -0.7309$. In the case of *Jubileum 75*, correlations of the PSV/PSY ratio with cluster yield and berry weight proved to be significant at the level $p = 0.05$: $r = 0.8953$ and $r = 0.8720$, respectively. The adequate regression lines are shown in *Fig. 5*.

5. *Conclusions*

(1) The effect of the yearly weather is different on the two varieties of the investigated vine grape.

(2) The phenological and production parameters of the long growing grape are more weather dependent than those of the short growing grape.

(3) The berry diameter and acidity are the most weather dependent characteristics of the grape varieties.

(4) The extract content of the vine seems to be independent of the yearly weather.

(5) To obtain good production, the long growing grape requires warm year, the short growing grape requires wet year.

Fig. 3. Regression between production feature of Zenit vine variety and the meteorological elements.

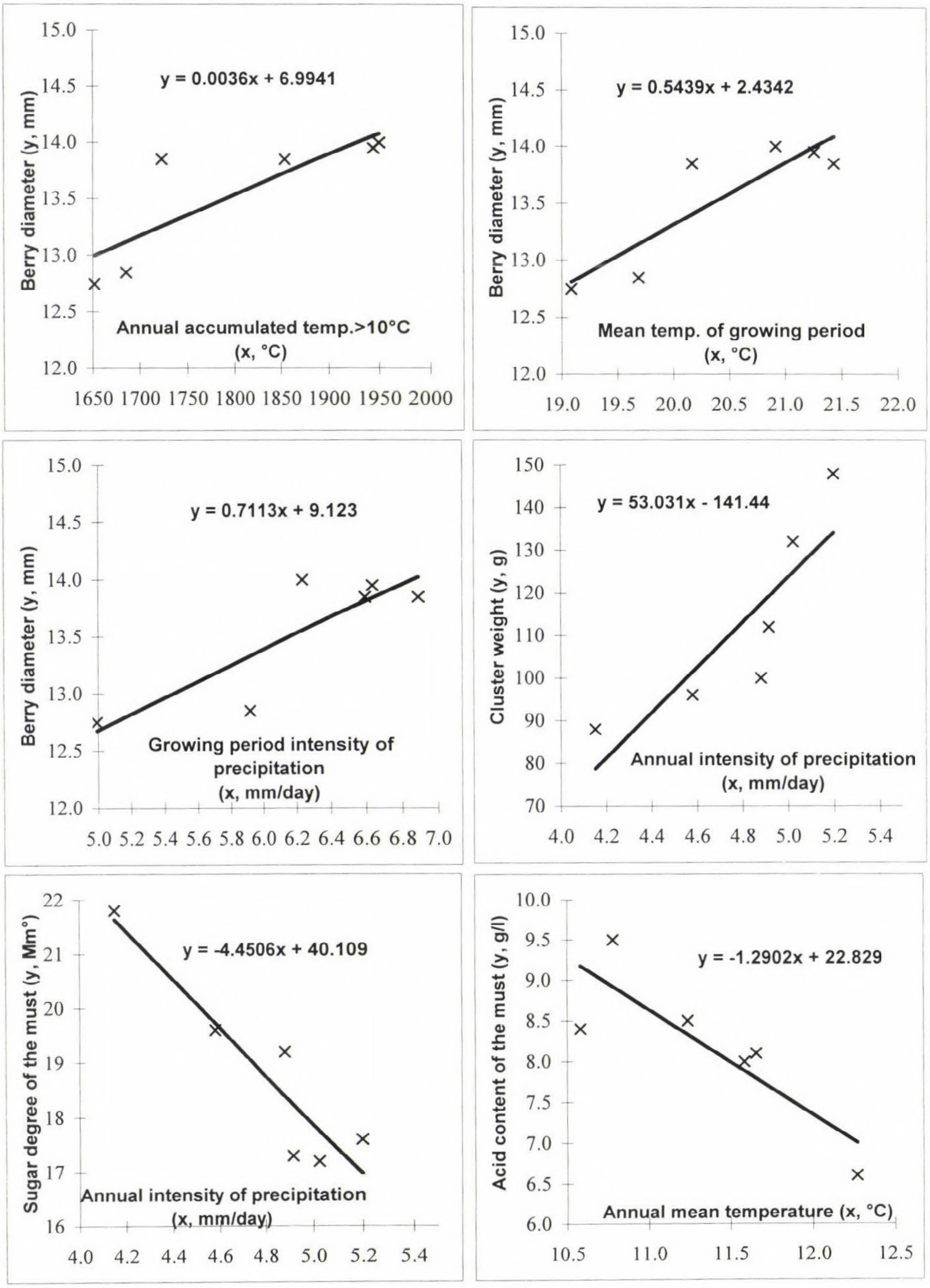

Fig. 4. Regression between production feature of Jubileum 75 vine variety and the meteorological elements.

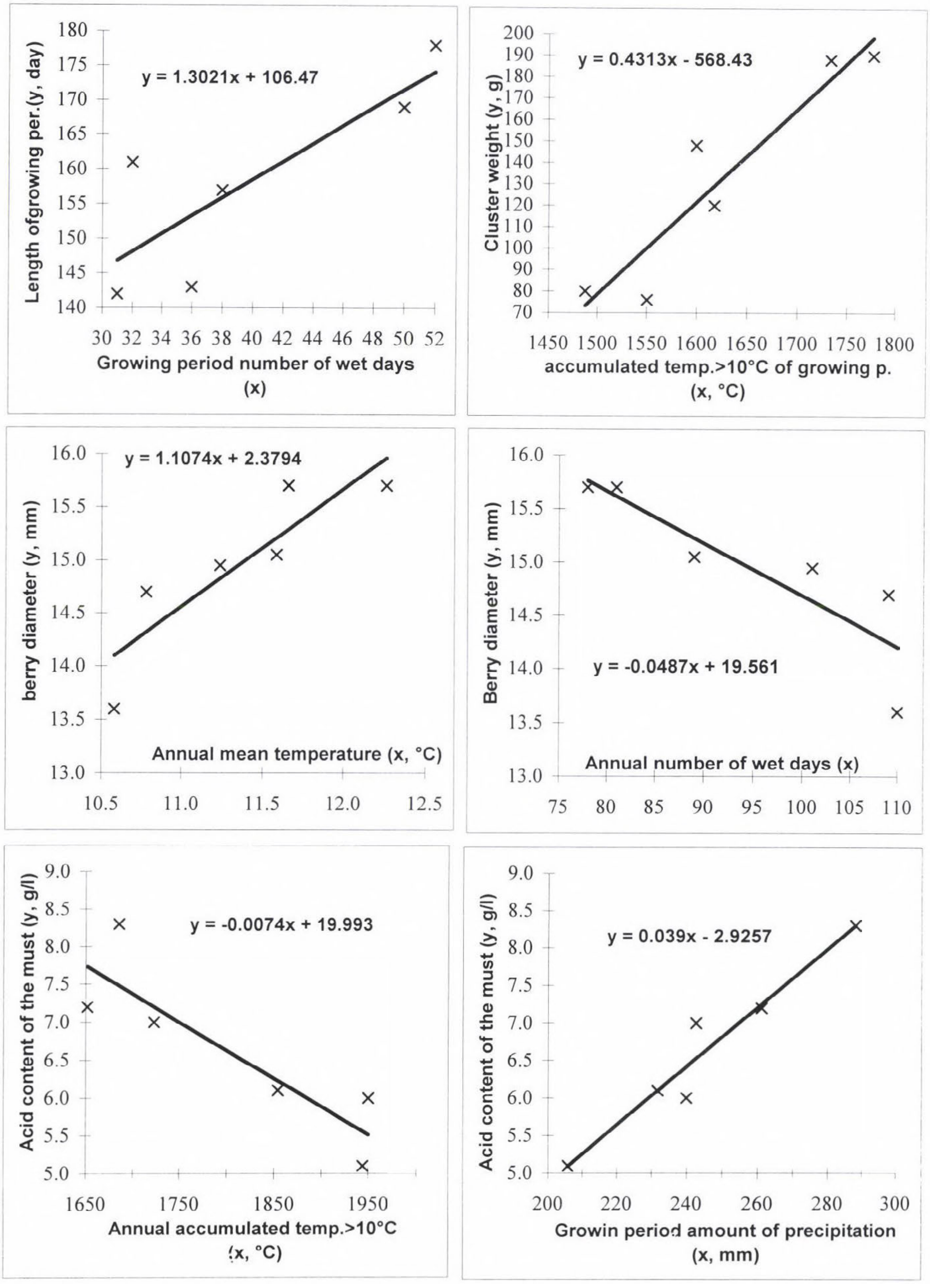

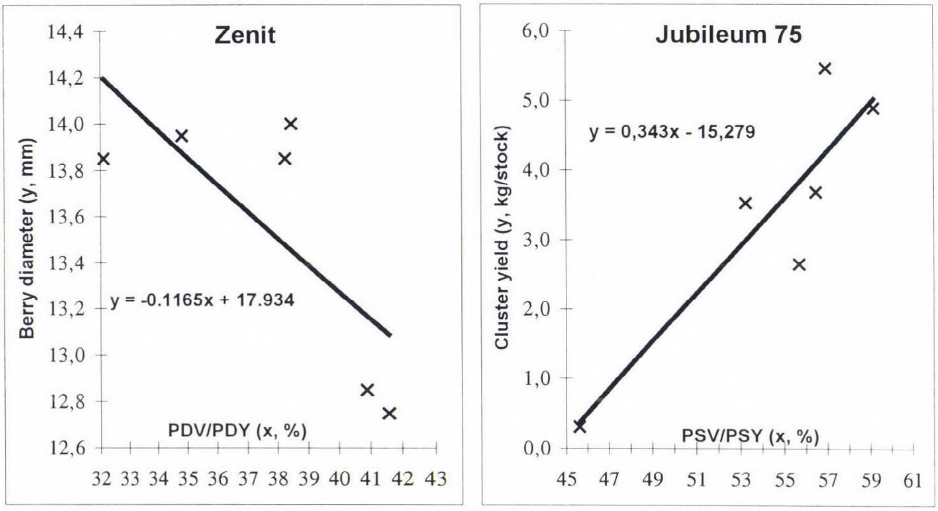

Fig. 5. Regression between production features of vine varieties and parameters containing the annual and vegetation seasonal meteorological elements (see Table 3).

References

Csepregi, P. and *Zilai, J.*, 1998: *Knowledge and Using of Vine Varieties* (in Hungarian). *Mezőgazdasági Kiadó*, Budapest, 508 pp.

Füri, J., Hajdu, E. and *Tar K.*, 1991: Relation of weather elements and product of vine (in Hungarian). *Acta Geographica Debrecina, XXVIII-XXIX*, 49-59.

Justyák, J., 1995: *Climatology* (in Hungarian). Kossuth Egyetemi Kiadó, Debrecen, 225 pp.

IDŐJÁRÁS

Quarterly Journal of the Hungarian Meteorological Service
Vol. 103, No. 3, July–September 1999, pp. 177–187

A climatological study of soil moisture and irrigation water requirement in Paraiba State (NE Brazil)

K. Karuna Kumar, Virgínia de F. Bezerra and **Paulo R. C. Dantas**

Department of Atmospheric Sciences, Federal University of Paraiba,
Campina Grande - PB - 58109-970, Brazil; e-mail: karuna@dca.vfpb.br

(Manuscript received 28 July 1998; in final form 16 March 1999)

Abstract—Results of a study of soil moisture conditions in Paraiba state (NE Brazil) are presented in this paper. Paraiba is one of the several states in NE Brazil which is frequently affected by droughts. Considerable parts of the state have a semiarid climate and the highly irregular nature of rainfall makes the practice of agriculture a risky proposition. Information on soil moisture conditions is hence a matter of importance.

The study is based on the estimation of daily soil moisture values for a minimum period of 25 years at twenty seven locations representing different parts of the state. A simple water balance model using daily precipitation and monthly mean temperature data is used for the estimation of soil moisture content. A first order Markov chain model is applied to the soil moisture data and the initial and conditional probabilities of days with dry and wet soil are computed for each decade of the year. Soil moisture averages and probabilities are used to evaluate the crop growing periods at the stations. The amounts of supplementary irrigation necessary to maintain the soil moisture content above selected levels during the crop growing periods are determined.

Key-words: soil moisture, Markov chain probabilities, crop growing periods, irrigation needs.

1. Introduction

The semiarid zone of Northeast Brazil is 860,000 km^2 in extent and contains nearly 10% of the country's population. The main climatic characteristics are: annual rainfall of 400–800 mm with a coefficient of variability of up to 80%, high air temperatures and high potential evapotranspiration rates (on average 2000 mm).

The frequent appearance of droughts in the region is responsible for the extreme poverty that affects the majority of the population. Various attempts are being made to reduce the impact of droughts on the region's economy.

In the semiarid zone the main constraint to crop production is the rainfall and it's extreme variability. The explanation and prediction of the rainfall fluctuations in this region is one of the challenging issues of tropical meteorology.

Agroclimatic studies based on long-term soil moisture information would be superior to those using rainfall averages and probabilities, since soil moisture information can be related to crop growth and production. Long-term soil moisture records are not often available. Models of varying degrees of complexity had been developed in the past for the evaluation of soil moisture conditions.

A simple water balance using long-term averages of monthly rainfall and potential evapotranspiration gives some indication of the availability of soil water and of water surplus (*Thornthwaite*, 1948). The simplicity of the model renders the results somewhat questionable. On the other hand, models such as the versatile soil moisture budget (*Baier* and *Robertson*, 1966; *Dyer* and *Mack*, 1984) involve several soil layers, information on the crop rooting depth, knowledge of the water holding and water releasing characteristics of the soil layers, etc.

Considering the large uncertainty in even the best measurement of soil moisture over a large area (*Robertson*, 1973), its estimation by models involving many parameters of unknown certainty may not be a very realistic approach. For agroclimatic purposes it seems preferable to use models and techniques which are simpler than the complex mathematical models, and still yield better results than those based on long-term averages of rainfall and temperature.

In the present study simple techniques are used to convert historical rainfall information to soil moisture data. These techniques integrate the knowledge of potential evapotranspiration, available moisture capacity as well as daily rainfall data and provide an estimate of available soil water on a daily basis.

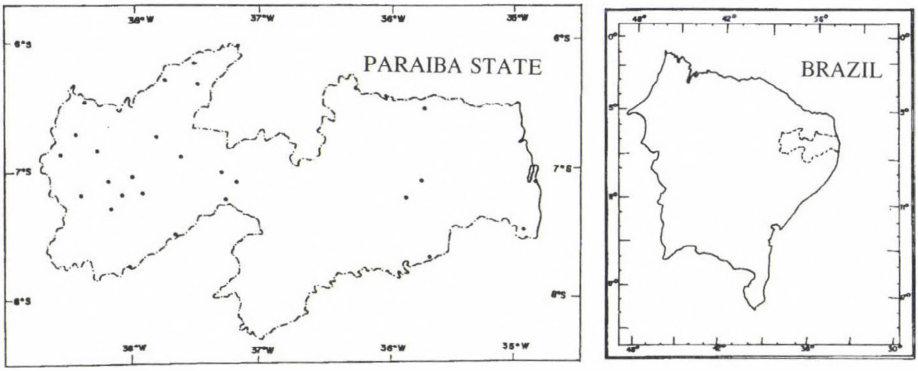

Fig. 1. Location of the stations.

The estimated daily soil moisture data are subjected to various types of analysis. Evaluation of crop growing periods and irrigation needs at the stations is the main objective of the study. *Fig. 1* shows the locations of the stations selected for this study.

2. *Methodology*

The evaluation of daily values of available soil moisture at the stations is based on the procedure suggested by *Thornthwaite* and *Mather* (1957). Mean monthly potential evapotranspiration (PE) values are computed using long-term mean monthly temperature data. The variation of PE during the year is used to obtain the PE values for each decade of the year. Each month is divided into three decades for this purpose; the last decade has 8, 9, 10 or 11 days depending on the month. The daily values are obtained from the decadal PE values and these together with the daily precipitation values are used to evaluate the daily soil moisture values. At each station the daily soil moisture content values are evaluated for the entire study period for each of five assumed available moisture capacity (AWC) values (25, 100, 150, 200 and 250 mm). The term 'available moisture capacity' represents the difference between the field capacity and the permanent wilting point.

A first order Markov chain model is applied to the estimated soil moisture data. Using the daily soil moisture values, the initial and conditional probabilities P(D), P(W), P(D/D) and P(W/W) are determined for each decade of the year. Here P(D) is the probability of soil being dry on a given day, P(W) is the probability of soil being wet, P(D/D) is the probability of soil being dry given that soil on the previous day is also dry and P(W/W) is the probability of soil being wet on a day given that on the previous day it was wet too. The threshold moisture content (VC) separating a dry day from a wet one is 50% of the AWC value adopted.

Mean soil moisture contents in individual decades and the corresponding probabilities for different AWC values are used to evaluate the growing periods at the stations.

In the simplified water balance studies the soil moisture fluctuation is regarded as the difference between the gain due to precipitation and the loss due to evaporation and transpiration. This method of computing soil moisture suggests a simple climatological approach to irrigation planning. One can set up limits below which soil moisture will not be allowed to decrease for a crop with a given root depth. Then, by means of daily water balance computations, it would be possible to know when the predetermined level of soil moisture is reached and how much to irrigate to bring the moisture back to a safe level.

The two important parameters in this study are the available moisture capacity and the critical soil moisture level (CV). The available moisture capacity depends on the soil characteristics and the crop rooting depth. Each crop has its own critical moisture level below which a reduction in yield will occur. Also for same crop the critical moisture level may vary with the phenological phase.

Due to lack of reliable soil and crop data, two AWC values (100 and 200 mm) and three critical moisture levels (55%, 70% and 85% of the AWC) are adopted in this investigation.

For a given station with a chosen AWC value, daily soil moisture values are evaluated for all the years of the study period. However, in each year during the crop growing season, whenever the soil moisture content decreases to a preselected level, the value on that day is replaced with that of corresponding to 95% of the AWC. In practical terms this means that each time soil moisture is depleted to a predetermined level, irrigation is applied to bring it back near to its maximum value.

The number of irrigation applications and the mean interval between irrigations are computed for each year and mean values for the study periods are derived from the results.

3. Results and discussion

Decadal mean values of soil moisture at Cathole de Rocha for different AWC values are averaged over all the years of the study period (*Fig. 2*). The period with the maximum soil moisture content seems to vary with variation in the AWC value. For example for AWC_{25} the three decades with the highest moisture content are the 8th, 9th and 10th decades while for AWC_{250} the three corresponding decades are the 11th, 12th and 13th, respectively.

A preliminary estimate of the growing season at Cathole de Rocha can be obtained from Fig. 2 on the assumption that the moisture content must be at least 50% of the maximum for favourable crop growth. Fig. 2 shows that the growing season at Cathole de Rocha has a duration of 140 days for AWC_{100} and 150 days for the other three AWC values.

The above information is based on mean soil moisture patterns. A better understanding of the soil moisture conditions can be obtained from the probabilities of sequences of days with dry and wet soil.

The probability of occurrence of five consecutive days with wet soil in each decade of the year is shown in *Fig. 3* for different AWC values. We now assume that a five day wet spell in each decade is sufficient for productive crop growth, and that successful agriculture is based on good crops being produced in at least seven out of ten years. From Fig. 3 we notice that the growing season at Cathole de Rocha extends from the 7th to 15th decades for AWC_{100} and from the 6th to 16th decades for AWC_{150}. For AWC values of 200 and 250 mm, the period starts at the 8th and 9th decades and ends at the 18th, respectively.

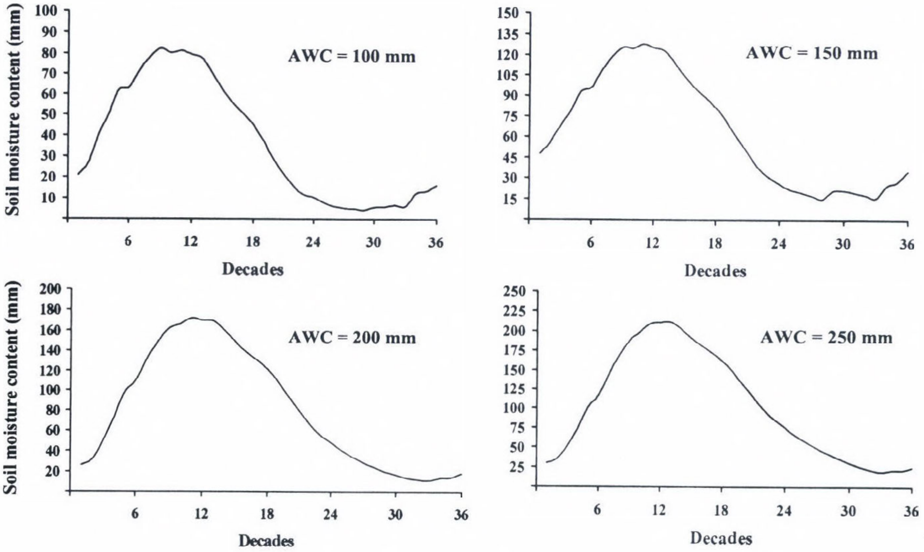

Fig. 2. Mean values of available soil moisture content at Catole do Rocha.

We assume that the seedbed holds 25 mm of moisture and that germination and early seedling growth require half of this amount for at least five days after sowing. We further assume that sowing is normally done after rain has sufficiently moistened the soil. From the mean decadal soil moisture content for AWC_{25} it is seen that for decades 5–13 the mean moisture content is more than half of the maximum value. The probability of occurrence of at least one wet day and of five consecutive wet days after a wet day is computed for decades 5–8, and it is found that the 6th decade is the most suitable for sowing purposes. If sowing is done in this decade, the growing seedling will enter a period when the expanding root system can tap moisture from greater depths (AWC values varying between 100 and 250 mm). The length of the growing season will be 100, 110, 150 and 150 days for AWC values 100, 150, 200 and 250 mm, respectively.

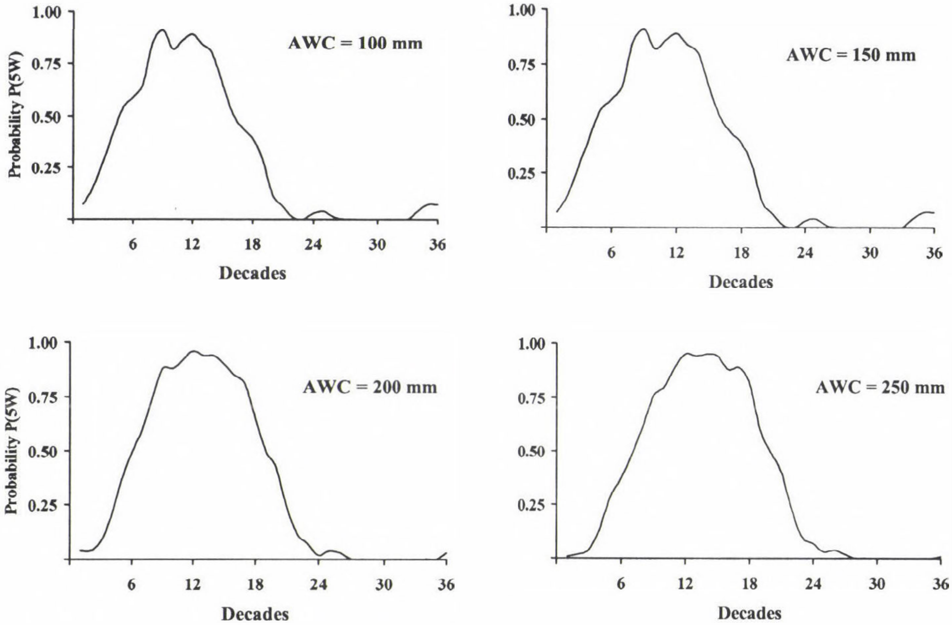

Fig. 3. Probability of occurrence of five consecutive wet days in each decade at Catole de Rocha.

Crop growing periods at the selected stations evaluated as discussed above are given in *Table 1* for two AWC values. Based on the results for all the stations, the following conclusions are arrived at:

(i) There is a significant phase postponement between the variation during the year of mean decadal values of precipitation and soil moisture content. This suggests that crop growing periods evaluated on the basis of precipitation data alone may not yield reliable results.

(ii) The period of the year with the maximum moisture content varies with the AWC value assumed. Also the ratio between soil moisture content and AWC varies with the AWC value considered.

(iii) Length of the growing season increases with increase in the AWC value adopted. This implies that at a given station with a given soil type the growing period for deep rooted crops will be longer than for shallow rooted crops.

Results of irrigation water requirement computations for São Gonçalo are discussed below and a summary of the results for all the stations is presented in *Table 2*.

Table 1. Crop growing periods in Paraiba State

Station	Available moisture capacity (mm)	Crop growing period		
		Start	End	Durations (days)
Barra de Jua	100 250	10 Mar	31 MAY 30 JUNE	80 110
Antenor Navarro	100 250	20 Feb	20 MAY 20 JUNE	90 120
Nova Olinda	100 250	10 Feb	10 MAY 10 JUNE	90 120
Serra Grande	100 250	01 Mar	20 MAY 10 JULY	80 130
Pianco	100 250	01 Mar	10 MAY 20 JUNE	70 110
Porcos	100 250	10 Feb	10 MAY 20 JUNE	90 130
Catole do Rocha	100 250	20 Feb	31 MAY 30 JUNE	100 130
Alhandra	100 250	10 Apr	20 SEPT 31 OCT	160 200
Joao Pessoa	100 250	10 Apr	30 SEPT 30 OCT	170 200
Imaculada	100 250	20 Mar	20 MAY 10 AUG	60 140
Belem do Brejo do Cruz	100 250	20 Feb	10 MAY 10 JUNE	80 110
Bom Jesus	100 250	10 Mar	20 MAY 30 JUNE	70 110
Itaporanga	100 250	10 Mar	20 MAY 20 JUNE	70 100
Princesa Isabel	100 250	01 Mar	31 MAY 20 JULY	90 140
Aguiar	100 250	01 Mar	10 MAY 10 JUNE	70 100
Araruna	100 250	01 Apr	30 SEPT 30 OCT	180 210
Sao Goncalo	100 250	20 Feb	20 MAY 20 JUNE	90 120
Agua Branca	100 250	20 Feb	20 MAY 31 JULY	90 160
Cajazeiras	100 250	10 Feb	10 MAY 20 JUNE	90 130
Piloes	100 250	10 Mar	20 MAY 20 JUNE	70 100
Condado	100 250	10 Mar	20 MAY 20 JUNE	70 100
Patos	100 250	10 Mar	20 APR 10 JUNE	40 90
Teixeira	100 250	10 Mar	10 MAY 20 JUNE	60 100
Umbuzeiro	100 250	10 Jun	31 AUG 30 SEPT	80 110
Pombal	100 250	20 Mar	20 MAY 20 JUNE	60 90
Alagoa Nova	100 250	01 Mar	10 OCT 20 NOV	220 260
Campina Grande	100 250	01 May	31 SEPT 30 OCT	150 180

Table 2. Irrigation needs at the stations

Station	Period	Available moisture capacity (mm)	Irrigation need (mm)
Barra de Jua	MAR – JUN	100 200	108 104
Antenor Navarro	MAR – JUN	100 200	148 112
Nova Olinda	MAR – JUN	100 200	168 144
Serra Grande	MAR – JUN	100 200	92 88
Pianco	MAR – JUN	100 200	152 120
Porcos	MAR - JUN	100 200	144 128
Catole do Rocha	MAR – JUN	100 200	108 96
Alhandra	MAR – OCT	100 200	176 160
Joao Pessoa	APR – OCT	100 200	96 80
Imaculada	MAR – JULY	100 200	120 104
Belem do Brejo do Cruz	MAR – MAY	100 200	124 104
Bom Jesus	MAR – JUN	100 200	112 104
Itaporanga	MAR – JUN	100 200	132 88
Princesa Isabel	MAR – JUN	100 200	108 88
Aguiar	MAR – MAY	100 200	96 88
Araruna	APR – OCT	100 200	124 104
Sao Goncalo	FEB – JUN	100 200	168 160
Agua Branca	APR - JULY	100 200	88 72
Cajazeiras	FEB – JUN	100 200	168 144
Piloes	MAR – JUN	100 200	144 120
Condado	MAR – JUN	100 200	148 128
Patos	MAR – JUN	100 200	168 144
Teixeira	MAR – JUN	100 200	120 104
Umbuzeiro	JUN – SEP	100 200	48 88
Pombal	APR – JUN	100 200	108 88
Alagoa Nova	MAR – NOV	100 200	160 128
Campina Grande	MAY – OCT	100 200	104 96

Limiting soil moisture value is 55% AWC

Irrigation requirements at São Gonçalo for AWC_{100} and limiting moisture level of 55% are shown in *Table 3*. In this case irrigation is applied whenever the soil moisture content decreases to 55 mm and thus the soil moisture content is maintained between 55 mm and 100 mm. It is seen that irrigation is needed in all years of the study period ranging from one application in 1974 to nine in 1958 and 1976. The mean interval between irrigations is 31 days and the mean irrigation water requirement during the five month crop growing period is 204 mm. It is noticed that in 15 out of 37 years the soil moisture deficit (difference between the AWC and the available moisture content) is more than 30 mm on at least 25% of the days.

A summary of the results for two AWC values and three limiting moisture levels is shown in *Table 4*. As it is to be expected, the number of irrigations increases and the mean interval between successive irrigations decreases as the limiting moisture level increases. However, the change in the total water need is not very pronounced since at higher moisture levels less water is applied in each irrigation.

For both AWC values, adoption of 70% level results in the soil moisture content remaining above 80% of the AWC on 70% of the days. Table 4 also suggests that to maintain similar moisture levels in the soil, less irrigation water seems necessary for AWC_{200} than for AWC_{100}. Similar result was obtained by *De Jong* (1985).

Long-term mean values of precipitation and potential evapotranspiration at Umbuzeiro during the six month wet season (May–October) are 468 mm and 463 mm, respectively. However, it is seen from Table 2 that even to maintain the soil moisture above 55% of the AWC, nearly 140 mm of irrigation is necessary. During the period February–May Terezina receives, on the average, 967 mm of precipitation. Potential evapotranspiration during the four month period is much less: 504 mm. Significant amount of supplementary irrigation is, however, necessary during the period to maintain the soil moisture content above half of the available moisture capacity.

This feature, also observed at the other stations, suggests that use of long-term mean monthly values of precipitation and potential evapotranspiration for the identification of crop growing periods may lead to erroneous conclusions in this region.

The crop growing periods shown in Table 1 are based on Markov chain probabilities of dry and wet days and represent the optimum months for crop growth at the stations. Results shown in Table 2 suggest that significant amounts of irrigation water are necessary even to maintain the soil moisture content near half of the available moisture capacity which is often considered as the minimum moisture level for plant growth (*Robertson*, 1985). In the case of corn and rice, the soil moisture levels are much higher and the irrigation needs increase correspondingly.

Table 3. Irrigation schedule for São Gonçalo. Available moisture capacity is 100 mm and minimum moisture content is 55 mm

Period: Feb–Jun

Year	Number of irrigations	Mean interval between irrigations	Number of days with soil moisture content between		
			55–70 mm	70–85 mm	85–100 mm
1944	4	43	44	46	54
45	5	36	30	43	77
46	4	22	55	47	48
47	3	15	21	42	87
48	5	35	28	44	79
49	6	27	26	49	75
50	6	28	31	45	74
51	8	17	31	59	60
52	5	33	38	57	56
53	6	27	39	53	58
54	6	28	38	44	68
55	4	19	25	53	62
56	7	22	34	47	70
57	8	19	42	46	62
58	9	16	59	50	41
59	5	29	48	46	56
60	6	28	34	49	68
61	4	32	25	56	69
62	6	27	29	49	72
63	6	27	33	40	77
64	4	43	31	47	73
65	4	40	27	35	88
66	5	26	35	53	62
67	4	49	19	23	108
68	6	29	28	43	80
69	3	27	38	46	66
70	8	18	48	44	58
71	2	21	16	45	89
72	2	82	38	60	53
73	3	58	25	55	70
74	1	0	14	25	111
75	4	44	39	38	73
76	9	16	39	39	73
77	2	52	30	55	65
78	5	18	40	40	70
79	7	22	34	52	64
80	7	23	45	52	54

Table 4. Water requirements at São Gonçalo during the period February-June

Available moisture capacity (mm)	Limiting soil moisture value (mm)	Number of irrigations	Mean interval between irrigations (days)	Number of days with soil moisture content between			Irrigation need (mm)
100	55	5	31	55-70	70-85	85-100 mm	204
				34	46	69	
	70	11	14	70-80	80-90	90-100 mm	270
				33	49	67	
	85	30	4	85-90	90-95	95-100 mm	299
				39	42	68	
200	110	2	83	110-140	140-170	170-200 mm	195
				26	44	80	
	140	5	39	140-160	160-180	180-200 mm	239
				31	45	72	
	170	14	11	170-180	180-190	190-200 mm	272
				41	49	58	

Irrigation needs evaluated from easily available climatological information by means of simple models such as that used in this study can be of use in land use and irrigation system planning. A detailed study along these lines has been carried out by *Robertson* (1970).

References

Baier, W. and *G.W. Robertson, G.W.*, 1966: A new versatile soil moisture budget. *Canadian J. of Plant Sci. 46*, 299-315.

De Jong, R., 1985: Soil water modelling using daily and mean-daily data derived from historical monthly values. *Atmosphere-Ocean 23*, No. 3, 254-266.

Dyer, J.A. and *Mack, A.R.*, 1984: The versatile soil moisture budget — version three. *Research Branch, Agriculture Canada.*

Robertson, G.W., 1970: Rainfall and soil water variability with reference to land use planning. *Tech. Ser. 1 UDC 551.5:63.* Department of Meteorology, University of the Philippines.

Robertson, G.W., 1973: Reliability of soil moisture determinations. *Soil Horizons 14* (1), Research Branch, Agriculture Canada, Ottawa, 24-29.

Robertson, G.W., 1985: *Rainfall and Soil-water Averages and Probabilities and Other Pertinent Agroclimatic Data for Mandalay (Socialist Republic of the Union of Burma).* MO/BUR/80/-016, WMO, Geneva, 17 pp.

Thornthwaite, C.W., 1948: An approach toward a rational classification of climate. *Geogr. Rev. 38*, 58-94.

Thornthwaite, C.W. and *Mather, J.R.*, 1957: Instructions and tables for computing potential evapotranspiration and the water balance. *Publ. Climatol. Vol. X* (3). Lab. Climatol. New Jersey.

IDŐJÁRÁS
Quarterly Journal of the Hungarian Meteorological Service
Vol. 103, No. 3, July–September 1999, pp. 189–213

Chemistry of rain in central India

C. K. Chandrawanshi and **K. S. Patel**[1]

School of Studies in Chemistry Pt. Ravishankar Shukla University
Raipur-492010, MP, India

(Manuscript received 2 January 1997; in final form 23 September 1998)

Abstract—The south-western Arabian summer monsoon loaded with local and distant pollutants causes heavy rainfalls in the central region of the Indian continent. The chemistry of summer rain water of the country (lies between 17° and 24°N latitudes, and 80°17' and 84°11'E longitudes at altitude >300 m) during hydrological years 1995 to 1997 is described. A total of 800 rain events at twelve sites, i.e., Raipur (during 1995–1997), Korba, Bilaspur, Kanker, Janjgir, Raigarh, Chirmiri, Bhatapara, Pithora, Gariyaband, Dallirajhara and Ambikapur of central India (during 1995) were occurred, from which 477 rain water events were collected in a polyethylene bucket kept over the roof of the houses. The chemical composition for ions, i.e., H^+, Na^+, K^+, Ca^{2+}, Mg^{2+}, NH_4^+, SO_4^{2-}, NO_2^- + NO_3^-, Cl^-, F^-, I^-, ionic balance, pH and conductivity of the rain water samples were determined. The concentration, flux, deposition patterns and trends of the ions and their sources in the monsoon rain water are described. The sulphate is a predominating ion and primary source of acid rain in central India. Most of the rain storms of India occur on its central areas. The rain water of these storms is mostly acid, especially in the monsoon season, probably due to blown of less amount of soil dust and higher humidity.

Key-words: pH, rainfall, acidity, chemical composition of rain water, concentration, flux and distribution of the ions, sources.

1. Introduction

Precipitation is a natural phenomenon through which pollutants from the atmosphere are scavenged out by natural processes, i.e., rain, fog, dew, snow, etc. Rain is the main source for getting large quantities of water to change the ground water aquifers and supporting the forest vegetation in the tropical countries. The rain water is not pure but contaminated with a variety of pollutants due to increased human activities. Acidic precipitation to the earth's surface is well known serious phenomenon due to adverse environmental

---

[1] Correspondig author

impacts (*Pitelka* and *Raynal*, 1989; *Longhurst et al.*, 1993; *Tuovinen et al.*, 1993). Acid rain is blamed for tree damage, acidification of water reservoirs, deterioration of marble structures and ancient monuments, etc. (*O'Sullivan*, 1985; *Cheng et al.*, 1987; *Vocom*, 1979; *Skoulikidis*, 1983). Much work have been carried out in the western countries in order to define the sources, causes, extent and consequences of acid precipitation (*Kasina*, 1980; *Hansen* and *Hidy*, 1982; *Kallend et al.*, 1983; *O'Sullivan,* 1985; *Blanchard* and *Stromberg*, 1987; *Lacaux et al.*, 1987; *Moldan*, 1988; *Goreham*, 1989; *Cowling*, 1989; *Falkengren-Grerup*, 1989; *Likens*, 1989; *Porteous* and *Barratt*, 1989; *Bowersox et al.*, 1990; *Udisti et al.*, 1991; *Cerceo*, 1983; *Atteia*, 1994; *Lynch et al.*, 1995; *Sanusi et al.*, 1996). The activities, i.e., generation of electricity by burning of coal, combustion of gasoline by automobile and smelting/refinement of metals and non-metals are major sources of the oxides of nitrogen and sulphur that are involved (*Mohnen*, 1988; *Galloway*, 1989; *Schwartz*, 1989; *Khemani et al.*, 1987; *Irwin* and *Williams*, 1988; *Khemani et al.*, 1994). The question of the extent of acidification in the tropical globe has received little scientific attention until recently, so the answers are unsatisfactory or unavailable. For this region, the scope project "acidification in tropical countries" was initiated in 1984, culminating in a workshop in Caracas, 1986 (*Nollor* and *Chadha*, 1990). It is a clear that the question of acidification is very relevant to the tropics. Some identified areas of acidification such as South-Western China, Thailand, Japan, etc. are probably occurring due to increased combustion of fossil fuel, smelting of sulphide minerals as well as poor buffering capacity of soil present (*Zhao et al.*, 1988; *Saylor et al.*, 1992; *Environment Agency*, 1996). The tropical region has large population and it is the area of the globe where changes in population, energy usage, industrial capacity and agricultural practices are the fastest (*Nollor* and *Chadha*, 1990). Another geographical feature is that about 40 percent of acid sulphate soil of the world occurs naturally in the tropics of Asian region (*Singh*, 1982). About half of the globe population resides in the Asian region and the use of fertilizers is increasing too fast due to multiple crop yields in the agriculture. Tropical regions are characterized by rice forming and biomass burning which provides sources for green house gases like CH_4, NMHC, CO, NO_x and NO_2 (*Clairac et al.*, 1988; *Suman*, 1988; *Talbot et al.*, 1988). The industrialization and production of energy in the tropics are mainly based on burning of fossil fuel such as coal with emission of an enormous amount of the acidic gases, SO_x, NO_x into the atmosphere. The expected emitted amount of SO_2 alone by 2000 AD in South Asia is 76 million tons, more than projected for the whole of Europe and North America (*Hordijk*, 1993). These anthropogenic pressures on atmospheric composition and chemistry are likely to be increased with time in this region.

The data on the atmospheric precipitation of India is fragmentary and even less data exist on the acidity of precipitation in particular. Some authors reported the acidity and ion composition of rain water of the northern and western part of the Indian continent in isolated pattern (*Mukherjee*, 1978; *Das et al.*, 1981; *Khemani et al.*, 1989; *Verma*, 1989; *Ravichandran* and *Padmanabhamurty*, 1994).

There is rapid industrialization and urbanization in the central region of the country (lies between 17° and 24°N latitudes and 80°17' and 84°11'E longitudes) due to availability of vast natural resourced materials, i.e., coal and minerals of Fe, Al, Cu, Mn, Sn, Nb, Ca, etc. More than 2000 small and more than 200 large scale industrial works and thermal power plants, mostly based on burning of coal, are operating in this region. Heavy rainfalls occur in this region by breaking of the south-west (SW) summer monsoon. The most of tropical rain forests of the country lie in this region where active exchange of gases and aerosol between the atmosphere and the biosphere takes place as a natural process. In this work, the chemistry of precipitation in central India has been investigated to define the concentration, amount, distribution pattern and sources of major ions, i.e., H^+, Na^+, K^+, Ca^{2+}, Mg^{2+}, NH_4^+, SO_4^{2-}, NO_3^-, Cl^-, F^-, I^- in rain water.

2. *Experiments*

2.1 Sampling sites

The choice of sampling network and location of sampling equipment were made according to internationally accepted specifications (*WMO GAW* No. 85; *Khemani et al.*, 1989). Twelve sampling sites were established in the central India: Raipur, Korba, Bilaspur, Kanker, Janjgir, Raigarh, Chirmiri, Bhatapara, Pithora, Gariyaband, Dallirajhara and Ambikapur (see *Fig. 1*). These sites were chosen as representatives of different geographical, geological and meteorological effects, and their summary descriptions are given in *Table 1.*

2.2 Sampling of precipitation water

Wet (rain water) samples were collected on an event basis. The sampling period was extended from January 1995 to December 1997 and the total number of rain water samples collected during these period were 477. The instrument consists of a bucket system covered with a lid which exposed and closed manually. A cylindrical polyethylene bucket (diameter = 30.5 cm and height = 32 cm) was fixed on a wooden stand mounted over the roof of a house (height = 4 m). The depth of rain amount was measured with a graduated scale. The rain water samples were filtered with Whatmann filter paper No. 42 and transferred into a one liter polyethylene bottle. Each collector was washed out from the container with 500 ml deionized double distilled water. Each collected sample was identified with a site identification code and sample collection data.

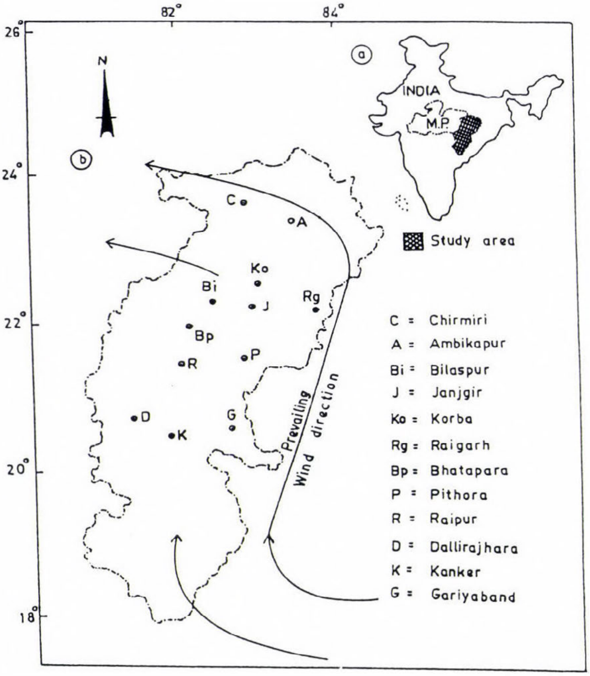

Fig. 1. Geographical map of (*a*) India, (*b*) central India.

2.3 Shipment and storage of samples

Sample bottles were packed with foam in wooden-board boxes and shipped to the laboratory by bus or train. The time between field sampling and receipt of samples was typically 3 to 4 days whereas between receipt of samples and subsequent chemical analysis ranged between 1 to 30 days. The samples were stored at 4 °C in the refrigerator and no preservatives were added to the samples at any time during shipping or storage. Interaction between sample solutions and storage bottle, effect of ambient gases and potential losses by evaporation were not studied.

2.4 Measurements and chemical analysis

All plastic equipments used in experiments were acid washed prior to use. They were soaked overnight in 1 N HNO_3 which was rised 3 times with distilled water. A Systronic μ-pH meter (type–361) and a Systronic conductivity-meter (type–304) were used to measure pH and conductivity values. A GBC flame AAS (type–932AA) equipped with air-acetylene and nitrous oxide-acetylene flames was used for monitoring of elements, i.e., Na, K, Ca, Mg. A Tecator flow injection analyzer (type–5012) equipped with ALPKEM UV–VIS spectrophotometer detector (type–510) with a 5.5 mm flow cell, and two peristaltic pumps of constant speed (48 cycle min^{-1}) were used for monitoring of ions F^-, Cl^-, I^-, NO_2^-, NO_3^-, and NH_4^+. A Systronic turbidimeter (type–131) was used for monitoring of SO_4^{2-}.

Table 1. Study site location and description

Site No.	Location	Type	Description
1.	Raipur	UA	Steel and cement industries and urban pollution source area
2.	Korba	UA	Thermal power plants, aluminum industry, coal mines and urban pollution
3.	Bilaspur	UA	Cement industries and urban pollution source
4.	Kanker	RUA	Forest area with deposition of iron ore
5.	Janjgir	SUA	Cement industry and agricultural land
6.	Raigarh	SUA	Ferro-alloy industry, agricultural land and forest area
7.	Chirmiri	SUA	Coal mines and urban pollution
8.	Bhatapara	SUA	Cement industry and agricultural land
9.	Pithora	RUA	Agricultural land
10.	Gariyaband	REA	Forest area with deposition of pyrites
11.	Dallirajhara	SUA	Iron ore processing industry and forest area
12.	Ambikapur	RE - SUA	Remote and forest area with deposition of coal

UA = urban area; RUA = rural area; SUA = suburban area; REA = remote area;

RE - SUA = remote suburban area

The pH of the solution was measured in the laboratory using μ-pH meter equipped with glass and calomel electrode calibrating with buffer 4 and 7.25 ml. The solution was taken into a plastic beaker, and the meter was allowed to equilibrants for 5 minutes before the pH value was recorded. Electrical conductivity of the solution was also recorded by using conductivity meter. The used 25 ml solution was discarded. The ions were analyzed with techniques AAS, FIA, turbidimetry. Their optimal analytical parameters are summarized in *Table 2*. For the analysis of the metals with AAS, a 25 ml aliquot of filtered rain water sample was treated with 0.2 ml concentrated HNO_3 (ultrapure, E. Merck) in a polyethylene tube covered with lid. A reagent blank was prepared using de-ionized distilled water in a similar way. Cations Na^+, K^+, Ca^{2+}, Mg^{2+} were analyzed with the flame-AAS as described in the literature. Filtered rain water samples were used for the analysis of the anions NO_2^-, NO_3^-, Cl^-, F^-, I^-, NH_4^+ with the flow injection analysis (FIA) technique by measuring the colour change as described in the literatures (*Tecator*, 1992b; *Tecator*, 1991; *Chandrawanshi et al.*, 1996; *Chandrawanshi* and *Patel*, 1998; *Tecator*, 1992a). Sulphate ions were analyzed turbidimetrically using $BaCl_2$ as reagent (*Vogel*, 1978).

3. Results and discussion

3.1 Geography and geology

The study area (central India) is situated between 17° and 24°N latitudes, and 80°17' and 84°11'E longitudes at altitude of $\geq$300 m a.s.l. Tropics of cancer passes through this region and the total area is about 1.4×10^5 km^2 (4.1% of the area of India). It is based on igneous and metamorphic rocks with heavy deposition of minerals like iron/copper/manganese pyrites, bauxite, dolomite, coal, etc. The soil is red-yellow or red in colour and it is low in silica with high levels of iron and aluminium. Both tropical moist and dry deciduous forests are present in this region. The area of the forest is about 6.0×10^4 km^2 and the tree, *Shore Robust* is the predominant species in this area. Other important trees found are *Terminals arjuna, Terminals belerica, Terminals chabula, Amblica officinales, Dalbergia sissoo, Tectona grandis, Acaccia catechu, Butea monosperma, Madhulica officinales,* etc. Rice is the main food crop of this region includes 60% of the total cropped area. The total of 1.2×10^6 tons yr^{-1} of rice grain is produced on this part of the country.

This part of the country has the highest summer temperature and the lowest summer atmospheric pressure profiles, probably due to emission of huge amount of green house gases by forest vegetation, rice field, combustion of fossil fuels, biomass burning, etc. Temperature rises steadily from January to May which is usually the hottest month of the year. The mean maximum

Table 2. Details of techniques used for rain water analysis

Species	Techniques	Wave length (nm)	Detection limit (mg ℓ^{-1})	Optimum concentration range (mg ℓ^{-1})
Na^+	AAS, air - C_2H_2 flame	589.0	0.004	0.18 - 0.7
K^+	AAS, air - C_2H_2 flame	766.5	0.008	0.40 - 1.5
Ca^{2+}	AAS, N_2O - C_2H_2 flame	422.7	0.02	1.00 - 4.0
Mg^{2+}	AAS, N_2O - C_2H_2 flame	285.2	0.003	0.10 - 0.4
NH_4^+	Colorimetric FIA gas-diffusion technique using dye as colour developing agent	590.0	-	0.10 - 1.0
SO_4^{2-}	Turbidimetric method using reaction SO_4^{2-} + $BaCl_2$	420.0	-	-
NO_2^- + NO_3^-	Colorimetric FIA technique using on line Cd-reductor and sulphanili-amide + N-(-1-Naphty1)-ethylenediamine dihydrochloride as colour developing agent	540.0	-	0.20 - 100
Cl^-	Colorimetric FIA technique based on destruction of the colour of $Hg(SCN)_2$ + Cl^- + Fe^{3+}	470.0	-	1.0 - 150
F^-	Colorimetric FIA technique based on destruction of the colour of Zr-SPADNS complex with F^-	580.0	0.01	0.05 - 0.7
I^-	Colorimetric FIA technique based on catalytic destruction of the colour of Fe(III)-SCN^--CP^- complex with NO_2^- and NO_3^-	470.0	0.0001	0.005 - 0.1

temperature in May 1995 was ranged from 26.5 to 46.5°C. The period of May and the early June prior to the arrival of south-western monsoon is rather hot. Towards the close of the monsoon season in September, the day temperature increases slightly, and the rise is maintained in October after the withdrawal of monsoon. December is usually the coolest with the mean daily temperature in the range of 7.0°C to 27°C. A decreasing trend of the atmospheric temperature at a rate of 1°C to 2°C from, 1995 to 1997 was observed. The mean monthly (from January to December) relative humidity (morning & evening) and evaporation in site Raipur during hydrological years from 1995 to 1997 are 88 & 41% and 4.1 mm, 75 & 33% and 5.2 mm, 60 &20% and 7.0 mm, 55 & 25% and 9.9 mm, 40 & 15% and 12.6 mm, 72 & 48% and 11.1 mm, 85 & 71% and 5.3 mm, 91 & 78% and 4.2 mm, 92 & 77% and 3.9 mm, 88 & 60% and 3.5 mm, 89 & 40% and 3.0 mm, 82 & 25% and 2.5 mm, respectively. The highest relative humidity was recorded during the south-west monsoon season. After the monsoon season, humidity decreases during the winter season and the air is fairly dry with lowest evaporation rate. The dry part of the year is the summer season when the evening relative humidity is rather low (12%) in May. The rate of evaporation increases steadily from January to May and decreases steadily from June to December. The evaporation rate is lowest in December whereas highest in May.

3.2 Air quality

Air pollution is considered to be any atmospheric substances that are foreign to the "natural" atmosphere. Before the independence in 1947 the whole central region of the country was covered with dense tropical rain forest. After 1960 a rapid industrialization and urbanization of this region started. Nowadays the most of the metal and non-metal industries and coal based thermal power plants of the country are operating in this region. An enormous increase in population, industries, thermal power plants and agriculture production intensified the environmental problems, which already are plaguing the area. The total population of this area according to 1991 census was 18 millions with growth rate of ± 2.5% and at present the population expected is about 21 millions. The average population density is 130 persons km^{-2}. The number of both two and four wheeler vehicles are about 0.5 millions. There are 200 large scale and 2000 small scale (i.e., agro, building, chemical, engineering, forest, leather, paper, polymer, textile, etc. based) industries and thermal power plants of high capacity operating in this region. The amount of fossil fuel and coal consumed by various sources in this region are estimated to be 8 million tons yr^{-1}. In addition, every year, a huge amount of minerals like copper, iron and manganese pyrites (13 million tons yr^{-1}), aluminium (0.21 million tons yr^{-1}), dolomite (0.75 million tons yr^{-1}) and coal (31 million tons yr^{-1}) are mined out from various open and under ground mines. The level of NO_x, SO_x and SPM in the Raipur city during the years 1995 to 1997 were determined by the pollution department and their mean concentration ranged between 13–14, 8–25, and 128–381 μg m^{-3} with increasing rate of 15, 17 and 10% in the ambient air, respectively. The highest reported level of NO_x, SO_x and SPM in the ambient air of the Korba city during January 1997 was 55, 73 and 500 μg m^{-3}, respectively. The relatively higher level of NO_x, SO_x and SPM in this region of the country is probably due to rapid industrialization, transportation of distant pollutants from other parts of the country and the globe, etc.

3.3 Rainfall

The central part of the country receives the highest rainfall excluding Himalayan and eastern regions of the country. Rainfall with a maximum of 1650 mm was recorded in this region due to raining of both south-west (SW) and south-east (SE) monsoons. The SW summer monsoon comes with high wind speed probably due to high temperature above 40°C and causes a heavy rainfall. The average annual rainfall at 12 sites of central India during the hydrological year 1995, is 1300 mm varied from 1176 mm at Bilaspur in the south-east to 1376 mm at Gariyaband in the north-east. The amount of rainfall is not the same at different sites and the excess rain causes floods. The period between June and October receives about 88.5% of the annual rainfall. Decreasing of the rainfall starts in September and shrinks to less than 50 mm. In October, SW monsoon returns and substitutes by SE monsoon. The period between November and May receives only about 110 mm and it is 8.5% of the total annual rainfall. The rainfall during the hydrological years 1995 to 1997 at site Raipur is 1283, 1123 and 1214 mm, respectively. A decreasing trend in the rainfall height with lower frequency and rainfall duration from 1995 to 1997 was observed.

3.4 Mean concentration and quality assurance of data

The details of rainfall chemistry at twelve sites of central India occurred in the hydrological year 1995 are summarized in Table 3. The overall mean rainfall amount, duration and events or storms were 1300 mm, 224 hr and 58, respectively.

The sampling precision was checked by collecting 2 × 10 rain water samples from two sites of Raipur city: Daganiya (R_1) and Tikarapara (R_2) during 1995 by analyzing their physical parameters and ionic concentrations. Their analytical precision was checked by using Eq. (1).

$$S_i = \left(\frac{\sum d_i^2}{2N_i} \right)^{\frac{1}{2}}, \tag{1}$$

where d_i = difference between two analyses of the same sample, N_i = number of sample pairs used, $i = 1,2$. The value of S_i for rainfall amount, pH, conductivity, H^+, Na^+, K^+, Ca^{2+}, Mg^{2+}, NH_4^+, SO_4^{2-}, NO_3^-, Cl^-, F^- and I^- for the 2×10 rain water samples collected at two sites of Raipur city in 1995 were 1.3, 0.4, 9.6, 2.0, 5.4, 1.8, 8.1, 20.7, 10.7, 19.8 and 3.5, respectively. Good sampling precisions for the most parameters were obtained except for the F^- and NO_3^-, probably because of the variation in rate of evaporation and reaction with the other materials of F^-, and biodegradation of NO_3^-.

The accuracy of the chemical analysis in the proposed results was checked by ion and conductivity balance of the rain water samples. The rain water samples with pH ≤ 5.8 and the concentration of HCO_3^- were considered to be negligible in the tropics, whereas for the samples with pH > 5.8 the bicarbonate concentration was not considered. A linear correlation between measured anion and cation equivalent concentrations was determined and found to be significantly excellent: $r = 0.996$ for $n = 373$ (see *Table 3*). The ratio of the sum of anionic concentrations $\Sigma(\text{anions}) = \{[F^-] + [Cl^-] + [I^-] + [NO_3^-] + 2[SO_4]^{2-}\}$ to sum of cationic concentrations $\Sigma(\text{cations}) = \{[H^+] + [NH_4^+] + [Na^+] + [K^+] + 2[Mg^{2+}] + 2[Ca^{2+}]\}$ in 12 sites during the hydrological year 1995 was calculated and ranged between 0.97 to 1.00. The agreement between measured and calculated conductivity was determined. The calculated conductivity of the rain water samples was evaluated by using Eq. (2), where the concentrations are expressed in n mol ℓ^{-1}, the conductivity in μS cm^{-1}.

$$\text{Conductivity}_{\text{calc.}} = 10^{(3-\text{pH})} \times 350 + 2(SO_4^{2-})79.6 + (NO_3^-)70.6 + (Cl^-)75.5 + (NH_4^+)74.5 + (Na^+)50.9 + (K^+)74.5 + 2(Ca^{2+})\,60.0 + 2\,(Mg^{2+})\,53.1, \tag{2}$$

where concentrations are expressed in m mol ℓ^{-1}, conductivity is expressed in μS cm^{-1} units. The correlation coefficient (r) between measured and calculated conductivity was found to be $+0.80$ ($n = 5$).

3.5 Rain water acidity

Table 4 shows the pH distribution (from 4.9 to 6.7) of samples over the period January to November 1995. About 32% of rain water samples appeared with pH ≤ 5.8 and only 8% of samples appeared with < 5.0 which could be considered as the lower pH of natural rain water (*Charlson* and *Rodhe*, 1982). Acid pH values revealed the presence of strong acid in rain water, while neutral and alkaline pH values occur because of the neutralized acids by soil dust and sea salt. High concentration of soil dust in small samples of rain water are responsible for the neutral pH values.

Table 3. The volume weighed mean physical and chemical parameters of rain water in central India in the hydrological year 1995

Sampling site	No. of site	Total rainfall events	Total rainfall height (mm)	Total rainfall duration (hour)	No. of sample analysis	Ave. pH	Ave. cond. (μS cm^{-1})	Volume weighed mean contcentration (μeq ℓ^{-1})											$\frac{\Sigma[\text{anions}]}{\Sigma[\text{cations}]}$	$\frac{\Sigma[SO_4^{2-}]}{\Sigma[NO_3^-]}$	$\frac{\Sigma[H^+]\text{obs.}}{\Sigma[H^+]\text{cal.}}$
								H^+	Na^+	K^+	Ca^{2+}	Mg^{2+}	NH_4^-	SO_4^{2-}	NO_3^-	Cl^-	F^-	I^-			
Raipur	3	57	1283	225	115	5.8	65	2.0	25.6	4.4	136	45.5	9.5	166	21.7	32.7	2.7	0.02	0.97	7.6	0.8
Korba	2	55	1198	230	31	4.9	42	16.8	20.7	3.7	183	42.8	15.3	213	25.1	31.8	11.6	0.04	0.99	8.5	0.7
Bilaspur	2	55	1176	227	60	5.9	65	1.6	50.1	6.1	112	35.4	12.3	138	17.5	59.0	2.8	0.02	1.00	7.9	0.8
Kanker	1	70	1518	221	25	6.7	97	0.3	54.7	6.8	140	33.8	2.8	149	21.5	62.0	7.5	0.04	1.00	6.9	0.7
Janjgir	1	59	1320	226	18	6.4	75	1.5	33.3	4.5	153	78.4	1.3	170	60.0	35.5	5.9	0.02	0.99	2.8	0.3
Raigarh	1	62	1376	231	20	5.8	46	2.7	39.7	5.8	101	32.2	9.3	123	15.5	49.9	2.5	0.04	1.00	7.9	0.6
Chirmiri	1	51	1297	223	15	5.7	33	5.7	47.8	5.9	117	25.3	18.9	153	12.7	53.0	2.3	0.02	1.00	12.0	0.4
Bhatapara	1	53	1252	219	13	6.7	84	0.9	60.2	8.4	147	34.8	12.1	170	16.6	73.0	3.7	0.02	1.00	10.2	0.2
Pithora	1	54	1191	217	12	6.6	90	1.2	46.2	7.0	114	63.0	8.6	163	19.6	52.0	3.2	0.02	0.98	8.3	0.3
Gariyaband	1	65	1376	224	30	5.8	66	3.5	30.6	2.3	121	44.9	21.6	156	21.9	34.2	3.9	0.02	0.97	7.1	0.5
Dallirajhara	1	58	1312	227	20	5.6	61	5.0	50.4	6.8	132	33.0	2.9	146	20.2	61.0	3.1	0.03	0.99	7.2	0.5
Ambikapur	1	60	1270	219	14	5.8	63	2.2	30.0	2.6	131	42.6	2.3	144	23.5	35.1	3.6	0.03	0.97	6.1	0.7
Overall mean concentration			1297	224		5.9	74	3.6	40.7	5.3	132	42.7	9.7	158	22.9	48.4	4.4	0.03			

obs. = observed; cal. = calculated

Table 4. pH distribution of event samples and volume weighed percentage acids in rain water at 12 sites of central India during the hydrological year 1995

Site No.	Sampling site	pH of rain water events (%)			Acid (%)		
		pH > 5.65	pH < 5.65	pH < 5.0	H_2SO_4	HNO_3	HCl + HF
1.	Raipur	75.5	24.5	–	74.4	9.7	15.8
2.	Korba	–	22.3	77.7	75.6	8.9	15.4
3.	Bilaspur	69.1	30.9	–	63.4	8.0	28.5
4.	Kanker	95.6	4.4	–	61.9	8.9	29.1
5.	Janjgir	88.3	11.7	–	62.7	22.1	15.2
6.	Raigarh	66.7	27.7	5.5	64.5	8.1	27.4
7.	Chirmiri	23.1	61.5	15.4	69.2	5.7	25.1
8.	Bhatapara	91.6	8.4	–	64.3	6.3	29.4
9.	Pithora	90.0	10.0	–	68.5	8.2	23.2
10.	Gariyaband	55.2	44.8	–	72.3	10.1	10.1
11.	Dallirajhara	68.4	26.3	5.3	63.4	8.7	27.8
12.	Ambikapur	66.6	66.6	–	69.8	11.4	18.7
Overall volume weighed mean % concentration of acid					67.5	9.8	22.6

Detailed statistics of the rain water acidity during the hydrological year 1995 is summarized in *Tables 4–5*. It is obvious that "acid rain" commonly occurred in central India specially in the monsoon periods. Korba was the site with the lowest volume weighed mean pH value (4.9) of the event samples and the lowest pH value (4.1) of the event samples. Other seven locations: Raipur, Bilaspur, Raigarh, Chirmiri, Gariyaband, Dallirajhara, Ambikapur were the sites where the overall volume weighed mean pH values of rain water was 5.8. Thus, these eight sites commonly faced acid rain problems with pH values well below the neutral pH, 5.8, specially in the monsoon season as shown Table 4. In the sites: Janjgir, Pithora, Kanker and Bhatapara, relatively higher volume weighed mean pH values were recorded (6.4, 6.6, 6.7 and 6.7, respectively). The high pH values were probably due to neutralization of acids with alkaline particulates emitted from the cement factories and soil dust.

The effect of meteorological parameters, i.e., rainfall amount, frequency, rainfall duration on the pH value of rain water was examined. Results are shown on *Fig. 2*. The pH values decrease as the number of frequency of rainfall amount and the duration of rainfall increase, probably due to blown of lower amount of soil dust. Similarly, the pH values of rain water decrease as the relative humidity increase, probably due to relatively more absorption and hydrolysis of the acidic oxides, i.e., NO_2 and SO_3 from distant area. However, no exact trend was observed with variation in atmospheric temperature and wind speed.

The monthly and annual variations in pH values of rain water samples at site Raipur were studied. The pH values of the rain water decreased from May to August probably due to blown of lower amount of soil dust and higher humidity. From August the pH values gradually increased probably due to lower rainfall amounts. The pH of the rain water samples decreased in hydrological years 1995–1997 during the monsoon period probably duo to either increase in emission rate of acidic gases or decrease in soil buffering capacity or both.

3.6 Ionic species relationship

The pair correlation coefficient dataset of 11 ions in the rain water of 1995 is computed for entire central India. The highest correlations appear for the ion pairs: Na^+ and Cl^- ($r = 0.97$), K^+ and Cl^- ($r = 0.91$), Na^+ and K^+ ($r = 0.87$), Ca^{2+} and SO_4^{2-} ($r = 0.8$), Ca^{2+} and F^- ($r = 0.84$), Mg^{2+} and NO_3^- ($r = 0.8$), F^- and SO_4^{2-} ($r = 0.74$), Ca^{2+} and F^- ($r = 0.72$), H^+ and SO_4^{2-} ($r = 0.67$), H^+ and F^- ($r = 0.66$), H^+ and Ca^{2+} ($r = 0.58$), NH_4^+ and NO_3^- ($r = 0.57$), F^- and I^- ($r = 0.55$). Most of these well correlating pairs have either common sources, (they occur in precipitation as a result of a common source) or they exist in the form of compounds like $NaCl$, KCl, $CaSO_4$, CaF_2, $Mg(NO_3)_2$, NH_4NO_3, etc. The ion-pair Na^+ and K^+ has good correlation due to common occurrence in

Table 5. Statistical descriptions of the chemical composition of precipitation at each sampling station

Site No.	Sampling site	Statistical parameter	pH	Cond. (µS cm^{-1})	Ions (µeq ℓ^{-1})										
					H^+	Na^+	K^+	Ca^{2+}	Mg^{2+}	NH_4^+	SO_4^{2-}	NO_3^-	Cl^-	F^-	I–
1.	Raipur	V. M. Mean	5.8	65	2.0	25.6	4.4	135.9	45.5	9.5	165.8	21.7	32.7	2.7	0.02
		A. Mean	–	–	4.0	30.8	9.5	145.8	52.6	11.4	175.9	26.9	38.6	5.5	0.08
		Median	6.1	39	0.7	29.7	3.1	144.0	18.3	6.1	18.7	18.5	42.5	2.1	0.40
		Minimum	5.0	13	0.01	4.3	0.5	75.0	12.1	0.0	81.0	1.7	1.8	1.0	0.02
		Maximum	7.9	476	7.1	265.0	71.8	800.0	136.6	272.2	745.8	224.2	352.1	54.3	2.15
		Sd (±)			1.9	46.8	11.9	149.7	25.7	48.0	118.9	39.2	71.6	8.5	0.02
2.	Korba	V. M. Mean	4.9	42	16.8	20.7	3.7	182.7	42.8	15.3	213.1	25.1	31.8	11.6	0.04
		A. Mean	–	–	19.7	26.1	6.9	197.6	49.3	19.8	226.2	35.4	38.5	19.2	0.06
		Median	4.9	41	18.5	19.2	2.6	73.7	19 9	14.7	81.2	23.9	26.5	12.4	0.60
		Minimum	4.4	13	0.5	6.5	1.3	25.0	7.2	0.8	42.3	10.1	11.8	4.2	0.08
		Maximum	5.6	80	40.6	89.4	23.1	290.0	64.0	158.9	278.2	53.0	128.3	42.1	5.40
		Sd (±)			11.7	26.1	5.3	69.7	18.1	36.6	75.9	12.0	34.7	7.6	0.03
3.	Bilaspur	V. M. Mean	5.9	65	1.6	50.1	6.1	111.8	35.4	12.3	138.4	17.5	59.5	2.8	0.02
		A. Mean	–	–	3.8	58.2	12.3	131.7	42.8	21.4	167.1	29.2	68.4	5.4	0.05
		Median	6.0	31	0.8	21.7	6.9	75.0	66.7	1.6	287.4	22.5	28.2	1.8	0.30
		Minimum	5.4	7	0.1	0.0	0.0	0.0	7.4	0.0	15.0	0.6	4.2	0.5	0.03
		Maximum	7.0	490	4.4	180.4	669.2	130.0	135.8	67.3	1120.8	214.5	701.4	62.1	1.70
		Sd (±)			1.2	41.7	17.9	159.3	29.3	21.6	154.1	51.1	108.9	9.5	0.02
4.	Kanker	V. M. Mean	6.7	97	0.3	54.7	6.8	140.5	33.8	2.8	148.8	25.5	62.4	7.5	0.04
		A. Mean	-	-	1.1	59.5	10.8	155.2	41.5	5.4	159.7	33.8	68.2	11.8	0.07
		Median	6.7	59	0.2	25.2	8.5	161.0	63.4	1.7	304.2	32.2	29.6	3.7	0.50
		Minimum	5.8	8	0.03	0.0	0.7	0.0	7.4	0.0	133.4	0.8	8.4	1.1	0.14
		Maximum	7.5	380	0.7	652.2	127.5	925.2	127.6	15.0	650.0	417.7	971.8	33.7	2.90
		Sd (±)			0.3	276.8	78.8	270.4	42.6	6.5	160.3	120.8	262.4	9.3	0.02

Continued Table 5

Site No.	Sampling site	Statistical parameter	pH	Cond. (μS cm^{-1})	Ions (μeq ℓ^{-1})										
					H^+	Na^+	K^+	Ca^{2+}	Mg^{2+}	NH_4^+	SO_4^{2-}	NO_3^-	Cl^-	F^-	I^-
5.	Janjgir	V. M. Mean	6.4	75	1.5	33.3	4.5	152.8	78.4	1.3	170.3	60.0	35.5	5.9	0.02
		A. Mean	-	-	2.6	38.4	7.8	159.1	84.5	5.1	179.5	68.5	42.7	8.1	0.07
		Median	6.5	59	0.3	25.2	33.3	135.0	51.8	1.7	245.8	39.3	34.1	3.7	0.40
		Minimum	6.2	17	0.1	0.0	0.0	30.0	9.0	0.0	175.0	8.2	9.8	2.1	0.01
		Maximum	7.2	210	5.5	221.7	405.1	1125.0	224.6	20.5	408.4	227.4	112.8	18.9	1.60
		Sd (±)			1.5	54.9	82.6	321.9	55.2	5.1	61.5	57.5	24.9	5.2	0.01
6.	Raigarh	V. M. Mean	5.8	46	2.7	39.7	5.8	101.5	32.2	9.3	123.2	15.5	49.9	2.5	0.04
		A. Mean	-	-	5.8	44.8	12.0	110.1	36.8	12.5	134.5	26.2	55.1	6.2	0.08
		Median	6.1	40	0.7	9.8	5.1	105.0	73.6	1.7	260.5	14.1	13.4	2.1	0.50
		Minimum	5.0	9	0.1	0.0	0.0	0.0	7.4	0.0	62.4	0.6	7.0	0.5	0.10
		Maximum	6.9	128	9.7	47.8	38.5	385.0	132.4	60.5	825.0	237.1	59.7	17.9	7.50
		Sd (±)			2.6	14.8	11.1	123.1	37.0	15.6	173.7	69.7	16.3	4.2	0.03
7.	Chirmiri	V. M. Mean	6.6	90	1.2	46.2	7.0	114.2	63.6	8.6	163.0	19.6	52.0	3.2	0.02
		A. Mean	-	-	3.4	52.4	12.8	126.9	71.2	11.8	185.2	25.8	60.3	7.1	0.06
		Median	6.8	58	0.2	30.9	12.8	110.0	79.7	1.7	229.1	19.4	35.0	2.1	0.30
		Minimum	5.5	6.0	0.02	3.5	5.1	5.0	14.2	0.0	150.0	0.8	12.7	1.1	0.02
		Maximum	7.8	144	3.3	320.8	58.9	2063.4	773.6	27.7	1120.8	83.4	1135.2	12.6	1.30
		Sd (±)			4.5	31.1	4.1	28.0	10.9	16.2	32.9	8.6	80.9	1.3	0.02
8.	Bhatapara	V. M. Mean	6.7	84	0.9	60.2	8.4	147.2	34.8	12.1	169.6	16.6	73.7	3.7	0.02
		A. Mean	-	-	2.8	67.5	13.5	157.5	41.2	15.4	175.1	19.8	77.2	5.5	0.06
		Median	6.9	90	0.1	71.7	5.2	36.2	81.5	1.7	272.2	33.0	98.7	4.2	0.40
		Minimum	5.5	17	0.03	0.0	1.0	10.0	22.2	0.0	170.8	2.7	7.0	1.6	0.02
		Maximum	7.5	106	3.1	369.6	112.8	330.0	138.2	577.7	637.4	674.2	300.0	19.5	2.10
		Sd (±)			0.8	130.9	199.6	245.6	34.2	165.5	144.5	104.5	107.5	5.7	0.03

Continued Table 5

Site No.	Sampling site	Statistical parameter	pH	Cond. (μS cm^{-1})	Ions (μeq ℓ^{-1})										
					H^+	Na^+	K^+	Ca^{2+}	Mg^{2+}	NH_4^+	SO_4^{2-}	NO_3^-	Cl^-	F^-	I^-
9.	Pithora	V. M. Mean	6.6	90	1.2	46.2	7.0	114.2	63.6	8.6	163.0	19.6	52.0	3.2	0.02
		A. Mean	-	-	2.5	52.2	13.0	122.2	68.7	12.1	175.2	26.8	61.0	7.1	0.08
		Median	6.8	58	0.2	30.9	12.8	110.0	79.7	1.7	229.1	19.4	35.0	2.1	0.30
		Minimum	5.5	6	0.02	3.5	5.1	5.0	14.2	0.0	150.0	0.8	12.7	1.1	0.02
		Maximum	7.8	144	3.3	320.8	58.9	2063.4	773.6	27.7	1120.8	83.4	1135.2	12.6	1.30
		Sd (±)			1.0	124.2	20.5	631.3	226.8	3.8	289.6	22.5	349.2	18.8	0.03
10.	Gariyaband	V. M. Mean	5.8	66	3.5	30.6	2.3	120.6	44.9	20.6	156.5	21.9	34.2	3.9	0.02
		A. Mean	-	-	5.8	36.8	4.5	131.7	51.0	27.1	167.9	29.1	43.2	7.9	0.06
		Median	6.1	32	0.7	43.5	1.8	136.0	36.2	20.0	173.4	20.9	48.7	2.1	0.20
		Minimum	5.1	4	0.02	10.0	0.4	0.0	12.2	0.0	92.4	0.9	11.3	0.6	0.01
		Maximum	7.7	583	7.4	161.7	16.7	542.4	138.6	213.9	786.4	202.9	202.2	23.7	2.20
		Sd (±)			2.3	39.0	4.2	98.7	35.1	57.8	126.8	42.9	49.1	4.6	0.02
11.	Dallirajhara	V. M. Mean	5.6	161	5.0	50.4	6.8	132.4	33.0	2.9	146.0	20.2	60.9	3.1	0.03
		A. Mean	-	-	7.5	59.5	12.9	143.6	39.0	6.1	162.0	30.3	68.0	7.8	0.06
		Median	5.9	72	1.1	18.3	7.7	254.4	76.6	0.0	300.0	14.0	547.0	2.6	0.30
		Minimum	5.0	8	0.3	0.0	1.3	0.0	26.4	0.0	116.6	0.6	8.4	0.5	0.02
		Maximum	6.5	735	9.7	303.9	230.7	1175.0	888.8	66.1	787.4	529.1	2642.2	17.0	2.40
		Sd (±)			2.9	89.5	51.6	344.5	295.5	15.2	201.5	123.4	592.7	14.1	2.80
12.	Ambikapur	V. M. Mean	-	63	2.2	30.0	2.6	130.8	42.6	2.3	143.9	23.5	35.1	3.6	0.03
		A. Mean	55.8	-	5.5	38.0	6.8	135.8	50.5	5.4	156.1	34.6	43.2	7.8	0.07
		Median	0.9	44	1.0	43.9	21.8	145.0	63.8	0.0	224.9	48.0	33.9	2.1	0.40
		Minimum	5.2	12	0.2	3.5	4.1	15.0	27.2	0.0	62.4	2.7	5.6	1.1	0.06
		Maximum	6.5	166	5.6	200.0	195.4	1125.0	157.8	27.8	454.2	109.2	126.8	12.1	2.30
		Sd (±)			2.3	57.9	52.2	211.1	36.3	7.9	163.8	35.0	35.1	3.5	0.02

V. M. Mean = Volume Weighed Mean; A. Mean = Arithmetic Mean the sea water and in soil dust, while other pairs, e.g., H^+ and SO_4^{2-}/F^-, F^- and SO_4^{2-}, Ca^{2+} and F^-/SO_4^{2-} have good correlationship probably due to their similar way of emission from burning of coal, smelting of pyrite minerals and dolomite, etc. The relatively high correlation of Mg^{2+} and NO_3^-, Ca^{2+} and SO_4^{2-}, Ca^{2+} and F^-, H^+ and Ca^{2+}, NH_4^+ and NO_3^- are probably due to either their occurrence in the rain water or reaction of acids with the alkaline metals and NH_3. The relatively high correlation of Ca^{2+} and F^- and F^- and I^- show that they apparently steam from a common source, i.e., burning of coal, smelting of pyrite minerals and dolomite, etc.

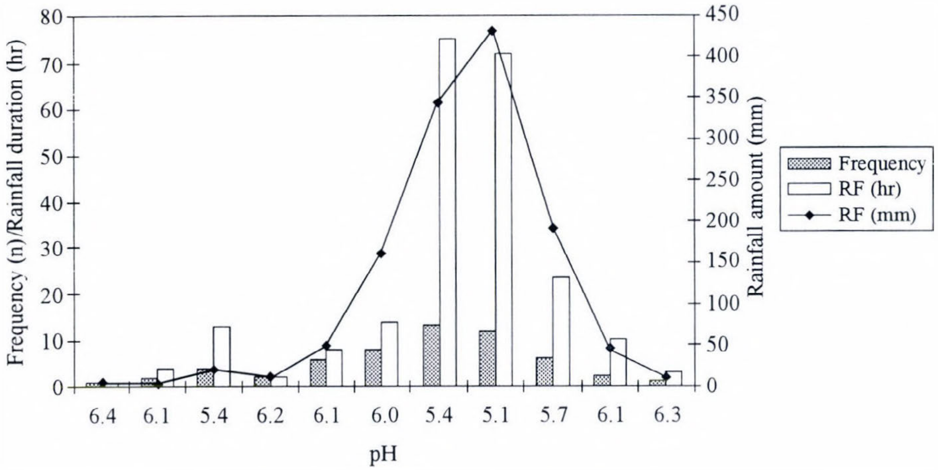

Fig. 2. The effect of frequency (n), rainfall duration (hr) and rainfall amount (mm) on monthly pH of rain water at site Raipur city in hydrological year 1995.

3.7 General relationship

The statistical analytical data base of 11 ions in the total of 373 rain water samples, collected during hydrological year 1995, has been established. Arithmetic and volume weighed means, range and median values have been calculated for each species of each site and for entire data set of 12 sites during hydrological year 1995 as shown in Tables 3 and 5. The average relieve magnitude of ionic species concentrations shows the following decreasing order: $SO_4^{2-} > Ca^{2+} > Cl^- > Mg^{2+} > Na^+ > NO_3^- > NH_4^+ > K^+ > F^- > H^+ > I^-$. This relative abundance relationship holds for both arithmetic and volume weighed mean concentration.

Fig. 3 shows a typical plot of SO_4^{2-} concentration versus amount of precipitation. It is observed that the highest SO_4^{2-} concentration generally occurred in samples of the smallest amount of precipitation, whereas lower concentration occurred with higher amount of precipitation. Generally, similar trends have been observed for other ions, Na^+, K^+, Ca^{2+}, Mg^{2+}, NO_3^-, Cl^-, F^-, I^-. However, a reverse trend has been noticed for concentration of H^+ and NH_4^+.

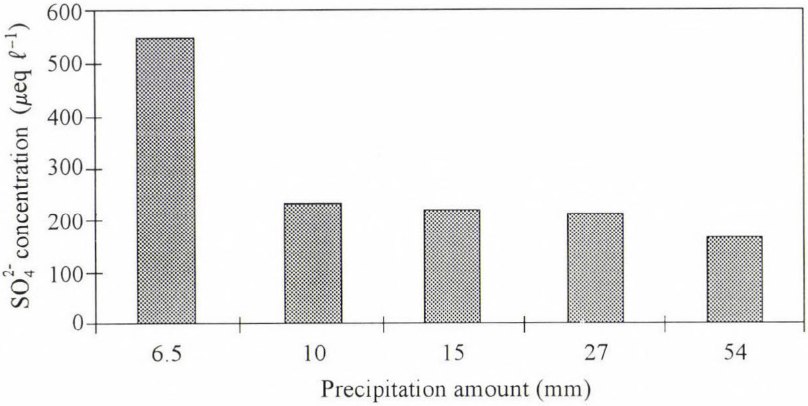

Fig. 3. Variation of SO_4^{2-} concentration with respect to the amount of precipitation in July 1995 at site Raipur.

3.8 Seasonal, temporal and spatial variations

Monthly and annual volume weighed mean concentration of H^+, Na^+, K^+, Ca^{2+}, Mg^{2+}, NO_3^-, Cl^-, F^-, I^- and values of pH and conductivity were calculated over the entire operating interval of 1995–1997, see *Figs. 4* and *5*. The concentration of Na^+, K^+, Ca^{2+}, Mg^{2+}, SO_4^{2-}, NO_3^-, Cl^- and F^- was in top during the period from March to June probably due to dusty air. In the rainy season, from July to October, the concentration of seven ions, Na^+, K^+, Ca^{2+}, Mg^{2+}, NO_3^-, Cl^- and F^- in rain water was decreased due to higher amount of precipitation or blown of lower amount of dust or both. However, the concentration of H^+, NH_4^+, I^- and SO_4^{2-} have different trends. The concentration of free acid, H^+ was the highest during August probably due to blown of lower amount of alkaline soil dust. Similarly, the concentration of NH_4^+ was the highest in the rainy season from July to August probably due to more rapid biodegradation of the forest biomass and municipal waste, wide cropping of rice plants, etc. The concentration of SO_4^{2-} was the highest from April to August probably due to high amounts of dust in the dry season (April to June) and formation of more sulphuric acid in the rainy season (July to

August). I^- ion has no exact variation trend. The annual variation in concentration of H^+, Na^+, K^+, Ca^{2+}, Mg^{2+}, SO_4^{2-}, NO_3^-, Cl^-, F^-, I^- in rain water samples of the period 1995–1997 was found to be increasing probably due to increased emission rates of the ions and other factors, see Fig. 5.

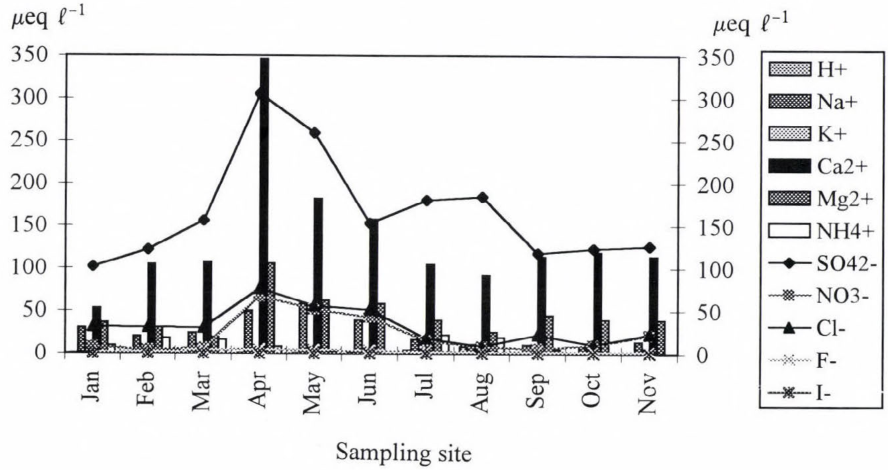

Fig. 4. Seasonal variation of concentration of major ions at Raipur during hydrological year 1995.

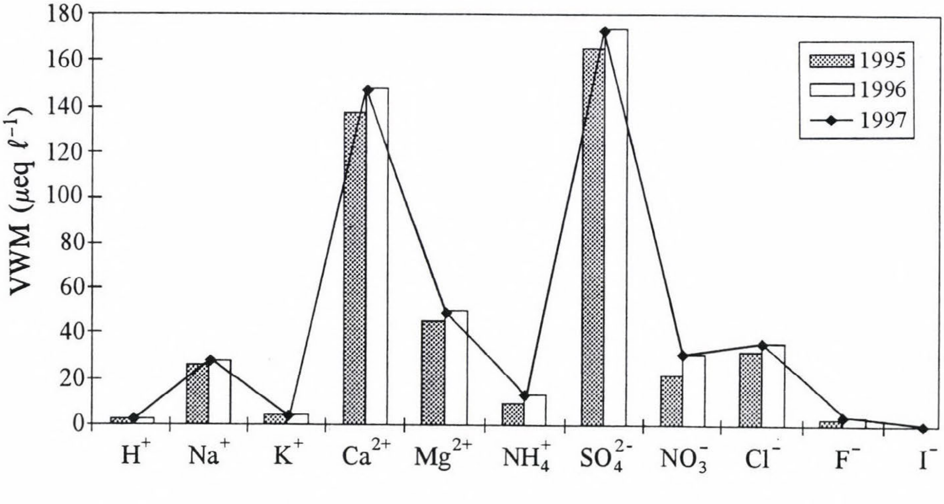

Fig. 5. Temporal variation of volume weighed mean (VWM) concentration at Raipur during hydrological year 1995–1997.

Spatial variations of the volume weighed annual mean concentrations of H^+, Na^+, K^+, Ca^{2+}, Mg^{2+}, SO_4^{2-}, NO_3^-, Cl^-, F^- and I^- in rain water of central India were examined in detail. Among them, the concentration of H^+, NH_4^+, F^- shows high spatial variations. The rain water acidity (concentration of free H^+) was the highest at site Korba, whereas the lowest at site Kanker. The concentration of SO_4^{2-} was also the highest at Korba but almost the same in the other eleven sites. Ammonium concentration was the higher in coal and pyrite mineral sites, Korba, Chirmiri, Gariyaband. The concentration of free H^+, NH_4^+ and SO_4^{2-} have positive correlation. NO_3^- and Mg^{2+} ions had the highest concentration at rice growing site Janjgir and almost the same in the other sites. The concentration of Cl^- was higher in sub-urban, rice growing and forest areas than in urban and industrial areas, i.e., Raipur, Korba. Fluoride was the highest in sites Korba, Janjgir and Kanker due to operation of an aluminum plant (capacity about 0.2 million tons yr^{-1}) or cement plant (capacity about 0.4 million tons yr^{-1}) and contamination of soil with fluorite minerals, respectively. Iodide was present at higher levels in the remote and forest sites probably due to atmospheric temperature and more evaporation from the forest sites. The concentration variation of alkali and alkaline metals was higher in sub-urban and urban sites.

3.9 Annual deposition

The overall mean fluxes of H^+, I^-, F^-, NH_4^+, K^+, Mg^{2+}, Na^+, NO_3^-, Cl^-, Ca^{2+} and SO_4^{2-} were 5, 5, 146, 221, 267, 657, 1203, 1830, 2550, 3399 and 9781 kg km^{-2} yr^{-1} in 1995 with median and standard deviation of 2.7, 4.0, 111, 219, 290, 603, 1266, 1680, 2437, 3357, 9805 and ± 5.7, 1.4, 110, 156, 99, 232, 381, 1005, 1167, 566, 1232, respectively. H^+, I^-, F^-, NH_4^+, K^+, Mg^{2+}, Na^+, NO_3^-, Cl^-, Ca^{2+} and SO_4^{2-} ions were precipitated with weighted ratio of 1, 1, 29, 44, 131, 240, 366, 510, 680 and 1956, respectively. Very high amounts (>99%) of acids like HF, HCl, HNO_3, H_2SO_4 are neutralized by alkaline particulates. Their standard deviation ranges from ± 1.4 to 1232 showing high variation in the nature, the strength of emission sources as well as the loading of distant pollutants. We analysed the spatial variations in the flux of ions at 12 sites of central India. The flux of free acid (H^+) was the highest in the sites where large amount of coal is burnt (Korba), several coal mines are in operation (Korba, Chirmiri, Raigarh) or pyrite minerals are deposited or processed (Gariyaband, Dallirajhara). The flux of SO_4^{2-} was the highest in site Korba where large amount of coal is burnt. Deposition trend of SO_4^{2-} in central India in decreasing order is Korba > Janjgir > Kanker > Gariyaband > Raipur > Bhatapara > Chirmiri > Pithora > Dallirajhara > Ambikapur > Raigarh > Bilaspur. The fluxes of NO_3^- and Cl^- were in top in rice cropping site Janjgir with different deposition patterns. The fluoride flux was the highest in sites where either aluminum industry (Korba) or soil is loaded with fluorite mineral (Kanker). The iodide flux was the highest in the forest areas (Kanker, Raigarh, Dallirajhara, Ambikapur) probably due to lower atmospheric temperature, higher emission rate from the forest vegetation, higher rainfall, etc. Similarly, the ammonia has some sort of similarity with I^- in deposition pattern and found to be the highest in the forest areas Gariyaband and Chirmiri. The deposition patterns of alkali and alkaline elements have some similarity, and the alkali metal fluxes were in top in sites Bhatapara and Kanker, however, the alkaline metal fluxes were in top in sites Korba, Kanker and Bhatapara.

Deposition trends, rainfall amount, pH, conductivity and ionic concentration H^+, Na^+, K^+, Ca^{2+}, Mg^{2+}, NH_4^+, SO_4^{2-}, NO_3^-, Cl^-, F^-, I^- at site Raipur during hydrological years from 1995 to 1997 were determined and shown in *Table 6*. The precipitation amount decreased in the hydrological period 1995–1997, whereas their pH values were almost the same. The value of conductivity and ionic concentrations of H^+, Na^+, K^+, Ca^{2+}, Mg^{2+}, NH_4^+, SO_4^{2-}, NO_3^-, Cl^-, F^- and I^- showed increasing trends but fluxes of some ions were the lowest in 1996.

3.10 Sources

Gases like NO_x, SO_x, hydrocarbon, etc. are emitted into the atmosphere by both natural and anthropogenic sources, rice paddy, biodegradation of forest vegetation and municipal waste, burning of coal and forest biomass, combustion of gasoline, smelting of pyrite minerals and dolomite, etc. The production and consumption of fossil fuels like coal, pyrites (Cu, Fe, Mn), aluminum and dolomite in this region are 31.0 and 8.0, 13.0 and 10.0, 0.2 and 0.16, 0.75 and 0.60 million tons yr^{-1}, respectively. In summer the Arabian SW monsoon causes heavy rainfall in central India. The air masses while crossing the Arabian sea proportionally enriched with sea salt particles which are incorporated with cloud droplets. The monsoon generally breaks into central India on the 2nd or 3rd week of June. During this long travel (about 1500 km), the cloud profiles are contaminated with soil dusts, acids, gases, metals, non-metals, etc. The monsoon loaded with both local and distant pollutants breaks in the central India. The main ions associated with sea salt are Na^+ with Cl^- with smaller amounts of Mg^{2+}, Ca^{2+}, K^+ and SO_4^{2-}. The ratio is modified when the air masses move inland due to presence of calcite, clay minerals, soil components and ions emitted from anthropogenic sources in the air. Various authors used Na^+ as tracer and claimed the ionic ratio of Cl^-, SO_4^{2-}, Mg^{2+}, Ca^{2+}, K^+, Cl^- and NO_3^- to Na^+ in sea water to be 1.17, 0.12, 0.22, 0.044, 0.021, 0.0008, and 0.0006, respectively (*Mamane*, 1987). Thus, sea salts account the most of Cl^-, partially K^+ and Mg^{2+}, very less amount of SO_4^{2-} and Ca^{2+} and negligible amount of other ions (F^- and NO_3^-). The ionic ratio of Cl^-, SO_4^{2-}, Mg^{2+}, Ca^{2+}, K^+, F^- and NO_3^- to Na^+ in the rain water of central India were found to be 1.2, 4.4, 1.2, 3.7, 0.14, 0.11 and 0.56, respectively. The contribution of the natural and anthropogenic sources in the rain water of central India accounts to be 2.5, 97.3, 81.7, 98.8, 85.0, 99.3 and 99.9% for the ions Cl^-, SO_4^{2-}, Mg^{2+}, Ca^{2+}, K^+, F^- and NO_3^-, respectively.

Table 6. Trend of rainfall height, pH, conductivity and major ion concentrations at site Raipur during hydrological years from 1995 to 1997

Station No.	Parameters	Volume weighted mean concentration (μeq ℓ^{-1})			Flux (kg km^{-2} yr^{-1})		
		1995	1996	1997	1995	1996	1997
1.	Rainfall (mm)	1283	1123	1214	1283	1123	1214
2.	pH	5.8	5.9	5.8	5.8	5.9	5.8
3.	Cond. (μS cm^{-1})	65	70	72	65	70	72
4.	H^+ (μeq ℓ^{-1})	2.0	1.2	2.0	2.6	1.3	2.4
5.	Na^+ (μeq ℓ^{-1})	25.6	24.4	28.2	770	630	787
6.	K^+ (μeq ℓ^{-1})	4.4	3.8	4.2	218	166	199
7.	Ca^+ (μeq ℓ^{-1})	138	145	148	3464	3733	3589
8.	Mg^+ (μeq ℓ^{-1})	45.5	47.2	49.5	706	699	733
9.	NH_4^+ (μeq ℓ^{-1})	9.5	12.3	13.9	218	249	303
10.	SO_4^{2-} (μeq ℓ^{-1})	166	171	174	10211	9207	10163
11.	NO_3^- (μeq ℓ^{-1})	21.7	25.6	31.5	1719	1782	2371
12.	CL^- (μeq ℓ^{-1})	32.7	34.6	35.8	1488	1379	1543
13.	F^- (μeq ℓ^{-1})	2.7	3.4	3.9	110	121	150
14.	I^- (μeq ℓ^{-1})	0.02	0.03	0.03	3.8	4.3	4.6

4. Conclusion

(1) Acid rain occurs in central India specially in the monsoon period. Mean pH of storms in 1995 at the twelve sampling sites varied from 4.9 at Korba to 6.7 at Bhatapara, and the lowest pH of any storm was 4.1 at Korba. Thus, rain water was about 10–100 times more acidic than unpolluted rain which has a theoretical pH of 5.8 at the tropics.

(2) On chemical-equivalent basis, more sulphate is present in the precipitation than nitrate. Sulphate is the anion most closely correlated with H^+ at eight of the twelve sampling sites, thus air pollution by SO_2 forming sulphuric acid (H_2SO_4) is presumed to be the primary cause of the acidity of rain; NO, forming nitric acid (HNO_3) appears to be the secondary cause at the present time.

(3) Total deposition of ionic constituents of rain precipitation is a function of both ionic concentration and total volume of rain. Total weighted deposition of both sulphate and H^+ ions were the highest at sites Korba and Gariyaband. These sites are about 150 km apart from Raipur in opposite directions. It is concluded that acid rain is widely distributed from pollution source areas to sub-urban, receptor areas. The ecological effect may be expected in the urban and sub-urban area where soil has poor buffering capacity.

Acknowledgements—We are thankful to the national and international finding agencies DST, New Delhi, Alexander von Humboldt Foundation, Bonn, Germany and TWAS, Trieste, Italy for the financial support provided for this study.

References

Atteia, O., 1994: Major and trace elements in precipitation on western Switzerland. *Atmos. Environ.*, *28*, 3617-3624.

Blanchard, C.L. and *Stromberg, M.R.*, 1987: Acidic precipitation in south eastern Arizona. SO_4^{2-}, NO_3^- and trace metal deposition. *Atmos. Environ. 21*, 2375-2381.

Bowersox Van, C., *Douglas, L.*, *Sisterson* and *Anthony, R.O.*, 1990: Acid rain, a world -wide phenomenon : A perspective from the United States. *Intern. J. Environ. Studies 36*, 83-101.

Cerceo, E., 1983: Acid rain and climate warming in southern New Jersay. Global implication. *Atmos. Environ.*, 26-29.

Chandrawanshi, C.K. and *Patel, K.S.*, 1998: Fluoride deposition in central India. *Environ. Monitoring and Assess. 1-15*, in press.

Chandrawanshi, C.K., *Chandrawanshi, S.K.* and *Patel, K.S.*, 1996: Flow analysis determination of iodide at nanogram levels in water. *J. Auto. Chem. 18*, 181-186.

Charlson, R.J. and *Rodhe, H.*, 1982: Factor controlling the acidity of natural rain water. *Nature 295*, 683-685.

Cheng, R.J., *Hwu, J.R.*, *Kim, J.T.* and *Leu, S.M.*, 1987: Deterioration of marble structures. The role of acid rain. *Anal. Chem. 59*, 104A-106A.

Clariac, B., *Delmas, R. Cros, B.*, *Cachier, H.* and *Buat-Menard, P.*, 1988: Formation and chemical composition of aerosols in an equatorial forest area. *J. Atmos. Chem. 6*, 301-322.

Cowling, E.B., 1989: Recent changes in chemical climate and related effects on forests in North America and Europe. *Ambio 18,* 171-176.

Das, D.K., Dev Burman, G.K. and *Kidwai, A.L.*, 1981: Chemical composition of monsoon rain water over Bhopa, Madhya Pradesh (India): *Mausam 32*, 221-228.

Environment Agency, 1996: *Acid Rain Deposition Monitoring Network in East Asia Tokyo, Japan.* 1-62.

Falkengren-Grerup, U., 1989: Soil acidification and its impacts on ground vegetation. *Ambio 18,* 179-183.

Galloway, J.N., 1989: Atmospheric acidification: Projections for the future. *Ambio 18*, 161-166.

Goreham, E., 1989: Scientific understanding of ecosystem acidification: a historical review. *Ambio 18*, 150-154.

Hansen, D.A. and *Hidy, G.M.*, 1982: Review of questions regarding rain acidity data. *Atmos. Environ. 16*, 2107-2126.

Hordijik, L., 1993: Halting acidification in Asia. *Acid rain 3*, 20.

Irwin, J.G. and *Williams, M.L.*, 1988: Acid rain: chemistry and transport. *Environ. Pollut. 50*, 29-59.

Kallend, A.S., Marsh, A.R.W., Packles, J.H. and *Proctor, M.V.*, 1983: Acidity of rain in Europe. *Atmos. Environ. 17*, 127-137.

Kasina, S., 1980: On precipitation acidity in southeastern Poland. *Atmos. Environ. 14*, 1217-1221.

Khemani, L.T., Momin, G.A., Medha, S. Naik, Prakasa Rao, P.S., Safai, P.D. and *Murty, A.S.R.*, 1987: Influence of alkaline particulates on pH of cloud and rain water in India. *Atmos. Environ. 21*, 1137-1145.

Khemani, L.T., Momin, G.A., Prakasa Rao, P.S., Safai, P.D., Singh, G. and *Kapoor, R.K.*, 1989: Spread of acid rain over India. *Atmos. Environ. 23*, 757-762.

Khemani, L.T., Monin, G.A., Rao, P.S.P., Pillai, A.G., Safai, P.D., Mohan, K. and *Rao, M.G.*, 1994: Atmospheric pollutants and their influence on acidification of rain water at an industrial location on the west coast of India. *Atmospheric Environment 19,* 3145-3154.

Lacaux, J.P., Servant, J. and *Baudet, J.G.R.*, 1987: Acid rain in the tropical forests of the Ivory Coast. *Atmos. Environ. 21*, 2643-2647.

Likens, G.E., 1989: Some aspects of air pollutant effects on terrestrial ecosystems and prospects for the future. *Ambio 18*, 172-178.

Longhurst, J.W.S., Roper, D.W., Lee, D.S., Health, B.A., Conlan, B. and *King, H.J.*, 1993: Acid deposition. A selected review 1852-1990. Effect on materials and health: abatement strategies and programmes. *Atmos. Environ. 73*, 1363-1380.

Lynch, J.A., Grimm, J.W. and *Bowersox, V.C.*, 1995: Trends in precipitation chemistry in the United States : A national perspective, 1980-1992. *Atmos. Environ. 29*, 1231-1246.

Mamane, Y., 1987: Chemistry of precipitation in Israel. *Sci. Total Environ. 61*, 1-13.

Moldan, B., 1988: Chemical composition of atmospheric precipitation in Czechoslovakia, 1978-1984-II event samples. *Atmos. Environ. 22*, 1901-1908.

Mohnen, V.A., 1988: The challenge of acid rain. *Scientific American 259*, 30-38.

Mukherjee, A.K., 1978: pH of monsoon rain water over the Bay of Bangal. *Ind. J. Met. Geophys. 29*, 749.

Nollor, B.N. and *Chadha, M.S.*, 1990: *Chemistry and the Environment*. Comm. Sci. Council, London.

O'Sullivan, D.A., 1985: European concern about acid rain is growing. *Chem. Eng. News 63*, 12-18.

Porteous, A. and *Barrett, R.S.*, 1989: A short term survey of daily rainfall acidity in the U.K. *Atmos. Environ. 23*, 509-512.

Pitelka, L.F. and *Raynal, D.J.*, 1989: Forest decline and acidic deposition. *Ecology 70*, 2-10.

Ravichandran, C. and *Padmanabhamurty, B.*, 1994: Acid precipitation in Delhi, India. *Atmos. Environ. 28*, 2291-2297.

Sanusi, A., Wortham, H., Millet, M. and *Mirabel, P.*, 1996: Chemical composition of rainwater in eastern France. *Atmos. Environ. 30*, 59-71.

Saylor, R.D., *Butt, K.M.* and *Peters, L.K.*, 1992: Chemical characterization of precipitation from a monitoring network in the lower Ohio river valley. *Atmos. Environ. 26A*, 1147-1156.

Schwartz, S.E., 1989: Acid deposition: Unraveling a regional phenomenon. *Science 243*, 753-763.

Singh, V.P., 1982: Management of acid sulphate soil for brackish water fishponds : Experience in the Philippines. In *Proc. 2nd Int. Symp. on Acid Sulphate Soils*. International Institute for Land Reclamation. The Netherlands.

Skoulikidis, T.N., 1983: Effect of primary and secondary air pollutants and acid depositions on (ancient and modern) buildings and monuments. In *Proc. of the EEC Symposium: "Acid Deposition a Challenge for Europe"*. 193-226. Karlsruhe, F.R.G.

Suman, D.O., 1988: The flux of charcoal to the troposphere during the period of agricultural burning in Panama. *J. Atmos. Chem. 6*, 21-34.

Talbot, R.W., *Andreae, M.O.*, *Andreae, T.W.* and *Harriss, R.C.*, 1988: Regional aerosol chemistry of the Amazon basin during the dry season. *J. Geophys. Res. 93*, 1499-1508.

Tecator, 1991: Application short note, ASN 135-01/91, Hoganas, Sweden.

Tecator, 1992a: Application short note, ASN 151-01/92, Hoganas, Sweden.

Tecator, 1992b: Application short note, ASN 110-02/92, Hoganas, Sweden.

Tuovinen, J.P., *Laurila, T.* and *Lattila, H.*, 1993: Impact of the sulphur dioxide sources in the Kola Peninsula on air quality in Northern most Europe. *Atmos. Environ. 27A*, 1379-1395.

Udisti, R., *Bellandi, S.*, *Barbolani, E.* and *Pantani, F.*, 1991: Acid deposition in the Tuscan appennines during the dry period. *Chemistry and Ecology 5*, 129-137.

Verma, G.S., 1989: Background trends of pH of precipitation over India. *Atmos. Enviro. 23*, 747-751.

Vogel, A.I., 1978: *Textbook of Quantitative Inorganic Analysis*. Fourth Edition, Longman Group Ltd, England.

Vocom, J.E., 1979: Air pollution damage to buildings on the Acropolis. *J. Air Pollut. Control Ass. 29*, 333-338.

WMO GAW No. 85, *Chemical Analysis of Precipitation for GAW: Laboratory Analytical Methods and Sample Collection Standards.*

Zhao, D., *Xiong, J.*, *Xu, Y.* and *Chan, W.H.*, 1988: Acid rain in South Western China. *Atmos. Environ. 22*, 349-358.

ATMOSPHERIC ENVIRONMENT

an international journal

To promote the distribution of Atmospheric Environment *Időjárás* publishes regularly the contents of this important journal. For further information the interested reader is asked to contact *Prof. P. Brimblecombe*, School for Environmental Sciences, University of East Anglia, Norwich NR4 7TJ, U.K.; e-mail: atmos_env@uea.ac.uk

Volume 33 Number 10 1999

Volume 33 Number 11 1999

Volume 33 Number 12 1999

A. Bott: A numerical model of the cloud-topped planetary boundary-layer: chemistry in marine stratus and the effects on aerosol particles, 1921-1936.

D.J. Carruthers, A.M. Mckeown, D.J. Hall and *S. Porter*: Validation of ADMS against wind tunnel data of dispersion from chemical warchouse fires, 1937-1953.

M.C. Green: The project MOHAVE tracer study: study design, data quality, and overview of results, 1955-1968.

T. Zhu, D. Wang, R.L. Desjardins and *J.I. Macpherson*: Aircraft-based volatilc organic compounds flux measurements with relaxed cddy accumulation, 1969-1979.

Volume 33 Number 13 1999

L. Morawska, G. Johnson, Z.D. Ristovski and *V. Agranovski*: Relation between particle mass and number for submicrometer airborne particles, 1983-1990.

T.M. Araújo, J.A. Carvalho Jr., N. Higuchi, A.C.P. Brasil Jr. and *A.L.A. Mesquita*: A tropical rainforest cleaning experiment by biomass burning in the state of para, Brasil, 1991-1998.

S. Uchiyama and *S. Hasewaga*: A reactive and sensitive diffusion sampler for the determination of aldehydes and keton in ambient air, 1999-2005.

P. de Haan: On the use of density kernels for concentration estimations within particle and puff dispersion models, 2007-2021.

R.W. Dixon and *H. Aasen*: Measurement of hydroxymethanesulfonate in atmospheric aerosols, 2023-2029.

S. Heinz and *H. van Dop*: Buozant plume rise described by Lagrangian turbulent model, 2031-2043.

S.C. Pryor, R.J. Barthelmie, L.L.S. Geernaert, T. Ellermann and *K.D. Perry*: Speciated particle dry deposition to the sea surface, results from ASEPS '97, 2045-2058.

H. Hauck, H. Kromp-Kolb and *E. Petz*: Requirements for the completeness of ambient air quality data sets with respect to derived parameters, 2059-2066.

C.-J. Lin and *S.O. Pehkonen*: The chemisty of atmospheric mercury: a review, 2067-2079.

W.F.J. Evans and *E. Pucckrin*: Combined measuruments of thermal emission and solar absorption of atmospheric carbon monoxide, 2081-2088.

V.-M. Kerminen, K. Teinilä, R. Hillamo and *T. Mäkelä*: Size-segregated chemistry of particulate dicarboxylic acids in the Arctic atmosphere, 2089-2100.

N.A. Kelly and *T.Y. Chang*: An experimental investigation of incremental reactivities of volatile organic compounds, 2101-2110.

Technical Note

L.F. Salter and *B. Parsons*: Field trials of the TEOM® and Partisol for PM_{10} monitoring in the St Austell china clay area, Cornwall, UK, 2111-2114.

Volume 33 Number 14 1999

M. Kulmala, A. Asmi and *L. Pirjola*: Indoor air aerosol model: the effect of outdoor air, filtration and ventilation on indoor concentrations, 2133-2144.

M. Kulmala, J. Hienola, L. Pirjola, T. Vesala, M. Shimmo, N. Altimir and *P. Hari*: A model for NO_x-O_3-terpene chemistry in chamber measurements of plant gas exchange, 2145-2156.

W.J. Riley, A.L. Robonson, A.J. Gadgil and *W.W. Nazaroff*: Effects of variable wind speed and direction on radon transport from soil into buildings: model development and exploratory results, 2157-2168.

S. Huang, K.A. Rahn and *R. Arimoto*: Testing and optimizing two factor-analysis techniques on aerosol at Narragansett, Rhode Island, 2169-2185.

J.E. Sickles, II, L.L. Hodson and *L.M. Vorburger*: Evaluation of the filter pack for long-duration sampling of ambient air 2187-2202.

C.H. Song and *G.R. Carmichael*: The aging process of naturally emitted aerosol (sea-salt and mineral aerosol) during long range transport, 2203-2218.

M. Piringer and *G. Schauberger*: Comparison of a Gaussian diffusion model with guidelines for calculating the separation distance between livestock farming and residential areas to avoid odour annoyance, 2219-2228.

Y.L. Xie, P.K. Hopke, P. Paatero, L.A. Barrie and *S.-M. Li*: Locations and preferred pathways of possible sources of Arctic aerosol, 2229-2239.

D.S. Lee, R.D. Kingdon, J.M. Pacyna, A.F. Bouwman and *I. Tegen*: Modelling base cations in Europe–sources, transport and deposition of calcium, 2241-2256.

J.E. Pleim, P.L. Finkelstein, J.F. Clarke and *T.G. Ellenstad*: A technique for estimating dry deposition velocitics based on similarity with latent heat flux, 2257-2268.

P. Chýlek, L. Kou, B. Johnson, F. Boudala and *G. Lesins*: Black carbon concentrations in precipitation and near surface air in and near Halifax, Nova Scotia, 2269-2277.

M.J. Navas, A.M. Jiménez and *G. Galán*: Air analysis: determination of hydrogen peroxide by chemiluminescence 2279-2283.

Volume 33 Number 15 1999

C.J. Weschler and *H.C. Shields*: Indoor ozone/terpene reactions as a source ofindoor particles, 2301-2312.

M. Chang, S. Kim and *C. Sioutas*: Experimental studies on particle impaction and bounce: effects of substrate design and material, 2313-2322.

H.Y. Tong, W.T. Hung and *C.S. Cheung*: Development of a driving cycle for Hong Kong, 2323-2335.

P. Franzese, A.K. Luhar and *M.S. Borgas*: An efficient Lagrangian stochastic model of vertical dispersion in the convective boundary layer, 2337-2345.

M. Kessler: Development and analysis of an adaptive transport scheme, 2347-2360.

R.L.R. Salcedo, M.C.M. Alvim Ferraz, C.A. Alvez and *F.G. Martins*: Time-series analysis of air pollution data, 2361-2372.

M.R. Bassford, G. Nickless, P.G. Simmonds, A.C. Lewis, M.J. Pilling and *M.J. Evans*: The concurrent observation of methyl iodide and dimcthyl sulphide in marine air; implications for sources of atmospheric methyl iodide, 2373-2383.

F. Lena and *F. Desiato*: Intercomparison of nocturnal mixing height estimate methods for urban air pollution modelling, 2385-2393.

R. Meininghaus, T. Salthammer and *H. Knöppel*: Interaction of volatile organic compounds with indoor materials–a small-scale screeningmethod, 2395-2401.

H. Liu, W.L. Chang, S.J. Oltmans, L.Y. Chan and *J.M. Harris*: On springtime high ozone events in the lower troposphere from Southeast Asian biomass burning, 2403-2410.

Published by the Hungarian Meteorological Service

Budapest, Hungary

INDEX: 26 361

HU ISSN 0324-6329

NOTES TO CONTRIBUTORS OF *IDŐJÁRÁS*

The purpose of the journal is to publish papers in any field of meteorology and atmosphere related scientific areas. These may be

- reports on new results of scientific investigations,
- critical review articles summarizing current state of art of a certain topic,
- shorter contributions dealing with a particular question.

Each issue contains "News" and "Book review" sections.

Authors may be of any nationality, but the official language of the journal is English. Papers will be reviewed by unidentified referees.

Manuscripts should be sent to

Editor-in-Chief of IDŐJÁRÁS
P.O. Box 39
H-1675 Budapest, Hungary

in three copies including all illustrations. One set of illustrations has to be of camera ready quality, the other two might be lower quality.

Title part of the paper should contain the concise title, the name(s) of the author(s), the affiliation(s) including postal and E-mail address(es). In case of multiple authors, the cover letter should indicate the corresponding author.

Abstract should follow the title, it contains the purpose, the data and methods as well as the basic conclusion.

Key-words are necessary to help to classify the topic.

The text has to be typed in double spacing with wide margins. Word-processor printing is preferred. The use of SI units are expected. The negative exponent is preferred to solidus. Figures and tables should be consecutively numbered and referred to in the text.

Mathematical formulas are expected to be as simple as possible and numbered in parentheses at the right margin. Non-Latin letters and hand-written symbols should be indicated and explained by making marginal notes in pencil.

Tables should be marked by Arabic numbers and printed in separate sheets together with their captions. Avoid too lengthy or complicated tables.

Figures should be drawn or printed in black and white, without legends, on separate sheets. The legends of figures should be printed as separate list. Good quality laser printings are preferred as master copies.

References: The text citation should contain the name(s) of the author(s) in Italic letter and the year of publication. In case of one author: *Miller* (1989), or if the name of the author cannot be fitted into the text: *(Miller,* 1989); in the case of two authors: *Gamov* and *Cleveland* (1973); if there are more than two authors: *Smith et al.* (1990). When referring to several papers published in the same year by the same author, the year of publication should be followed by letters a,b etc. At the end of the paper the list of references should be arranged alphabetically. For an article: the name(s) of author(s) in Italics, year, title of article, name of journal, volume number (the latter two in Italics) and pages. E.g. *Nathan, K.K.,* 1986: A note on the relationship between photosynthetically active radiation and cloud amount. *Időjárás 90*, 10-13. For a book: the name(s) of author(s), year, title of the book (all in Italics except the year), publisher and place of publication. E.g. *Junge, C. E.,* 1963: *Air Chemistry and Radioactivity.* Academic Press, New York and London.

The final version should be submitted on diskette altogether with one hard copy. Use standard 3.5" or 5.25" DOS formatted diskettes. The preferred word-processors are WordPerfect 5.1 and MS Word 6.0.

Reprints: authors receive 30 reprints free of charge. Additional reprints may be ordered at the authors' expense when sending back the proofs to the Editorial Office.

More information: gmajor@met.hu
Information on the last issues:
http://www.met.hu/firat/ido-e.html

IDŐJÁRÁS

QUARTERLY JOURNAL
OF THE HUNGARIAN METEOROLOGICAL SERVICE

CONTENTS

****

http://www.met.hu/firat/ido-e.html

VOL. 103 * NO. 4 * OCTOBER–DECEMBER 1999

IDŐJÁRÁS

Quarterly Journal of the Hungarian Meteorological Service

Editor-in-Chief
T. PRÁGER

Executive Editor
M. ANTAL

Editorial Office: P.O. Box 39, H-1675 Budapest, Hungary or
Gilice tér 39, H-1181 Budapest, Hungary
E-mail: prager@met.hu or *antal@met.hu*
Fax: (36-1) 290-7387

Subscription by

mail: IDŐJÁRÁS, P.O. Box 39, H-1675 Budapest, Hungary;
E-mail: prager@met.hu or *antal@met.hu*; *Fax: (36-1) 290-7387*

IDŐJÁRÁS

Quarterly Journal of the Hungarian Meteorological Service
Vol. 103, No. 4, October–December 1999, pp. 219–235

Arctic climate empirical diagnostics: a contribution to the climate change debate

V. N. Adamenko[1], **K. Ya. Kondratyev**[2] and **C. A. Varotsos**[3]

[1]*Polar Marine Academy, Butlerova Str., 8-227, St. Petersburg 195220, Russia*
[2]*Research Centre for Ecological Safety, Russian Academy of Sciences, Korpusnaya Str., 18, St. Petersburg 197110, Russia; e-mail: nansen@online.ru*
[3]*University of Athens, Panepistimioupolis, Build. PHYS-V, Athens, Greece, e-mail: kvarots@atlas.uoa.gr*

(Manuscript received 5 January 1999; in final form 17 September 1999)

Abstract—A hypothesis that global climate warming observed during the last century has been due to anthropogenically induced carbon dioxide concentration growth provoked controversial response. In this context, general considerations have been discussed supporting the viewpoint that the "greenhouse" global warming hypothesis is doubtful, although, of course, the greenhouse effect contribution should be taken into account. One of the strongest arguments in favor of the above hypothesis is a conclusion drawn from numerical climate modeling data that there must be an enhancement of the "greenhouse signal" with latitude. In this paper some results of surface air temperature (SAT) observations in the Arctic during the last 20–30 years have been discussed which demonstrate a reduction in SAT in a number of Arctic regions. Some dendroclimatic data relevant to tree growth near the northern forest boundary have also been considered. Analysis of these data (covering larger time periods) reveals that not only the conclusion about polar enhancement of climate warming is wrong but the warming itself could hardly be realistic. So it may be concluded that no noncontroversial information exists that can support the hypothesis of global "greenhouse" warming.

Key-words: global climate change, polar warming enhancement, dendrochronology data, Framework Convention on Climate Change, climate modeling, the Arctic.

1. Introduction

The problem of global climate change has attracted great attention during the recent decades (see *Adamenko,* 1985a; *Barnett,* 1999; *Bengtsson et al.,* 1999; *Brauch,* 1996; *Browning* and *Gurney,* 1999; *Emsley,* 1996; *Flower,* 1999; *Hansen et al.,* 1998; *Houghton et al.,* 1996; *Jain et al.,* 1999; *Kondratyev,* 1992, 1998, 1999; *Manabe,* 1998; *Mason,* 1995; *Mysak* and *Venegas,* 1998;

Postmentier et al., 1999; *Raschke,* 1996; *Schoenwiese,* 1996; *Scorer,* 1996; *Singer,* 1997; *Storch* and *Floeser,* 1999; *Warnecke,* 1997; *Watanabe* and *Nitta,* 1999; *Weber,* 1996; *Wigley,* 1998; *Wiin-Nielsen,* 1998; *Yao* and *Del Genio,* 1999, and others). The problem has mainly been discussed in the context of the "greenhouse stereotype", which proceeds from the assumption that global climate warming which took place in the course of the current century had been due to an enhancement of the atmospheric greenhouse effect caused by the growing concentration of carbon dioxide and other greenhouse gases (GHGs) in the atmosphere.

Even according to the assessment presented in the Report of the Intergovernmental Panel on Climate Change (IPCC), it is stated that "the balance of evidence suggests a discernible human influence on global climate" (*Houghton et al.,* 1996). The assessment of this kind of ideas, discussed in detail earlier (*Kondratyev,* 1992, 1996, 1997, 1998, 1999; *Kondratyev et al.,* 1996; *Kondratyev* and *Cracknell,* 1998, etc.), is not only of academic interest. It is in this context that the Framework Convention on Climate Change (FCCC) approved by the UN General Assembly recommends to reduce the amount of carbon dioxide emissions to the atmosphere by the year 2000 to the level of the year 1990, and this is a minimum demand. Later much stronger reductions have been recommended by the Third Conference of the Parties in Kyoto (*Schneider,* 1998) which, however, have not been quantitatively substantiated so far.

In this context, a non-biased evaluation of the justification of broadly spread estimates of anthropogenic impacts on climate acquires an exceptional importance. Evaluations, which are in discordance with the IPCC conclusions, can be found in quite a number of recent publications (see, for instance, *Ellsaesser,* 1992; *Emsley,* 1996; *Jastrow et al.,* 1990; *Kahl et al.,* 1993; *Kondratyev,* 1992, 1996, 1998; *Singer,* 1997; *Weber,* 1996, etc.). These evaluations, however, have not met adequate attention or have been ignored altogether. In the meanwhile, it is a matter of not minor remarks (concerning, for example, the IPCC reports) but of judgements of principal nature.

In this connection, *Singer* (1997) has been quite right to state that the science of climate is full of uncertainties of principal importance resulted from the fact that relevant observational data are insufficient and numerical climate models are far from being perfect. Here are some of the causes of these uncertainties.

- The problem of the global carbon cycle has not been solved so far, especially in the part relevant to the acquisition of anthropogenic carbon dioxide emissions by the ocean (the "biological pump" role) and the functioning of the land biosphere as a source or sink of carbon (the problem of the "missing" carbon sink). This creates great uncertainties in predicting the carbon dioxide concentration growth in the next century, especially if one takes into account the difficulty of prediction of time changes in using fossil fuels in the future.

- The quality of data on the surface air temperature for the recent century is not quite up to the mark.
- Discrepancies between the results of temperature change calculations made with different climate models sometimes reach 300%; many of the climate models do not take into account meso- and microscale processes in clouds or numerous processes of the interaction between the atmosphere and ocean which are of crucial importance.
- Climate models are incapable of adequately reproducing and accounting for climatic changes in the 20th century, such as a SAT rise from 1920 to 1940, a cooling before 1975 and the absence of warming in satellite data on the tropospheric climate, beginning with 1979 (*Ellsaesser,* 1992) (see also more recent publications, such as *Kondratyev,* 1998, 1999; *Postmentier et al.,* 1999).
- Climate models are incapable of explaining rapid paleovariations (on a decadal level) discovered from the data of the analysis of tree rings, ice cores, sea and lake sediments (*Fischer et al.,* 1999). Such significant events as El Niño/Southern Oscillation (ENSO), the North-Atlantic Oscillation and other rapid contemporary climatic changes have not been predicted from numerical modeling (although significant progress has been recently achieved in predictions of ENSO).
- Estimates of potential World Ocean Level (WOL) rise due to global warming have been broadly discussed but proved unreliable. One cannot exclude the possibility that enhanced evaporation from the sea surface may lead to a faster accumulation of polar glaciers, and consequently, to a drop in the ocean level. The suggestion can be supported by the presence of a negative correlation between the WOL rise and SAT in the tropics (see also recent papers published in *Annals of Glaciology*, 1998, Vol. 27).
- The repetition rate of strong storms and hurricanes has not increased during the recent 50 years, whereas under conditions of a global warming (following from the calculated decrease of the latitudinal temperature gradient) the opposite situation must prevail (see a recent paper by *Fu et al.,* 1999).
- Because the increase of carbon dioxide concentration stimulates photosynthesis, and the increase in SAT mostly observed in the nighttime and in winter leads to a longer duration of the vegetative season, this should be favorable for agriculture under conditions of a global warming and sufficient moistening. It is also important that agriculture has ample capacity for adaptation to climatic changes (*Kondratyev,* 1998).

Perhaps, the least expected and rather paradoxical aspect of contemporary research in climate and its variability is related to the conclusions of studies on the empirical diagnostics of observational data and indirect indicators of the state of the climatic system. The continuing analysis of observational data revealed new regular features of SAT variations and other climate characteristics. In particular, this is relevant to the high latitudes of the Northern Hemisphere (*"Are Human Activities...?"*, 1995; *Grotefendt et al.*, 1998; *Kahl et al.*, 1993; *Kondratyev et al.*, 1996; *Lovelius*, 1997; *Vaganov et al.*, 1996; *Report*, 1998, etc.).

2. Some results of the analysis of observational data and indirect indicators of the state of the climatic System as global climate change (CC) indicators

2.1 The "anthropogenic" CC signal

The discussion on the detection of the so-called "anthropogenic" signal is being continued (*Kondratyev*, 1998). Numerical climate models (CM) and their paleoclimatic analogs are inadequate to assess the reality: for example, predictions of a "polar enhancement" of warming have not been confirmed by empirical data (*Adamenko*, 1985a,b; *Adamenko et al.*, 1982; *Anisimov*, 1998; *Grotefendt et al.*, 1999; *Kahl et al.*, 1993; *Kondratyev*, 1998; *Vaganov et al.*, 1996; *Woodcock*, 1999; *Zakharov*, 1996). The numerical forecasting of precipitation does not reproduce the present-day climate either (*Anisimov*, 1998; *Vaganov et al.*, 1996; *Drozdov* and *Lugina*, 1998; *Zakharov*, 1996). This is doubtless in the inadequate results of the description of physical processes such as feedbacks due to cloudiness, sea ice dynamics, the halocline state in polar oceans, etc.

As it has been revealed by *Anisimov* (1998), the correlation between the summer temperatures over the continents and the carbon dioxide concentration variations predicted by means of paleoreconstructions and CM is negative. Variations in precipitation predicted by CM are often statistically unreliable. Most paleoreconstructions indicate an enhanced humidification of the continents during warming. A great uncertainty in the assessment of future precipitation makes it very difficult to assess many of CC consequences.

2.2 Mountain and sea ice dynamics as an indicator of CC

The frequently used conclusion that the state of mountain and sea ice dynamics is a reliable indicator of CC, is in fact controversial. The location of glacier edges, i.e., their retreat or advance, depends not only (and not so much) on climate as on the rheological state of glaciers: motion speed, bed friction, surface inclination, thermophysical parameters of the firn and ice thickness. Glaciology cannot offer a reliable explanation of the causes of the time-dependent motion of glaciers (*Adamenko*, 1985a). That is why the data on periods of the retreat or advance of mountain glaciers can only be used as very approximate indicators of anthropogenic or natural changes in the climatic system (CS) (*Zakharov*, 1996).

The use of "the environment-glaciers" models for the diagnostics and predictions is only possible in some particular cases, and only if the physical nature of the processes of the external mass-energy-exchange and of boundary and initial conditions is well known.

2.3 Sea ice cover dynamics

An equal degree of uncertainty is present in the characteristics of sea ice cover dynamics: the sea ice cover extent, thickness, age, motions and structure, in spite of the fact that the data of satellite remote sensing made it possible to obtain a realistic picture of the phenomenology of the processes—the boundaries dynamics and extent changes. However, the cause-and-effect features of the ice cover dynamics have not been adequately explained (*Kondratyev*, 1998; *McPhee et al.,* 1998; *Zhang et al.,* 1998, and others). According to Zakharov's concept (*Zakharov,* 1996), CC is not simply the cause of ice cover transformations; the sea ice cover dynamics at high latitudes, which is dependent upon the thickness and specific features of the three-dimensional structure of the halocline, the advection of water masses and ice and other factors, should be regarded as an interactive climate-forming factor (here the non-linearity of relevant dependences is important). When analyzing the sea ice dynamics, it is important to adequately consider the spatial-temporal variability of the processes of the ice accretion, ablation and motions. Of course, it is obvious that, in general, the interrelationships between sea ice dynamics and climate change are of interactive nature.

As an illustration, we examine the causes of the well-known reduction in the extention of sea ice cover in the Arctic seas during the 1920s–1930s, as well as that of the mountain and surface ice changes in the Arctic and Sub-Arctic and other mountain regions of the Northern Hemisphere. It is known that the climate change at that time mainly revealed itself as a warming of the cold season and an enhancement of precipitation. It was due to or accompanied by a certain transformation of macrocirculation conditions (*Adamenko,* 1985a,b; *Drozdov* and *Lugina,* 1998; *Vaganov et al.,* 1996; *Zakharov,* 1996)—a higher frequency of cyclonic circulations and a less frequent repetition of anticyclonic ones, a shift of cyclone trajectories to relatively higher latitudes. Considering these observational data, one cannot attribute the decrease of ice cover extent to the enhancement of ice ablation. The causes may be due to the following causes: (a) the advection of sea ice to lower latitudes; (b) the decrease of the ice formation intensity; (c) the increase of the duration of sea ice ablation, etc.

2.4 Possible causes for the retreat of mountain glaciers

During an Arctic warming, the retreat of mountain glaciers can hardly be explained by enhanced ablation (*Adamenko,* 1985a). Among possible causes of glaciation degradation in the mountains during the warming epoch, there are the following:

- The speed of motion of glaciers, and consequently, the advection of ice to the apron parts of glaciers can decrease as a result of the approaching "negative" component of the anomalies of the Nay-Shumsky kinematic wave (*Shumsky,* 1968). As a result, the weakening of ice advection from the firn glacier parts to the apron ones takes place. It is known that every glaciation centre, every glacier has its characteristic time of response to changes in the mass-energy exchange in time and space. This time depends on many causes, part of which influences non-linearly the ice advection and has not been adequately studied thus far. The weakening of the ice advection of mountain glaciers may be a response to the decrease of the accumulation of firn and ice during the minor glacial epoch (the 1870s–1880s).
- Decrease in the cooling of glaciers in the cold season which might be a result of wintertime warming and possible increase of cloud amount under conditions of the high cyclonic activity during the period climate warming in the Arctic.
- Longer duration of the ablation period in the warming periods at high latitudes (*Adamenko,* 1985a; *Anisimov,* 1998).

3. Empirical diagnostics of climate change

Observational data for the aquatic areas of the Northern Hemisphere indicate the existence of some ocean areas where, during the recent 3–4 decades, a decrease in air temperature and sea surface temperature (SST) occurred. Analysis of these data makes it possible to conclude that a uniform "polar enhancement" of climate warming does not actually exist.

Large regions, where inter-latitudinal temperature contrasts have enhanced, are clearly pronounced. Such regions have stably existed during the recent decades. It is essential that the appearance of these regions is connected with a well-known (and unpredicted by theory) phenomenon: increased moistening over the water catchment area of the Caspian Sea (*Adamenko,* 1985a). The phenomenon revealed itself as a substantial sea level rise and a considerable transformation of macrocirculation conditions over vast territories from the Atlantic to Western Siberia and Central Asia (*Adamenko,* 1980, 1985a,b; *Kondratyev,* 1992; *Vaganov et al.,* 1996, etc.).

These phenomena have not been predicted by numerical modeling and have been quite unexpected. Their causes should be sought in the manifestations of a whole number of factors that have not been adequately studied thus far, viz., autooscillations in the "ocean-atmosphere-polar ice" system, changing of the atmospheric optical transparency, which, in its turn, depends on quite a number of causes (volcanic eruptions, time-dependency of cloudiness fields, transport of aerosols from natural and anthropogenic sources, etc.).

Analysis of aerological data from high latitudes makes it possible to draw the following conclusions:

- The speed of motion of glaciers, and consequently, the advection of ice to the apron parts of glaciers can decrease as a result of the approaching "negative" component of the anomalies of the Nay-Shumsky kinematic wave (*Shumsky,* 1968). Instead of the expected warming, in a number of sectors of the Northern Hemisphere—from the equator to the high latitudes—the process of cooling took place during the periods 1961–1970 and 1981–1990 (*Drozdov* and *Lugina,* 1998).
- According to the data of the "North Pole" stations summarized for the entire period of their operation, the process of cooling was taking place in Central Arctic with a centre mainly in the American sector of the Arctic (*Zakharov,* 1996). This conclusion can be confirmed by independent data (*Kahl et al.,* 1993) which reveal the lack of evidence of anthropogenic warming predicted by numerical climate modeling. During the time period 1950–1990, seasons and regions of cooling near the surface and in the troposphere have been found out in the polar region of the Northern Hemisphere.
- It is important that, in connection with a cooling in the Arctic, in a number of its sectors regions have appeared where temperature gradients increased between the high and middle latitudes in the European sector of Eurasia during the recent 2–3 decades. This kind of increase is mostly characteristic for cold epochs observed in the past. The marked increase of temperature contrasts between the middle and low latitudes during the recent decades may be in correspondence with the discovered enhancement of cyclogenesis in the south-western part of the North Atlantic (*Adamenko,* 1985a; *Drozdov* and *Lugina,* 1998; *Radionov et al.,* 1996).
- Forecasts of increased dryness in the European Russia, which should follow from the anticipated warming at the end of the 20th century, have proved wrong; one of indicators of the above is the fact that the Caspian Sea level ceased to drop but started rising instead. It is important that similar phenomena have been discovered (from instrumental and paleoclimatic data) for cold epochs (*Adamenko,* 1985a).

It can therefore be concluded that the hypothesis of anthropogenic warming and its variability in time and space has not been confirmed by the empirical climate diagnostics. It is not confirmed either by the analysis of some indirect CC indicators which will be examined below.

4. The state of large lakes as an indicator of climate change

The liquid water and heat balance of water catchment regions and aquatic areas of large lakes are responsible, to a great extent, for their level regime, trophic status, natural and anthropogenic variability (*Adamenko*, 1985a). For shallow and relatively small lakes, their hypsometric and morphometric specific features may result in situations when the same changes of components of the heat and water balances due to CC can result from very different, non-linear response of the level regime. This means that it is not always and not for all closed waterbodies true that their level regimes and their variations may be considered to be indicators of climate change (in this respect, an analogy can be found with the above-considered state of glaciers).

As has been noted above with regard to the Caspian Sea water catchment area, its response to CC should be considered taking account of the specific atmospheric conditions over the vast territory from the Atlantic to Western Siberia and Central Asia, from the Arctic to the subtropical latitudes (*Adamenko,* 1985a).

Analysis of the air temperature and precipitation anomalies in the water catchment area of the lake of Taimyr located at high latitudes has shown that the present epoch is rather characteristic of a cooling than a warming of climate in the region (*Adamenko,* 1985b). This is revealed by the higher frequency of negative temperature anomalies and precipitation during almost every month of the year; by the level regime and trophic state of the waterbody. The present-day decrease in the atmospheric moisture content and the cooling are very similar to the conditions of the end of the past and beginning of the present century.

5. Dendroclimatic indicators of climate change

5.1 Introductory remarks

Because the data of instrumental observations are limited in time, it is necessary to seek for and use indirect indicators of the state of the climatic system (CS) (see *Adamenko,* 1985a,b; *Anisimov,* 1998; *Brauch,* 1996; *Cheddadi et al.,* 1997; *Duursma* and *Carroll,* 1996; *Houghton et al.,* 1996; *Jaenicke* and *Weidner,* 1996; *Jastrow et al.,* 1990; *Kahl,* 1993; *Kondratyev,* 1998; *Report,* 1998; *Vaganov et al.,* 1996; *Warnecke,* 1997; *Weber,* 1996, etc.). Analysis of dendroclimatic indices makes it possible to assess long-term climate dynamics. Individual trees are known whose age is over 1000 years (in the Central Asian mountains, at the upper forest boundary), up to 600–800 years (in the forest-tundra, at the northern forest boundary): archa and larch, respectively; the gigantic sequoia in North America can be several thousand years old. The use of fossil and flooded wood makes it possible to obtain dendrochronological data for periods over 5 thousand years and more. Information obtained from tree rings allows to determine the temporal variation of various carbon isotopes, carbon dioxide, heavy metals penetrating the trees from the soil, as well as brought from the atmosphere due to dry and wet deposition (*Adamenko,* 1985a).

The main difficulty in reconstructing the climate signal from dendrochronological data is the necessity to filter out the contribution of other factors which influence the growth rate of tree rings. Such factors may be the photosynthetically active radiation, the state of the soils during the vegetation period, wintertime climatic conditions, the possible Markov type of tree growth processes (the dependence of subsequent conditions on the prehistory), the state of mineral and organic nutrition, photosynthesis conditions, etc.

Various methods have been developed in dendrochronology (*Lovelius,* 1997; *Vaganov et al.,* 1996) for taking into account the biological curve of growth. These methods make it possible to obtain the so-called dendrochronological growth rate indices I, which depend only on changing external conditions: the heat-to-moisture relationships, the photosynthetically active radiation (PAR), aeration, mineral nutrition, etc. Biologists assume (although this should be verified) that for trees which have reached the limit of growth conditions (or tolerance conditions), the value of index I is determined by a certain principal limiting factor. If $I > 1.00$, the external conditions determining the annual productivity are considered to be close to the average, and factors determining the annual production are considered to be favorable; if $I \leq 1.0$, a decrease in the annual productivity (inhibition) is considered to take place.

It is supposed that near the northern boundary of forest propagation the annual production is limited by the thermal regime, whereas at the southern boundary the decisive factor for the annual production is the moisture regime. In reality, analysis of the influence of the external environmental factors on forest productivity, and consequently, on tree ring width and other indicators of the state of trees in the sites of their growth, requires an individual and complex approach to the study of dendrochronological indices for the purpose of detecting different “signals”, including those due to the effects of heat and moisture.

5.2 Observation data

Vaganov et al. (1996) and *Lovelius* (1997) discussed the indicative properties of dendrochronological indices. Their monographs contain information databases obtained from vast territories of the northern forest boundary in the Sub-Arctic and other regions. The initial data processing answered the following questions: (1) Is reconstruction of various CC indices from these data possible? (2) Are various CS indices, reconstructed from qualitative indicators, homogeneous in time and space? (3) What are present-day CC trends if one obtains them from qualitative CS indicators? (4) Can the so-called anthropogenic signal be detected from qualitative CC indicators? (5) Are variations in the qualitative CS indicators during the period of instrumental observations and in recent decades very different from the data for the last 5–6 centuries? Here are brief answers to these questions.

Analysis of the information considered (*Fig. 1*, regions 3 and 4), obtained from areas separated one from the other by thousands of kilometres, about the temporal variation of various indicators of biological productivity (*Figs. 2, 3*) near the northern boundary of forest propagation makes it possible to draw the following conclusions:

- Temporal variations of indices *I* during a nearly 70-year period are distinctly synchronous.
- Since the variations of the indices analyzed (Figs. 2, 3), as will be shown later, are in agreement with the summertime input of heat (*Adamenko,* 1985a,b), their temporal variations indicate that the changes have not been unidirectional.
- During the 1930s (the trend is shown in Fig. 2 corresponding to the data for the northern forest boundary at the Taimyr Peninsula) and the 1960s (the trends are in Fig. 2) and up to now, a trend towards the decrease of indices *I* reveals itself in the low-frequency variability range.
- Analysis of dendrochronological data shows, on the one hand, the lack of extraordinary features in the temporal variation of indices *I*; but, on the other hand, it reveals a long-term trend towards their decrease during the recent 30–60 years (the trends are in Fig. 2). As can be seen from a multifactor linear and nonlinear correlation analysis (see below), the temporal variation of indices *I* is 60–80%-determined by the conditions of heat input. Therefore, one can draw the conclusion about the presence of a clearly pronounced trend at the northern forest boundary (regions 3 and 4 in Fig. 1) towards cooling. This is revealed by the fact that the maximums of productivity (indices *I*) during the period from 1930s to 1990s were becoming lower and lower with time, and the minimums were becoming deeper (Fig. 2).

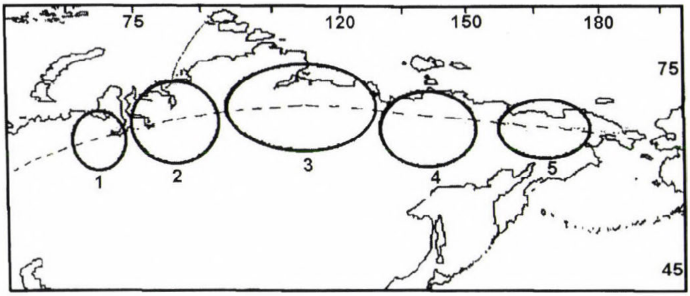

Fig. 1. Regions where samples of trees have been taken near the polar forest propagation boundary. 1 – Polar-Urals; 2 – West-Siberian; 3 – Taimyr-Putoran; 4 – East-Siberian; 5 – Chukotka

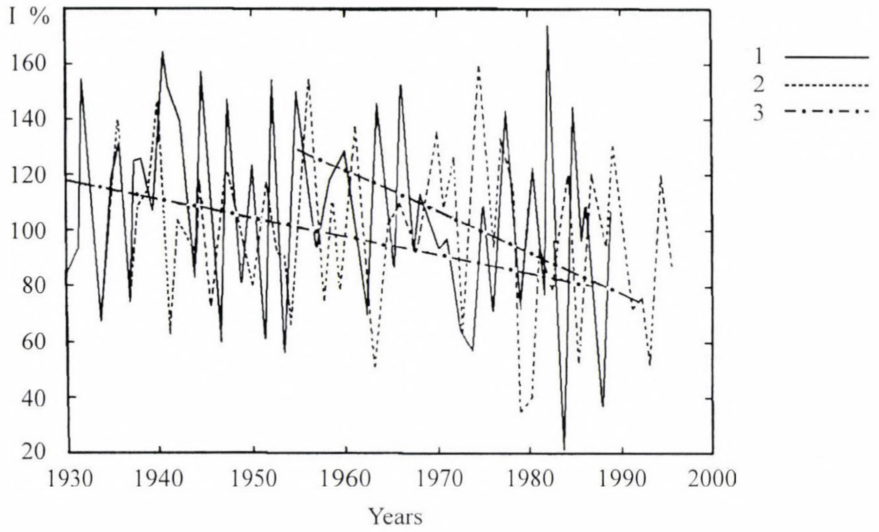

Fig. 2. Variations of dendrochronological index I (%) near the polar forest boundary. (Data of the Institute of Forests of the Siberian Branch of the Russian Academy of Sciences.)
1 – Ary-Mas; 2 – the Indigirka River basin; 3 – linear trend

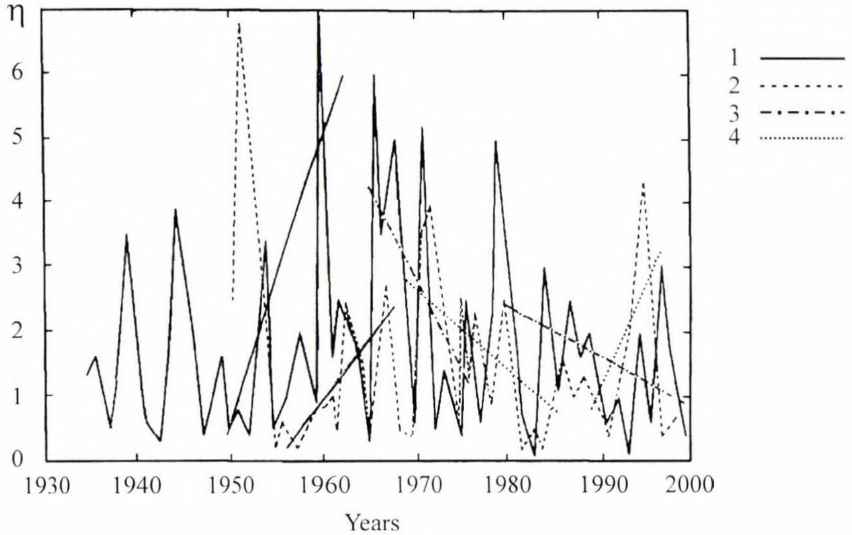

Fig. 3. Variation of the comfort index of bioproductivity η and its linear trends.
1 – the Novaya River (Taimyr); 2 – the Indigirka River (Eastern Siberia); 3, 4 – trends

5.3 Bioproductivity parameter

To more comprehensively characterize the variations of conditions favorable for forest productivity at the northern forest boundary during the last 5–6 centuries, analysis has been made of the temporal variation of the index of comfort for bioproductivity η determined by the ratio (Fig. 3):

$$\eta = \frac{I \geq 1.20}{I \leq 1.20}, \tag{1}$$

where $I \geq 1.20$ is the growth repetition rate which exceeds by 20% and more the average long-term norm calculated for running averages; $I \leq 1.20$ is the growth repetition rate which is 20% and more lower than the norm.

The values of the dimensionless parameter η determine, therefore, the ratio of the frequency of the years favorable for the biological productivity to that of the years unfavorable for it; thus, these values may be considered to be indices of the comfort for forest bioproductivity at its northern boundary.

An analysis performed earlier has revealed that index η depends on the summertime air temperature and the correlation coefficient exceeds 0.80 ± 0.03 (*Adamenko,* 1985a,b).

Analysis of the temporal variation of index η (Fig. 3) makes it possible to draw the following conclusions:

- Throughout the time period considered (5–6 centuries), there has not been any significant trend of a regular increase of index η with time, which could be comparable with the global air temperature variation or the independently recorded progressive increase of the carbon dioxide (or other greenhouse gases) concentration in the atmosphere.
- In contrary to the idea that global warming has been more pronounced at high latitudes, during nearly two centuries (the trend of decreasing η in Fig. 3) a significant tendency towards the decrease of η with time has revealed itself in the East-Siberian sector of the Sub-Arctic.
- During the late 1970s and early 1980s, a tendency towards the decrease of η took place also on the Taimyr Peninsula. The decrease of η reflects a reduction in the heat supply, i.e., the deterioration of conditions for biological productivity of forest at its northern boundary (region 3 in Fig. 1). This may be interpreted as some evidence in favor of a stronger cooling in the region considered in comparison with other ones (region 4 in Fig. 1). The variation of index η is in agreement with the results obtained by other investigators (*Anisimov,* 1998; *Lovelius,* 1997; *Vaganov et al.,* 1996, etc.), as well as with the above-mentioned decrease in heat and moisture reservoirs in the water catchment region of Lake Taimyr, the lowering of its level, the reduction of its area and changes in its biotic state.

- The variations of η during the 20th century are not exceptional (Fig. 3). The only specific feature of the changes is a greater intensity of the cooling processes. This fact is at variance with the well-known statement concerning universal anthropogenic warming and its enhancement at high latitudes.
- The climate warming of the 1930s at high latitudes has not clearly revealed itself in the variation of the η index: its relatively high values had also been observed in the past (Fig. 3). Comparison of the Arctic warming in the 20th century with the paleodata shows that the effect of the warming on biological productivity has been 2–5 times weaker than that in the past (see curve peaks in Fig. 3 relevant to the 16th and 17th centuries). This conclusion is in agreement with the data of a number of publications (*Vaganov et al.,* 1996; *Walland* and *Simmonds,* 1997; etc.).

5.4 Correlation analysis

In the context of the range of problems discussed, of interest is the analysis of the agreement between the variability in time for some CC indices used in the literature, which have been obtained from instrumental data on air temperature, assessments of the sea ice extent in the Arctic, and dendrochronological indices. Limiting ourselves to a very brief consideration, we present data on the correlation matrix of the 6th order in the truncated form (*Table 1*), with the level of confidence above 99.9%.

Not a single one of the *I* values of the time series presented by *Vaganov et al.,* (1996) has been in satisfactory agreement with the average air temperature variation in the Northern Hemisphere. This indicates that the values of *I* for each of over 60 points of observation within 5 regions considered (Fig. 1) cannot be regarded as indicators of global climate change but are connected with the regional-scale impacts. The averaging of the *I* values for certain sectors (Fig. 1, regions 1–5), performed by making use of the image recognition method developed by *Adamenko* (1985a), somewhat increased the values of correlation coefficients r with the averaged air temperature but did not make them statistically significant. No statistically significant correlation coefficients have either been discovered between the summarized index series presented by *Lovelius* (1997) and each of the 61 time series borrowed from the monograph by *Vaganov et al.* (1996). The values of the correlation coefficients between the *I* values for the series summarizing the growth rates of conifers at the northern forest boundary, obtained by *Lovelius* (1997), and all the other matrix parameters (Table 1) have proved to be statistically reliable and significant on a high level of confidence.

Hence it follows that the summarizing of *I* indices performed by *Vaganov et al.* (1996) or that of the results of measurements of the annual ring width of conifers near the northern forest boundary makes it possible to eliminate the influence of environmental conditions on the micro- and mesoscale levels, suppresses measurement noises and the effects of various artefacts, but singles out signals on a global or regional level. This conclusion is in accordance with the discovered by *Adamenko* (1985b) lack of a significant correlation of *I* indices for three regions on the Taimyr Peninsula with any indicators of heat and moisture regime on a local or mesoscale level, as well as a certain agreement between the *I* index anomalies and atmospheric circulation conditions which determine to a great extent the entire complex of conditions for biological productivity.

Table 1. Correlation matrix for growth rate indices of conifers near the northern boundary of forest propagation (I_{SA}, according to *Lovelius,* 1997), air temperature of the Northern Hemisphere (T_{NH} from the GRID data) and sea ice cover extent in the Arctic (S_{NE}, S_{EG}, S_{AA}, S_{BS}), according to *Zakharov* (1996)

		(1) T_{NH}	(2) I_{SA}	(3) S_{NE}	(4) S_{EG}	(5) S_{AA}	(6) S_{BS}
(1)	T_{NH}	1.00					
(2)	I_{SA}	0.55	1.00				
(3)	S_{NE}	-0.66	-0.58	1.00			
(4)	S_{EG}	-0.43	-0.34	0.79	1.00		
(5)	S_{AA}	-0.55	-0.44	0.93	0.84	1.00	
(6)	S_{BS}	-0.65	-0.57	0.91	0.47	0.79	1.00

Note: (1) T_{NH} is air temperature in the Northern Hemisphere during the 20th century; (2) I_{SA} values cover the latitude circle from the Kola Peninsula to Chukotka; (3)–(7) are data on sea ice cover extent in the Arctic; (3) S_{NE} – the North-European basin seas; (4) S_{EG} – the East-Greenland region seas; (5) S_{AA} – the Atlantic Arctic seas; (6) S_{BS} – the Barents Sea. The value of confidence of the correlation coefficient at the level of significance above 99.9% equals 0.31, by the module; correlation coefficient estimates have errors within the range from r ± 0.02 to r ± 0.05.

The accordance between some indirect climate indicators and data on surface air temperature, averaged over the Northern Hemisphere, may be considered a physical reality (*Adamenko,* 1985b). This statement is based on the fact that the correlation coefficient values between *I* and *T* are positive, and between *I* and *S* negative (see Table 1). Of interest is the fairly good agreement between various data on sea ice cover extent obtained independently for different Arctic seas (*Zakharov,* 1996), on the one hand, and between *I* and *S*, on the other hand.

6. Conclusions

The results considered above make it possible to draw the following general conclusions:

(1) The problem of the assessment of global climate change on the basis of the currently existing climate models is still far from being solved.

(2) The use of empirical diagnostics results shows that the anthropogenic climate warming signal has not revealed itself convincingly enough thus far either in the data of instrumental observations, or in indirect CC indicators (climate dynamics is far more complex than has ever been assumed).

(3) Analysis of the results of instrumental observations at high Northern latitudes indicates a considerable spatial-temporal inhomogeneity of temperature fields both during warming and cooling periods; the variations of humidity fields are even more complicated.

(4) The present-day trends in the variations of the indirect indicators of the state of the climatic system—the levels and areas of lakes, the state of marine and mountain ice cover, dendrochronological indices, etc.—show that model climate predictions have not been adequate, and the anthropogenic signal in indirect CC indicators has not revealed itself clearly during the recent 2-3 decades. The temporal variation of indirect CC indicators reveals the lack of polar enhancement of climate change, as well as the presence of stable tendencies towards climate cooling in a number of regions of the high latitudes of the Northern Hemisphere. Variations of the latitudinal gradients in the thermal regime indices, the presence of a number of specific features in the variations of the state of large lakes are rather characteristic for the cooling than warming epochs (in the regions mentioned).

(5) Any global climate change is characteristic of the presence of vast regions of multidirectional transformation of the heat and moisture reservoirs on the land and in the ocean, and the interrelated conditions of the existence of the biota and humans. This conclusion may be drawn from both the consideration of numerical climate modeling results and the analysis of the instrumental observation data, as well as indirect CC indicators.

References

Adamenko, V.N., 1980: Barico-circulation conditions of the latest millennium over the territories of Western Siberia and Central Asia (the Middle Region). In *Contemporary Climate Formation Problems* (ed.: *P.S. Khromov*) (in Russian). Moscow Univ. Press, 130-143.

Adamenko, V.N., 1985a: *Climate and Lakes* (in Russian). Leningrad, Gidrometeoizdat, pp. 263.

Adamenko, V.N., 1985b: Dendrochronological indication of long-term variability of barico-circulation processes. In *The Geography of the Taimyr Lakes* (in Russian). Nauka Publ., 87-99

Adamenko, V.N., Masanova, M.D. and *Chetverikov, A.F.*, 1982: *Climate Change Indication. Methods of Analysis and Interpretation*. Leningrad, Gidrometeoizdat, pp. 112.

Anderson, D.L.T. and *Willebrand, J.* (eds.), 1996: *Decadal Climate Variability. Dynamics and Predictability*. Springer Verlag, Berlin e.a., pp. XIII/467.

Anisimov, O.A., 1998: Climate change in the region of the cryolithozone of the Northern Hemisphere and the assessment of its consequences. Abstract of *Ph.D. dissertation*, St. Petersburg State Univ.

Are Human Activities Causing Global Warming?, 1995. George C. Marshall Inst. Publ., Washington, DC, pp. 45.

Barnett, T.P., 1999: Comparison of near-surface air temperature variability in II coupled global climate model. *J. Climate 12*, 511-518.

Bengtsson, L., Roeckner E. and *Stendel, M.*, 1999: Why is the global warming proceeding much slower than expected? *J. Geophys. Res. 104*, 3865-3876.

Brauch, H.G. (ed.): 1996. *Klimapolitik*. Springer Verlag, Berlin e.a., pp. XXX+450.

Browning, K.A. and *Gurney, R.J.* (eds.), 1999: *Global Energy and Water Cycles*. Cambridge Univ. Press, pp. 292.

Cheddadi, R.Yu.G., Guiot, J., Harrison, S.P. and *Prentice, I.C.*, 1997: The climate of Europe 6000 years ago. *Climate Dynamics 13*, 1-9.

Drozdov, O.A. and *Lugina, K.M.*, 1998: The climatic system dynamics and geographic conditions. *In Ecologo-Geographic Assessment and Monitoring of the Environment*. St.Petersburg State Univ. Publ., 8-35.

Ellsaesser, H.W. (ed.), 1992: *Global 2000 Revisited. Mankind's Impact on Spaceship Earth*. Paragon House, New York, pp. 436.

Emsley, J. (ed.), 1996: *The Global Warming Debate*. The Report of the European Science and Environment Forum. Bourne Press Ltd., Bornemouth, pp. 288.

Fischer, H., Wahlen, M., Smith, S., Mastroianni, D. and *Deck, R.*, 1999: Ice core records of atmospheric CO_2 around the last three glacial terminations. *Science 283*, 1712-1714.

Flower, B.P., 1999: Warming without high CO_2? *Nature 399*, 313-314.

Fu, C., Diaz, H.F., Dong, D. and *Fletcher, J.O.*, 1999: Changes in atmospheric circulation over Northern Hemisphere oceans associated with the rapid warming of the 1920s. *Int. J. Climatol. 19*, 581-606.

Grotefendt, K., Lagemann, K., Quadfasel, D. and *Ronski, S.*, 1998: Is the Arctic warming? *J. Geophys. Res. 103*, 27679-27688.

Hansen, J.E., Sato, M., Ruedy, R., Lacis, A. and *Glascoe, J.*, 1998: Global climate data and models: a reconciliation. *Science 281*, 930-932.

Houghton, J.T., Meira-Filho, L.G., Callander, B.A., Harris, N., Kattenberg, A. and *Maskell, K.* (eds.) 1996: *Climate Change 1995. The Science of Climate Change*. Cambridge Univ. Press, pp. 572.

Jain, S., Lall, U. and *Mann, M.E.*, 1999: Seasonality and interannual variations of Northern Hemisphere temperature: Equator-to-pole and ocean-land contrasts. *J. Climate 12*, 1086-1100.

Jastrow, R., Nierenberg, W. and *Seitz, F.*, 1990: *Global Warming. What Does the Science Tell Us?* George C. Marshall Inst. Publ., Washington, DC, pp. 72.

Jones, P.D. and *Hegerl, G.C.*, 1998: Comparisons of two methods of removing anthropogenically related variability from the near-surface observational temperature field. *J. Geophys. Res. 103*, 13777-13786.

Kahl, J.S. et al., 1993: Absence of evidence for greenhouse warming over the Arctic Ocean in the past 40 years. *Nature 361*, 335-337.

Kondratyev, K.Ya., 1992: *Global Climate*. Nauka Publ., pp. 359.

Kondratyev, K.Ya., 1997: Global ecodynamics and sustainable development: the natural science aspects and the human dimension. *Izvestiya of Russian Geograph. Soc. 129*, No. 6, 1-12.

Kondratyev, K.Ya., 1998: *Multidimensional Global Change*. Wiley/Praxis, Chichester, U.K., pp. 761.

Kondratyev, K.Ya., 1999: *Climatic Effects of Aerosols and Clouds*. Springer/Praxis, Chichester, U.K., pp. 264.

Kondratyev, K.Ya., Johannessen, O.M. and *Melentyev, V.V.*, 1996: *High-Latitude Climate and Remote Sensing*. Wiley/Praxis, London, pp. 200.

Kondratyev, K.Ya. and *Cracknell, A.P.*, 1998: *Observing Global Climate Change.* Taylor & Francis, London, pp. 562.

Lovelius, N.V., 1997: *Dendroindication of Natural Processes and Anthropogenic Influences* (in Russian). St. Petersburg, *World & Family-95*, pp. 320.

Manabe, S., 1998: Study of global warming by GFDL climate models. *Ambio 27*, 182-186.

Mason, B.J., 1995: Predictions of climate changes caused by man-made emissions of greenhouse gases: a critical assessment. *Contemporary Physics 36*, 299-319.

McPhee, M.G., Stanton, T.P., Morison, J.H. and *Martinson, D.G.*, 1998: Freshening of the upper ocean in the Arctic: Is perennial sea ice disappearing? *Geophys. Res. Lett 25*, 1729-1732.

Mysak, L.A. and *Venegas, S.A.*, 1998: Decadal climate oscillations in the Arctic: A new feedback loop for atmosphere-ice-ocean interactions.

Postmentier, E.S., Soon, W.H. and *Baliunas, S.L.*, 1999: *Natural Variability in an Ocean-atmosphere Climate Model.* Harvard-Smithsonian Center for Astrophysics, Cambridge, MA, No. 4802, pp. 16.

Radionov, V.F., Briazgin, N.N. and *Alexandrov, E.I.*, 1996: *Snow Cover in the Arctic Basin* (in Russian). Gidrometeoizdat, St. Petersburg, pp. 124.

Raschke, E. (ed.), 1996: *Radiation and Water in the Climate System. Remote Measurements.* Springer Verlag, Berlin e.a., pp. X+614.

Report on Study of the Arctic Change Workshop held November 10-12, 1997, 1998: Univ. of Washington, Seattle, Washington, Polar Science Center Publ. No. 8, pp. 63.

Schneider, S.H., 1998: Kyoto Protocol: The unfinished agenda. *Climatic Change 39*, 1-21.

Schoenwiese, C., 1996: *Klimaaenderungen. Daten, Analysen, Prognosen.* Springer Verlag, Berlin e.a., pp. XIII+224.

Scorer, R.S., 1996: *Dynamics of Meteorology and Climate.* J. Wiley & Sons, Ltd., Chichester, U.K., pp. 400.

Shumsky, P.A., 1968: *Dynamical Glaciology* (in Russian). VINITI Press, pp. 178.

Singer, F.S., 1997: *Hot Talk, Cold Science: Global Warming, Unfinished Debate.* Oakland, CA, Independent Inst., pp. 120.

Storch, H., von and *Floeser, G.*, 1999: *Anthropogenic Climate Change.* Springer, Berlin e.a., pp. XIV + 372.

Vaganov, E.A., Shiyatov, S.G. and *Mazepa, V.S.*, 1996: *Dendroclimatic Studies in the Urals-Siberian Sub-Arctic* (in Russian). Novosibirsk, Nauka Publ., pp. 246.

Walland, D.J. and *Simmonds, I.*, 1997: Modelled atmospheric response to changes in Northern Hemisphere snow cover. *Climate Dynamics 13*, 25-34.

Warnecke, G., 1997: *Meteorologie und Umwelt. Eine Einführung.* Springer Verlag, Berlin e.a., pp. XII + 266.

Watanabe, M. and *Nitta, T.*, 1999: Decadal changes in the atmospheric circulation and associated climate variations in the Northern Hemisphere winter. *J. Climate 12*, 494-510.

Weber, G.R., 1996: *Global Warming. The Rest of the Story.* Dr. Boettiger Verlags GmbH, Wiesbaden, pp. 188.

Wigley, T.M., 1998: The Kyoto Protocol: CO_2, CH_4 and climate implications. *Geophys. Res. Lett. 25*, 2285-2288.

Wiin-Nielsen, A., 1998: Limited predictability and the greenhouse effect—a scientific view. *Energy & Environm. 9*, 639-646.

Woodcock, A., 1999: Global warming—a natural event? *Weather 54*, No. 5, 162-163.

Yao, M.-S. and *Del Genio, A.D.*, 1999: Effects of cloud parameterization on the simulation of climate changes in the GISS GCM. *J. Climate 12*, 761-779.

Zakharov, V.F., 1996: *Sea Ice in the Climatic System* (in Russian). Gidrometeoizdat, St. Petersburg, pp. 213.

Zhang, J., Rothrock, D.A. and *Steele, M.*, 1998: Warming of the Arctic Ocean by a strengthened Atlantic inflow: Model results. *Geophys. Res. Lett. 25*, 1745-1748.

Zubov, N.N., 1945: *The Arctic Ice* (in Russian). The Arctic Sea Route Publ., Moscow, pp. 360.

IDŐJÁRÁS

Quarterly Journal of the Hungarian Meteorological Service
Vol. 103, No. 4, October–December 1999, pp. 237–247

Application of some statistical tests for detecting hidden periodicity in the Serbian annual precipitation sums

J. Mališić[1], **M. Unkašević**[2] and **I. Tošić**[2]

[1]*University of Belgrade, Faculty of Mathematics, Studentski trg 16, 11 000 Belgrade, Yugoslavia*

[2]*University of Belgrade, Faculty of Physics, Department of Meteorology, Dobračina 16,*
11000 Belgrade, Yugoslavia; e-mail: itosic@afrodita.reub.bg.ac.yu

(Manuscript received 9 November 1998; in final form 9 March 1999)

Abstract—Research on periodicity in the climatological time series has been receiving a lot of attention. It is important for studies of climatic fluctuations and changes. This paper deals with hidden periodicities in time series of annual precipitation sums of five stations in Serbia in the period 1925–1995. The Siegel's test is used to perform the analysis. This is an extension of the Fisher's test in the way that it may be able to detect even so-called compound periodicities hidden in random white noise. New critical values of test statistics from 5 to 100 years are calculated by using the Wei's approximation. Certain conditions, such as homogeneity and Gaussian distribution of the data have to be fulfilled to apply the test. Compound periodicity in the Serbian annual precipitation sums has not been found.

Key-words: hidden periodicity, climatological statistical tests, annual precipitation sums.

1. Introduction

Many time series in the natural sciences seem to exhibit periodical structures. In such a case, a series repeats more or less the same pattern over time. Two classical examples are the Wolf sunspots number and the annual number of Canadian Lynx. Some climatologic time series seem to have periodical structures as well.

Standard approaches to such time series are the fast Fourier transform method (*Cooley* and *Tukey*, 1965; *Mališić*, 1990), estimation of the spectrum and fitting of an autoregressive–moving average (ARMA) model or an autoregressive–integrated–moving average (ARIMA) model (*Kay*, 1980; *Thompson*, 1982).

Fitting of periodical phenomena by means of trigonometric functions has a long tradition in meteorology. Lots of different methods have been used for discovering hidden periods (*Blackman* and *Tukey*, 1959; *Anderson*, 1971; *Bloomfield*, 1976; *Siegel*, 1980; *Damsleth* and *Spjotvoll*, 1982; *Newton* and *Pagano*, 1983). However, during the last 20 years some new and non-traditional methods have been investigated: the maximum enthropy spectral estimation (*Andersen*, 1974; *Padmanabhan* and *Rao*, 1988; *Padmanabhan,* 1991), the maximum likelihood spectral estimation (*Friedlander*, 1982), etc.

This paper is inspired by the Fisher's and Siegel's tests (*Fisher*, 1929, 1939, 1940; *Siegel*, 1980) and presents an attempt of application of these tests to annual precipitation sums. Section 2 describes the used data and the results of the inhomogeneity tests. A short review of the Fisher's and Siegel's tests is given in Section 3. The new tests for periodicity containing the Fisher's test as a special case, and calculations of the test-statistics and its critical values are proposed in Section 4. Some conclusions about applicability of the *Fisher*'s (1940) and *Siegel*'s (1980) tests to examine periodicity in the annual precipitation sums during the period 1925–1995, and in the annual maximum precipitation sums during the period 1888–1994 are given in Section 5.

2. Data used

This paper takes into analysis the annual precipitation sums measured at the stations Belgrade-Observatory (44°48'N, 20°28'E, 132 m a.s.l.), Loznica (44°33'N, 19°14'E, 121 m a.s.l.), Vršac (45°08'N, 21°19'E, 85 m a.s.l.), Senta (45°56'N, 20°05'E, 80 m a.s.l.) and Sremska Mitrovica (44°58'N, 19°38'E, 81 m a.s.l.) in the period 1925–1995. These stations are located in the lowland of the northern part of Serbia (*Fig. 1*), which is spatially homogeneous.

Examination of homogeneity is necessary before any serious study of periodicity in climatological time series. In this paper the Kolmogoroff-Smirnoff's, the bivariate (*Maronna* and *Yohai*, 1978) and the *Alexandersson*'s (1986) tests for examination of inhomogeneity are used. The bivariate test is based on the assumptions of normality and independence. Assumption of normality is not rigorously met the by five annual precipitation series, as the coefficient of skewness shows, while the lag-one correlation coefficient is satisfied (*Table 1*). Namely, all series show positive skewness, indicating that the series are only approximately normal, while low values of lag-one correlation coefficients indicate that the series are independent.

The bivariate and Alexandersson's tests are based on second correlated series which are assumed to be unchanged and also give the maximum likelihood estimates of the time and amount of change. These tests allow to determine the year of inhomogeneity (T_1), the size of change and its statistical significance (level 0.05). The test statistics $T_0 = \max_{i<n}\{T_i\}$, ($n = 71$) is calculated and then compared to the critical value on the significance level 0.05 (*Potter*, 1981; *Alexandersson*, 1986). The statistics T_0 is used to test whether a shift in mean has occurred. The tests used indicated that there are no inhomogeneity in the annual precipitation series at the five stations.

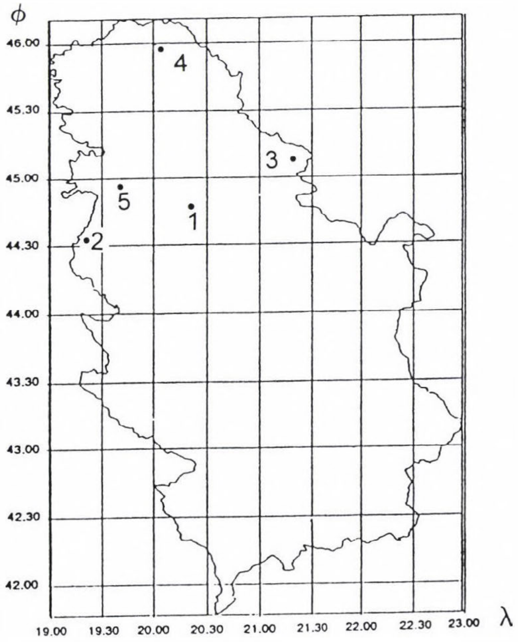

Fig. 1. Location map of the precipitation stations:
1. Belgrade-Observatory, 2. Loznica, 3. Vršac, 4. Senta, 5. Sremska Mitrovica.

Table 1. Statistics: A – coefficient of skewness, B – lag-one correlation coefficient

Stations	Belgrade-Obs.	Loznica	Vršac	Senta	Sr. Mitrovica
A	0.195507	0.442214	0.529956	0.122999	0.348323
B	0.210460	0.188676	0.087799	0.078852	0.063636

3. Review of the Fisher's and Siegel's tests

To examine periodicity in the time series of the annual precipitation sums (*Fig. 2*) we use the following analytical procedure.

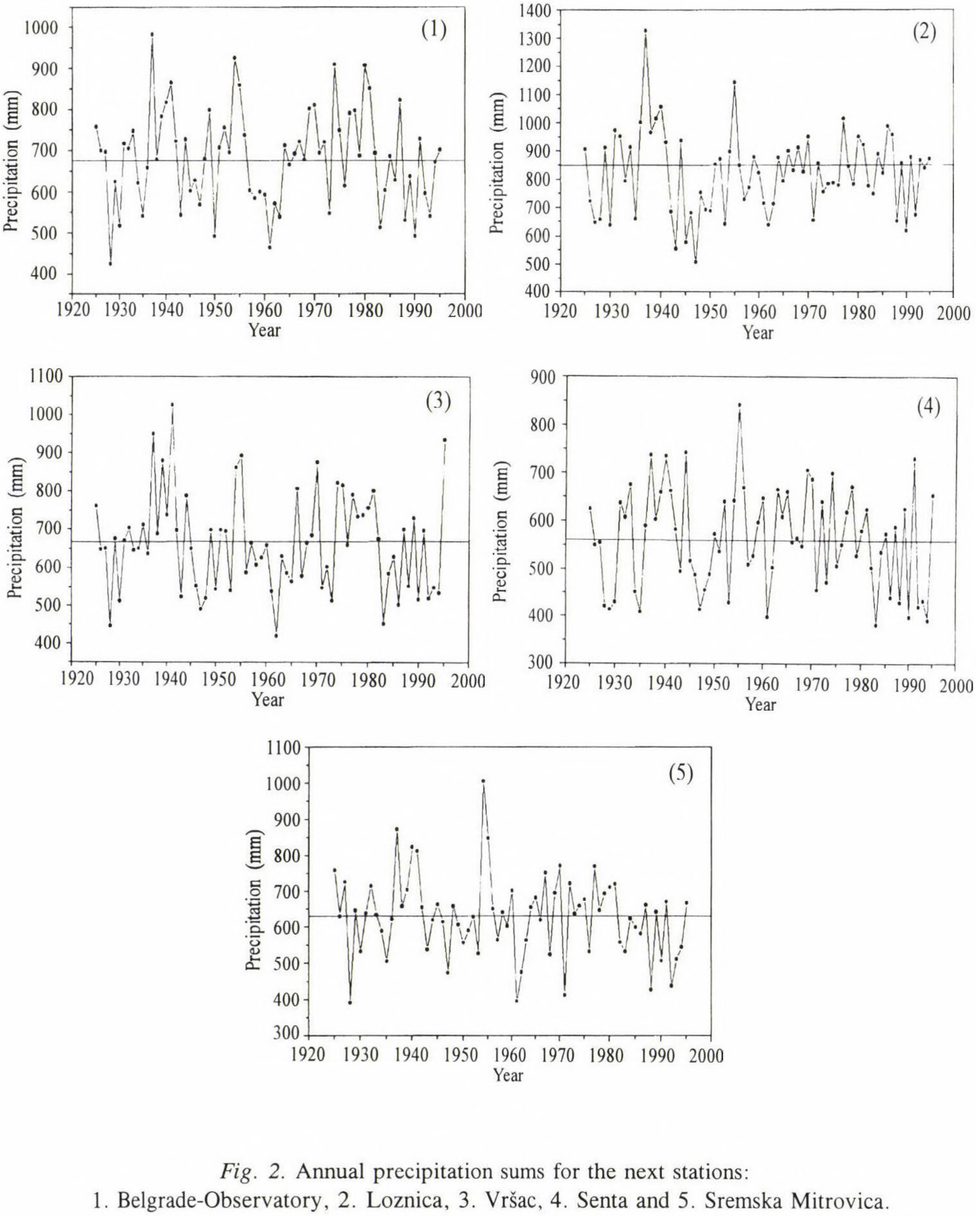

Fig. 2. Annual precipitation sums for the next stations:
1. Belgrade-Observatory, 2. Loznica, 3. Vršac, 4. Senta and 5. Sremska Mitrovica.

First, let $\{X_t, t = 1,2,\dots,N\}$, $N = 2n + 1$, n is positive integer, be a series of observations taken at equally spaced time intervals and

$$X_t = \zeta_t + \varepsilon_t, \quad t = 1,\dots,N, \tag{1}$$

where ζ_t represents the unobservable value of the annual precipitation at the moment t. The series $\{\varepsilon_t\}$ is assumed to be a strong Gaussian white noise, a sequence of independent, identically Gaussian-distributed random variables with zero mean and unknown variance σ^2. Let

$$a_0 = \bar{\zeta} = \frac{1}{N}\sum_{t=1}^{N}\zeta_t\,,\ a_j = \frac{2}{N}\sum_{t=1}^{N}\zeta_t\cos\left(\frac{2\pi jt}{N}\right),\ b_j = \frac{2}{N}\sum_{t=1}^{N}\zeta_t\sin\left(\frac{2\pi jt}{N}\right),\ j = 1,\dots,n \tag{2}$$

be the Fourier coefficients of the decomposition

$$\zeta_t = a_0 + \sum_{j=1}^{n}\left[a_j\cos\left(\frac{2\pi jt}{N}\right) + b_j\sin\left(\frac{2\pi jt}{N}\right)\right]. \tag{3}$$

Further, we introduce the periodogram values

$$R_j^2 = A_j^2 + B_j^2 = \left[\frac{2}{N}\sum_{t=1}^{N}X_t\cos\left(\frac{2\pi jt}{N}\right)\right]^2 + \left[\frac{2}{N}\sum_{t=1}^{N}X_t\sin\left(\frac{2\pi jt}{N}\right)\right]^2,\ j = 1,\dots,n. \tag{4}$$

and statistics

$$Y_j = \frac{R_j^2}{R_1^2 + R_2^2 + \dots + R_n^2},\ j = 1,\dots,n \tag{5}$$

Let the null hypothesis H_0 that there is no periodic activity, i.e.,

$$H_0\ (\zeta_1 = \zeta_2 = \dots = \zeta_N), \tag{6}$$

and let the compound alternative hypothesis $H_{i_1,i_2,\dots,i_m}$ means the periodicities at the frequencies $i_1/N,\dots,i_m/N$. Then the Fisher's and Siegel's tests (*Fisher*, 1940; *Siegel*, 1980) are based on the statistics

$$G = \max_{1\le j<n} Y_j\,. \tag{7}$$

We reject H_0 if the statistics G exceeds the appropriate critical value $g_{F;\alpha}$, corresponding to the level of significance α ($\alpha = 0.01$ or 0.05 for example). Thus, if the sample value g of the statistics G exceeds the critical value $g_{F;\alpha}$, we conclude that the series $\{X_t\}$ has the periodic component at the frequency i/N, i.e., N/i is the period.

It is clear that any increase in a smaller Y_j will tend to decrease their maximum G in Eq. (7). We remedy this case by choosing a threshold value $g_\alpha^* < g_{F;\alpha}$, i.e., we define a coefficient λ between 0 and 1 as

$$\lambda = \frac{g_\alpha^*}{g_{F;\alpha}}. \tag{8}$$

Then, the proposed statistics is

$$T_\lambda = \sum_{j=1}^{n} (Y_j - g_\alpha^*)_+ \equiv \sum_{j=1}^{n} (Y_j - \lambda g_{F;\alpha})_+ = \sum_{j=1}^{n} \varphi_+ , \tag{9}$$

where φ_+ is the positive-part of the function φ, defined as

$$\varphi_+ = \max\{\varphi, 0\} = \begin{cases} \varphi, & \text{if } \varphi \geq 0, \\ 0, & \text{if } \varphi < 0. \end{cases}$$

If $\lambda = 1$, we obtain the Fisher's test, because $T_1 > 0$ if and only if some value Y_j exceeds $g_{F;\alpha}$. A value of λ near 1 might be used when the simple periodicity is expected; smaller values of λ might be used when compound periodicities are expected.

4. *Calculations of test-statistics and critical values*

In the case of the compound alternative hypothesis $H_{i_1 i_2 \ldots i_m}$ we have

$$\frac{(N-1) - 2m}{2m} Z_{i_1, i_2, \ldots, i_m} = F_{2m;\, N-1-2m} , \tag{10}$$

where

$$Z_{i_1 i_2 \ldots i_m} = \frac{R_{i_1}^2 + R_{i_2}^2 + \ldots + R_{i_m}^2}{\sum\limits_{j \notin \{i_1, i_2, \ldots, i_m\}} R_j^2} \tag{10'}$$

the denominator is the sum of all values R_j^2 except $R_{i_1}^2, R_{i_2}^2, \ldots, R_{i_m}^2$ and $F_{2m;N-1-2m}$ are Fisher's random variables with $2m;N\text{-}1\text{-}2m$ degree of freedom.

New critical values $g_{F;\alpha}$ were obtained by using the Wei's approximation (*Wei*, 1990):

$$P_{H_0}(G \geq g_{F;\alpha}) \approx n(1 - g_{F;\alpha})^{n-1}, \tag{11}$$

for significance levels $\alpha = 0.05$ and $\alpha = 0.01$, and for $n = 5, 6, \ldots, 100$ (*Table* 2). We use the Siegel's equation (*Siegel*, 1978, 1980) in the form

$$P_{H_0}(T_\lambda > t) = \sum_{l=1}^{n} \sum_{k=0}^{l-1} (-1)^{k+l+1} \binom{n}{l} \binom{l-1}{k} \binom{n-1}{k} t^k (1 - \lambda \lg_{F;\alpha} - t)_+^{n-k-1}, \tag{12}$$

Critical values of t_λ, calculated for T_λ, are listed in Table 2. The estimates have been performed for the same significance levels of α and the same values of n as for the critical values of $g_{F;\alpha}$. Note that calculated critical values coincided with critical values obtained by using the Siegel's test (*Siegel*, 1980) for $n = 5,\ldots,50$.

5. Periodicity in the Serbian annual precipitation sums

The periodicity of the annual precipitation sums measured at the five stations during the period 1925–1995 is examined. After detrending, tapering and using the Hamming window (*Blackman* and *Tukey*, 1959), the values of the Fourier coefficients A_j and B_j, the periodogram values R_j^2 and the values of inferences Y_j are calculated. The same results are obtained by using other windows, for example, the Tukey and Parzen windows. The estimated values of Y_j for $n = 1,\ldots,35$ are shown on *Fig. 3*.

Following the Siegel's suggestion (*Siegel*, 1980) for $\lambda = 0.6$ and on the significance level 0.05, we obtained $\lambda g_{F;\alpha} = 0.105$. For the Belgrade-Observatory annual precipitation sums T_λ is equal to 0.0361 (Eq. 9). This value is smaller than the critical value $t_{0.6} = 0.0792$ (Table 2a) which indicates that the compound periodicity does not exist. Also, we have not found compound periodicity for the stations Loznica ($T_\lambda = 0.0164$), Vršac ($T_\lambda = 0.0038$), Senta ($T_\lambda = 0$) and Sremska Mitrovica ($T_\lambda = 0$).

We examined the periodicity of the annual maximum precipitation sums measured at the Belgrade-Observatory station during the period from 1888 to 1994 (107 years). The estimated values of Y_j for $n = 1,\ldots,53$ are shown in *Fig. 4*. For the annual maximum precipitation sums we have found $\lambda g_{F;\alpha} = 0.0752$

Table 2. Critical values $g_{F;\alpha}$ and t_λ for $\lambda = 0.8$, $\lambda = 0.6$ and $\lambda = 0.4$, when *(a)* $\alpha = 0.05$, *(b)* $\alpha = 0.01$

(a)

n	$g_{F;\alpha}$	$T_\lambda(0.8\ g_{F;\alpha})$	$T_\lambda(0.6\ g_{F;\alpha})$	$T_\lambda(0.4\ g_{F;\alpha})$
5	0.6837720	0.1365720	0.2733720	0.4101720
6	0.6161480	0.1260390	0.2465490	0.3808140
7	0.5611540	0.1123540	0.2249750	0.3556940
8	0.5156870	0.1028910	0.2074440	0.3340430
9	0.4774940	0.0959269	0.1937030	0.3160420
10	0.4449530	0.0890349	0.1812600	0.2995150
15	0.3346310	0.0669604	0.1398900	0.2460830
20	0.2704590	0.0549320	0.1162640	0.2137930
25	0.2281320	0.0462535	0.0997710	0.1905390
30	0.1979500	0.0400885	0.0878783	0.1732720
35	0.1752530	0.0358162	0.0792266	0.1603900
40	0.1575160	0.0324966	0.0724347	0.1500800
50	0.1314890	0.0268405	0.0614358	0.1329250
51	0.1293810	0.0264177	0.0605771	0.1315640
52	0.1273450	0.0260092	0.0597460	0.1302240
53	0.1253770	0.0256141	0.0589414	0.1289710
54	0.1234720	0.0252318	0.0581614	0.1277340
55	0.1216290	0.0248617	0.0574054	0.1265360
60	0.1132310	0.0231745	0.0539457	0.1209690
70	0.0996654	0.0204455	0.0482983	0.1114940
80	0.0891612	0.0183288	0.0438682	0.1039630
90	0.0807706	0.0166354	0.0402879	0.0977606
100	0.0739035	0.0152477	0.0373264	0.0925198

(b)

n	$g_{F;\alpha}$	$T_\lambda(0.6\ g_{F;\alpha})$	$T_\lambda(0.6\ g_{F;\alpha})$	$T_\lambda(0.4\ g_{F;\alpha})$
5	0.7885260	0.1573260	0.3151260	0.4729260
6	0.7217920	0.1441920	0.2885920	0.4335800
7	0.6644040	0.1332040	0.2660040	0.3992500
8	0.6151660	0.1231670	0.2461670	0.3716520
9	0.5727130	0.1143130	0.2289220	0.3486910
10	0.5358410	0.1070410	0.2143120	0.3293540
15	0.4068890	0.0813024	0.1636450	0.2620020
20	0.3297120	0.0657631	0.1335240	0.2215180
25	0.2781960	0.0558841	0.1138340	0.1943460
30	0.2412490	0.0485633	0.0994930	0.1742640
35	0.2133840	0.0431182	0.0887140	0.1587890
40	0.1915750	0.0381133	0.0795814	0.1457610
50	0.1595520	0.0317022	0.0669352	0.1269290
51	0.1569590	0.0315165	0.0662218	0.1258630
52	0.1544540	0.0314203	0.0656144	0.1247760
53	0.1520320	0.0305923	0.0643279	0.1234020
54	0.1496900	0.0298447	0.0631322	0.1215180
55	0.1474220	0.0299904	0.0628064	0.1210250
60	0.1370940	0.0276589	0.0584460	0.1142430
70	0.1204230	0.0245975	0.0520665	0.1044270
80	0.1075300	0.0212835	0.0461404	0.0959648
90	0.0972442	0.0198151	0.0426058	0.0894190
100	0.0888372	0.0177937	0.0388304	0.0843026

and $T_\lambda = 0.0417$, which is smaller than the critical value $t_{0.6} = 0.0589$ (Table 2a). Therefore the compound periodicity is not revealed in this case.

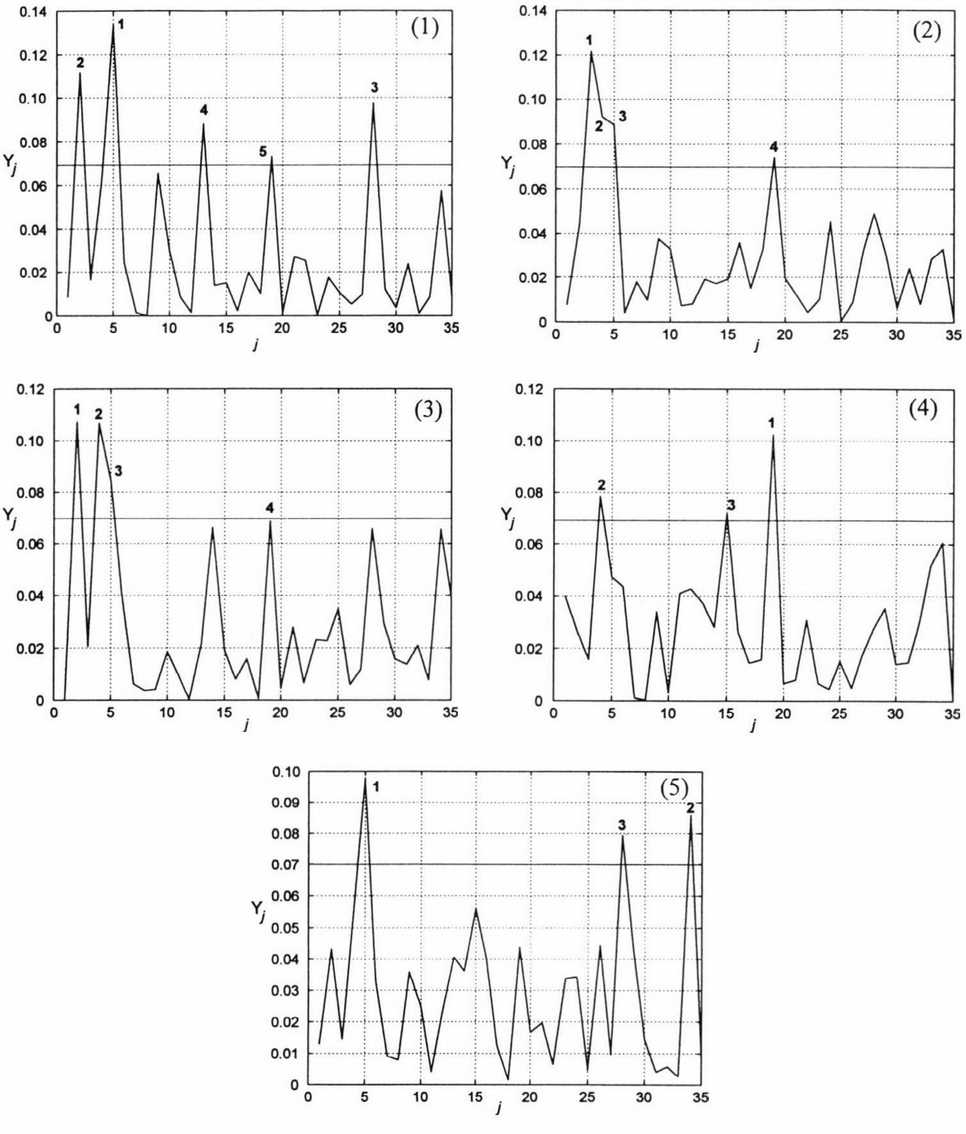

Fig. 3. Periodogram of the annual precipitation sums at 1. Belgrade-Observatory, 2. Loznica, 3. Vršac, 4. Senta and 5. Sremska Mitrovica stations, during 1925–1995. Horizontal lines represents the critical values Y_j.

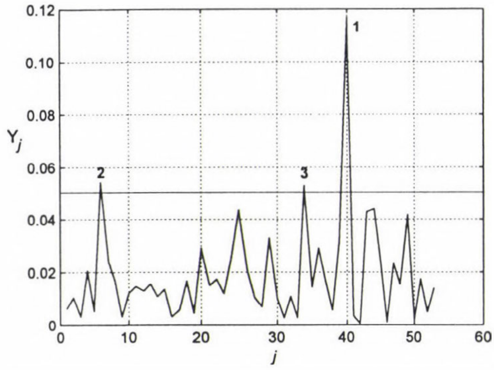

Fig. 4. Periodogram of the annual maximum precipitation sums at the Belgrade-Observatory station, during the period 1888–1994. Horizontal lines denotes the critical values Y_j.

6. Conclusion

We examined hidden periodicity in the annual precipitation sums measured at five stations in the northern part of Serbia, during the period 1925–1995 (71 years), using the Fisher's and Siegel's tests. The new critical values $g_{F;\alpha}$ and t_λ were obtained using the Siegel's test according to Wei's approximation for significance levels $\alpha = 0.05$ and $\alpha = 0.01$, for $n = 5,\ldots,100$, and for $\lambda = 0.4$, $\lambda = 0.6$ and $\lambda = 0.8$. The annual precipitation sums as well as the annual maximum precipitation sums did not exhibit compound periodicity according to the Fisher's and Siegel's tests.

References

Alexandersson, A., 1986: A homogeneity test applied to precipitation data. *J. Climatol. 6*, 661-675.

Andersen, N. 1974: On the calculation of filter coefficients for maximum entropy spectral analysis. *Geophysics 39*, 69-72.

Anderson, T.W., 1971: *The Statistical Analysis of Time Series*. John Wiley & Sons, New York.

Blackman, R.B. and *Tukey, J.W.*, 1959: *The Measurement of Power Spectra from the Point of View of Communications Engineering*. Dover, New York.

Bloomfield, P., 1976: *Fourier Analysis of Time Series: An Introduction*. John Wiley & Sons. New York.

Cooley, J.W. and *Tukey, J.W.*, 1965: An algorithm for machine calculation of complex Fourier series. *Math. Comput. 19*, 297-301.

Damsleth, E. and *Spjotvoll, E.*, 1982: Estimation of trigonometric components in time series. *J. Amer. Statist. Assoc. 77*, 381-387.

Fisher, R.A., 1929: Tests of significance in harmonic analysis. *Proc. of the Royal Society*, *Ser. A, 125,* 54-59.

Fisher, R.A., 1939: The sampling distribution of some statistics obtained from non-linear equations. *Annals of Eugenics 9*, 238-249.

Fisher, R.A., 1940: On the similarity of the distributions found for the test of significance non harmonic analysis, and in Steven's problem in geometrical probability. *Annals of Eugenics 10*, 14-17.

Friedlander, B., 1982: A recursive maximum likelyhood algorithm for ARMA spectral estimation. *IEEE Trans. Inform. Theory*, IT-28, 639-646.

Kay, S.M., 1980: A new ARMA spectral estimator. *IEEE Trans. Acoustics, Speach. Signal Processing*, ASSP-28, 585-588.

Maronna, R. and *Yohai, V.J.*, 1978: A bivariate test for the detection of a systematic change in mean. *J. Amer. Statis. Assoc. 73* 640-645.

Mališić, J., 1990: Stochastic Processes: Theory and Applications (in Serbian). Gradjevinska knjiga, Belgrade.

Newton, H.J. and *Pagano, M.*, 1983: A method for determining periods in time series. *J. Amer. Statist. Assoc. 78*, 152-157.

Padmanabhan, G. and *Rao, A.R.*, 1988: Maximum entropy spectral analysis of hydrologic data, *Water Resour. Res. 24*, 1519-1533.

Padmanabhan, G., 1991: Non-harmonic spectral analysis to investigate periodicity in hydrologic and climatologic time series. *Theor. Appl. Climat 43*, 31-42.

Potter, K.W., 1981: Illustration of a new test for detecting a shift in mean in precipitation series. *Mon. Wea. Rev 109*, 2040-2045.

Siegel, A.F., 1978: Random areas on the circle. *J. Appl. Probab. 15*, 774-789.

Siegel, A.F., 1980: Testing for periodicity in a time series. *J. Amer. Statist. Assoc. 75*, 345-348.

Thompson, D.J., 1982: Spectrum estimation and harmonic analysis. *Proc. IEEE 70*, 1055-1096.

Wei, W.W.S., 1990: *Time Series Analysis: Univariate and Multivariate Methods*. Addison-Wesley Publ. Company, Redwood City.

IDŐJÁRÁS

Quarterly Journal of the Hungarian Meteorological Service
Vol. 103, No. 4, October–December 1999, pp. 249–260

Instrumental problems of UV and UV-B radiometers: regression models to derive UV and UV-B irradiance from global solar radiation data

I. Galindo, A. T. Elizalde and **J. Fonseca**

Centro Universitario de Investigaciones en Ciencias del Ambiente,
Universidad de Colima,
25 de Julio 965, Villas San Sebastián, Colima, Mexico
e-mail: galindo@volcan.ucol.mx

(Manuscript received 11 October 1998; in final form 5 July 1999)

Abstract—Direct evidence of increased ground level ultraviolet radiation is fragmentary mainly due to scarce measurements and instrumental problems such as calibration shifts. The problem is more critical at the tropics, therefore regression models are used to relate global solar radiation measurements made at Colima, Mexico with UV and UV-B irradiance under all sky conditions, thus expanding the UV-B data set from October 1995 to June 1999. Aging of total ultraviolet radiometer (TUVR) is also documented. Results show no trends in the synthetic UV-B time series. Remarkable calibration shifts occur in the total ultraviolet radiometer suggesting that the mean lifetime of these instruments under tropical conditions is about 4 years.

Key-words: UV and UV-B irradiance, global solar radiation, total UV radiometer, instrumental calibration.

1. Introduction

Stratospheric ozone depletion, which became evident in the 1970s, has produced a great concern in the scientific community in the last years. Ozone depletion trends are now well established in both hemispheres (*Gleason et al.*, 1993; *Jones* and *Shanklin*, 1995). Solar radiation that reaches the surface of the Earth´s contains approximately 5% ultraviolet, 55% infrared and 40% visible radiation. Stratospheric ozone absorbs essentially all the highest energy (i.e., 100–290 nm, UV-C, the shortest wavelength radiation), approximately three-quarters of the next highest energy band (i.e., 290–315 nm, UV-B) but only a small part of the lowest energy radiation (i.e., 315–385 nm, UV-A). Further ultraviolet radiation is absorbed in the troposphere via clouds, dust and gaseous and particulate air pollutants. In particular, in the vicinity of active volcanoes there is UV absorption due to volcanic sulphur dioxide and large silicate particles. As human-induced depletion of stratospheric ozone is much greater at higher latitudes, about 30–60°N (*McMichael et al.*, 1996), ozone measurements are scarce at the tropics, therefore ozone depletion trends at the tropics are not yet established even that ozone variability in these latitudes is very low.

Spectral measurements of ultraviolet-B radiation made at Toronto indicate that the intensity of light at wavelengths near 300 nm has increased by 35 percent per year in winter and 7 percent in summer. These trends indicate that the increase is caused by the downward trend in total ozone measured at Toronto during the same period (*Kerr* and *McElroy*, 1993).

Since UV measurements are difficult to made and scarce all over the world, indirect methods to determine UV-B irradiance have been attempted, either through radiative transfer modelling (*Box* and *Loughlin*, 1997; *Dave* and *Furukawa*, 1966, *Lemus-Deschamps et al.*, 1997, *Ruggaber et al.*, 1997) or using simple regression models (*Feister et al.*, 1996; *Nagaraja et al.*, 1984).

On the other hand, statistics of skin cancer incidence show percentage increases as a function of latitude for the period 1979–1994. The highest increases are reported on the middle and high latitudes (*UNEP*, 1994). The latitude span for Mexico shows skin cancer incidence increases of about 3% for that period. Though these figures are not yet verified, there are relevant skin cancer incidence figures for the Colima state located in the western part of Mexico (*Galindo* and *Loya*, 1998) which justify *per se* the need of reliable high quality systematic ground-level UV measurements.

Although most of Colima sites are free from anthropogenic aerosols, Volcán de Fuego de Colima (see *Fig. 1*), which is one of the most active volcanoes of Mexico, has a permanent plume delivering gases (mainly SO_2) and large silicate particles into the atmosphere. Sulphur dioxide is transformed through the gas-to-particle conversion mechanism into small sulphate particles and sulphuric acid drops. It is necessary to study the effects of volcanic aerosols on the UV radiation field.

In this study regression models are used to relate global solar radiation (290–2900 nm) to UV (290–385 nm) and UV-B (290–320 nm) irradiance measurements. The regression equation obtained let us expand the UV-B data set from October 1995 to June 1999 and the UV data set from June 1993 to June 1999. Unfortunately, at the time that these UV measurements were made no ozone measurements were made within this region. Therefore the stratospheric ozone depletion does not appear in the expanded data set here reported. The new UV-B data set will be used only to support medical statistics on increasing skin cancer incidence. Finally, the calibration shift of the instrument with the time of total ultraviolet radiometers (TUVR) is also presented.

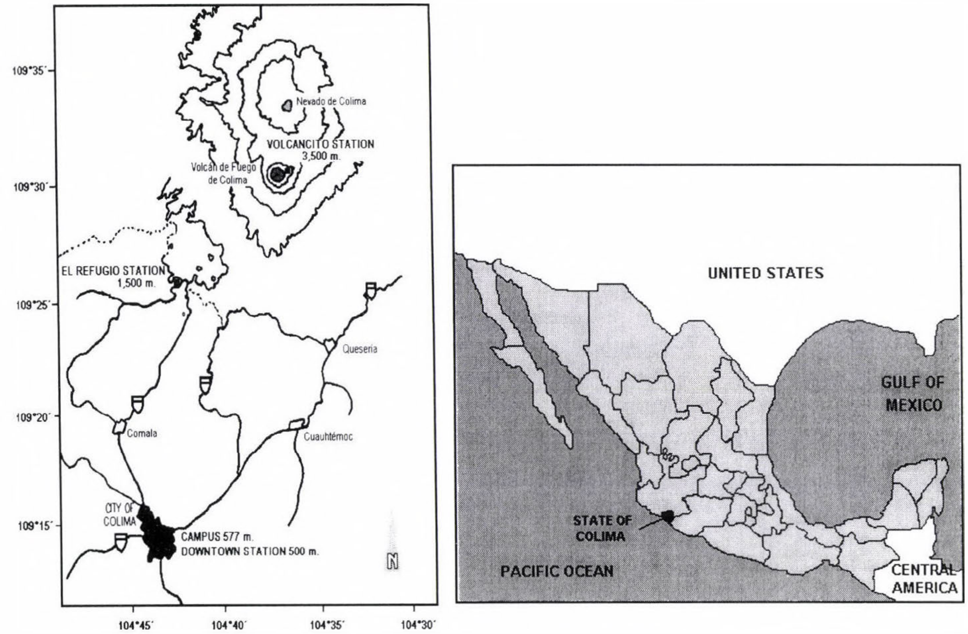

Fig. 1. Localization of the state of Colima in Mexico.
The two measurement sites are also depicted.

2. Methods

2.1 Measurement sites

2.1.1 University campus

A meteorological station was installed on the roof of a 4 m high building located at the University Campus (577 m a.s.l.) in April 1994. In June 1995 an Eppley precision spectral pyranometer (PSP) No. 29102F3 was added to measure global solar irradiance (290–2900 nm). From October 1995 to November 1996 a Solar Light Model 501 UV-Biometer S/N 1471 (290–320 nm) was operating. Finally, from November 1996 to January 1997 a UV-Biometer S/N 1458 was operating. All the instruments are coupled to a Campbell data logger sampling time in every 5 minutes. Unfortunately, the UV-Biometers are not protected electrically against shortcuts. Due to heavy storms, an electrical short circuit damaged very badly the UV-B sensors interrupting the measurements. Since the photodiode of these instruments were damaged, no attempts to repair and calibrate them were made. The data set of UV-B irradiance and global solar radiation measurements used for the regression analysis is from October 16, 1995 to December 31, 1996.

2.1.2 Rancho El Refugio

Our second station, installed in April 1994, is located in a rural zone at Rancho El Refugio (1,500 m a.s.l). The station operates two radiometers, Eppley Model TUVR S/N 27988 and 28928 (290–385 nm) to measure total and diffuse ultraviolet irradiance. Also there is an Eppley PSP No. 29102 that measures global solar radiation. All the instruments are coupled to a Campbell data logger sampling time in every 5 minutes. The data set for the year 1997 of total ultraviolet irradiance and global solar irradiance is used for the regression analysis.

A calibration program of all our pyranometers is regularly done against our Eppley H-F cavity radiometer No. 28965 which is one of the regional radiometer instruments of the Regional Radiation Center of Mexico for the Regional Association IV of the World Meteorological Organization (WRC, 1995). A conservative estimate of the accuracy of the measured global solar radiation is $\pm 2\%$. The observing site affords optimum exposure to the radiation sensors, with practically no obstructions extending beyond 3° above the plane of the sensors. The results are expressed in physical units (W m^{-2}).

The intensity of incoming solar radiation at the surface varies locally with the angle of incoming solar radiation and hence with the day, season, latitude and cloudiness (*Kuik* and *Kelder*, 1994), therefore local natural conditions are better represented performing regression analyses using measurements under all-sky conditions. Data sets of UV-B, UV and G were matched on time forming $n \times 2$ matrices (G_i, UV-B_i) and (G_j, UV_j), where i,j is the sampling time. The regression analyses were made using the MATLAB interactive system.

3. Calibration shift UV radiometers

The Eppley ultraviolet pyranometer (TUVR) sensor is a Weston selenium barrier-layer photoelectric cell (*Coulson*, 1975). The value of the original instrumental constant of these instruments is quite similar to the values shown in *Table 1*.

The instrument used as reference (TUVR S/N 28656) was received in January 1993, since then it has been on storage most of the time. In order to check irradiance levels of the other UV radiometers in operation, the instrument was exposed under high irradiance conditions only for several days. The other three radiometers were exposed under all sky conditions most of the time.

The photocell loses sensitivity with time. To study this effect, known as aging effect, a comparison was made under clear conditions. All the instruments were simultaneously exposed to the sun and coupled to a datalogger with five minutes sampling time.

Table 1. Original instrument constants of total ultraviolet radiometers (TUVR)

TUVR Nr.	k [mW cm^{-2} mV^{-1}]	Date
27831	0.518	09.18.1989
27988	0.469	11.09.1990
28656*	0.538	11.02.1992
28928	0.559	04.14.1992

* Reference instrument

4. Results

4.1 Ultraviolet-B irradiance

The degree of correspondence that exists between *UV-B* irradiance and global solar radiation *G* under all weather conditions is given by a polynomial of degree 2, which is the best fit for such regression models. Regression equation for UV-B irradiance from global solar radiation measurements made at campus Colima from October 16, 1995 to December 31, 1996 is as follows (see *Fig. 2a*):

$$UV\text{-}B = 1.28 \cdot 10^{-7}\, G^2 + 7.42 \cdot 10^{-5}\, G - 1.01 \cdot 10^{-3} \qquad (1)$$
$$c = 0.999, \quad e = +7.6\%,$$

where c is the correlation coefficient, e is the determination error.

The comparison of measured UV-B irradiance and that obtained using the regression equation for a particular day (January 10, 1996) is shown in *Fig. 2b*. The agreement is quite good around noon (10:30–14:30), however, for low solar height the estimated UV-B is relatively higher than the measured. The differences between modelled and measured UV-B are shown in *Fig. 2c*. The largest differences ($\sim$12 mW m^{-2}) are observed in the afternoon, whereas in the morning the difference is not larger than 9 mW m^{-2}. At noon there is a negative difference ($\sim$5 mW m^{-2}).

Synthetic time series were constructed for the time period from October 1995 up to present (June 1999). No trends were observed during this period.

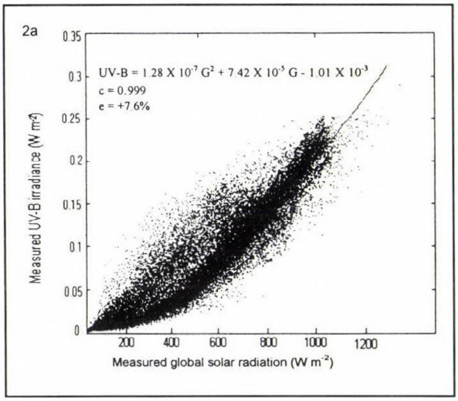

Fig. 2a. Regression equation for UV-B irradiance from global solar radiation measurements made at campus Colima from October 16, 1995 to December 31, 1996.

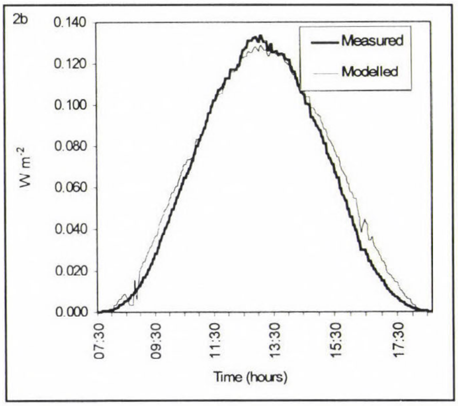

Fig. 2b. Comparison of UV-B measurements with calculated values of the regression equation for a particular day, January 10, 1996.

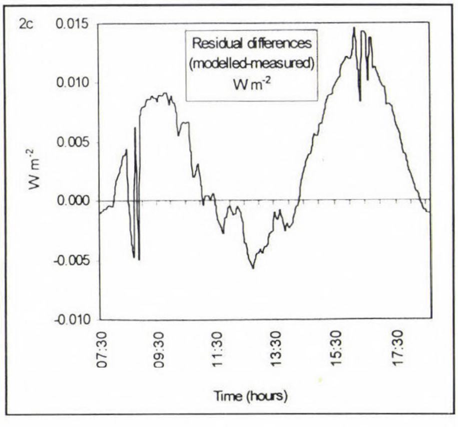

Fig. 2c. Difference between modelled and measured UV-B for January 10, 1996.

4.2 Ultraviolet irradiance

The degree of correspondence that exists between *UV* irradiance and global solar radiation (*G*) is given by a linear regression equation which is the best fit for such regression models. Regression equation for UV irradiance from global solar radiation measurements made at rancho El Refugio from January 1 to December 31, 1997 (see *Fig. 3a*) is as follows:

$$\begin{gathered} UV = 0.0741\ G + 1.8471 \\ c = 0.962,\ e = +8.4\%. \end{gathered} \tag{2}$$

The comparison of measured UV irradiance and that obtained using the regression equations for a particular day is shown in *Fig. 3b*. The agreement is relatively good, however the model produces systematically higher values. The differences between modelled UV and measured UV are shown in *Fig. 3c*. The largest differences ($\sim$7 W m^{-2}) are observed in the early morning, whereas during the rest of the day the differences rank between 4 and 1 W m^{-2}. At noon the fit lies around 2 W m^{-2}.

4.3 Calibration shifts

Fig. 4a shows the mean hourly voltage output of each instrument, and *Fig. 4b* shows the records in physical units. It is noticed that one of the instruments (S/N 28928) shows significantly higher values of incoming UV radiation, whereas the rest of the instruments respond quite similarly but with much lower signals. It is remarkable how the rest of the radiometers have degraded, between 40–50%, including the reference instrument (TUVR S/N 28656). Comparing the actual recorded values with previous records for the same time and place, one observes a significant loss of sensitivity (-14%) for the instrument S/N 28928, which shows, that this instrument was less degraded than the others. The above results suggest that the TUVR instrument mean lifetime under tropical conditions is about 4 years.

The instrument TUVR S/N 27988 was send to the manufacturer for photocell replacement and calibration against their standards. The new instrumental constant enables us to assume that the measured UV intensity with the reference instrument is proportional to the measured signals of the other radiometers:

$$K_N L_N \approx K_i L_i, \tag{3}$$

where the K is the instrumental constants and the L is the measured voltage. N stands for the new instrument S/N 27988, i stands for the test instruments.

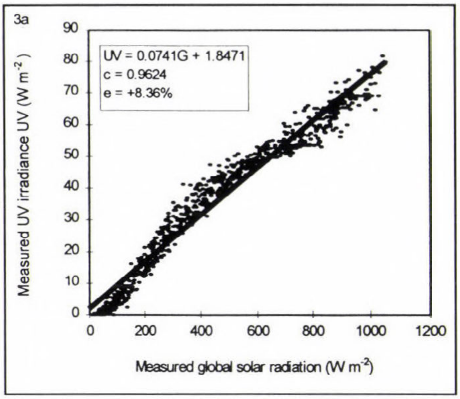

Fig. 3a. Regression equation for UV irradiance from global solar radiation measurements made at rancho El Refugio from January 1 to December 31, 1997.

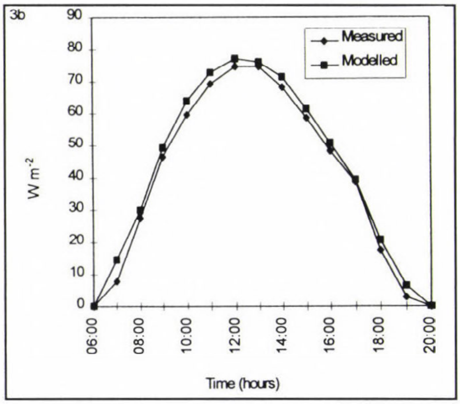

Fig. 3b. Comparison of UV measurements with calculated values of the regression equation for a particular day, May 1, 1998.

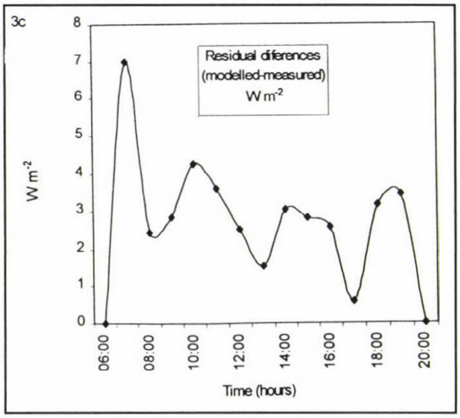

Fig. 3c. Difference between modelled and measured UV for May 1, 1998.

Using the proportionality constant one can raise the sensitivity of the test instrument in reference to the new instrumental constant:

$$K_i = K_N \, (L_N / L_i). \tag{4}$$

Using the above expressions, new calibration constants were obtained for the operational radiometers. A new comparison between all the instruments was made. We have selected one particular day (July 24, 1998) to show the new instruments response. *Fig. 5a* depicts the measured UV values with the TUVR S/N 27831, whereas *Fig. 5b* is for TUVR S/N 28656 and *Fig. 5c* is for TUVR S/N 28928. All of them were compared to the new reference instrument (S/N 27988). It is observed that there is still a response difference between the different radiometers.

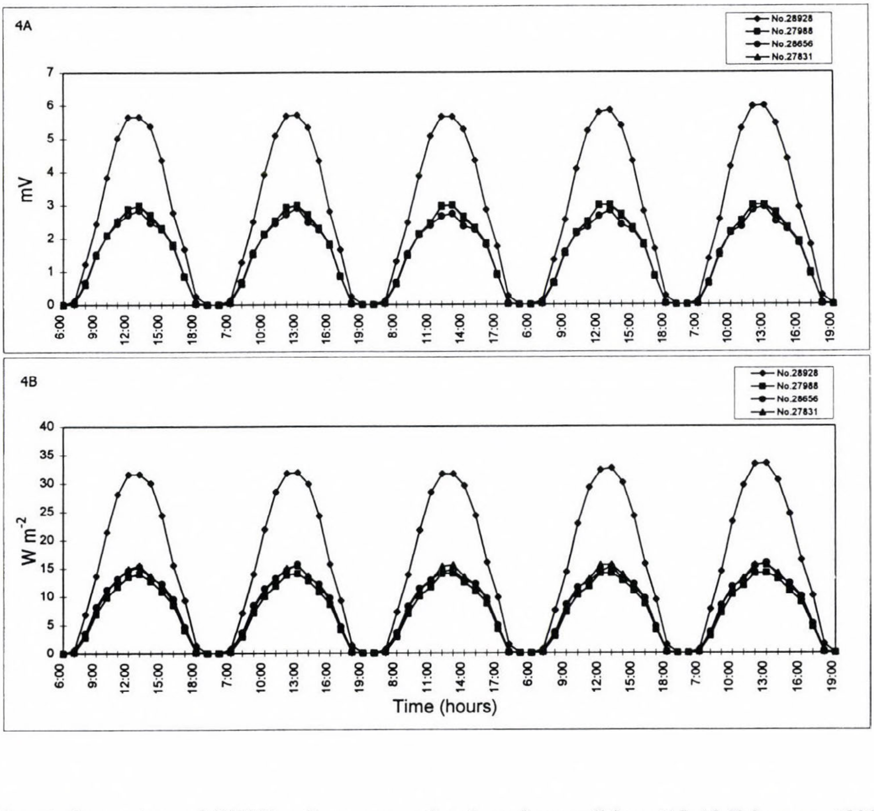

Fig. 4. Comparison of TUVR radiometers under clear sky conditions (15–19 February, 1998): (*a*) Mean hourly voltage output, (*b*) mean hourly UV irradiance (W m^{-2}).

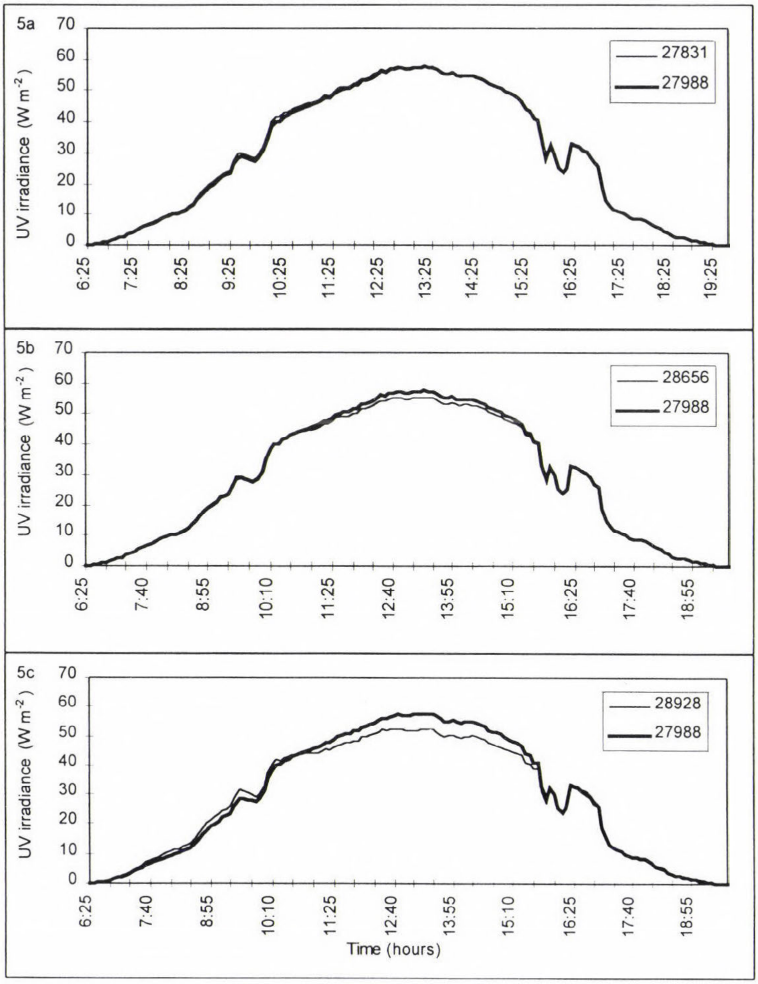

Fig. 5. Comparison of TUVR instruments: (*a*) S/N 27831; (*b*) S/N 28656; (*c*) S/N 28928 for a particular day (July 24, 1998).

Let us take the ratios of the measured values to UV $\geq$ 40 W m^{-2}, i.e., for high UV intensities which obviously occur around noon. The results are shown in *Table 2*.

The above results show that it is not enough to refer the instrumental response to a new instrumental constant since sensitivity loss of the photocell does not reach the actual incoming high UV intensities. The TUVR S/N 28928 instrument obviously needs a new photocell.

Table 2. Ratio of the measured values to UV ≥ 40 W m^{-2}, referred to a new instrumental constant

TUVR S/N	Ratio (%)
27831	1.06
28656	2.42
28928	5.81

5. Conclusions

Regression methods for global solar radiation and ultraviolet irradiance data permit to extend UV records which, in turn, may be used to analyze time variations of incoming UV-irradiance.

The analysis of synthetic UV-B series obtained shows no trends for the period 1995 up to present (June, 1999).

The best fit is obtained between global solar radiation (290–2900 nm) and ultraviolet irradiance-B (290–320 nm) through a second order polynomial. Whereas the best fit obtained between global solar radiation and UV irradiance (290–385 nm) obeys a linear regression.

Significant calibration shifts occur in the total ultraviolet radiometers. Therefore frequent instrumental comparisons and calibrations should be made. It is found that the mean lifetime of this kind of instruments is about 4 years at the tropics.

References

Box, M. and *Loughlin, P.*, 1997: Efficient calculation of UV indices using radiative perturbation theory. In *Proc. of the First Sparc General Assembly*. Melbourne, Australia, 2-6 December 1996 Vol. II, WCRP-99, WMO/TD-NO. 814, 525-528.

Coulson, K.I., 1975: *Solar and Terrestrial Radiation. Methods and Measurements*. Academic Press, New York, 322 pp.

Dave, J.V. and *Furukawa, P.M.*, 1966: Scattered radiation in the ozone absorption bands at selected levels of a terrestrial Rayleigh Atmosphere. *Meteorol. Monogr. 7*, 1-353.

Feister, U., Nöthlich, A. and *Grewe, R.*, 1996: Short-term forecasts of biologically effective UV radiation; comparison between modelled and measured irradiation. *Meteorol. Appl. 3*, 75-89.

Galindo, I. and *Loya, L.*, 1998: Ground level ultraviolet irradiance (UV-B), ozone and incidence of skin cancer at the tropics. Submitted to *Int. J. Epidemiol.*

Gleason, J.F., Bhartia, P.K., Herman, J.R., McPeters, R., Newman, P., Stolarski, R.S., Flynn, L., Labow, G., Larko, D., Seftor, C., Wellemeyer, C., Komhyr, W.D., Miller, A.J. and *Planet, W.*, 1993: Record low global ozone in 1992. *Science 260*, 523-524.

Jones, A.E. and *Shanklin, J.D.*, 1995: Continued decline of total ozone over Halley, Antarctica since 1985. *Nature 376*, 409-411.

Kerr, J.B. and *McElroy, C.T.*, 1993: Evidence for large upward trends of ultraviolet-B radiation linked to ozone depletion. *Science 262*, 1032-1034.

Kuik, F. and *Kelder, H.*, 1994: Spectral ultraviolet radiation measurements and correlation with atmospheric parameters. *Final Report NOP Project 852088*, Koninklij Netherlands Meteorologisch Institut. Scientific Report WR-94-05, 38 pp.

Lemus-Deschamps, L., Rikus, L., Atkinson, R., Grainger, S. and *Paevere, J.*, 1997: Ultraviolet index analyses and forecasts. In *Proc. of the First Sparc General Assembly*. Melbourne, Australia 2-6 December 1996 Vol. II, WCRP-99, WMO/TD-NO. 814, 549-552.

McMichael, A.J., Haines, A., Slooff, R. and *Kovats, S.* (eds.), 1996: *Climate and Human Health*. World Health Organization, Geneva, 297 pp.

Nagaraja Rao, C.R., Takashima, T., Bradley, A.W. and *Lee, Y.T.*, 1984: Near ultraviolet radiation at the earth´s surface; measurements and model comparisons. *Tellus 36B*, 286-293.

Ruggaber, A., Schwander, H. and *Nakajima, T.*, 1997: Modelling of UV radiation. In *Proc. of the First Sparc General Assembly*. Melbourne, Australia 2-6 December 1996, Vol. II, WCRP-99, WMO/TD-NO. 814, 553-556.

United Nations Environmental Programme, 1994: Environmental effects of ozone depletion: 1994 assessment. Nairobi, UNEP.

IDŐJÁRÁS

Quarterly Journal of the Hungarian Meteorological Service
Vol. 103, No. 4, October–December 1999, pp. 261–273

Source characterisation of airborne particles in Seville (Spain) by multivariate statistical analyses

A. J. Fernández Espinosa[1], **M. Ternero Rodríguez,**
F. J. Barragán de la Rosa and **J. C. Jiménez Sánchez**

Department of Analytical Chemistry, University of Seville,
E-41012 Seville, Spain; e-mail: anjose@cica.es

(Manuscript received 10 August 1998; in final form 19 July 1999)

Abstract—Metal contamination (Al, Cr, Mn, Fe, Co, Ni, Cu, Zn, Cd and Pb) in suspended particles was studied at twelve monitoring stations in Seville. The metal concentrations in cellulose filter samples were analyzed by FAAS (flame atomic absorption spectrophotometric) and GFAAS (graphite furnace atomic absorption spectrophotometry). We found that the sum and the percentages of metals analyzed with respect to the Total Suspended Particles (TSP) were low. The study shows that Al and Fe are the major metal elements with concentrations of around 860 ng m^{-3} which together represent 90.6% of the sum of metals. Three statistical groups of metals were found by factor analysis and cluster analysis: Fe, Al and Mn; Zn, Cd and Cr; and Pb and Cu. These techniques, applied in the 1monitoring stations, were effective at associating the groupings obtained with the different environmental locations of the city and with the origin of the metals in different areas of the same city. Areas of the city influenced by traffic and industry were distinguished, especially those influenced by metal foundry industries (Camas, Puerto Este, Pinomontano and La Liebre). A second group comprises areas influenced by traffic alone (Los Remedios, Laraña, Resolana, Recaredo and Luis Montoto). The remaining sites correspond to areas influenced by emission sources (Reina Mercedes, Bellavista and Torreblanca).

Key-words: heavy metals, factorial analysis, particulate matter, air pollution.

1. Introduction

The presence of harmful substances in the atmosphere is particularly worrying because of the number of people that can be affected. Also, air pollution can have significant negative effects on a wide range of living organisms and on the rocky materials of monumental buildings. The danger depends on the nature of

---

[1] Corresponding author

the pollutants and on its content in the atmosphere. Although there are considerable amount of data on gaseous pollutants (CO, SO_2, NO_x and O_3) this is not the case for heavy metals. Heavy metals have an important effect on biochemical mechanisms especially because they accumulate in the biomass.

In large urban areas, the considerable amount of particulate matter in the air is an important problem. The main sources of airborne particulate matter are: agriculture, industry, fuels for domestic use and motor traffic. Particles in suspension comprise the most representative variable, and determination of heavy metals in unsedimentable particles is also of great value. Because of their small size, these particles have a direct incidence on health by affecting respiration. On the other hand, they are easily transported large distances and can stay in the air for some time depending on meteorological conditions.

The aim of the present work was to determine the metal content of suspended particulate matter in Seville, which is the most densely populated city of southern Spain. It presents an extension of 142 km^2 and is situated only 10 meters above the sea level on an extensive plain crossed by the Guadalquivir River. In 1993 it had a population of 716,937 inhabitants, but on workdays the effective population increases to one million mainly with commuters from nearby towns. Seville has a Mediterranean climate with an annual average temperature of 19°C and rainfall of 580 mm. Other climatological conditions (poor winds, thermal investments) do not favour pollutant dispersion. Industry as a source of metal pollutants is rather scarce and represents about 5% of the city's economic activities. Metallic products represent only 15% of this industry.

Several studies on contamination by particulate matter in the city of Seville have been carried out in order to determine metals in sedimentable particles (*Usero et al.,* 1983a, b) and in suspended particles (*Melgarejo et al.,* 1986; *Usero et al.,* 1988; *Luis-Simón et al.,* 1995). Consequently, one of the main goals of this work was to study the evolution of the situation after the economic and urban changes experienced in the city after 1992, when the World Fair of Seville (EXPO 92) was celebrated.

2. Experimental

2.1 Sampling

Sampling network with twelve monitoring stations was elaborated (*Fig. 1*). It is designed to encompass practically all urban areas and some peripheral zones of Seville. In this network stations are located near to focuses of emission (industries and zones of high traffic density) as well as to others with cleaner air.

The stations can be classified into three categories according to the nearest and most significant possible pollution sources:

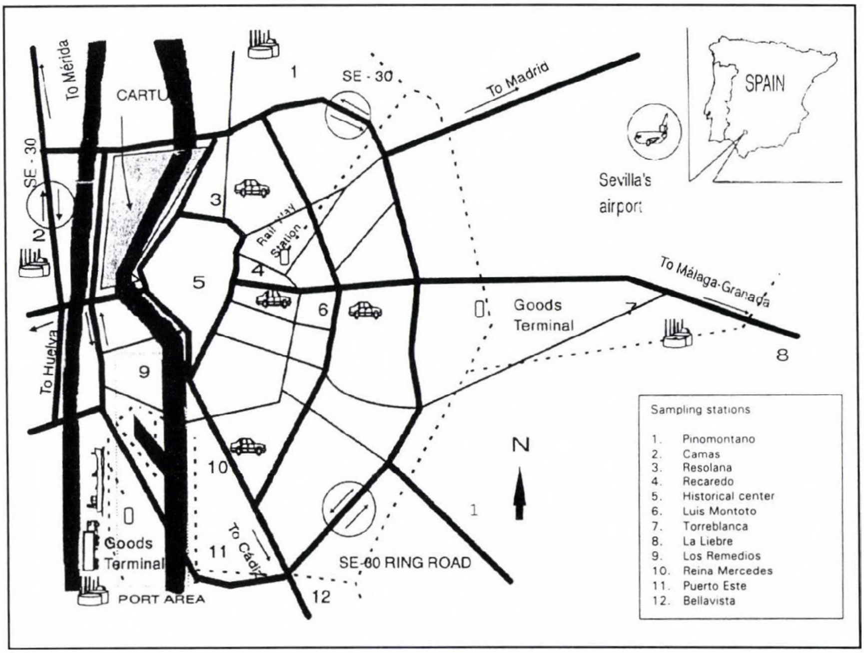

Fig. 1. Sampling network in Seville with the location of the twelve sampling.

(i) *Stations under the influence of industrial emissions.* Camas (station 1) is 6 kilometres far from the city centre, near to two foundries of iron and aluminium. Puerto Este (station 3) is near to Seville Harbour in the estuary of the Guadalquivir, in which important loading and unloading activities take place. There is a certain amount of industry nearby (fertilisers, oils, cement and construction materials, small metallurgy and shipyards). Pinomontano (station 10) is near to fertiliser and building material production plants. La Liebre (station 12) is 15 kilometres far from the city. It is next to an important cement factory, and there is a glass factory and metal foundries nearby.

(ii) *Stations under the influence of vehicle emissions.* Los Remedios (station 2), Laraña (station 5) in the historic centre, Resolana (station 6), Recaredo (station 7) and Luis Montoto (station 9). The last three sites are next to important communication routes inside the city.

(iii) *Peripheral stations with few sources of industrial emissions or traffic.* Reina Mercedes (station 4), Bellavista (station 8), near to a factory of fiber-cement and Torreblanca (station 11).

In this study, 48 samples were collected (four samples in each monitoring station on different days of the week) from February to October, 1993.

Atmospheric suspended particles were collected on 20.3 × 25.4 cm cellulose filters (Whatman-41) using a Quimisur-SMAV high volume sampler on the top roof of buildings at 4–6 m high. Approximately 1500 m^3 air was collected in each 48 hour sampling period with a nominal aspiration flow of 40 m^3 h^{-1}.

In order to obtain a sufficient quantity of sample and absolute concentration of metals, the relationship between the duration of the sampling and results of subsequent analytical determinations was studied. Because of the low levels of metals and the small amounts of particles collected, a sampling period of 48 hours was chosen.

Beforehand, a preliminary assay was done to select the most suitable filter. Although some authors prefer to use glass-fiber filters (*Obiols et al.,* 1986; *Clevenger et al.,* 1991), in our experience cellulose ones were preferable for the analyzed parameters (*Usero et al.* 1988; *Luis-Simón et al.,* 1995), because of the chemical stability, low concentration of blanks and low cost. These filters can easily break down, and values corresponding to blanks are lower than glass-fiber values. These showed high levels of impurities of iron, aluminium and especially zinc (*Berg et al.,* 1993), and reactivity with metals (*Zatka et al.,* (1992). In addition, several experiments were done to improve the method for chemical attack of samples in teflon vessels. The proportions and types of acids used in the digestion mixture, temperature, time and other variables were noted in order to optimise the blanks and efficacy of attacks. Other mixtures and heating procedures (*Obiols et al.,* 1986; *Frenzel*, 1991), have been studied, but we obtained the best results in the method recorded below.

2.2 Apparatus and reagents

Samples were analyzed by flame atomic absorption spectrophotometry (FAAS Perkin-Elmer 3100) for the majority metals Fe, Al, Zn, Cu and Pb, and by graphite furnace atomic absorption spectrophotometry (GFAAS Perkin-Elmer 2380 with HGA Programmer Perkin-Elmer 300) for the trace metals Cd, Co, Ni, Mn and Cr.

All the reagents employed were of analytical grade, and Milli-Q water was used.

2.3 Methodology for the chemical analysis

A quarter of cellulose filter was finely divided into 1 cm^2 pieces prior to chemical treatment, consisting of acid digestion by heating in a closed teflon vessel under pressure.

First, the sample was treated in an open vessel with 20 mℓ of concentrated nitric acid and then it was evaporated to half of the volume in a sandbath at 180°C. Afterwards, 20 mℓ of water plus 2 mℓ of perchloric acid were added. The closed vessel was introduced into a stove at 120°C for six hours. The treated sample solution was decanted from the washed silica-carbonaceous residue, placed in a 50-mℓ standard flask and diluted to the mark with Milli-Q water. Treated samples were then analyzed by FAAS or GFAAS.

Blanks were determined for all metals. The previously described procedure was repeated with four unused filters and the average value of the blanks was subtracted from samples.

2.4 Multivariate analyses

To draw conclusions from the data, multivariate analyses were applied to the average of the four concentrations obtained for each metal in each monitoring station. Statistical models of parameter correlation, factor analysis and cluster analysis of variables and cases were applied using the CSS:STATISTICA (StatSoft) software package. The data matrix represents the total contents for the 10 metals and the 12 monitoring stations. Another matrix with an additional column corresponding to values of total suspended particles (TSP) was also studied.

3. Results and discussion

To interpret the data, in addition to plots and basic statistics of the results, other models of multivariate statistics, called pattern recognition, were also applied. These models can handle a large amount of numerical data reducing the variables to a few factors, which allow us to evaluate their combined effect and to classify metals by emission sources.

3.1 Heavy metal composition

Concentration values for total particles in suspension (TSP) and metal concentrations appear in *Table 1* (expressed in nanogram of the element per cubic meter of sampled air).

Values for TSP, the sum of metals (S) and their relative percentages in the TSP (S/TSP%) for each sample are recorded in *Fig. 2.* Regarding these data globally, the following considerations can be made:

The sites with the highest levels of TSP are 5 and 1, and these, therefore, have low S/TSP% values. Stations 8 and 2 behave similarly, due to the even lower absolute amounts of metals.

The sites with the lowest levels of TSP (stations 9, 10 and 4) coincided with the areas of the city with the highest relative metal percentages.

These observations can be explained as follows: Evolution of S/TSP% in the graph follows the same profile as the total sum of metals (Fig. 2), because the largest variation among the different stations is given for this variable. If the TSP value is low and the sum of metals is medium or high, the metallic richness is high (sites 9, 10, 4), but if the TSP value is high and the sum of

Table 1. Average metals concentrations (ng m^{-3}) and total suspended particles (TSP) in Seville from February to October, 1993

Station	Al	Fe	Zn	Pb	Cu	Mn	Ni	Co	Cr	Cd	TSP × 10^{-3}
N° 1	895.3	1131.2	74.1	16.4	9.3	11.6	4.7	1.8	0.9	0.9	176.8
N° 2	467.1	421.0	53.5	43.6	19.0	8.3	3.1	1.2	0.8	0.4	155.1
N° 3	1179.4	1491.6	158.4	48.5	24.4	23.0	24.5	9.3	3.9	1.3	140.6
N° 4	445.9	621.3	79.1	91.5	38.8	8.5	4.9	2.0	1.2	0.8	75.3
N° 5	859.5	818.8	70.3	74.5	39.6	10.2	6.7	2.6	2.1	0.6	186.1
N° 6	1299.2	1217.2	75.7	76.3	53.7	18.2	5.6	4.0	2.7	0.4	139.2
N° 7	694.2	938.1	111.5	198.1	80.9	12.2	3.3	5.9	1.1	1.1	123.9
N° 8	276.1	213.5	143.9	26.1	27.0	3.3	3.9	2.7	2.5	1.4	146.8
N° 9	1192.4	1058.2	52.0	66.5	51.1	15.8	4.4	3.5	1.2	0.3	94.3
N° 10	1036.8	636.1	64.3	35.9	39.1	9.6	4.6	1.8	0.9	0.5	80.7
N° 11	1268.0	876.8	134.4	34.3	21.4	18.8	17.8	3.7	1.5	0.5	138.8
N° 12	708.0	893.8	73.7	18.0	45.6	17.5	4.7	5.2	0.3	0.5	143.1
Mean	860.2	859.8	90.9	60.8	37.5	13.1	7.4	3.6	1.6	0.7	133.4
Range	276-1299	214-1492	52-158	16-198	9-81	3-23	3-25	1.2-9.3	0.3-3.9	0.3-1.4	75-186

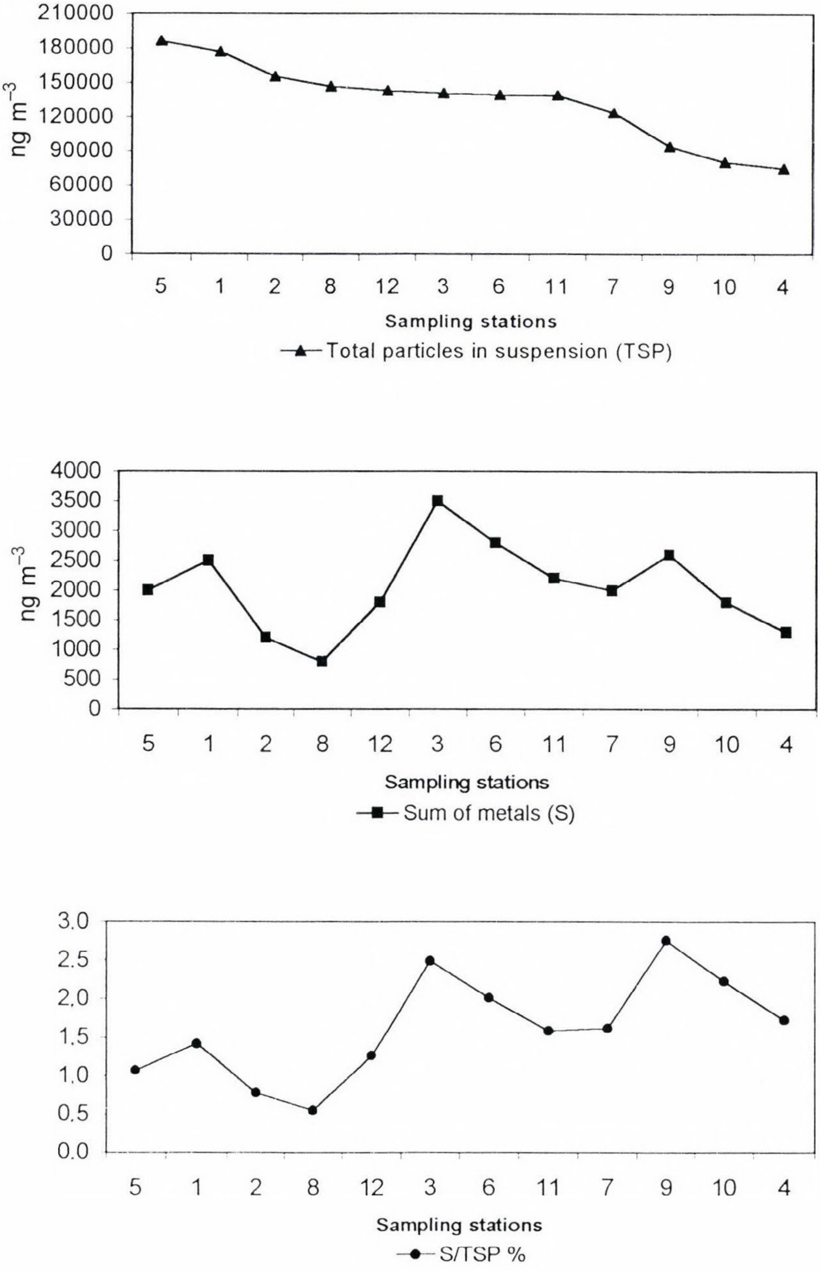

Fig. 2. Average of total particles in suspension (TSP), sum of metals (S) and their relative percentages in the TSP (S/TSP%) parameters at the twelve sampling stations of Seville.

metals is low, the metallic richness is low (sites 2, 8). Therefore, the values of S/TSP% reflect the metallic richness of particles, although the parameter that measures the degree of metal pollution is the total sum of all the metals (S). However, the parameter S/TSP% is useful to assess the level of metal contamination in conditions in which, mainly due to the rains, TSP and S levels diminish considerably. Therefore, in spite of varying meteorological conditions, metal concentrations on different days or in different seasons would give some indication of the degree of metal contamination of the particles.

Values of metal pollution (S) (Fig. 2) reflect that the highest levels are found in Puerto Este (3), Resolana (6), Luis Montoto (9) and Torreblanca (11). The least contaminated sites are Bellavista (8), Los Remedios (2) and Reina Mercedes (4).

Regarding individual heavy metal contents (Table 1) we observed the highest average concentrations for Al and Fe with 860 ng m^{-3} for both elements. The metals Zn, Pb and Cu presented concentrations an order of magnitude below the above value (91–38 ng m^{-3}), and finally, Mn, Ni, Co, Cr and Cd showed even lower amounts (13–0.7 ng m^{-3}).

Table 2 presents the results of two experiments: the average individual metal content (C), the metallic fractions (C/TSP%) and the relative metallic composition (C/S%) obtained in 1985 (*Usero et al.,* 1988) and 1993. The comparison reveals a reduction in metal concentrations (C) from 1985 to the present day. They are four times lower for Al, Fe, Zn, Ni and Cd and even ten times lower for Pb and Cr. On the other hand, these parameters remained more or less constant for Mn and Co. Similar values of relative composition (C/S%) show that the same contamination sources remained in Seville. However, lead and chrome are notable exceptions, since their concentrations suffered a greater decrease. The metallic fraction on particulate matter (C/TSP%) was also diminished since TSP levels were only reduced from 210,000 to 133,400 ng m^{-3}.

3.2 Correlation of metals

Table 3 includes the correlation matrix of the studied parameters. Tabulated values show that Mn significantly correlates with Fe, Al and Co ($r > 0.73$) and to a lesser extent with Ni ($r = 0.69$). These elements are presumably of soil or agricultural origin. A good correlation between elements mainly from vehicular emissions such as Pb and Cu ($r = 0.81$) is also observed. Zn correlates with Cd and Cr moderately well ($r > 0.64$) and to a lesser extent with Co and Ni (r coefficients of 0.62 and 0.69). All these elements are from waste stored in uncontrolled dumps, where burning and incineration often take place. Also, in the case of Ni and Co the significant correlation with earth metals marks a mixed origin. In the following factor and cluster analysis, TSP was ignored because of its low correlation with the remaining parameters.

Table 2. Comparative study of 1985 and 1993 in Seville

		1985*			1993**	
TSP		210.000 ng m^{-3}			133.400 ng m^{-3}	
Metal	C	C/TSP%	C/S%	C	C/TSP%	C/S%
Al	3070.0	1.462	39.72	860.2	0.645	45.32
Fe	3570.0	1.700	46.18	859.8	0.644	45.30
Zn	340.0	0.162	4.40	90.9	0.068	4.79
Pb	680.0	0.324	8.80	60.8	0.046	3.20
Cu***				(37.5)	(0.028)	
Mn	19.6	0.009	0.25	13.1	0.010	0.69
Ni	26.0	0.012	0.34	7.4	0.006	0.39
Co	4.6	0.002	0.06	3.6	0.003	0.19
Cr	16.0	0.008	0.21	1.6	0.001	0.08
Cd	3.3	0.002	0.04	0.7	0.001	0.04
Sum	7729.5	3.681	100.00	1898.1	1.424	100.00

C: total contents in ng m^{-3}
C/TSP%: metallic fraction
S: sum of total contents in ng m^{-3}
C/S%: relative composition
* see *Usero et al.*, 1988
** present work
*** the metal not was analyzed in 1985

3.3 Factor analysis of the metals

The previous correlations were confirmed by factor analysis of the variables revealing three factors which together explained 87% of the variance. The factors that contributed to less than 5% of the variance were rejected. Percentages and loadings explained in each case are included in *Table 4*. The variables obtained in each factor are the following:

Factor 1. This is formed by Al, Fe, Mn, Co and Ni (it is noteworthy that these last two elements can also be found in Factor 2). This factor explains 43% of the variance and it prevails in stations Puerto Este (11), Resolana (3), Torreblanca (7) and Luis Montoto (6) (see *Fig. 3*). These elements contribute to almost 90% of metal content in the atmosphere of Seville. Factor 1 shows the presence of elements (*Usero,* 1988) of earth crustal origin.

Factor 2. This consists of elements such as Zn, Cd and Cr. This factor explains 24% of the variance and this grouping is significant at stations of

Puerto Este (11) and Bellavista (12) (Fig. 3). This factor is associated mainly with waste combustion (*Usero,* 1988) and represents 5% of all the metals.

Table 3. Correlation coefficients (r) for the ten analyzed metals and TSP

Al	1										
Cd	-0.39	1									
Co	0.36	0.41	1								
Cr	0.29	**0.51**	**0.55**	1							
Cu	0.06	-0.11	0.29	-0.11	1						
Fe	**0.77**	-0.04	**0.67**	0.37	0.14	1					
Mn	**0.79**	-0.20	**0.73**	0.32	0.10	**0.86**	1				
Ni	**0.52**	0.30	**0.67**	**0.64**	-0.34	**0.54**	**0.69**	1			
Pb	-0.07	0.16	0.26	0.00	**0.81**	0.12	-0.03	-0.19	1		
Zn	0.02	**0.78**	**0.62**	**0.64**	-0.14	0.13	0.23	**0.69**	0.03	1	
TSP	-0.04	0.14	0.05	0.21	-0.38	0.12	0.03	0.12	-0.24	0.14	1
	Al	Cd	Co	Cr	Cu	Fe	Mn	Ni	Pb	Zn	TSP

Factor 3. This is formed by Cu and Pb corresponding to 5% of the metal content. This factor explains 20% of the variance and its highest influence is observed at the Recaredo (4) station (Fig. 3). This reflects the effect of vehicle emissions.

Table 4. Factor loadings for the varimax rotation

Variable	Factor 1	Factor 2	Factor 3	Communality (%)
Al	**0.91**	0.16	-0.06	86
Cd	-0.27	**-0.91**	0.07	91
Co	**0.63**	**-0.61**	0.31	87
Cr	0.36	**-0.73**	-0.09	66
Cu	0.09	0.13	**0.95**	93
Fe	**0.90**	-0.10	0.14	85
Mn	**0.97**	-0.09	0.02	94
Ni	**0.66**	**-0.60**	-0.32	89
Pb	-0.03	-0.11	**0.93**	88
Zn	0.13	**-0.93**	-0.06	89
% of total variance	43.2	23.8	19.9	

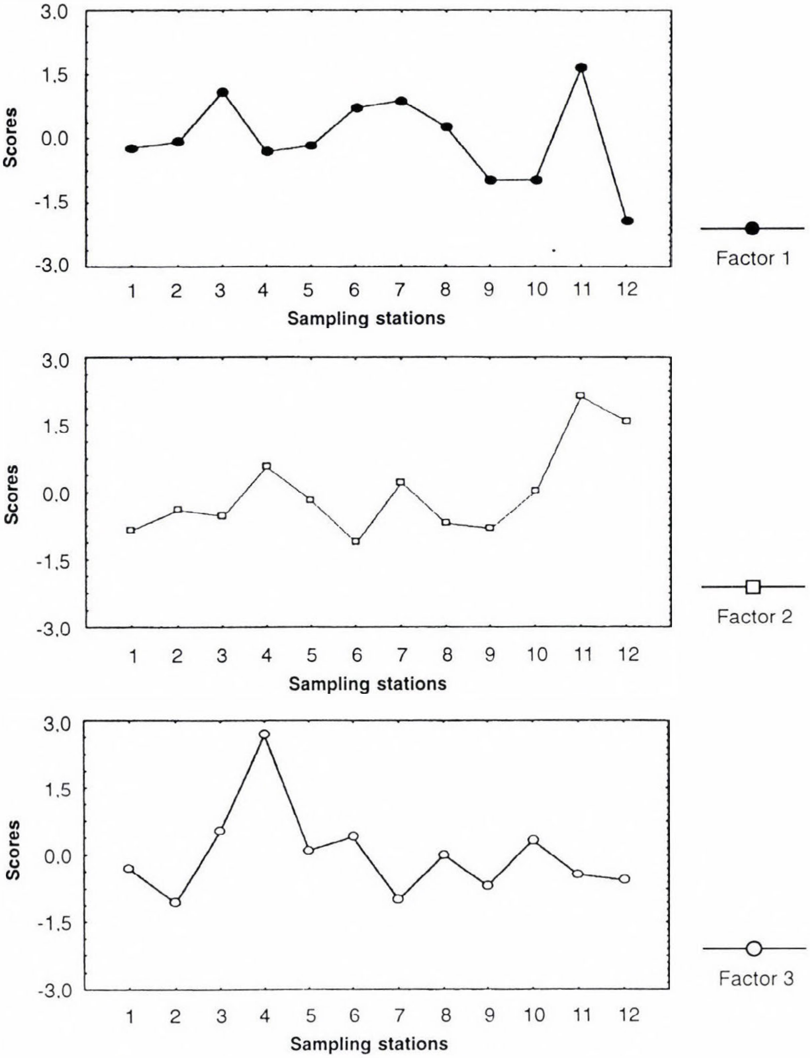

Fig. 3. Graphical representation of the three factors in the twelve sampling stations of Seville.

3.4 Cluster analysis

Cluster analysis of variables with the standardised matrix (*Fig. 4*) was also carried out. This analysis groups together Al, Fe and Mn, the other cluster is formed by Cd, Zn, Co, Ni and Cr, and the last cluster consists of Cu and Pb.

Metals are practically classified in the same groups obtained by factor analysis, while Co and Ni show a mixed behavior between Factor 1 and Factor 2.

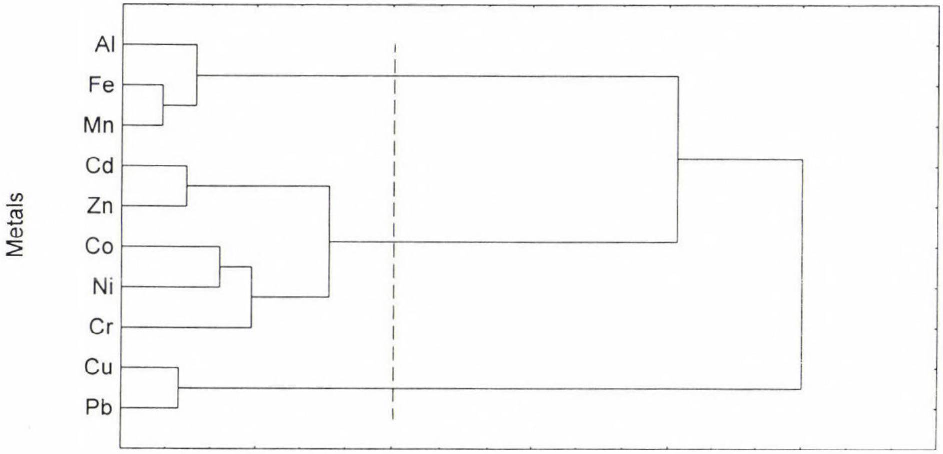

Fig. 4. Dendrogram of the cluster analysis of the ten metals.

4. Conclusions

From our results we can conclude that, in general, atmosphere of Seville is cleaner now than several years ago. This is indicated by the average value of TSP that has reduced from 210,000 to 133,400 ng m^{-3}. On the other hand, the metal fraction in TSP has diminished considerably, i.e., suspended particles now contain smaller amounts of metals. The decrease observed for lead and chromium is especially significant. In the first case, this is due to the new underground network of railways and ring roads constructed in 1992 for the World Fair. The latter has certainly alleviated dense inner city traffic. The continual increase of the proportion of vehicles with unleaded fuel also plays an important role. The decrease in chromium is especially pronounced because of the conversion of many former uncontrolled garbage dump sites into large controlled urban waste installations far from the city center also as a consequence of urban and environmental restructurization.

The absolute metal content has also decreased. Similarly to above, this is also partially due to improvement in traffic and waste management. However, the relative concentration of the ten heavy metals studied has not changed. Metals which present with the highest concentrations are still iron and aluminium, clearly derived from soil or building activities. Zinc, lead and copper present in lower levels, manganese, nickel, cobalt, chromium and cadmium in still smaller amounts. Unexpectedly, the percentages of each metal with respect to the sum (the metal fraction) also remained constant in the last few years (Table 2). This suggests that the pollutant sources have not experienced substantial changes with time, although absolute levels have decreased. Lead and chromium are two clear exceptions to this behavior since, because of the aforementioned reasons, they are now present in much lower percentages.

Factor analysis of variables detects the principal metal sources for atmospheric particles. The main one is the land, due to agricultural works on the periphery. Thus, the metals included in this group are iron, aluminium, manganese, nickel and cobalt. Other important sources are urban wastes and traffic. Thus, Zn, Cd and Cr are components of different waste sources, while Cu and Pb are grouped as components of vehicle emissions. The soil and waste components in particles come from the city's outskirts, whereas the components of traffic origin are emitted in city centre. In this way, zones predominantly affected by the different metal sources in the city have been identified.

Acknowledgements—We would like to thank the "Consejería de Medio Ambiente de la Junta de Andalucía" for their financial assistance to carry out a research project in our Department.

References

Berg, T., *Royset, O.* and *Steinnes, E.*, 1993: Blank values of trace elements in aerosol filters determined by ICP-MS. *Atmos. Environ.* 27A, 2435-2439.

Clevenger, T.E., *Saiwan, C.* and *Koirtyohann, S.R.*, 1991: Lead speciation of particles on air filters collected in the vicinity of a lead smelter. *Environ. Sci. Technol. 25*, 1128-1133.

Frenzel, W., 1991: Microanalytical concept for multicomponent analysis of airborne particulate matter. *Fresenius J. Anal. Chem. 340*, 525-533.

Luis-Simón, F.J., *Gómez-Camacho, J.* and *Respaldiza, M.A.*, 1995: Study of the elemental composition of the air pollution in Seville. *Int. J. PIXE, 5*(1), 43-56.

Melgarejo, P.L., *Ternero, M.* and *Gracia, I.*, 1986: A study of the atmospheric lead pollution in Seville, Spain. Influence of meteorology and traffic, and relationship with other traffic-generated pollutants. *Intern. J. Environ. Anal. 24,* 283-296.

Obiols, J., *Devesa, R.* and *Sol, A.*, 1986: Speciation of heavy metals in suspended particulates in urban air. *Toxicol. Environ. Chem. 13*, 121-128.

Usero, J., *Ternero, M.* and *Gracia, I.*, 1983a: Estudio de la contaminación atmosférica de la ciudad de Sevilla por partículas sedimentables. I. Fracción insoluble. *Ingeniería Química.* 176, 149-153.

Usero, J., *Ternero, M.* and *Gracia, I.*, 1983b: Estudio de la contaminación atmosférica de la ciudad de Seville por partículas sedimentables. II. Fracción soluble. *Ingeniería Química. 189*, 57-62.

Usero, J., *Rosa, F.*, *Ternero, M.* and *Gracia, I.*, 1988: A determination of the sources in the Seville urban aerosol. *Intern. J. Environ. Anal. Chem.* 33, 233-244.

Zatka, V.J., *Warner, J.S.* and *Maskery, D.*, 1992: Chemical speciation of Nickel in airborne dusts: Analytical methods and results of an interlaboratory test program. *Environ. Sci. Technol.* 26, 138-144.

BOOK REVIEWS

Rudolf Czelnai: **The World Ocean** (in Hungarian; A világóceán. Modern fizikai oceanográfia). Vince Kiadó, Budapest, 1999, 182 pages. Price: 1295 HUF.

Hungary has neither sea, nor ocean. Therefore the Hungarian experts of earth sciences had learned only the very basic knowledge about the oceans, that is better to say the world ocean, since the "geographic" oceans are not isolated from each other, so they form one complet system. Now, we have a book, written in Hungarian, about the modern physical oceanography! The author thinks that each nation and each person has relations to the ocean, since it has defining role in the future of the humankind. He hopes that in the future Hungarian scientists might take part in exploring of the oceanic secrets, since the science becomes more and more international.

The book consists of a foreword and seven chapters. The different chapters present different parts of the scientific knowledge about the ocean but in each case in a "easy to read easy to understand" way. The author has the remarkable ability to describe very complicated things in a simple way, however the reader always feels that the reality is much more complex, but he or she receives the essence of it. The other general feature of the book is that the reader sees the fast increase of our knowledge about the ocean (or the whole Earth system), but he or she learns the limits of this knowledge and understands the we must make all efforts to learn much more since we are responsible for our environment and for the future of our children.

I am sure: each reader of this book will learn a lot and, at the same time, enjoy this learning!

G. Major

Wilfried Schröder: **Aurora in Time** (in German; Das Polarlicht). Science Edition, D-28777 Bremen, 1999, 156+10 pages. Price: $20.

This book is a reprint edition of the book "Das Phaenomen des Polarlichts", besides it contains a 10 page English introduction/summary titled: "Some Aspects of the History of Auroral Research". Not only the introduction, but the whole text deals with the history of observations and understanding of aurora from the Ancient Age till the end of the last century. (Developments in the 1900's are supposed to be known.) Besides the European history, the Arabic and Far-Eastern (Korean, Chinese and Japanese) historical observations and their descriptions are mentioned. Until the 18th century the aurora was regarded as miracle or astrological sign. Then the connection between the appearance of aurora and the irregular variations of the terrestrial magnetic field was recognised. It was also observed, that auroras are more frequently seen in those years when the sunspot number is high. More detailed investigations were made when auroras could be recorded on photos.

The history of any field of science is interesting. This is specially true for auroral research, since its development was driven only by the human curiosity until the last decades.

G. Major

ATMOSPHERIC ENVIRONMENT

an international journal

To promote the distribution of Atmospheric Environment *Időjárás* publishes regularly the contents of this important journal. For further information the interested reader is asked to contact *Prof. P. Brimblecombe*, School for Environmental Sciences, University of East Anglia, Norwich NR4 7TJ, U.K.; e-mail: atmos_env@uea.ac.uk

Volume 33 Number 16 1999

Volume 33 Number 17 1999

Carbonaceous Particles in the Atmosphere

The 6th International Conference, Vienna, Austria, 22–24 September 1997

Volume 33 Number 18 1999

IDŐJÁRÁS

VOLUME 103 * 1999

BUDAPEST, HUNGARY

AUTHOR INDEX

TABLE OF CONTENTS
I. Papers

Book review

III. News

Contents of journal Atmospheric Environment, 1999

IV. SUBJECT INDEX

The asterisk denotes book reviews

NOTES TO CONTRIBUTORS OF *IDŐJÁRÁS*

The purpose of the journal is to publish papers in any field of meteorology and atmosphere related scientific areas. These may be

- reports on new results of scientific investigations,
- critical review articles summarizing current state of art of a certain topic,
- shorter contributions dealing with a particular question.

Each issue contains "News" and "Book review" sections.

Authors may be of any nationality, but the official language of the journal is English. Papers will be reviewed by unidentified referees.

Manuscripts should be sent to
Editor-in-Chief of IDŐJÁRÁS
P.O. Box 39
H-1675 Budapest, Hungary

in three copies including all illustrations. One set of illustrations has to be of camera ready quality, the other two might be lower quality.

Title part of the paper should contain the concise title, the name(s) of the author(s), the affiliation(s) including postal and E-mail address(es). In case of multiple authors, the cover letter should indicate the corresponding author.

Abstract should follow the title, it contains the purpose, the data and methods as well as the basic conclusion.

Key-words are necessary to help to classify the topic.

The text has to be typed in double spacing with wide margins. Word-processor printing is preferred. The use of SI units are expected. The negative exponent is preferred to solidus. Figures and tables should be consecutively numbered and referred to in the text.

Mathematical formulas are expected to be as simple as possible and numbered in parentheses at the right margin. Non-Latin letters and hand-written symbols should be indicated and explained by making marginal notes in pencil.

Tables should be marked by Arabic numbers and printed in separate sheets together with their captions. Avoid too lengthy or complicated tables.

Figures should be drawn or printed in black and white, without legends, on separate sheets. The legends of figures should be printed as separate list. Good quality laser printings are preferred as master copies.

References: The text citation should contain the name(s) of the author(s) in Italic letter and the year of publication. In case of one author: *Miller* (1989), or if the name of the author cannot be fitted into the text: *(Miller,* 1989); in the case of two authors: *Gamov* and *Cleveland* (1973); if there are more than two authors: *Smith et al.* (1990). When referring to several papers published in the same year by the same author, the year of publication should be followed by letters a,b etc. At the end of the paper the list of references should be arranged alphabetically. For an article: the name(s) of author(s) in Italics, year, title of article, name of journal, volume number (the latter two in Italics) and pages. E.g. *Nathan, K.K.,* 1986: A note on the relationship between photosynthetically active radiation and cloud amount. *Időjárás 90,* 10-13. For a book: the name(s) of author(s), year, title of the book (all in Italics except the year), publisher and place of publication. E.g. *Junge, C. E.,* 1963: *Air Chemistry and Radioactivity.* Academic Press, New York and London.

The final version should be submitted on diskette altogether with one hard copy. Use standard 3.5" or 5.25" DOS formatted diskettes. The preferred word-processors are WordPerfect 5.1 and MS Word 6.0.

Reprints: authors receive 30 reprints free of charge. Additional reprints may be ordered at the authors' expense when sending back the proofs to the Editorial Office.

More information: gmajor@met.hu
Information on the last issues:
http://www.met.hu/firat/ido-e.html

Published by the Hungarian Meteorological Service

Budapest, Hungary

INDEX: 26 361

HU ISSN 0324-6329